PHENOTYPIC PLASTICITY AND GENETIC VARIATION IN TWO DIVERSE GROUPS OF MOLLUSKS

by

Denise Furr

A dissertation submitted to the faculty of
The University of North Carolina at Charlotte
in partial fulfillment of the requirements
for the degree of Doctor of Philosophy in
Biology

Charlotte

2023

Approved by:

_____
Dr. Adam Reitzel

_____
Dr. Paola Lopez-Duarte

_____
Dr. Bao-Hua Song

_____
Dr. Matthew Parrow

_____
Dr. Sara Gagne

ABSTRACT

DENISE FURR: Phenotypic Plasticity and Genetic Variation
in Two Diverse Groups of Mollusks
(Under the direction of DR. ADAM REITZEL)

Mollusks are a highly diverse phylum with some of the most extremes of body forms from wormlike Aplacophora to tentacled cephalopods. The relationship between phenotype and phylogeny is studied here in two very different groups of mollusks, the bivalves and the terrestrial gastropods. The eastern oyster, *Crassostrea virginica*, being a nearly amorphic organism, expresses its phenotype as physiological responses to its environment. This ancient group has a huge distribution over a range of climates and conditions, lives either submerged or exposed along the edge of the water and faces assault from storms and floods that make its habitat one of the harshest on earth. The physiology of the eastern oyster is investigated to determine its response as a physiological phenotype to different tidal elevations, salinities, and environmental conditions, including the aftermath of a hurricane and a bacterial pathogen. This research investigates the immunity gene expression and mitochondrial genes to determine if selection has any effect in the oyster response. *Triodopsis* snails, on the other hand, generally have small ranges that appear to be similar habitats but have many morphological forms that may have evolved in sympatry. The morphology, biogeography and phylogenetics of the *Triodopsis* genus is studied to determine the status of recognized species, and probable evolutionary history. Both groups of mollusks have incredible adaptations to their respective lifestyles. Oysters have an amazing ability to acclimate to a wide range of conditions without changes in their genetics, whereas the snails have mtDNA that appears to function in spite of extreme variation and holds evidence of volatile climate change and migration of a slow animal. The oyster and the snail are extreme examples of diversity and adaptation to adverse habitats and conditions with different life strategies.

DEDICATION

To my family for enduring my time away from them but always believing I would be successful, and to the many colleagues who encouraged me to take this giant leap. This dissertation is lovingly dedicated.

ACKNOWLEDGMENTS

I would like to send my heart-felt gratitude to my mentors, Dr. Adam Reitzel and Dr. Anna Ivanina, and my committee members Bao Hua Song, PhD, Paola Lopez-Duarte, PhD, Matthew Parrow, PhD, and Sara Gagne, PhD for their patience and guidance through this process. I also thank my lab mates, Whitney Leach and Remi Ketchum, and many undergraduates, Raya Boyd, Maria Kanawati, Zan Atwell, Katrina Gurdyumov, Mariah Graves, Renee Hill, Justin Castillo, and Joshua Nguyen for their contribution to this research.

I would like to thank the following fellow malacologists and institutions for providing permits or specimens, or helping in the field: Schiele Museum of Natural History, Gastonia, NC; N.C. Wildlife Resources Commission; Cherokee National Forest Service; Pisgah National Forest Service; Baruch Research Station; NC Fisheries, SEAP Grant; NSF Graduate Research Fellowship; John Slapcinsky, MS and University of Florida Museum; Art Bogan, PhD, Jamie Smith, MS and the NC Museum of Natural History, Raleigh, NC; Amy Van Devender, MS and R. Wayne Van Devender, PhD; David Campbell, PhD, Gardner Webb University, NC; Zachary Felix, PhD and Reinhardt University, GA; Barbara Dinkins, MS, Dinkins Biological Consulting; Gerald Dinkins, MS, McClung Museum, University of Tennessee; Kathryn Perez, PhD, University of Texas Rio Grande Valley; Dr. Mike Ferro, PhD, Clemson University; Anthony Deczynski, PhD, Clemson University; Emily Phifer, MS and Amanda Wilkerson, MS. This is truly a work of many helpful hands.

TABLE OF CONTENTS

LIST OF TABLES x

LIST OF FIGURES xi

LIST OF ABBREVIATIONS xiv

CHAPTER ONE - INTRODUCTION
- Plasticity and adaptation 1
- Mollusks as a large, diverse phylum 2
- Genetic markers and barcoding 4
- Aims 5
- Relevance to Malacological Research 8

CHAPTER TWO - PHYSIOLOGICAL VARIATION OF *CRASSOSTREA VIRGINICA* BETWEEN LOCATIONS/SALINITIES AND MICROHABITATS
- Abstract 10
- Introduction 11
  - Mitochondrial stress and damage 15
  - Energy storage capacity 17
  - Cellular component damage due to oxidative stress 20
- Materials and Methods 22
  - Animal collection and culture 22
  - Mitochondrial function and damage 24
  - Energy storage capacity 26
  - Cellular component damage 28
  - Statistical analysis 29
- Results 29
  - Mitochondrial respiration and damage 29
  - Energy storage capacity 31
  - Cellular component damage 32
- Discussion 32
  - Mitochondrial respiration and damage 32
  - Energy storage compounds 35
  - Cellular component damage 36
- Conclusion 36
- Chapter two tables 38
- Chapter two figures 43

CHAPTER THREE – EFFECTS OF A HURRICANE ON OYSTER BIOENERGENTICS
- Abstract 50
- Introduction 51
  - Mitochondrial stress and damage 52
  - Energy Storage capacity 53
  - Cellular component damage due to oxidative stress 54
- Materials and Methods 55
  - Animal collection and culture 55

Mitochondrial function and damage 56
Energy storage capacity 56
Cellular component damage 57
Statistical analysis 57
Results 57
Discussion 59
Conclusion 61
Chapter three tables 62
Chapter three figures 66

CHAPTER FOUR - PHYLOGENETICS AND IMMUNITY GENE EXPRESSION IN EASTERN OYSTERS OF NORTH AND SOUTH CAROLINA
Abstract 72
Introduction 73
Immunity factor gene expression 74
Oyster genetics 75
Materials and Methods 76
Animal collection and culture 76
Immunity gene expression 77
Oyster genetics of COI and 16S 79
Results 80
Immunity gene expression 80
Oyster genetics of COI and 16S 81
Discussion 82
Immunity gene expression 82
Oyster genetics of COI and 16S 82
Conclusion 85
Chapter four tables 87
Chapter four figures 91

CHAPTER FIVE - IMMUNITY GENE EXPRESSION BASED ON PATHOGEN SUSCEPTIBILITY AND TIDAL ELEVATION
Abstract 98
Introduction 99
Materials and Methods 103
Animal collection and maintenance 103
Genetic variation 104
Hypoxia exposure 105
Bacterial exposure – Bacterial strains and culture conditions 106
Bacteria uptake experiments 106
Mitochondrial isolation and respiration 107
Hemocyte collection and gene expression 108
Statistical analysis 109
Results 110
Genetic variation 110
Establishing normalized oyster husbandry conditions 111

Response to hypoxia; mitochondrial physiology 112
Crassostrea virginica gene expression in normalized husbandry conditions 112
Crassostrea virginica location comparison: hypoxia 113
Crassostrea virginica location comparison: bacteria 113
Discussion 114
Chapter five tables 118
Chapter five figures 119

CHAPTER SIX - RELATIONSHIP OF MORPHOLOGY, PHYLOGENETICS AND BIOGEOGRAPHY IN *TRIODOPSIS* RAFINESQUE, 1819 (STYLOMMATOPHORA: POLYGYRIDAE) LAND SNAILS
Abstract 125
Introduction 126
The Stylommatophoran land snails 129
History of *Triodopsis* taxonomy and research 130
Materials and Methods 132
Tissue procurement and collection 132
DNA extraction and PCR 133
Phylogeny tree construction 135
Morphology measurements and biogeography maps 136
Results 137
Triodopsis genus 16S phylogeny 137
The *Triodopsis fallax* group 16S phylogeny 139
The *Triodopsis fraudulenta* and *Triodopsis tridentata* groups 16S tree 140
Population statistics 141
ITS2 and 16S/ITS2 Concatenation 142
H3 phylogeny and molecular clock 143
Morphology measurements and biogeography maps 143
Discussion 145
Triodopsis 16S Phylogeny 145
The *Triodopsis fallax* group 146
The *Triodopsis fraudulenta* group and *Triodopsis burchi* 147
The *Triodopsis tridentata* group 148
Triodopsis population statistics 151
ITS2 and H3 gene sequencing 154
Relationship of morphology and 16S phylogenetics 157
Extreme mitochondrial genome variation in Polygyridae 158
Phylogeography and speciation in *Triodopsis* 160
Conclusion 163
Chapter six tables 167
Chapter six figures 172

CHAPTER SEVEN – CONCLUSION 193

REFERENCES 197

APPENDICES 210

A.1 Lipid Determination 210

A.2 Glucose/Glycogen Assay 211

A.3 DNA Degradation Protocol 214

A.4 Carbonyl Groups in Oxidized Proteins 218

A.5 ELISA protocols for HNE Determination 220

A.6 Protein Extraction and Determination by Bradford Dye 222

A.7 Perchloric Acid Extracts of Tissues for Carbohydrates 224

A.8 DNA Extraction Method with SDS for Museum Specimens in Alcohol 226

SUPPLEMENTAL FIGURES AND TABLES 228

S. 5.1 Chapter 5 Primer sequences for target genes in *Crassostrea virginica* 228

S. 5.2 Population pairwise F-Statistics by Haplotype and Distance 229

S. 5.3 Haplotype distribution from Four Locations of Oysters 230

S. 5.4 Effect of Acclimation Husbandry Conditions on Mitochondrial Respirations 231

S. 5.5 Effect of Hypoxia Conditions on Mitochondrial Respiration 232

S. 5.6 Basal Expression of Stress-sensing and Stress-response Molecules 233

S. 6.1 *Triodopsis* Specimens Sequenced in Chapter 6 232

S. 6.2 GenBank Specimens used as Outgroups in Phylogeny Trees 241

S. 6.3 Morphological Measurements for *Triodopsis fallax* Group 242

S. 6.4 16S polymorphism of major *Triodopsis* clades 244

LIST OF TABLES

TABLE 2.1: Mitochondrial Respiration - Federal Point, Harker's Island, Baruch Research Station 38

TABLE 2.2: Amount of Proton Leak - Federal Point, Harker's Island, Baruch Research Station 39

TABLE 2.3: Energy Storage Components - Federal Point, Harker's Island, Baruch Research Station 40

TABLE 2.4: Sum of Energy Components - Federal Point, Harker's Island, Baruch Research Station 41

TABLE 2.5: Cellular Oxidation Damage - Federal Point, Harker's Island, Baruch Research Station 42

TABLE 3.1: Mitochondrial Respiration and Damage – Harker's Island Pre- and Post-hurricane 62

TABLE 3.2: Energy Storage Components - Pre- and Post- Hurricane Harker's Island 63

TABLE 3.3: Sum of Energy Components – Harker's Island Pre- and Post-Hurricane 64

TABLE 3.4: Cellular Component Damage - Pre- and Post- Hurricane Harker's Island 65

TABLE 4.1: Immunity Gene Expression in *Crassostrea virginica* 87

TABLE 4.2: Primer sequences for Target Genes in *Crassostrea virginica* 88

TABLE 4.3: *Crassostrea virginica* COI Mismatch Distribution Statistics 89

TABLE 4.4: *Crassostrea virginica* COI Genetic Distance 90

TABLE 5.1: ANOVA: Effects of Experimental Conditions and/or Populations on the Expression of Studied mRNAs in *Crassostrea virginica* 118

TABLE 6.1: Key to *Triodopsis* Clade Numbers Used in Phylogenies 167

TABLE 6.2: 16S Pairwise Polymorphism Statistics of All *Triodopsis* Clades 168

TABLE 6.3: 16S/ITS2 Pairwise Polymorphism Statistics of All *Triodopsis* Clades 171

TABLE 6.4: A History of the *Triodopsis* genus Nomenclature 172

LIST OF FIGURES

FIGURE 2.1: Oyster Collection Locations in North Carolina and South Carolina 43

FIGURE 2.2: Mitochondrial Respiration - Federal Point, Harker's Island, Baruch Research Station 44

FIGURE 2.3: Mitochondrial Damage - Federal Point, Harker's Island, Baruch Research Station 45

FIGURE 2.4: Energy Storage Components - Federal Point, Harker's Island, Baruch Research Station 46

FIGURE 2.5: Sum of Energy - Federal Point, Harker's Island, Baruch Research Station 47

FIGURE 2.6: Percentage of Total Energy Storage - Federal Point, Harker's Island, Baruch Research Station 48

FIGURE 2.7: Cellular Oxidation Damage - Federal Point, Harker's Island, Baruch Research Station 49

FIGURE 3.1: Harker's Island Oyster Collection Site 66

FIGURE 3.2: Mitochondrial Respiration – Harker's Island Pre- and Post- hurricane 67

FIGURE 3.3: Mitochondrial Damage - Harker's Island Pre- and Post- hurricane 68

FIGURE 3.4: Energy Storage Components – Harker's Island Pre- and Post-hurricane 69

FIGURE 3.5: Sum of Energy Components – Harker's Island Pre- and Post- hurricane 70

FIGURE 3.6: Cellular Oxidation Damage - Harker's Island Pre- and Post-hurricane 71

FIGURE 4.1: Immunity Gene Expression - Part 1 91

FIGURE 4.2: Immunity Gene Expression - Part 2 92

FIGURE 4.3: COI Phylogeny with Bootstrap Values 93

FIGURE 4.4: *Crassostrea virginica* COI Mismatch Distributions by Location 94

FIGURE 4.5: *Crassostrea virginica* COI Mismatch Distributions by Location and Tidal Zone 95

FIGURE 4.6: *Crassostrea virginica* COI Mismatch Distributions by Tidal Zone 96

FIGURE 4.7: DNA Analysis of 16S Gene with Bootstrap Values..... 4.7

FIGURE 5.1: Collection Locations of *Crassostrea virginica* and Haplotype Network..... 119

FIGURE 5.2: Stress-sensing Molecules under Hypoxia Stress..... 120

FIGURE 5.3: Expression of Stress-response under Hypoxia Stress 121

FIGURE 5.4: *Vibrio vulnificus* Loads in Oyster Tissue under Normoxic Conditions 122

FIGURE 5.5: Expression of Stress-sensing Molecules under Bacterial Stress 123

FIGURE 5.6: Expression of Stress-Response Molecules under Bacterial Stress..... 124

FIGURE 6.1: *Triodopsis* Shell Morphology..... 173

FIGURE 6.2: *Triodopsis* Morphology Two-Variable Measurement Graphs - Part 1 174

FIGURE 6.3: *Triodopsis* Morphology Two-Variable Measurement Graphs - Part 2 175

FIGURE 6.4: Morphological measurements of *Triodopsis fallax* Group Clades - Part 1..... 176

FIGURE 6.5: Morphological measurements of *Triodopsis fallax* Group Clades - Part 2..... 177

FIGURE 6.6: 16S Phylogeny of All *Triodopsis* and other Polygyridae 178

FIGURE 6.7: 16S Phylogeny of *Triodopsis fallax* group only 179

FIGURE 6.8: 16S Phylogeny of *Triodopsis fraudulenta* and *tridentata* groups only..... 180

FIGURE 6.9: ITS2 Phylogeny of *Triodopsis,* Others in Triodopsini and Mesodontini..... 181

FIGURE 6.10: Concatenation of *Triodopsis* 16S and ITS2 Genes 182

FIGURE 6.11: H3 Phylogeny for *Triodopsis* and Stylommatophora 183

FIGURE 6.12: H3 *Triodopsis* Molecular Clock Tree..... 184

FIGURE 6.13 Population Stability in *Triodopsis* Clades..... 185

FIGURE 6.14: Expected 16S Genetic Differentiation Estimates - Population Size vs. Observed in *Triodopsis* Genus..... 186

FIGURE 6.15 Statistical Parsimony Haplotype Network with *Triodopsis* 16S and ITS2 ... 187

FIGURE 6.16: Expected 16/ITS2 Genetic Differentiation Estimates - Population Size vs. Observed in *Triodopsis* Genus 188

FIGURE 6.17: *Triodopsis fallax* Group Distributions 189

FIGURE 6.18: *Triodopsis fraudulenta* Group Distributions 190

FIGURE 6.19: *Triodopsis tridentata* Group Distributions 191

FIGURE 6.20: Reciprocal Fertilization Creates Mitochondrial Haplotype Diversity 192

LIST OF ABBREVIATIONS

16S, 5.8S, 28S	Subunits of ribosomes
A, T, G, C	Nucleotides Adenine, Thymine, Guanine, Cytosine
ADP	Adenosine diphosphate
ANOVA	Analysis of variance
ASV	Amy Van Devender Personal Collection
ASW	Artificial seawater
ATP	Adenosine triphosphate
ATP/G6P-DH	ATP per glucose-6-phosphate dehydrogenase
Bacto HI	Bacto Heart Infusion agar
bacto LB	Bacto Luria-Berani broth
bp	Base pairs
BR	Baruch Research Station
BSA	Bovine serum albumin
C1q	Complement proteins
C3, D2, E9	Seafood zones on NC coast
cDNA	Complementary DNA
CFUs	Colony Forming Unit – concentration of bacteria
Cg	Crassostrea gigas
CO	Carbon monoxide
CO^2	Carbon dioxide
COI	Cytochrome oxidase I
Conc	Concentration
C3q	Complement compound 3q
C-type	Cysteine - like
CU	Clemson University
Cv	Crassostrea virginia
DAMPs	Damage-associated molecular patterns on pathogens
df	Degrees of Freedom
DNA	Deoxyribonucleic Acid
DNP/HCL	2,4-Dinitrophenylhydrazine in HCl
DS breaks	Double strand DNA breaks
ELISA	Enzyme linked immunoassay
ETS	Electron transport chain
F Statistic	Ratio of two variances
F_1	First generation offspring
F_1F_0-ATPase	Adenosine tri-phosphate synthase
FAA	Free amino acids
FP	Federal Point
F_{ST}	Fixation index - measure of heterozygosity
g ml^{-1}	Grams per milliliter
gRT -PCR	Quantitative Realtime Polymerase Chain Reaction
h	Number of haplotypes in a population
H_2O_2	Hydrogen peroxide

H3	Histone 3 nuclear gene
HC	Hematocytes
Hd or Hs	Haplotype diversity
HI	Harker's Island
HNE (or 4-HNE)	4- Hydroxynonenal
HSP	Heat Shock Proteins
IFNLP	Interferon-like proteins
ITS2	Internal transcribed spacer 2
JMP Pro 16 (SAS Institute, Cary, NC 2021)	Statistics software
JSO-2	A *Vibrio vulnificus* strain
kJ	KiloJoules
kJ mol^{-1} O^2	KiloJoules per mole of oxygen
Ks	Number of nucleotide differences in a sequence
K-T	Cretaceous / Triassic boundary
LSD	Fisher's Least Significant Differences test
Meso	Mesodontini tribe
ml	Milliliter
mmol l^{-1}	Millimoles per liter
MO_2	Metabolic rate based on oxygen consumption
MR2	Mannose Receptor 2
mRNA	Messenger ribonucleic acid
MT	Mitochondrial
mtDNA	Mitochondrial DNA
natom O min^{-1} mg^{-1}	Respiration rate of mitochondria
NC	North Carolina
NCSM	North Carolina State Museum
nmol CO/mg	nanomoles of CO per milligram
NOAA	National Oceanic and Atmospheric Association
NSF	National Science Foundation
O2	Oxygen molecule
^oC	Degrees Celsius
ol	With addition of oligomycin
$OsHV^{-1}$	Ostreid herpesvirus
p	Statistical significance factor
PAMPs	Pathogen-associated molecular patterns
PCA	Perchloric Acid
PCR	Polymerase Chain Reaction
pH	Acidity/alkalinity based on hydrogen concentration
Pi (π)	Nucleotide diversity
PMSF	Proteinase inhibitor
ppt	Parts per thousand
PUFA	Polyunsaturated fatty acids
RCR	Respiratory Control Ratio
RCR+	Respiratory Control Ratio with addition of oligomycin

Rec2	Receiver 2 (as in Mannose Rec2)
ROS	Reactive Oxygen Species - oxidants
s	Number of segregated sites in sequences
SC	South Carolina
SDS	Sodium dodecyl sulfate (sodium lauryl sulfate)
SEAP	NC Fisheries Permit and Grant
SEM	Standard Error of the Mean
SMNC	Schiele Museum of Natural History
SNPs	Synonymous nucleotide polymorphisms
SOD	Antioxidant superoxide dismutase
SRCR	Scavenger receptor cysteine-rich
SS breaks	Single strand DNA breaks
Taq	Thermal tolerant polymerase
TLR	Toll-like Receptors
TNF	Tumor necrosis factor
Trio	Triodopsini tribe
UF	University of Florida Museum
ug/ml	Micrograms per milliliter
$\mu mol\ l^{-1}$	Micromoles per liter
umb	Width of umbilicus
UT or UTRGV	University of Texas Rio Grande Valley
VA	Virginia
wdht	Width / height ratio
wdsp	Width / spire height ratio
wdum	Width / umbilicus width ratio

CHAPTER ONE

INTRODUCTION

Plasticity and adaptation

Response to the environment differs greatly from species to species based on ability to conform to changes in abiotic parameters such as temperature, salinity, etc. Many animals are mobile and can escape to more suitable environments when conditions change. Mollusks vary tremendously in their ability to move depending on phylogeny and stage in the life cycle. For example, cephalopods are highly mobile, but terrestrial snails move very little. Species with biphasic life cycles, like oysters, are sessile as adults, but larvae can be dispersed widely, although maybe not as homogeneously as once thought (Eierman and Hare 2016; Hellberg et al. 2002). Terrestrial snails have a very limited range of movement over a lifetime unless passively transported by other means, such as floods or other animals (Aubry et al. 2006). The mismatch between the scale of environmental variation and the ability of species to move or disperse is likely to promote phenotypic plasticity and/or local adaptation.

A species is classified as a generalist or specialist based on its range of tolerance and optimal fitness (Gilchrist 1995). In an ideal constant environment, optimal fitness could occur within a narrow band with a restricted tolerance for deviations from that ideal. In contrast, in a broad range of environmental conditions within one generation, organisms must be able to tolerate those varying conditions even though optimal fitness may occur at shortened time periods (Gilchrist 1995). Generalists with plasticity have broad physiological tolerance, whereas the specialists have a narrow optimal fitness range for environmental conditions and generally occupy more restricted niches. Generalists generally have larger ranges, while specialists usually have

limited or sporadic distributions and therefore, are at higher risk of extinction from environmental change (Saupe et al. 2015).

There is no dispute that *Crassostrea virginica*, the Eastern Oyster, is a generalist. They range from Canada to Brazil through many climates, exist in coastal waters that range in salinity from 5 ppt to 35 ppt, and occupy some of the harshest niches in the marine environment. The presumed phenotypic plasticity of oysters is physiological rather than morphological. Terrestrial snails, on the other hand, although in the seemingly broad environment of woodland leaf litter, are usually limited in distribution due to temperature as well as other factors like plant community. They have characteristics of specialists. The numbers of closely related land snail species living in sympatry such as in the *Triodopsis* genus suggests they underwent a change in morphology in response to environmental change. Evidence and potential mechanisms for phenotypic plasticity and adaptation of the two groups of mollusks are investigated in this research.

Mollusks as a large, diverse phylum

Phylum Mollusca, as the second largest phylum of metazoans (Sun et al. 2017), has radiated into highly adaptable clades with varying abilities to survive in highly diverse aquatic and terrestrial environments. In my thesis, I examined species from two diverse groups of mollusks and their adaptation to the environment. My research will address questions primarily at two levels: physiological and phylogenetic. A comparison of the genetic variability of the two groups will provide information about molluscan plasticity and speciation, which will be useful in accessing the future of molluscan groups in a changing climate. As climate change is ongoing and will continue well into the future, organisms will be challenged to survive in fluctuating or abrupt changes to temperature, CO_2 concentrations, and water availability (Malhi et al. 2020).

Having originated early in the Cambrian or possibly pre-Cambrian, mollusks radiated throughout the world in marine habitats, eventually diverging into dissimilar forms with different life histories (Fig. 1). Bivalves diverged in a deep node in the animal tree over 500 million years ago (Wanninger and Wollesen). Many families of marine bivalves have a world-wide distribution where they occupy diverse habitats, depths, temperatures, etc. True oysters (Ostreidae) are one of the oldest families of extant bivalves. They have continuously adapted as the world's climate changed in a continuous marine environment (Bayne 2017). For example, the plasticity of bivalve species that reside in intertidal and subtidal environments indicates a wide range of environmental tolerance without diversifying into separate morphological or phylogenetic species (as defined as groups with very little or no gene flow) (Wanninger and Wollesen 2018).

Gastropods originated in the marine environment around the same time as bivalves but some groups only invaded land about 150 mya, having undergone numerous adaptations to air-breathing, terrestrial life (Liu et al. 2021). Although land snails are a recent divergence, they have radiated quickly into many morphologically similar species. Most speciation in Polygyrid land snails occurred during the last 20 million years, during a time of repeated climate fluctuations in North America (Emberton 1995a; Liu et al. 2021). Most terrestrial snails are hermaphroditic, possibly allowing opportunities to produce offspring for an animal with limited mobility. They lay egg clutches, and the young have limited dispersal. Land snails have limited options in a changing environment and could be some of the most imperiled species due to ongoing climate change (Nicolai and Ansart 2017).

How each of these molluscan life history strategies have contributed to the success of these groups has been understudied. Both molluscan lifestyles will be investigated to better understand the molluscan response to environment and how their evolved strategy may relate to survival in

the future. Some mollusks show great tolerance to environmental challenges with phenotypic plasticity that can mask population and species divergence.

Genetic markers and barcoding

Barcoding became a common approach for species identification about 15 years ago and has been used extensively in species determination (DeSalle and Goldstein 2019; Sauer and Hausdorf 2012). The idea of a single gene, usually cytochrome c oxidase subunit 1 (COI or cox1), identifying unique species was appealing in theory but was found to be unsuccessful in some groups of organisms. For example, standard primers failed to amplify the gene (Geller et al. 2013). For others, the genetic resolution was not high enough at the species level due to lack of variability in the COI gene (Madeira et al. 2017; Thomaz et al. 1996). Still, it is useful for museum specimens that have been alcohol preserved for years since high throughput sequencing may not be possible due to DNA degradation. The use of additional genetic loci beyond COI may increase the probability of successful species differentiation.

The attempts to use COI barcoding on some mollusk groups have been largely uninformative due to high intraspecies variability (Madeira et al. 2017; Thomaz et al. 1996). Barcoding with COI was used because of the large number of reference sequences through the Barcode of Life and related biodiversity initiatives. However, other loci with different phylogenetic resolution have also been used for questions at higher taxonomic levels. These targeted regions have been largely nuclear genes to compare and potentially refine results at multiple taxonomic scales. Single genetic markers must be dependable and efficient in determining species or population differentiation in phylogeny tips that are a) highly variable physiologically

but morphologically indistinguishable single species, or b) morphologically distinguishable, and possibly reproductively compatible, sister species in sympatry.

Rapid radiations of species are particularly challenging for barcoding, as incomplete lineage sorting and introgression may prevent species separation (Sauer and Hausdorf 2012). Stylommatophoran terrestrial snails have been found to have a high rate of sequence divergence (Sauer and Hausdorf 2012) and high intraspecies variability in mitochondrial DNA (Madeira et al. 2017; Thomaz et al. 1996), but sequencing of multiple loci may afford species resolution. Genetic variation in COI should relate to oyster physiology differences between populations and microhabitat.

Aims

The specific Aims and Hypotheses of this research are listed below. My purpose is to investigate the relationship between phenotypic and genetic variation in the two mollusk groups that diverged in ancient times and have extremely different life histories and habitats. Marine bivalves and terrestrial gastropods are both mollusks, but very different in genetic, morphometric, and physiological attributes. The different life histories are compared in this research to reveal divergent examples of phenotypic plasticity and adaptative strategies.

Aim 1 – Determine physiological differences between locations /salinities and microhabitats of a stress tolerant mollusk species.

The eastern oyster provides an excellent model organism to study environmental impacts on physiology. Chapter 2 will examine the three hypotheses below to determine differences in locations (which also correspond to different salinities) and habitats in the tidal zone. These

physiological responses will be tested again in Chapter 3, where I investigate the effects of a hurricane on an oyster population over a period of two years on the same physiological processes.

Hypothesis 1.1

Mitochondrial stress as measured by respiration and carbonyls will be higher in intertidal oysters than subtidal oysters due to the hypoxia experienced by emersion during heat and cold .

Hypothesis 1.2

Energy storage capacity of intertidal oysters will be less than that of subtidal oysters due to stress because of the shorter feeding period intertidal oysters experience.

Hypothesis 1.3

Cellular components will experience more damage due to stress in intertidal oysters than in subtidal oysters due to the oxidative stress of hypoxia and extreme temperatures during emersion.

Aim 2 – Determine if a genetic component is correlated with differences in oysters from different microhabitats.

Adaptation to the environment will be investigated by examining immunity gene expression with and without a pathogen challenge and hypoxia in Chapter 4 and 5. In Chapter 4, I will compare differences in gene expression of intertidal and subtidal oysters using. Variation in gene expression is then compared with genetic diversity of oyster individuals determined with two mitochondrial loci, COI and 16S. In Chapter 5, I will explore the synergistic effects of a bacterial pathogen plus hypoxia on gene expression, and the genetic structure of cultured oysters.

Hypothesis 2.1

Subtidal oysters will have higher expression of immune genes due to their higher exposure

to pathogens in the water than intertidal oysters.

Hypothesis 2.2

Subtidal oysters will show a higher expression of related gene. Gene expression will be dependent on pathogen susceptibility and tidal elevation.

Hypothesis 2.3

Intertidal oysters will have a higher expression of stress related genes in the transcriptome due to emersion and extreme temperatures.

Hypothesis 2.4

Native wild oysters will show little genetic variation between locations, but more variation between microhabitats in the same location. These locations are biogeographically close; therefore, no population variation is expected. There may be genetic differences in oysters at each tidal habitat due to local selection.

Aim 3 – Determine relationship of "species" with morphological similarity within a sympatric genus of land snails.

Hypothesis 3

Recognized species of land snails that are similar morphologically and that are overlapping in distribution will be similar genetically. Living in sympatry with similar morphology may indicate gene flow and incomplete speciation, limiting genetic differentiation.

In Chapter 6, I will analyze the mitochondrial and nuclear DNA of the *Triodopsis* genus of land snails. This study was designed to determine the relationship between morphological and genetic variation in a recently diverged genus of Polygyrid land snails. Morphological characters will be compared to cladistic grouping to determine the species status of very taxonomically difficult groups.

Relevance to Malacological Research

The research reported in this dissertation should provide insight into the relationship between phenotypic plasticity and genetic variation in two different groups of mollusks – one very ancient and stable species, and one group of species that may have radiated quickly in a relatively small geographic area.

The oysters have been used extensively as models of hypoxic research, but never on a scale of microhabitat. This study will provide evidence to show the acclimation or genetic adaptation of a highly plastic oyster to specific lifestyles.

Conversely, the non-vagile lifestyle of the terrestrial snail may lead to rapid speciation in a very static habitat. Land snails are facing possible extinction of numerous species as the climate changes faster than this non-mobile species can adapt. The genetics and mechanisms of speciation of this group are very understudied, so the number of species is only reported from morphological data. This research will hopefully add to our bank of knowledge in this area to better understand the relationship of morphology to genetic diversity, as well as the consequences of climate change and the effect it will have on smaller, less obvious, but no less important organisms in the ecosystem. It will also provide insight into the adaptive strategies of understudied species during a period of rapid climate change.

The results of this research may help to determine the future of these groups in the prospect of a rapidly changing environment. Both groups of mollusks may experience difficulty during times of rapid climate change.

A final, but also important objective of this research is to develop techniques for DNA analysis that can be used safely in small institutions in the field of systematics without a full

biotechnology lab and with a limited budget. This study will give direction and guidance to the malacologists working in small institutions on best practices for using genetic tools to assist morphological systematics. As genetic research becomes more automated and technology is simplified, larger sequences may become available with less need of costly equipment and expertise for individuals and smaller institutions.

CHAPTER TWO

PHYSIOLOGICAL VARIATION OF *CRASSOSTREA VIRGINICA* BETWEEN LOCATIONS/SALINITIES AND MICROHABITATS

(Furr, Denise; Reitzel, Adam; Ivanina, Anna)

ABSTRACT

Environmental variability in tidal zones and in different geographic locations requires that estuarine species like the eastern oyster *(Crassostrea virginica)* must maintain homeostasis to specialize in such highly variable abiotic conditions, effecting mitochondrial function and the ability to store energy compounds as well as the ability to repair cell damage. As a result, these oysters exhibit highly plastic physiological responses dependent on the local environment. Sessile adult oysters, with no ability to migrate to more suitable conditions, must modify a suite of physiological and cellular processes, including mitochondrial bioenergetics, energy storage capacity and cellular damage control from conditions where they settle. I examined intertidal and subtidal oysters at the multiple locations to compare the effects of tidal and geographic location (Federal Point, Harker's Island, Baruch Research Station) in the southeastern United States. There was little difference in each of the parameters (mitochondrial function, energy storage capacity and cellular damage control) regardless of tidal location; however, physiological differences were recorded between geographic location. Site salinity appeared to have a strong effect on oyster physiology. Mitochondrial damage potential was greater at the extremes of salinity. Energy storage reserves also differed between the sites, with higher protein but lower glycogen stores at the intermediate salinity site, Baruch Research Station, with no significant difference between tidal locations. Oysters can acclimate to a wide range of oxygen availability, stress, and conditions that effect the ability to store energy compounds and repair cell damage, but salinity appears to be a

major factor in modulating adult physiology in the field. This study underscores the extensive phenotypic plasticity and potential weaknesses of eastern oyster physiology and how salinity may result in significant physiological variation in native oyster populations.

INTRODUCTION

Crassostrea virginica, the eastern oyster, is a reef-building bivalve that once created huge beds along shores of estuaries on the East Coast until overharvesting and pollution reduced populations to isolated and smaller beds (Kirby 2004). The eastern oyster inhabits the shore high above the water in the intertidal zone to submerged below in the subtidal zone in these congregate beds. Oysters can live diurnally exposed to air in the intertidal zone, where they can only gill-breathe and feed when covered with water, and they can also live submerged constantly, more exposed to fouling organisms and aquatic predators. They are usually found in estuaries, where the salinity changes with the tidal surge, but may occur in open sounds in ocean level salinity.

We will investigate native oysters from beds from geographic locations with different salinities and habitats. The Federal Point location is an oyster bed in a river estuary with low salinity, Harker's Island location is in the sound on a small island, and the Baruch Research Station location is a large open marsh in a protected sound, exposed to the sun. The ambient temperature difference in all three locations is considered negligible since the locations are within 200 miles of each other.

Other authors have studied environmental effects on oyster larval development, dispersal, and survival (Burford et al. 2014), but all have considered a single oyster bed location to be homogenous in respect to habitat. Water and air temperature, and salinity have been studied as if all oysters at a specific location experience the same conditions (Bartol et al. 1999; Casas et al.

2018; Ivanina et al. 2012). Few studies have considered the intertidal oysters exposed to air and daily heat may have different adaptive strategies than the subtidal oysters that remain submerged, and that juveniles may be selected differentially for survival of specific stresses in these microhabitats during a high mortality stage. Larvae are also found to have lower physiological tolerances than those of adults, so larval planktonic connectivity is not as homogenous as predicted (Eierman and Hare 2016; Puckett and Eggleston 2012).

While intertidal oysters must deal with exposure, subtidal oysters must contend with epibiont coverage, which also causes physical stress and competition for suspended food, exposure to aquatic predators and suspended sediments in the water from wave action (Boyd and Burnett 1999). Subtidal oysters have 97% coverage of fouling organisms as opposed to 21 – 38% in intertidal oysters in the spring, contributing to reduced feeding and interference with shell growth (Bishop and Peterson 2006; Boyd and Burnett 1999). Even so, shell growth in terms of height and dry tissue weight revealed no significant difference in intertidal and subtidal oysters at the same age (Boyd and Burnett 1999), showing that the oysters from the two zones were morphologically the same despite enduring two different environmental conditions during growth. Subtidal oysters grew faster in the winter and early spring, with intertidal oysters catching up quickly in the warmer air exposure in the spring as fouling organisms grew even faster on subtidal oysters (Bayne 2017; Bishop and Peterson 2006). Even though there are advantages and disadvantages to both lifestyles, the ability to live in such diverse habitats is an amazing feat for a single species.

The relationship of adaptive physiological phenotype to intertidal and subtidal habitats has been little studied in oysters (Meng et al. 2018). In one of the very few studies including these habitats as a parameter, Meng et al. (2018) found F_1 intertidal oysters reached metabolic depression and displayed anaerobic responses sooner under hypoxia than F_1 subtidal oysters. The difference

in survival mechanisms could be a trait that is adaptive in the settling stage because of environmental conditions. If so, intertidal oysters may have undergone selectivity in the settling phase, genetically differentiating intertidal from subtidal oysters. Meng et al. (2018) has shown that F_1 oysters from intertidal and subtidal stock performed differently to hypoxia in a common garden design and may have a genetic basis to their differences. Parker et al. (2021) however, suggests that a type of "transgenerational plasticity" is exhibited by offspring of parents that have been subjected to environmental challenges. Meng et al (2018) also determined that there is a difference in ATP production and gene expression of metabolism-related genes in intertidal and subtidal oysters of *Crassostrea gigas*.

Another mollusk, the Antarctic limpet *Nacella concinna,* (Strebel, 1908) has shown distinct physical and physiological differences in intertidal vs. subtidal morphs with the intertidal limpet able to function emersed without anaerobiosis and breathe air; whereas, the subtidal morph switches to anaerobic respiration quicker upon exposure to air (Weihe and Abele 2008). In most soft-bodied aquatic animals, however, a hyperoxic environment, i.e., exposure to air, is associated with even higher levels of oxidative stress due to excess O_2 infusion (Abele et al. 2007). Even though intraspecific differences in invertebrate physiology due to environmental conditions are not unusual, the comparison of mitochondrial function in intertidal and subtidal habitats has not been well investigated in oysters.

In estuaries, it has been found that reduced salinity and higher temperatures can cause metabolic and physiological stresses that affect respiration, heart rate, energy metabolism and rate of growth of oysters (Heilmayer et al. 2008). Oysters have adapted to everchanging conditions in estuaries, where salinity may fluctuate greatly with tidal surges and rainfall and may become low with freshwater outflow. *Crassostrea virginica* can survive a broad range of salinities, 5 – 40 ppt

according to La Peyre et al. (2013), with salinity influencing stages such as recruitment and scope of growth, with no recruitment at a salinity of 10 ppt or less (La Peyre et al. 2013). Salinity has the most influence on bioenergetics, although the effects are synergistic with other environmental conditions (Heilmayer et al. 2008). Low salinity causes osmoregulation imbalances which affect metabolic requirements (Heilmayer et al. 2008). The high mortality at the combination high temperatures and low salinity occurs from a failure to control cellular osmolarity (La Peyre et al. 2013). Acidification and pH fluctuations in low salinity estuaries are also more of a problem than in higher ocean level salinities because of a lower buffering effect (Dickinson et al. 2012). High variability in environmental conditions make a low salinity site unpredictable for long term survival (Miller et al. 2017). The oysters used in this study were living in established beds in these areas, but the bioenergetic cost of survival in these extreme salinities is not known.

Biotic challenges are affected by salinity levels as well. It was found that although growth was greater in higher salinities, the incidence of disease such as *Perkinsus marinus* and predators was higher, with up to 100% mortality in studies (Miller et al. 2017). Oyster drills, mud crabs and other predators of new recruits are present in high numbers in high salinity sites along with more fouling of subtidal oysters (personal observation). Subtidal oysters are particularly susceptible to the biotic hazards of high salinity (Miller et al. 2017).

The goal of this research is to determine the differences in oyster phenotype in these different habitats and the physiological consequences of living in the extremes. Phenotypic information in *Crassostrea virginica* is best collected as physiological differences since the morphology of oysters is highly unpredictable and depends on spatial structure of the individual oyster's immediate surroundings. In my research, the physiological plasticity of the eastern oyster,

Crassostrea virginica, is investigated to determine evidence of population and habitat differences in mitochondrial function, energy storage and cell damage repair.

Mitochondrial stress and damage

Oysters of the species *Crassostrea virginica* can live in the intertidal or subtidal zones of the ocean shore. Since oysters are gill-breathing aquatic animals, an oyster does not respire during shell closure, which occurs nearly immediately upon being exposed to air (in addition to other rapid or desirable events) to avoid desiccation. Subtidal oysters are constantly submerged and rarely experience this diurnal stressor. Subtidal oysters must contend with competition and predation, but rarely physical abiotic stressors, except by localized heavy silting or organic decomposition. High fluctuations in temperature, such as experienced by intertidal oysters exposed in the sun, can also cause oxidative stress when rapid cooling occurs during tidal immersion.

Abele (2007) found elevated oxygen species, hydrogen peroxide (H_2O_2), in mitochondria from marine mollusks subjected to elevated temperature. Above certain temperatures, antioxidants and other critical proteins for heat stress are no longer synthesized, exacerbating oxidative stress (Abele et al. 2007). When oxygen consumption is interrupted as in intermittent hypoxia then suddenly resumed, the reoxygenation of tissues can create reactive oxygen species (ROS) due to excess O_2. The ROS generated by the mitochondria in aquatic ectotherms such as bivalves have been shown to correlate in part to proton leak in State 4 (Abele et al. 2007). The resulting oxidative stress causes reactive oxygen species (ROS) such as H_20_2 to increase, which can damage proteins, resulting in carbonyls.

Carbonyls include ketones and aldehydes, products of protein degradation as free radicals that cause irreversible modifications to protein structures. This protein carbonylation converts side

chains into ketones and aldehydes and is highly destructive to cells and tissues (Letendre et al. 2012). HNE causes cross-linking and clumping of the fatty acids, especially linoleic and arachidonic acid, and is particularly destructive to mitochondrial and cell membranes (Zhong and Yin 2015). Mollusks in general, particularly intertidal bivalves, have a robust antioxidant production during hypoxia in anticipation of reoxygenation, but in times of high stress these defenses can be overwhelmed. Measurements of carbonyl and lipid peroxidation levels can still be informative of oxidative protein and lipid modification in mitochondria (Levine et al. 2000). Carbonyls and 4- hydroxynonenal (4-HNE or HNE) concentration will be measured in the mitochondria as indicators of oxidative stress in this study.

Many other studies have used them as model organisms for hypoxia/anoxia research (Furr et al. 2021; Ivanina et al. 2010; Ivanina et al. 2011b; Ivanina et al. 2016b). Besides being able to withstand intermittent anoxia during regular diurnal tide cycles, oysters have shown incredible tolerance to long term anoxia over periods of day or weeks due to dead zones or pollutants (Kurochkin et al. 2009). Anoxia/hypoxia tolerance in oysters is credited to physiological adaptations that include metabolic depression, alternative glycolytic cycles, and production of antioxidants and non-toxic waste products (Sokolova et al. 2012). Oyster anaerobic metabolic pathways have been studied extensively (Letendre et al. 2012), showing that alternate glycolysis pathways allow more energy per glycogen molecule (Hochachka and Somero 2002; Müller et al. 2012). This alternate, branched pathway for the electron transport system in the mitochondrial membrane in *Crassostrea* oysters bypasses complexes III and IV of the electron transport system and also reduces excess O_2 to water, reducing the creation of ROS (Liu and Guo 2017). The oyster's ability to switch to sustainable anaerobiosis allows long-term survival without oxygen. An intertidal oyster can not only survive the tidal period of 6-12 hours exposed in the sun on the

shore, but metabolic depression and glycolytic fuel can sustain the bivalve in an anaerobic state for weeks (Bayne 2017).

Long term hypoxia and shell closure can also cause the build-up of metabolic waste products (Ivanina and Sokolova 2013); however, buffering systems in oysters prevent toxicity by storing waste as non-toxic end products (Hochachka and Somero 2002). Boyd and Burnett (1999) found that decreased pH due to hypoxia influenced reactive intermediates that serve a role in disease fighting mechanisms but admittedly did not test extremes of hypoxia and stress in intertidal oysters. However, they predicted the results to be more significant in intertidal oysters than in the subtidal oysters they tested. Ivanina et al. (2016b) determined that mitochondrial proteases are found to have a protective role in hypoxia-induced toxicity in oysters and clams, unlike other organisms including other mollusks not adapted to these extremes.

These physiological adaptations and antioxidants plus metabolic depression allow oysters to survive days or even weeks of limited oxygen without suffering extensive damage from toxic end-products from anaerobic respiration and waste removal (Letendre et al. 2012). Even juvenile oysters can conserve their ATP reserves for prolonged periods of anoxia (Dickinson et al. 2012). Together, these novelties can make intermittent hypoxia in the tidal zone not only possible but possibly a preferred niche for the eastern oyster. Mitochondrial respiration rate will be measured *in situ* in oyster mitochondria to determine effects of intermittent hypoxia stress by exposure to air during diurnal tidal cycles.

Energy storage capacity

Oysters rely on carbohydrates, lipids and proteins as energy reserves, just as most other eukaryotes do. Marine bivalves use carbohydrates (glycogen and glucose) first as quick energy

compounds, then resort to lipids and even proteins as carbohydrates are depleted. In *Crassostrea gigas*, sister species to *C. virginica*, adults have a high protein component at 60-80% dry weight with an increase of about 20% in the spring; lipids are generally 10 - 20% and glycogen about 6% (Berthelin et al. 2000). The stores of lipids and proteins help sustain the oyster through the hot summer until fall, when algal blooms allow the oyster to restore the glycogen, lipid, and protein stores for the winter. Protein and lipid levels rise again in spring associated with gonadal development (Berthelin et al. 2000). Lipid content generally reaches its maximum in September, along with a second peak for glycogen, and these serve as winter reserves (Berthelin et al. 2000).

Energy storage is closely associated with stages in reproduction and gametogenesis. Most of the glycogen is stored during the sexual resting phase from October to February in specialized vesicular cells around the gonads and labial palps as the adult oyster prepares for spawning (Berthelin et al. 2000). The stored glycogen is regulated by two enzymes, glycogen phosphorylase and glycogen synthase, transcribed at different rates depending on tissues and season correlated with the reproductive cycle (Bacca et al. 2005). Gametogenesis and spawning use nearly all the stored glycogen in June, the typical time for oyster spawning in North and South Carolina when water temperature is between 18 – 20^{o}C (Gao et al. 2021). Glycogen drops to a minimum and remains there through the summer (Li et al. 2007). Cotter et al. (2010) found this to be true especially of males in oyster beds in Wales.

Lipids are precursors to many enzymes and hormones and can be converted to glycerol and fatty acids for energy. Lipid reserves are established in oysters in early winter along with protein, and reach a peak in the September in the digestive gland, as well as in gonads and mantle (Berthelin et al. 2000). Polyunsaturated fatty acids (PUFA) are an important component of gametes and are a major source of energy (Gao et al. 2021). In a study of oyster nutrition primarily for the food

market, Gao (2021) found that lipids vary in composition by season with correlation to the sexual resting period November to April, gamete maturation and spawning from May to July, and summer post-spawn period from August to October with the highest unsaturated glycerides in August and the highest unsaturated phospholipids in April.

Proteins, being a structural component as well as energy source, are a major component of oyster dry weight (Berthelin et al. 2000). In the cell, proteins are constantly being synthesized and broken down, so free amino acids are always available for use in energy production or other processes, such as osmoregulation (Bayne 2017). Proteins are generally not used for reproductive energy expenses, so are therefore available to sustain the animal in the summer after spawning (Berthelin et al. 2000). Mollusks are more likely to use protein as an energy source than mammals that would only use protein if in starvation. Bivalves, on the other hand, can use free amino acids from proteins to fuel glycolysis and actually lose body mass in the process (Hochachka and Somero 2002). Proteins are also utilized for osmoregulation; free amino acids (FAA) act to stabilize cellular concentration in a world of constantly changing external salinity (Bayne 2017). FAA change in composition with the phytoplankton available at different seasons and environmental conditions, which according to Gao (2021), produce different tastes and nutritional value for oyster consumers.

For osmoconformers like oysters at lower salinity, more water enters the cell to adjust osmotic pressure. The concentration of the cell is never completely isosmotic to that of the surrounding water at low salinity; therefore, energy is required to actively maintain the osmotic balance slightly hyperosmotic (Bayne 2017; Fuhrmann et al. 2018). While glycogen and lipids are not used in osmolarity, they provide energy necessary during osmotic stress (Fuhrmann et al. 2018). Since protein concentration increased when salinity was temporarily lowered, Fuhrman

(2013) concluded that protein synthesis was a means of reducing the amount of FAA in the cell, which also requires energy. Carbohydrate levels were higher in lower salinity, likely due to decreased activity of hexokinase, as were lipids; however, as oysters acclimated to the lowered salinity after 11 weeks, the lipid content dropped substantially (Fuhrmann et al. 2018). This shows the oyster's ability to meet osmoregulation demands for short periods of time during temporary fluctuations of salinity. These higher levels of energy reserves also seem to help protect against certain pathogens, such as the Ostreid herpesvirus, OsHV-1 (Fuhrmann et al. 2018). Oysters in lower salinity have a lower incidence of pathogens overall (Miller et al. 2017).

In this study, I will use the energy component content as a comparison between sites with different salinities and the habitats, intertidal and subtidal. All oysters in this study were collected in the spring just before spawning. Some were full of gametes when dissected, showing that spawning was eminent. I hypothesize that the energy demands of intertidal oysters will interfere with the energy storage capability, and the intertidal oysters will show lower storage of these energy compounds. Hepatopancreas tissue was used for determination of energy stores, which is not a primary glycogen storage site, but should be independent of the spawning process.

Cellular component damage due to oxidative stress

Reactive oxidative species (ROS), especially H_2O_2, can disrupt normal cell processes by degrading and destroying critical cell components. Lipid peroxides are particularly destructive compounds that can result in carbonylation of proteins and DNA damage. By measuring the amount of lipid peroxides, or the resulting carbonyls and DNA damage, the amount of oxidative stress in the cell can be quantified. Identification of total carbonyls and 4-HNE are useful

biomarkers for high oxidative stress in tissues that experience oxygen deficiency (Levine et al. 2000). Gill tissue was used for carbonyl and lipid peroxidation determination in this study.

Carbonyls include ketones and aldehydes, products of protein degradation, which as free radicals, cause irreversible modifications to protein structures. This protein carbonylation converts amino acid side chains into ketones and aldehydes and is highly destructive to cells and tissues (Letendre et al. 2012). Carbonyls may be produced from lipid peroxides or from any number of oxidation reactions, through direct oxidation from free radicals or from secondary reactions with other compounds oxidized by free radicals (Levine 2002). These carbonyl residues accumulate over a lifetime, becoming more prevalent in the proteins in the aging organism even though antioxidant mechanisms exist to repair them, likely causing detrimental effects on bodily functions and organs (Levine 2002).

Lipid peroxidation of polyunsaturated fatty acids (PUFA) results in a highly reactive product called 4-hydroxynonenal (Csala et al. 2015). Lipids are attacked by free oxygen radicals to form lipid peroxyl and hydroperoxide radicals, with resulting electrophilic aldehydes such as 4-hydroxynonenal (HNE) as an intermediate product (Mihalas et al. 2017; Pannunzio and Storey 1998). Elevated 4-HNE is caused by oxidative stress, and results mainly in the peroxidation and destruction of lipids (Mihalas et al. 2017), but also proteins and DNA (Csala et al. 2015). HNE causes cross-linking and clumping of the fatty acids, especially linoleic and arachidonic acid, and is particularly destructive to mitochondrial and cell membranes (Zhong and Yin 2015). It also contributes to heat shock by disabling heat shock proteins (HSP's) (Csala et al. 2015). The antioxidants superoxide dismutase (Söderhäll 2010) and glutathione peroxidase tend to disrupt the production of HNE and protect against further damage (Pannunzio and Storey 1998). Even though HNE is found at a low level flux in all tissues, it was discovered that intertidal gastropods, genus

Littorina, had a depressed level of HNE in the hepatopancreas during anoxia even though the foot muscle experienced a strong increase, attributed to the strong metabolic depression in the hepatopancreas (Pannunzio and Storey 1998). The suppression of oxidative phosphorylation protects against these oxidative products during estivation.

ROS produced by oxidative stress can also affect DNA integrity by disrupting DNA repair mechanisms (Meng et al. 2017) with toxic results. DNA modifications due to oxidative stress can be caused directly by ROS or by oxidative products such as lipid peroxides. This repair malfunction results in SS and DS breaks, base modifications, and purine/pyrimidine substitutions (Salmon et al. 2004). These oxidative modifications understandably interfere with gene expression and transcription, possibly causing an inappropriate hypoxia response. Comparisons of the amounts of toxic DNA breaks and lesions are informative to differentiate because intertidal oysters and those in lower salinity should suffer an increase in the effects of DNA damage due to repeated oxidative stress. Carbonyls, lipid peroxidation, and DNA degradation will be investigated in the oyster tissue to determine levels of oxidative damage of geographic locations and tidal zone.

MATERIALS AND METHODS

Animal collection and culture

Wild native oysters were field collected from three sites, two in North Carolina (Federal Point, Harker's Island) and one in South Carolina (Baruch Research Station) (see Figure 2.1). Both intertidal and subtidal oysters were taken at each site. For one of these populations, Harker's Island, collections were made in different seasons to show seasonal variability. The North Carolina sites were covered under N.C. Fisheries SEAP Permit Number 929729. Baruch Research Station in Georgetown, South Carolina, issued a collection permit for that site. All oysters were collected in seafood safe zones. All sites were collected in the spring from May 25 – June 10.

All study animals for this research were collected within two weeks of the same time of year and are biogeographically close, and the intertidal and subtidal oysters experience very different temperature conditions that are difficult to quantify. Therefore, the temperature measurement was not included in the study, but was considered a component of the habitat conditions.

The study sites in this research are all different average salinities on a range of low (12 ppt) at Federal Point to high (ocean salinity of 35 ppt) at Harker's Island, with an intermediate (25 ppt) at Baruch Research Station. The three sites are in different macrohabitats as well as different salinities. Harker's Island oyster bed is beside a road which acts as a causeway between the mainland and Harker's Island proper. It is on an island in the sound serving as a base for the drawbridge. The oysters were on a rocky slope next to the road and along the edge of the beach-like area. Being in the open sound near an inlet allows the salinity to be as high as the ocean. Federal Point oysters were in a marsh, covered with marsh grass, near the parking area for the Wildlife Commission Boating Access near Fort Fisher. The Federal Point site is also in the middle of the Cape Fear River as it interacts with the ocean in tidal cycles, but approximately a mile from the mouth of the river, and so is highly influenced by freshwater outflow. Baruch Research Station, at the Baruch Institute of Marine Sciences, has a huge marsh accessible by boardwalk. It is mostly bare of grass, with beds of oysters in silty mud, and oysters were obtained from the open tidal marsh at the end of the boardwalk. Although the marsh salinity fluctuates with tides, it is consistently in the intermediate range.

At each site and date of collection at least 10 oysters each were collected from the intertidal and subtidal zones at low tide. Oysters were kept on ice overnight, then acclimated in aerated tanks in artificial sea water for 24 hours at native salinity and room temperature ($22\pm1^{o}C$) before

dissection and collection of tissues. Optimum temperature for *Crassostrea virginica* has been determined experimentally to be 20±1ºC in other studies (Kurochkin et al. 2009); therefore, room temperature was near this lowest stress level.

Mitochondrial function and damage

To determine how environmental conditions impact oysters from each studied location, mitochondria were isolated from oysters from each location and habitat. Mitochondria were isolated from oyster gills pooled from two individuals per replicate and assayed using a method modified from Sokolova (2004). Briefly, gills (2–4 g) were homogenized with several passes of a Potter–Elvenhjem homogenizer and a loosely fitting Teflon pestle, centrifuged to remove cell debris, and then the supernatant was centrifuged again to obtain a mitochondrial pellet. The mitochondrial pellet was resuspended, washed with homogenization buffer, and resuspended in ice-cold assay medium. Oxygen uptake by mitochondria (MO_2) was measured in 1 ml water-jacked, temperature-controlled chambers using Clarke-type oxygen electrodes (Qubit Systems, Kingston, Ontario, Canada) at 18°C. To test the effects of anoxia and reoxygenation on mitochondrial capacity, mitochondrial MO_2 was measured in the presence 10 mmol l^{-1} succinate.

Respiration with succinate was measured in the presence of 2.5 g ml^{-1} rotenone to inhibit the upstream complexes of the electron transport chain (Furr et al. 2021). Mitochondrial MO_2 was measured at saturating O_2 concentrations according to the standard practice in mitochondrial physiology. All assays were completed within 2 hours of isolation of the mitochondria. State 3 (ADP-stimulated), state 4 (resting), and state 4ol (in the presence of 2.5 g ml^{-1} oligomycin) respiration rates were determined as described earlier (Sokolova 2004). State 3 of mitochondria respiration was achieved by the addition of 100–150 mmol l^{-1} of ADP. States 4 and 4ol MO_2

represent uncoupled respiration when most (or all, in the case of state 4ol) energy of substrate oxidation is used to counteract the proton and cation cycles (collectively known as proton leak) across the mitochondrial membrane (Brand et al. 1994; Skulachev 1998). Respiratory control ratio (Harrison et al.) was calculated as the ratio of state 3 to state 4 respiration and used as an index of mitochondrial integrity (Estabrook 1967; Skulachev 1998). Mitochondrial respiration rates were corrected for the electrode drift and non-mitochondrial respiration and then converted into natom O min^{-1} mg^{-1} mitochondrial protein as described in Sokolova (Sokolova 2004). Protein concentrations in isolated mitochondria (treated with 0.1% Triton X-100 to solubilize mitochondrial membranes) were measured using the Bio-Rad protein assay (Bio-Rad Laboratories, Hercules, California, USA).

Mitochondria were also tested for presence of carbonyls and 4-hydroxynonenal (HNE) as evidence of oxidative damage. Carbonyls such as ketones and aldehydes are products of reactive oxidative compounds in the mitochondria, the possible results of anaerobiosis or heat stress. Hydroxynonenal (HNE) is the result of peroxidation of unsaturated lipids, a degradation that also leads to mitochondrial damage. Carbonyls were determined on mitochondria as well as gill tissue using a protocol adapted from the Cayman Chemical Carbonyl Colorimetric Kit (http://www.caymanchem.com/pdfs/10005020.pdf) (Appendix A. 4). Mitochondrial slurries were suspended in buffer and incubated with streptomycin sulfate. DNP/HCL dye was added, and absorbance compared to controls. Concentration of carbonyls (nmol CO/mg protein) was determined by calculation:

$$\text{Nmol CO/mg proteins} = \frac{\text{Abs} * \text{Vol (Guanidine in ml)} * 10^9}{\varepsilon * 1000 * \text{proteins (mg/ml)}}$$

(ε = 22,000 $cm^{-1} * M^{-1}$)

Lipid peroxidation as HNE was determined with a standard ELISA antibody assay based on the Thermo Scientific ELISA technical guide, using the ELISA Buffer (ThermoScientific) and HNE standards (Appendix A.5). HNE was determined in an indirect ELISA antibody assay measured against a known standard of HNE-BSA (hydroxynonenal to Bovine Albumin Serum). Spectrophotometric absorbance was measured, and samples determined based on the standard. Absorbance of standards and samples yielded concentration of HNE in ug/ml HNE-BSA.

Energy Storage Capacity

Hepatopancreas tissues were immediately frozen in liquid nitrogen when dissected. All tissues were then stored at -80^{o}C. Hepatopancreas tissue was used as it is used as storage for glycogen and lipids in mammals.

Energy storage capacity of oysters was measured in hepatopancreas tissue in terms of carbohydrate, lipid, and protein assays (see Appendices A.1, A.2, and A.6). Amounts of these compounds relate to the amount of energy storage capacity for metabolism in the oyster. These were measured in the spring for all three sites, when spring algal bloom should have replenished lipids and proteins, and oysters were preparing for spawn.

Carbohydrates (glycogen and glucose) were measured with a protocol based on Keppler and Decker (1981). Hepatopancreas tissue from the oysters were homogenized in PCA (perchloric acid) and kept on ice (see Appendix A.7). Glycogen and glucose were determined independently. Glycogen was hydrolyzed with glucoamylase digestion at 40^{o}C to convert to glucose, then glycogen/glucose and free glucose absorption were spectrophotometrically measured against a standard using ATP/G6P-DH and hexokinase. Change in absorbance at 340 nm was recorded and concentration in the sample was calculated from a standard curve (0.00 – 0.28 mM) (see Appendix A.2).

Lipids were measured by dry weight after extraction with a chloroform/methanol mixture (Folch et al. 1957). Ground tissue was dissolved in the solvent and solids removed. Lipids remain after the aqueous layer is removed and chloroform is evaporated under a hood (see Appendix A.1).

Total protein was determined spectrophotometrically using a standard Bradford Dye (Bio-Rad) protocol. Frozen tissue was homogenized in buffer with PMSF (a proteinase inhibitor) on ice. A protein standard series was made with Bovine Serum Albumin (BSA). Bradford dye was used to measure absorbance spectrophotometrically at 595nm. Sample concentration was calculated from BSA standards. Protein concentration was also required for several other assays (carbonyls, lipid peroxidation, carbohydrates, lipids, DNA degradation) and was done on those aliquots using this standard method (see Appendix A.6).

Raw totals of each of the compounds was determined in each oyster. Total energy storage for each site and habitat was calculated from totaling energy values of the principle storage compounds – lipids, carbohydrates and proteins – based on those of Whitehill and Moran from Grieshaber (Grieshaber et al. 1994; Whitehill and Moran 2012) (See Figure 2.6). Each of these compounds has a different amount of potential energy per gram. By converting to kiloJoules per gram, the compounds can be combined for a total energy value. The total energy storage in kiloJoules per gram was calculated from the following values; Glycogen 473 kJ $mol^{-1}O_2$, lipids 441 kJ $mol^{-1}O_2$, and protein 527 kJ $mol^{-1}O_2$ (Whitehill and Moran 2012). Percentages of the total were then calculated.

Cellular component damage

Gill and hepatopancreas tissues were immediately frozen in liquid nitrogen when dissected. All tissues were then stored at -80^{o}C. Molecular damage by oxidation was determined in gill tissue by measuring products of reactive oxidative processes from heat stress or long term anaerobiosis.

Carbonyls, products of reactive oxygen damage to proteins including ketones and aldehydes, were measured using a protocol for small samples adapted from the Cayman Chemical Carbonyl Colorimetric Kit (http://www.caymanchem.com/pdfs/10005020.pdf) (see Appendix A.6). Tissue is homogenized in HEPES/KCl buffer and incubated with streptomycin sulfate. DNP/HCL dye was added, and absorbance measured. Protein concentration of the sample was measured using the standard protocol (see Appendix A.4). Concentration of carbonyls (nmol CO/mg protein) was determined directly by calculation:

$$\text{Nmol CO/mg proteins} = \frac{\text{Abs} * \text{Vol (Guanidine in ml)} * 10^9}{\varepsilon * 1000 * \text{proteins (mg/ml)}}$$

$$(\varepsilon = 22{,}000\ \text{cm}^{-1} * \text{M}^{-1})$$

DNA degradation in hepatopancreas tissue was determined with an assay adapted from Olive et al. (1988) and measured by fluorometer (see Appendix A.3). This protocol detects DNA damage including strand breaks and cross-links indicating possible environmental stress (Olive et al. 1988). Damaged DNA was detected with Hoechst dye in the presence of sodium cholate. Fluorescence was measured against a standard DNA solution made from salmon sperm and reported per unit protein (determined by standard assay on these samples).

Lipid peroxidation as HNE was determined with a standard ELISA antibody assay based on the ThermoScientific ELISA technical guide, using the ELISA Buffer (ThermoScientific) and HNE-BSA standards. HNE was determined in an indirect ELISA antibody assay measured against a known standard of HNE-BSA (4-hydoxynonenal to Bovine Serum Albumin).

Spectrophotometric absorbance was measured at 450nm, and the amount of lipid peroxidation determined based on the HNE standard curve. Protein in the sample was determined with the standard protocol (see Appendix A.5). Absorbance of standards and samples yielded the concentration of HNE in ug/ml HNE-BSA.

Statistical Analysis

All physiological data is analyzed using a two-factor experimental design and significance were determined by ANOVA in JMP Pro 16 (SAS Institute, Cary, NC 2021) at $p<0.05$ except % Proton Leak, which was run as a chi-square in the same application at the same significance level. Outliers were eliminated by the Grubbs method, detecting values outside normal distribution with $p<0.5$ using GraphPad outlier calculator (GraphPad QuickCalcs Web site: http://www.graphpad.com/quickcalcs/ConfInterval1.cfm (accessed 2019)). Graphs were produced in GraphPad version 9 for Windows (GraphPad Software, San Diego, California USA, www.graphpad.com).

RESULTS

Mitochondrial Respiration and Damage

To measure the ability of these oysters to control oxidative function in these very different habitats, metabolic rate is measured at different states in respiration. Metabolic rate may be measured as a function of oxygen consumption (MO_2) for oxygen-dependent organisms. MO_2 rates will be determined at different mitochondrial states, reflecting different processes in the electron transport chain. Active ATP production by F_1F_0-ATPase occurs mainly in State 3, when MO_2 is stimulated by ADP concentration. During the resting state, State 4, most of the ATP

produced is from proton leak to balance the membrane potential of the mitochondrion. With the addition of oligomycin, designated with a (+), all downstream ETS functions are halted, and ADP is used up, making all the O_2 used to make ATP due to proton leak. Respiratory Control Ratio (Harrison et al.) is the ratio of State 3 to State 4, and similarly, RCR+ is the ratio of State 3 to State 4+.

Oysters in different geographic locations, which correspond to different salinities, and tidal zones show overall significant differences in the ADP-stimulated state (State 3) of F_1F_0-ATP synthase function (see Table 2.1, Figure 2.2). Baruch Research Station at salinity of 25 ppt, was significantly lower than either of the other two locations. The interaction of the two factors, Site X Habitat, did prove to be a significant difference, with Harker's Island intertidal oysters comparable to all Baruch oysters and Harker's Island subtidal oysters comparable to all Federal Point oysters in State 3.

The resting state (State 4) and the resting, oligomycin-stimulated state (State 4+) showed no differences with any of the sites or habitats. The Respiratory Control Rate (Harrison et al.) was not significantly different between sites and habitats, either stimulated with oligomycin or unstimulated. In State RCR, however, subtidal oysters in Harker's Island and Baruch Research Station had significant differences between the two geographic locations.

The amount of proton leakage (see Table 2.2) was measured by determining the percentage drop of State 3 to State 4 values. A large percentage drop shows that little proton leakage is occurring. Harker's Island intertidal oysters showed little difference (8.5%) between State 3 and State 4, which was unusual in that all other sites/habitats had a 38 – 56% drop. The result, however, was not statistically significant.

For stress-related carbonyl concentrations in the mitochondria, which signifies oxidative stress, habitat again was not a significant factor (see Table 2.1, Figure 2.3). There was, however, a significant difference in location values overall (F = 10.6, p=0.0009) driven by a significant excess of carbonyls at the Harker's Island site, especially in the intertidal zone. This site had evidence for high oxidative stress as shown in protein degradation. In the HNE determination, Federal Point and Harker's Island both had high lipid peroxidation, signifying oxidative stress to lipid membranes, making lipid peroxidation values for site highly statistically significant (F = 77.9, p , 0.0001). The interaction of Site X Habitat is also statistically significant in carbonyls (F = 5.1, p = 0.0178) and lipid peroxidation (F = 4.1, p = 0.0359) due to the strongly significant Site component. Habitat shows no difference in any test.

Energy Storage Capacity

I found that habitat at a site showed no significant difference for any location in this study in glycogen, lipid or protein content in the hepatopancreas (see Table 2.3, Figure 2.4). However, there was a large and significant difference ($p < 0.0001$) in all components of hepatopancreas energy storage due to geographic location. Federal Point, and to a lesser extent, Harker's Island, showed a higher storage content of glycogen than Baruch at an intermediate salinity. Lipids were also significantly different for site ($p < 0.0001$), especially very high in the lower salinity Federal Point oysters, which were collected in lower salinity. Protein is also significantly different by site (F = 85.5, $p < 0.0001$). Even though the different energy compounds exhibited different outcomes, the total energy for each site was also significantly different, with Harker's Island having the lowest total energy storage of any site (F – 10.6, $p = 0.0003$) (see Table 2.4, Figure 2.5).

The percentage of total energy stores calculation (see Figure 2.6) showed little contribution of glycogen to the energy storage at the time of eminent spawning. There was a large difference in the percentage of protein vs. lipids in the different locations ($F = 10.6$, $p = 0.003$), with Baruch at the intermediate salinity having the highest percentage of protein and Federal Point at the lowest salinity having the least.

Cellular Component Damage

Oysters collected from Baruch Research Station at an intermediate salinity showed significantly lower level of carbonyls implicated in damaged proteins from oxidative damage (see Table 2.5, Figure 2.7). Federal Point with the lowest salinity had the highest carbonyls, especially in the subtidal zone. Harker's Island was intermediate in carbonyls. The same pattern was observed for DNA damage. Oxidative stress appeared to be specifically damaging proteins and causing DNA damage. However, there was no significant difference in lipid peroxidation damage in any of the sites, even though results were highly variable. There was also no significant difference in tidal zone habitat in any of the three parameters (mitochondrial damage, cellular component damage, energy storage) even though Federal Point subtidal oysters experienced high carbonyl and DNA damage levels.

DISCUSSION

Mitochondrial Respiration and Damage

It is apparent that State 3, which involves ADP stimulation of the F_1F_0-ATP synthase varies by geographic location, which are different salinities. If the rate of ATP production coinciding with oxygen consumption increases in extremes of salinities, it can be assumed that the energy demand is also higher. This was also found in oysters subjected to cadmium as in anthropogenic

pollution (Kurochkin et al. 2009). A long-term effect in ADP-stimulated oxygen uptake (State 3) was found in *C. virginica* by Kurochkin et al (2009) by subjecting oysters to hypoxia for an extended period of time, but resulting in no change in State 4, the resting state. This effect is also supported by my findings with intertidal oysters in high salinity experiencing intermittent hypoxia during normal life, and as a result, their State 4 resting state is not elevated.

Since the experimental optimum salinity for *Crassostrea virginica* is 30±1 ppt (Kurochkin et al. 2009), more energy is likely to be expended at the low (12 ppt) and high (35 ppt) end of the salinity range for osmotic balance than at the intermediate range. Baruch Research Station was consistently lower in mitochondrial respiration rate (although only statistically significant in Stage 3) than the other two, suggesting that the oysters were not actively respiring as quickly in an intermediate level salinity (25 ppt).

Increased oxygen consumption can result in higher oxidative stress, as is shown with the higher levels of carbonyls at Harker's Island at high salinity. The intertidal oysters at Harker's Island are on an inclined bank beside a road and bridge at the base of rocks, which may also exacerbate the heat stress in addition to raising the locally high salinity. They are also exposed to the air longer during low tide than those on level substrate as in a marsh. The synergistic combination of multiple stressors has been shown to exacerbate the effects of detrimental environmental conditions (Kurochkin et al. 2009).

Harker's Island oysters show high oxidative stress by the carbonyl values, which are extremely high in the intertidal oysters, and in the HNE values which show high lipid peroxidation present in oysters in both habitats. Both extremes of salinity, 12 ppt at Federal Point and 35 ppt at Harker's Island, provide evidence of oxidative stress to the point of damage to proteins and lipid membranes.

Harker's Island intertidal and subtidal oysters show a difference (although not significant due to variability) in the amount of proton leak as measured by percentage drop from State 3 to State 4. The intertidal oysters have more proton leak as the percentage drop from State 3 was only 8.5%, whereas all of the other Sites/Habitats have a 38 – 56% drop. This difference could be biologically important due to the oxidative stress damage as shown earlier in the carbonyl and HNE concentrations. This is evidence consistent with salinity as a factor in survival of oysters in this location, and these are perhaps close to their survival extremes at 35 ppt, typical ocean level salinities.

Federal Point had a low salinity of 12 ppt at time of collection which certainly fluctuated lower at times due to freshwater outflow during heavy rains. In fact, the Federal Point bed of oysters was not able to survive the heavy freshwater outflow from more than 30 inches of rain upstream from Hurricane Florence in 2018 even though the flooding period of several days was well within the survival time of estivating oysters. The additional stressor of summer-like temperatures was also a possible factor (La Peyre et al. 2013). It appears that an intermediate salinity (25 ppt in this case) is nearer the optimum fitness level for oysters, and it makes no difference whether they are in the intertidal or subtidal zone, at least for the majority of the physiological parameters measured in this study.

Based on the results of mitochondrial function, *Crassostrea virginica* is well-adapted to life in the estuary where salinities are fluctuating, but not usually as high as ocean salinities (35 ppt) or as low as freshwater/brackish salinities (< 12 ppt). They have an ability to survive a huge range of salinities, attesting to their ability to osmoregulate quickly. However, it comes at a cost at the extremes of their salinity range where they can experience oxidative damage, which may limit their survival in these salinities when compounded with temperature or other additional

stressors. This may be a greater factor as climate change causes extreme fluctuations in weather in addition to changes in average values. Intertidal or subtidal survival does not make a difference except in extremes of salinity, where the exposure and heat may cause osmoregulation challenges. Otherwise, oysters seem to possess the plasticity to acclimate to rapidly and wildly changing environments in either the intertidal or subtidal zone.

Energy Storage Compounds

I have found that although tidal zone did not result in significant differences in energy storage capacity of oysters, locations with differences in salinity (and perhaps other unmeasured variation) had a large impact. Federal Point had a high carbohydrate and lipid level, but very low protein. Since spawning generally depletes all glycogen stores, I suspect Federal Point oysters were not spawning. At the time of year these oysters were collected, spawning was eminent since mature gonads were observed in some oysters, so glycogen should have been very low. The lack of protein as compared to Baruch may indicate they are more susceptible to future stressors, since these stores are used as structural compounds as well as energy if needed, although the lipid content is very high.

The Harker's Island oysters had a moderate glycogen and lipid level. Because oysters were pooled for these measurements, some of them may have spawned or would have eminently. However, their protein and lipid levels were comparatively low, which may signal a problem with susceptibility to high summer mortality in this high salinity site.

Baruch Research Station oysters, being further south, may have already spawned out at the time of collection or were spawning at the time of collection. The high likelihood of spawning was supported by the very low glycogen content. Lipid and protein stores generally carry the oysters

through the summer, and these were moderate to high in the Baruch oysters. These oysters are in the best condition biochemically to survive possible summer mortality events until stores can be replenished in the fall.

Cellular Component Damage

Protein carbonylation and DNA damage show a relationship to salinity levels between each geographic location. There was significantly more protein and DNA damage in the location with the lowest salinity, potentially reflecting the costs of low salinity for these oysters. Harker's Island, being at the other end of the extreme in salinity is the next highest for protein and DNA damage, with the location with intermediate salinity showing the least amount of protein and DNA damage. Surprisingly, lipid peroxidation was the same in all three sites regardless of salinity. Tidal zone also has no significant difference in cellular component damage. Salinity makes a big difference when it comes to oxidative damage. Oysters can tolerate extremes of temperature at optimum salinity; oysters can tolerate extremes of salinity at lower temperatures (Heilmayer et al. 2008).

CONCLUSION

The overall conclusion points to salinity as the biggest factor in oyster bioenergetic fitness, and not position in the tidal zone. The oyster's incredible physiological plasticity allows it to osmoconform to estuarine conditions of extremely low and high salinity; however, there are costs to this ability. The cost of surviving these extremes of salinity may exclude the inability to reproduce in extreme habitats. Even though salinity levels are ultimately limiting the existence of these natural oyster beds, exposure to hypoxia at environmental levels, such as in tidal zones, does not appear to affect oyster fitness unless it is a component of multiple stressors acting

synergistically. Salinity, temperature, and hypoxia are natural stressors to which oysters can acclimate due to plastic regulation of physiological processes. However, these oysters may exist on the extreme limits of survival and reproduction so that the addition of stressors due to climate change and anthropogenic pollution may mean their demise.

TABLE 2.1

Mitochondrial Respiration and Damage - Federal Point, Harker's Island, Baruch Research Station

Parameters	Tissue	Site	Habitat	Site X Habitat
Carbonyl Concentration	Mitochondria	$F_{2,23}$= 10.6076 p= **0.0009***	$F_{1,23}$= 4.0797 p= 0.0585	$F_{5,23}$= 5.0769 p= **0.0178***
Lipid Peroxid. (HNE)	Mitochondria	$F_{2,23}$= 77.8875 p <**0.0001***	$F_{1,23}$= 0.0359 p= 0.8518	$F_{5,23}$= 2.0354 p= 0.1596
Stage 3	Mitochondria	$F_{2,22}$ = 5.7305 p= **0.0125***	$F_{1,22}$ = 3.9527 p= 0.0631	$F_{5,22}$ = 4.0702 p= **0.0359***
Stage 4	Mitochondria	$F_{2,23}$ = 2.7497 p= 0.0908	$F_{1,23}$ = 0.0088 p= 0.9262	$F_{5,23}$ = 0.3714 p= 0.6950
Stage 4+	Mitochondria	$F_{2,23}$ = 2.6008 p= 0.1018	$F_{1,23}$ = 0.2910 p= 0.5962	$F_{5,23}$ = 0.5144 p= 0.6064
RCR	Mitochondria	$F_{2,23}$= 1.7949 p= 0.1946	$F_{1,23}$= 0.9725 p= 0.3371	$F_{5,23}$= 0.9362 p= 0.4104
RCR+	Mitochondria	$F_{2,23}$ = 0.8313 p= 0.4515	$F_{1,\ 23}$= 0.9668 p = 0.3385	$F_{5,23}$ = 1.7416 p= 0.2035

Table 2.1. ANOVA: Effects of ex*p*erimental conditions and/or populations on the Mitochondrial Respiration in *Crassostrea virginica*. F ratios with the degrees of freedom for the factor effect and the error shown as a subscript, are given. Significant effects ($p < 0.05$) are highlighted in bold.

TABLE 2.2

Amount of Proton Leak - Federal Point, Harker's Island, Baruch Research Station

Location and Habitat	Average State 3	Average State 4	Percentage Drop (%)
Federal Point Intertidal	8.619	5.151	40.2
Federal Point Subtidal	9.904	4.486	54.7
Harker's Island Intertidal	5.058	4.630	8.5
Harker's Island Subtidal	14.111	6.108	56.7
Baruch Res Station Intertidal	4.734	2.576	45.6
Baruch Res Station Subtidal	3.407	2.081	38.9

Table 2.2. Average of active oxidative phosphorylation (State 3), average of resting oxidation (State 4) and the percentage of the drop, indicating the amount of proton leak in the mitochondrial membrane. ANOVA: df = 5, p = 0.4159 (Wilcoxon), not significant.

TABLE 2.3

Energy Storage - Federal Point, Harker's Island and Baruch RS

Parameters	**Tissue**	**Site**	**Habitat**	**Site X Habitat**
Protein Conc.	Hepatopancreas	$F_{2,57}$= 85.4836 p **<0.0001***	$F_{1,57}$= 1.8213 p=0.1830	$F_{5,57}$=0.6546 p=0.5239
Lipid Conc.	Hepatopancreas	$F_{2,56}$= 13.7511 p **<0.0001***	$F_{1,56}$= 0.2453 p=0.6226	$F_{5,56}$= 0.0613 p=0.9406
Glucose/glycogen	Hepatopancreas	$F_{2,42}$ = 14.9698 p **<0.0001***	$F_{1,42}$= 0.8283 p= 0.3686	$F_{5,42}$= 1.1042 p=0.3421

Table 2.3. ANOVA: Effects of ex*p*erimental conditions and/or populations on the Energy Storage Components in *Crassostrea virginica*. F ratios with the degrees of freedom for the factor effect and the error shown as a subscript, are given. Significant effects ($p < 0.05$) are highlighted in bold.

TABLE 2.4

Sum of Energy Components – Federal Point, Harker's Island, Baruch Research Station

Parameters	**Tissue**	**Before/After (Site)**	**Habitat**	**Before/after X Habitat**
Sum of Energy Component (KJ)	Hepatopancreas	$F_{2,34}$= 10.5601 p = **0.0003***	$F_{1,34}$= 0.0361 p = 0.8505	$F_{5,34}$= 1.1510 p = 0.3295

Table 2.4. ANOVA: Effects of ex*p*erimental conditions and/or populations on Sum of Energy Components in *Crassostrea virginica*. F ratios with the degrees of freedom for the factor effect and the error shown as a subscript, are given. Significant effects ($p < 0.05$) are highlighted in bold.

TABLE 2.5

Cellular Oxidation Damage - Federal Point, Harker's Island, Baruch Research Station

Parameters	Tissue	Site	Habitat	Site X Habitat
Carbonyl Conc.	Gills	$F_{2, 53}$=6.8417 p= **0.0024***	$F_{1,53}$= 0.1379 p= 0.7120	$F_{5,53}$= 0.1.7916 p= 0.1777
HNE (Lipid Perox)	Gills	$F_{2,28}$= 0.8269 p= 0.4500	$F_{1,28}$ = 0.6738 p= 0.4201	$F_{5,28}$= 1.0641 p=0.3614
DNA Damage	Hepatopancreas	$F_{2,35}$= 16.3046 p <**0.0001***	$F_{1,35}$= 0.2665 p = 0.6095	$F_{5,35}$= 3.5650 p = **0.0408***

Table 2.5. ANOVA: Effects of ex*p*erimental conditions and/or populations on the Cellular Oxidation Damage in *Crassostrea virginica*. F ratios with the degrees of freedom for the factor effect and the error shown as a subscript, are given. Significant effects ($p < 0.05$) are highlighted in bold.

FIGURE 2.1

Oyster Collection Locations in North Carolina and South Carolina

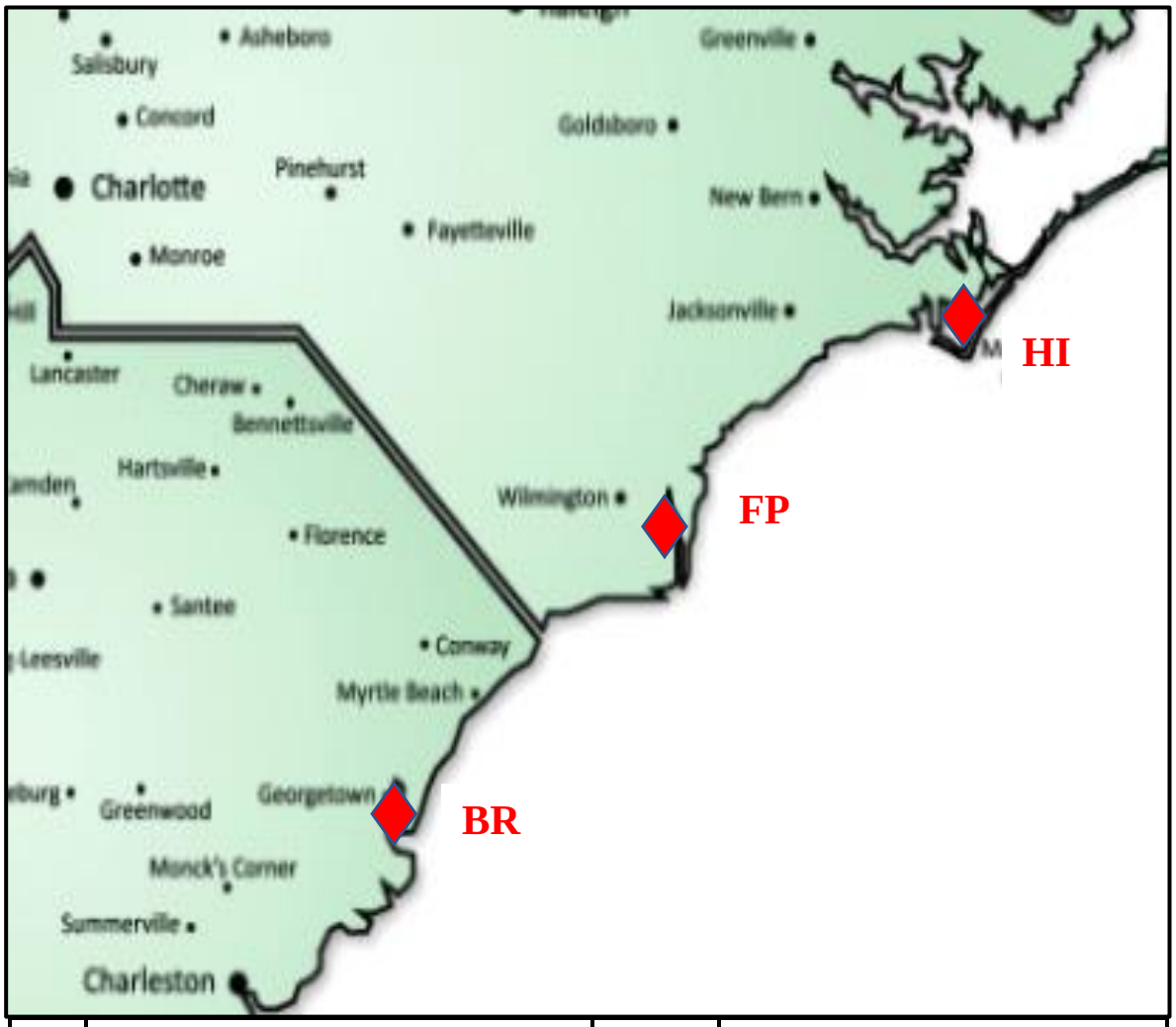

	Site	Salinity	Latitude/Longitude
HI	Harker's Island, NC	35 ppt	34.71917°N; 76.57619°W
FP	Federal Point, NC	12 ppt	33.95785°N; 77.94014°W
BR	Baruch Research Station, SC	25 ppt	33.32496°N; 79.18300°W

Figure 2.1. Oyster collection sites in North and South Carolina.

FIGURE 2.2

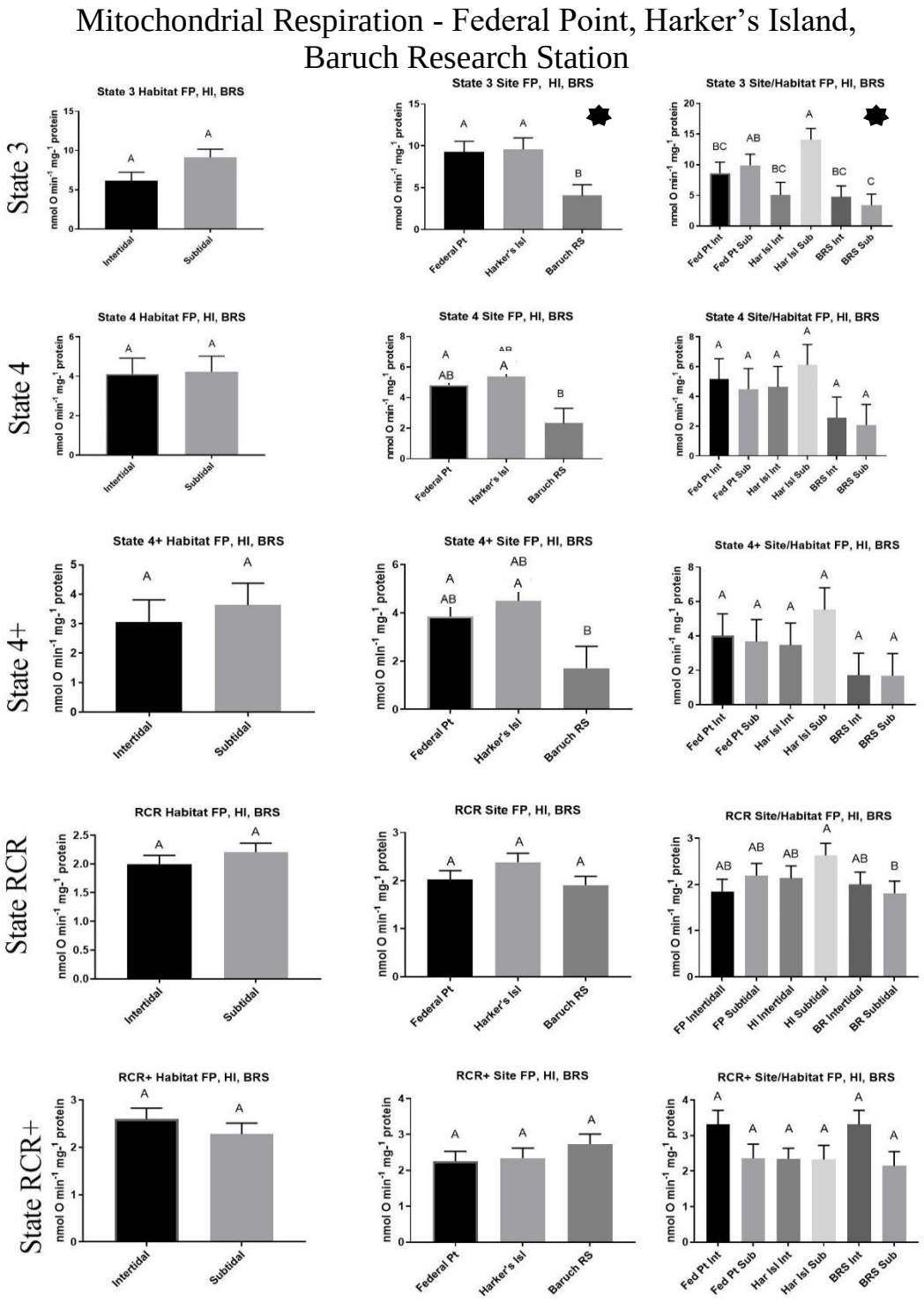

Figure 2.2. Different letters indicate the values that are significantly different among *C. virginica* from different zones ($p < 0.05$); if columns share a letter, the respective values are not significantly different ($p > 0.05$). Vertical bars represent the standard error of means. ✸ Indicates overall significance.

FIGURE 2.3

Mitochondrial Damage – Federal Point, Harker's Island, Baruch Research Station

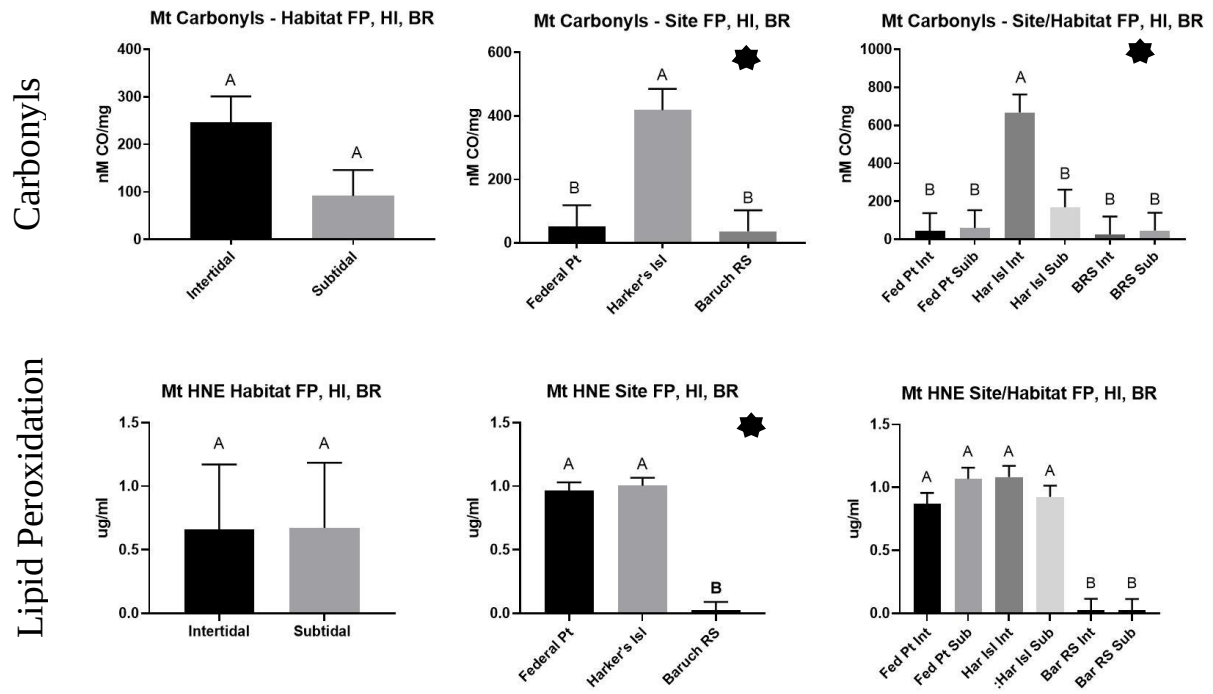

Figure 2.3. Different letters indicate the values that are significantly different among *C. virginica* from different zones ($p < 0.05$); if columns share a letter, the respective values are not significantly different ($p > 0.05$). Vertical bars represent the standard error of means. ✸ Indicates overall significance.

FIGURE 2.4

Energy Storage Components – Federal Point, Harker's Island, Baruch Research Station

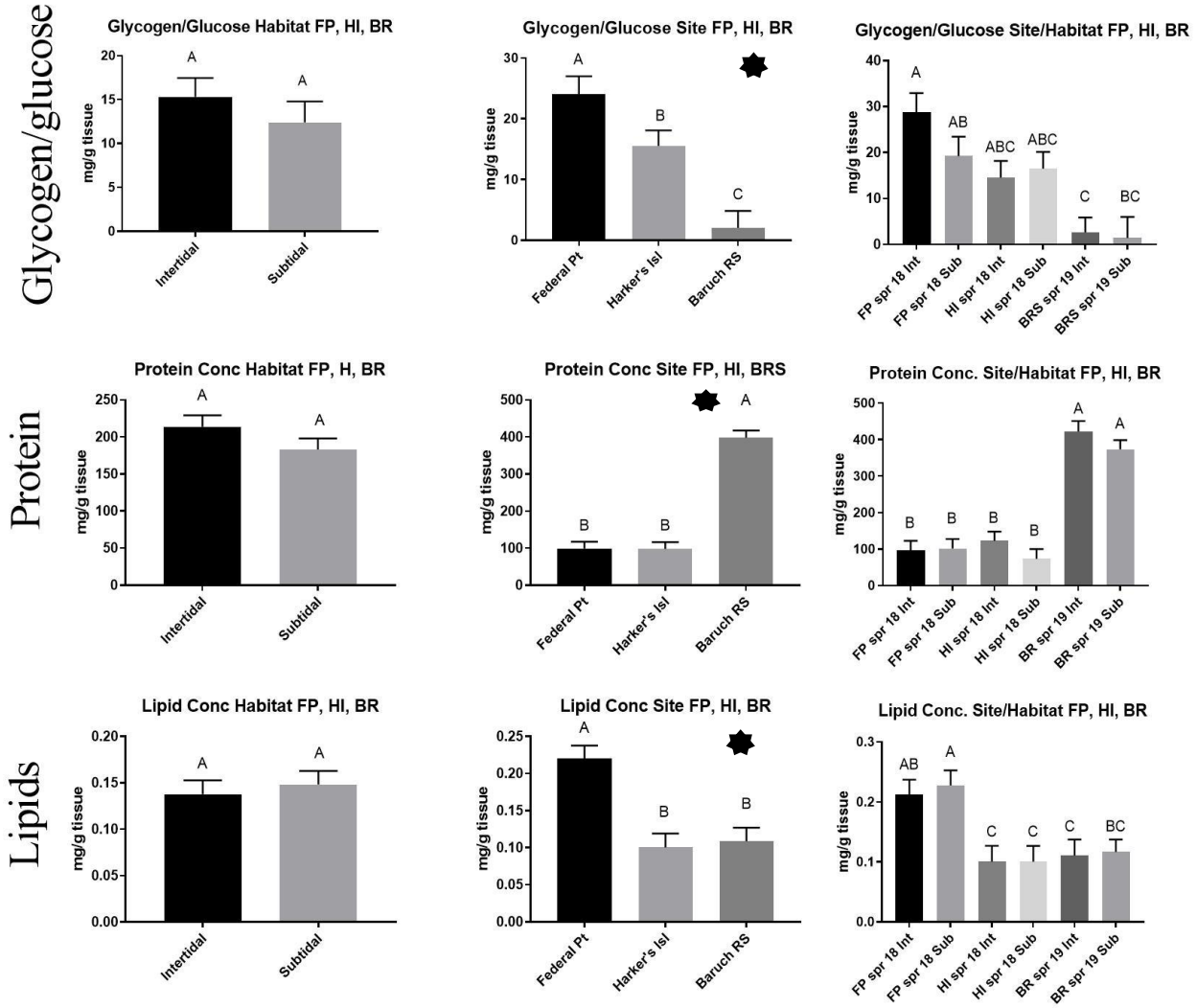

Figure 2.4. Different letters indicate the values that are significantly different among *C. virginica* from different zones ($p < 0.05$); if columns share a letter, the respective values are not significantly different ($p > 0.05$). Vertical bars represent the standard error of means. ✸ Indicates overall significance.

FIGURE 2.5

Sum of Energy – Federal Point, Harker's Island,
Baruch Research Station

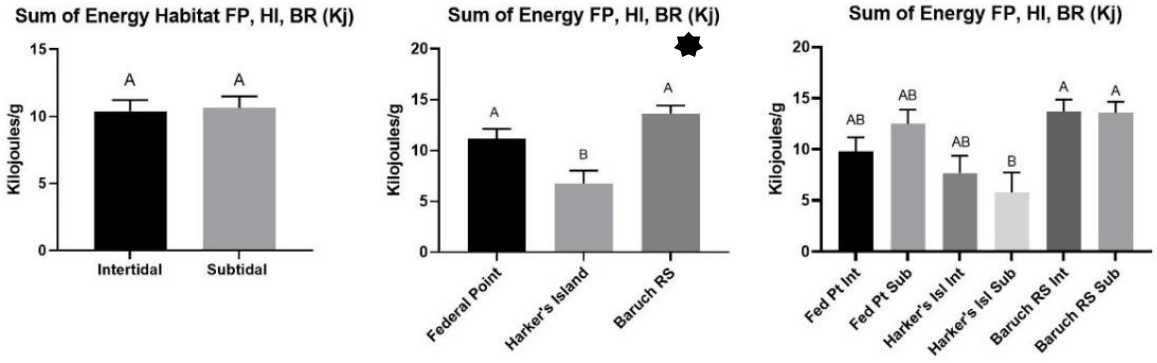

Figure 2.5. Different letters indicate the values that are significantly different among *C. virginica* from different zones ($p < 0.05$); if columns share a letter, the respective values are not significantly different ($p > 0.05$). Vertical bars represent the standard error of means. ✸ Indicates overall significance.

FIGURE 2.6

Percentage of Total Energy Storage - Federal Point, Harker's Island, Baruch Research Station

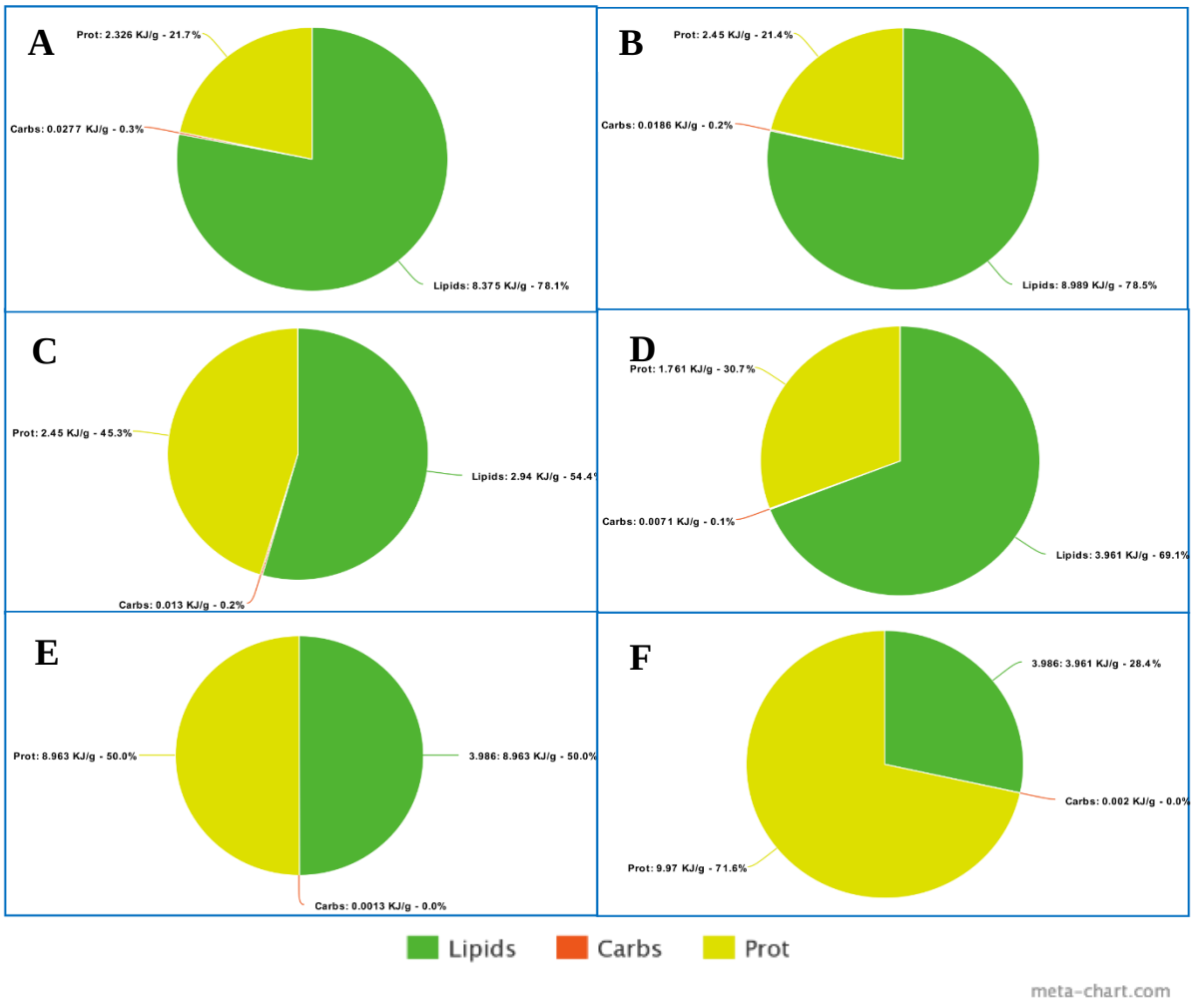

	Site/Habitat	Lipids %	Carbs %	Protein%
A	Federal Point/Intertidal – salinity 12.5ppt	78.1	0.3	21.7
B	Federal Point/Subtidal – salinity 12.5ppt	78.5	0.2	21.4
C	Harker's Island/Intertidal – salinity 35ppt	54.4	0.2	45.3
D	Harker's Island/Subtidal – salinity 35ppt	69.1	0.1	30.7
E	Baruch Research/Intertidal – salinity 25ppt	50.0	0.0	50.0
F	Baruch Research/Subtidal – salinity 25ppt	28.4	0.0	71.6

Figure 2.6. Total percentage of lipids, carbohydrates and protein in energy stores of the oyster hepatopancreas at different sites with different locations.

FIGURE 2.7

Cellular Oxidation Damage - Federal Point, Harker's Island, Baruch Research Station

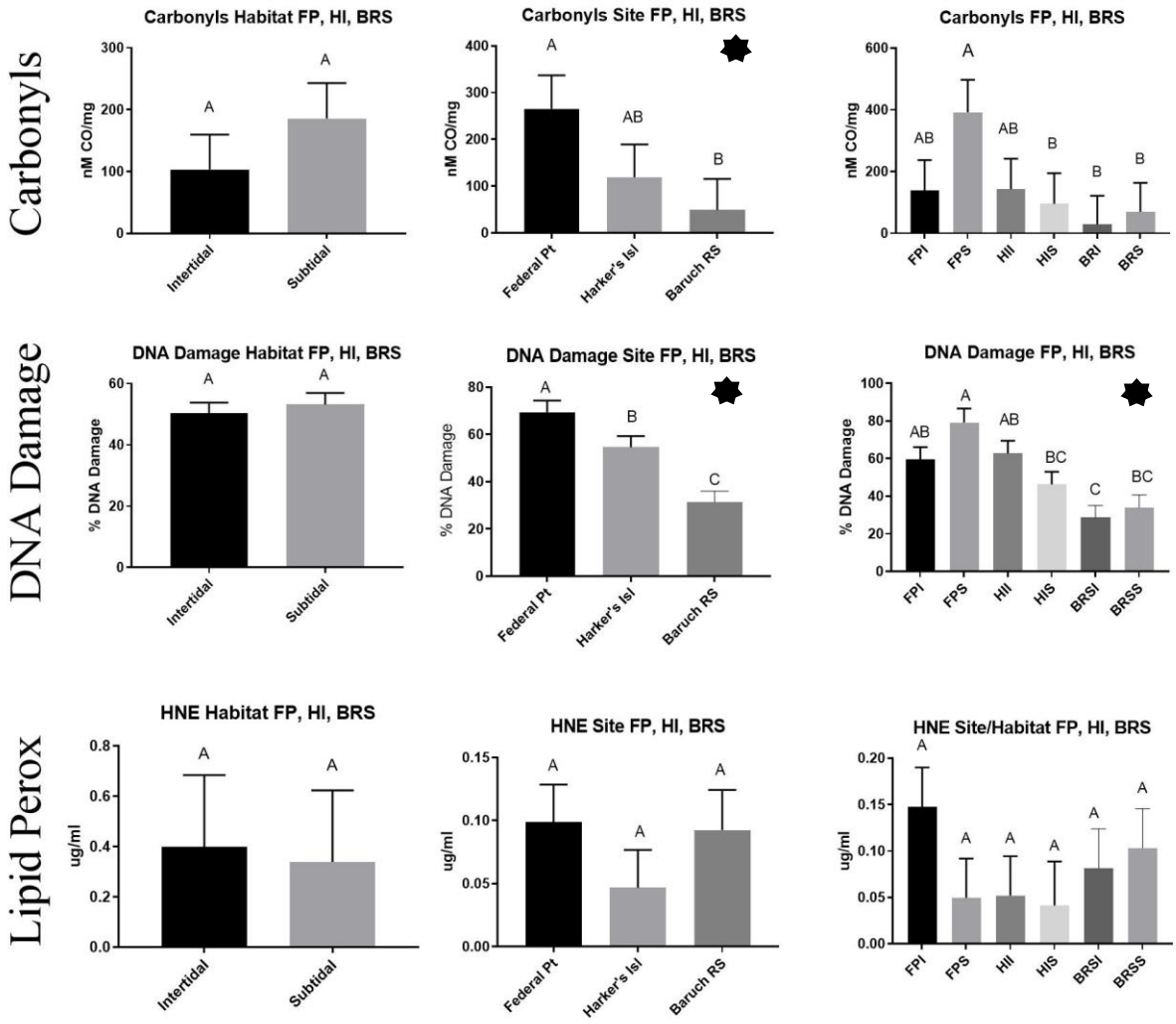

Figure 2.7. Different letters indicate the values that are significantly different among *C. virginica* from different zones ($P<0.05$); if columns share a letter, the respective values are not significantly different ($P>0.05$). Vertical bars represent the standard error of means. ✸ Indicates overall significance.

CHAPTER THREE

EFFECTS OF A HURRICANE ON OYSTER BIOENERGETICS

(Furr, Denise; Reitzel, Adam; Ivanina, Anna)

ABSTRACT

The Eastern Oyster, *Crassostrea virginica*, is a study model for physiological plasticity and environmental conformity. As a coastal organism, it is adapted to the saline aquatic environment; however, the range of salinities and habitats of the species is very broad. The oysters in the natural bed at the Harker's Island drawbridge site live in a high stress environment at the extreme of its survival range in a sound that experiences high salinity continuously, both in the intertidal and subtidal zones. The Harker's Island site, with a high ocean-level salinity in an open sound was also severely impacted by a climatic event, which left the oyster population with long-term physiological effects in mitochondrial damage and energy storage capabilities. Our study began as a study of seasonal variation in bioenergetics of the intertidal and subtidal oysters and transitioned into a study of the effects of a hurricane on mitochondrial and physiological stress. We were able to test the oysters before the hurricane, immediately after, and twice in the following year to see the impact on the surviving oysters in this already stressed population, as it has been shown to be susceptible to oxidative damage (See Chapter 2). This study found no evidence of effect on mitochondrial respiration states; however, mitochondrial damage was high, especially in intertidal oysters. Also impacted was the ability to store energy compounds that may impact survival through the winter. Conversely, we found a negative association with damage to cellular compounds, which dropped but then recovered over the course of the next year. Even though salinity at the site didn't change, and the only impact of the hurricane was physical wave action and debris, there was a discernible negative impact of a severe weather event on a natural oyster

bed in energy production and storage, which may affect survival. This impact may occur more frequently as climate conditions make severe weather events such as hurricanes more frequent occurrences on our coasts.

INTRODUCTION

On September 14, 2018, Hurricane Florence barreled ashore on the North Carolina coast, making landfall at Wrightsville Beach, near Wilmington, NC, after coming dangerously close to the Cape Lookout area near Harker's Island (see Figure 3.1). The storm was downgraded from a major hurricane with 140 mile/hour winds just offshore to a category 1 hurricane with 94 mile/hour winds just before landfall. According to NOAA records (https://www.nhc.noaa.gov/data/tcr/AL062018_Florence.pdf), the powerful storm pushed a 10-foot storm surge onshore at Morehead City, NC, and presumably as much at the Harker's Island site 20 miles east. Ocean waves washed over the roadway to Harker's Island from the east, dumping sand and debris on the west side. It also pushed ocean surge up the Cape Fear River, then stalled over southeastern North Carolina for three days, dumping record-setting flooding rains of over 30 inches on the area. Besides the heavy human toll from the storm, the oyster bed site used for research at Harker's Island was negatively affected.

The Harker's Island oyster bed being used for study is on the west side of the roadway connecting Harker's Island to the mainland. Winds from the east created a storm surge that over washed the road next to the oyster bed, depositing debris and sand on most of the subtidal oysters. Oysters at Harker's Island, having experienced the force of the hurricane, had survivors, although a large percentage of the bed was physically destroyed. There was likely little impact from the freshwater from hurricane flooding at the Harker's Island bed since it is surrounded by the large sound exposed to open ocean. The salinity at the site typically averages 32-34 ppt (Bishop et al.

2005), and the effect of river outflow was not a major factor. Therefore, the salinity is assumed to be constant over the study period. Natural and commercial oysters in other estuaries were totally destroyed by the heavy and persistent outflow of freshwater outflow from rivers feeding the tidal marshes for days after the hurricane, including the one at Federal Point, NC, an oyster bed used in Chapter 2.

Harker's Island oysters were collected in the spring of 2018 as part of a study comparing subtidal and intertidal oysters at three locations in the southeastern United States (see Chapter 2). As a high salinity site, Harker's Island had already shown some stress in the spring. The hurricane would add additional physical stress, such as wave action and sedimentation from overwash.

Mitochondrial Stress and Damage

Oysters of the species, *Crassostrea virginica*, can live in the intertidal or subtidal zones of the ocean shore. Conditions experienced by individuals at each of these zones are quite different. Since oysters are gill-breathing aquatic animals, an oyster does not respire during shell closure, which occurs nearly immediately upon being exposed to air (in addition to other rapid or desirable events) to avoid desiccation. Subtidal oysters are constantly submerged and rarely experience this diurnal stressor. Subtidal oysters must contend with competition and predation, but rarely abiotic stressors except by localized heavy silting or organic decomposition. Intertidal oysters should be particularly susceptible to mitochondrial disfunction due to the extreme environmental conditions of exposure and temperature in the intertidal zone.

When oxygen consumption is interrupted as in intermittent hypoxia, then suddenly resumed, the reoxygenation of tissues can create reactive oxygen species (ROS) due to excess O_2 (Abele et al. 2007). The resulting oxidative stress causes reactive oxygen species (ROS) such as

H_20_2 to increase, which can attack proteins, resulting in carbonyls. Carbonyls include ketones and aldehydes, products of protein degradation as free radicals that cause irreversible modifications to protein structures. This protein carbonylation converts side chains into ketones and aldehydes and is highly destructive to cells and tissues (Letendre et al. 2012). HNE causes cross-linking and clumping of the fatty acids, especially linoleic and arachidonic acid, and is particularly destructive to mitochondrial and cell membranes (Zhong and Yin 2015).

Energy storage capacity

Oysters rely on carbohydrates, lipids and proteins as energy reserves, just as most other eukaryotes do. Marine bivalves use carbohydrates (glycogen and glucose) first as quick energy compounds, then resort to lipids and even proteins as carbohydrates are depleted. Carbohydrates peak in the spring, then are depleted after spawning; protein and lipid levels rise in spring associated with gonadal development (Berthelin et al. 2000). Lipid content generally reaches its maximum in September, along with a second peak for glycogen, and these serve as winter reserves (Berthelin et al. 2000).

Energy storage levels are closely associated with stages in reproduction and gametogenesis. Gametogenesis and spawning use nearly all the stored glycogen in June, the typical time for oyster spawning in North Carolina when water temperature is between 18 – 20^{o}C (Gao et al. 2021). Glycogen drops to a minimum and remains there through the summer (Li et al. 2007). Lipid reserves are established in oysters in early winter along with protein, and reach a peak in the September (Berthelin et al. 2000). Proteins are generally not used for reproductive energy expenses, so are therefore available to sustain the animal in the summer after spawning (Berthelin et al. 2000). Mollusks are more likely to use protein as an energy source than mammals that would

only use protein if in starvation. Hepatopancreas tissue was used, which is not a primary glycogen storage site, but should be independent of the spawning process.

Cellular component damage due to oxidative stress

Reactive oxidative species (ROS), especially H_2O_2, can disrupt normal cell processes by degrading and destroying critical cell components. Identification of total carbonyls and 4-HNE are useful biomarkers for high oxidative stress in tissues that experience oxygen deficiency (Levine et al. 2000). Carbonyls include ketones and aldehydes, products of protein degradation, which as free radicals, cause irreversible modifications to protein structures.

Lipid peroxidation of polyunsaturated fatty acids (PUFA) results in a highly reactive product called 4-hydroxynonenal (Csala et al. 2015). Elevated 4-HNE is caused by oxidative stress, and results mainly in the peroxidation and destruction of lipids (Mihalas et al. 2017), but also proteins and DNA (Csala et al. 2015).

ROS produced by oxidative stress can also affect DNA integrity by disrupting DNA repair mechanisms (Meng et al. 2017) with toxic results. DNA modifications due to oxidative stress can be caused directly by ROS or by oxidative products such as lipid peroxides. This repair malfunction results in single-strand and double-strand breaks, base modifications, and purine/pyrimidine substitutions (Salmon et al. 2004). These oxidative modifications understandably interfere with gene expression and transcription, possibly causing an inappropriate hypoxia response.

Some of the Harker's Island survivors were collected three weeks after the hurricane, and then again, the next spring and fall. As the study had already begun in the spring, Harker's Island became a study in oyster bed recovery over the next year. Here I will investigate the after-hurricane

collections with the one in the spring before to see seasonal vs. hurricane effects. This study will show the long-term effects of the hurricane on mitochondrial respiration, energy storage and cellular component damage on adult oysters, all of whom survived the storm and were alive throughout the study period. Oysters from the intertidal as well as the subtidal zone will be compared to determine differences in habitat. Oysters should be able to handle these mechanical insults, so I hypothesize there will be no change after the hurricane in the Harker's Island oysters that survived. This study emphasizes the use of oyster beds as protective hard substrate against a storm during increasing incidents of severe weather in an era of climate change.

MATERIALS AND METHODS

Animal collection and culture

Harker's Island oyster collections were made in different seasons to show seasonal variability. Harker's Island was sampled four times over two years in 2018 and 2019 – twice in the spring and twice in the fall. The North Carolina site was covered under N.C. Fisheries SEAP Permit Number 929729. All oysters were collected in seafood safe zones, and an attempt was made to collect large adult oysters as determined by eye.

Harker's Island oyster bed is beside a road which acts as a causeway between the mainland and Harker's Island proper. It is on an island in the sound serving as a base for the drawbridge. The oysters were on a rocky slope next to the road and along the edge of the beach-like area on the west side. Being in the open sound near an inlet keeps the salinity as high as the ocean (see Figure 3.1).

At the Harker's Island site and each date of collection at least ten oysters each were collected from the intertidal and subtidal zones at low tide. These were kept on ice overnight, then acclimated in aerated tanks in artificial sea water for 24 hours at native salinity and room

temperature (22±1^{o}C). before dissection and collection of tissues. Optimum temperature for *Crassostrea virginica* has been determined experimentally to be 20±1^{o}C in other studies (Kurochkin et al. 2009); therefore, room temperature was near lowest stress level for temperature..

Mitochondrial function and damage

To determine how environmental conditions impact oysters from each studied location, mitochondria (n=4) were isolated from oysters from each location and habitat. Mitochondria were isolated from oyster gills pooled from two individuals per replicate and assayed using a method described in Chapter 2. Mitochondria were also tested for presence of carbonyls and 4-hydroxynonenal (4-HNE) as evidence of oxidative damage as in Chapter 2(see Appendices A.4 and A.5). Only Spring 2018, Fall 2018, and Spring 2019 collections were tested for mitochondrial respiration and damage.

Energy Storage Capacity

Hepatopancreas tissues were immediately frozen in liquid nitrogen when dissected. All tissues were then stored at -80^{o}C. Hepatopancreas tissue was used as it is used as storage for glycogen and lipids in mammals; however, in oysters, it was found that the hepatopancreas is not the primary site of energy storage (Berthelin et al. 2000), so values may be different than in other tissues such as mantle or gonad. Energy storage capacity of oysters was measured in hepatopancreas tissue in terms of carbohydrate, lipid, and protein assays as described in Chapter 2 (see Appendices A.1, A.2, and A.6).

Cellular component damage

Gill tissues were immediately frozen in liquid nitrogen when dissected. All tissues were then stored at -80^{o}C. Molecular damage by oxidation was determined in gill tissue by measuring products of reactive oxidative processes from heat stress or long term anaerobiosis. This provides a measure of recent environmental stress incurred during metabolism. Carbonyls, DNA degradation, and lipid peroxidation were assayed as in Chapter 2 (see Appendices A.3, A.4, and A.5).

Statistical Analysis

All physiological data was analyzed using a two-factor experimental design and significance were determined by ANOVA in JMP Pro 16 (SAS Institute, Cary, NC 2021) at $p < 0.05$. Outliers were eliminated by the Grubbs method, detecting values outside normal distribution with $p < 0.05$ using GraphPad outlier calculator (GraphPad QuickCalcs Web site: http://www.graphpad.com/quickcalcs/ConfInterval1.cfm (accessed 2019)). Graphs were produced in GraphPad version 9 for Windows (GraphPad Software, San Diego, California USA, www.graphpad.com).

RESULTS

Mitochondrial respiration function showed no significant differences in any states for any season/year or habitat (see Table 3.1, Figures 3.2 and 3.3). Mitochondrial damage, however, was significantly different after the first collection. Surprisingly, whereas previous studies (see Chapter 2) showed no significant difference in mitochondrial damage in habitat, it was different in the two habitats, intertidal and subtidal, over the two-year study. The data shows a significant drop ($p = 0.0499$) in mitochondrial carbonyls in the intertidal oysters from the spring of 2018 before the

hurricane to the spring of 2019. Subtidal oysters showed no significant difference in carbonyl damage from spring 2018 to spring 2019. Mitochondrial lipid peroxidation was also significantly different ($p = 0.0379$) in intertidal and subtidal oysters, with higher levels in intertidal oysters. These were the only significant differences between the intertidal and subtidal oysters in this study and the previous study in Chapter 2. Overall, Harker's Island oysters maintained a high level of lipid peroxidation in the fall of 2018 immediately after the hurricane, but in the spring of 2019, the level had dropped significantly ($p < 0.05$) in both tidal zones.

Cellular component damage (Table 3.4, Figure 3.6) shows a reduction in carbonyls ($p < 0.0001$), just as in the mitochondria, and no significant difference in DNA damage. Lipid peroxidation in the cells, while very low in the mitochondria, was a significantly high level in the cells ($p < 0.0001$) in the fall of 2019, after being very low before then. Lipid peroxidation levels varied over the sampling times, from a high in the spring to low in fall but fall of 2019 was several times the level of the previous fall after the hurricane.

Energy storage over the course of two years at Harker's Island showed cycle of spring and fall for total energy storage (see Table 3.2, Figure 3.4). This correlates with the spawning of oysters to have lower energy stores in the spring and higher energy stores in the fall. However, composition of energy stores between fall of 2018 and fall of 2019 significantly ($p < 0.0001$) differed. The collection taken three weeks after the hurricane showed a typical fall distribution of low carbohydrate level and high lipid storage. The spring of 2019 was comparable to spring of 2018. However, fall of 2019, is significantly different ($p < 0.0001$), and showed a reversal of energy storage from the previous fall, with carbohydrates high and lipids low. This is not the usual fall energy storage state, even though the total energy stored was within the range of a typical yearly cycle (see Table 3.3, Figure 3.5).

DISCUSSION

Mitochondrial respiration showed no change over the year data was collected (Data on mitochondrial respiration and damage was not taken in Fall of 2019). However, Harker's Island oysters showed a large reduction in mitochondrial damage as shown in carbonyls and lipid peroxidation after the hurricane. In the previous year, these oysters in spring 2018 were near spawning and showed high carbonyl and lipid peroxidation levels, which could have been due to the energy expenditure of spawning. The mitochondrial damage remained lower than spring of 2018 for the remainder of the study. This mitochondrial damage was also different among the tidal zones – intertidal oysters had more mitochondrial damage in terms of carbonyls and lipid peroxidation than subtidal oysters.

Energy storage compounds in the spring 2019 at Harker's Island matched the spring before. In the fall of 2019, however, energy storage components showed an atypical fall distribution with carbohydrates being high and lipids low, the opposite of usual energy storage winter preparation. The total energy in kilojoules, however, was the same as the fall before, but in a different composition. By all indications from the biochemical composition, the Harker's Island oysters did not spawn in 2019 and had accumulated unused carbohydrate stores from the spring. This might also explain the low mitochondrial damage in the spring of 2019 if the oysters did not experience the bioenergetic stress of spawning.

Cellular carbonyls also dropped immediately after the hurricane but began increasing each season afterward. The reason for this is unclear. There was no DNA damage evident, but lipid peroxidation in fall 2019 was as much as four-fold the fall before. This coincided with a reduction in lipid storage in fall 2019, most likely from lipid destruction due to the incremental rise in 4-HNE. Hydroxynonenal is a strong oxidation by-product that causes carbonyl protein damage as

well as DNA damage. The DNA appears to be unaffected; however, it could explain the rise in carbonyls. The source of this oxidative stress response the year after the hurricane is unknown but could be related to an interruption of the spawning cycle.

Other weather-related causes do not appear to be a factor. According to worldweatheronline.com, the average low temperature in winter of 2018 was 4^{o}C cooler than the year before; however, this was not an unusual range of differences over a 10-year period, and not the maximum nor the minimum during the period of 2012 to 2022. Average high temperatures during the same period did not change more than a degree, and no other potential weather causes could be found.

Crassostrea virginica individuals can live as old as ten years in the wild and start life generally as males. As they grow older and larger, the oysters can switch sexes and become female in a pattern of sexuality called *protandric dioecy* (Bayne 2017). This results in a life cycle where the larger individuals, having more energy capacity, can become female and produce eggs, an energy intensive task. One-year old oysters are likely to be mostly males. It is possible that the older, larger oysters were mostly females and were killed by mechanical trauma from the hurricane wave action or silting, and only the younger ones, mostly male, survived. I did not notice a difference in size of the oysters in the spring of 2019, but the amorphic shape of oysters makes it difficult to determine age and size. For whatever reason, it appears that Harker's Island oysters tested may not have spawned in the spring of 2019 after the hurricane, and the effects were still apparent in the fall one year after the storm.

CONCLUSION

As stressful as life in the intertidal zone is for oysters, episodic climate events can add another stress that can disrupt life functions of eastern oysters. The intertidal oysters at Harker's Island were more affected by the hurricane than the subtidal oysters physiologically among survivors, even though most of the subtidal oysters died from physical damage from silting. The seasonal patterns of energy storage and possibly spawning were impacted by a hurricane a year after the event. Even though the oysters took the brunt of the force of the storm, they did survive as a population. Other oyster beds in the estuaries were decimated by the freshwater flooding and did not recover. Severe climatic events, which may increase in frequency over the coming years, do affect oysters in negative ways and may put this ancient group of bivalves in jeopardy.

TABLE 3.1

Mitochondrial Respiration and Damage – Harker's Island Pre- and Post-hurricane

Parameters	**Tissue**	**Before/After (Season/year)**	**Habitat**	**Before/after X Habitat**
RCR	Mitochondria	$F_{2,23} = 2.2175$ $p = 0.1378$	$F_{1,23} = 0.4235$ $p = 0.5234$	$F_{5,23} = 0.8233$ $p = 0.4549$
RCR+	Mitochondria	$F_{2,23} = 7295$ $p = 0.4959$	$F_{1,23} = 1.3940$ $p = 0.2531$	$F_{5,23} = 0.9278$ $p = 0.4135$
Stage 3	Mitochondria	$F_{2,21} = 2.5131$ $p = 0.1106$	$F_{1,21} = 0.0042$ $p = 0.9490$	$F_{5,21} = 1.6752$ $p = 0.2167$
Stage 4	Mitochondria	$F_{2,23} = 2.0417$ $p = 0.1588$	$F_{1,23} = 0.2349$ $p = 0.6338$	$F_{5,23} = 0.5175$ $p = 0.6046$
Stage 4+	Mitochondria	$F_{2,23} = 1.8032$ $p = 0.1933$	$F_{1,23} = 0.1146$ $p = 0.7389$	$F_{5,23} = 0.5283$ $p = 0.5985$
Carbonyl Concentration	Mitochondria	$F_{2,23} = 10.1329$ $p =$ **0.0011***	$F_{1,23} = 4.4197$ $p =$ **0.0499***	$F_{5,23} = 4.7286$ $p =$ **0.0224***
Lipid Perox. (HNE)	Mitochondria	$F_{2,23} = 75.7818$ $p <$ **0.0001***	$F_{1,23} = 5.0183$ $p =$ **0.0379***	$F_{5,23} = 1.8898$ $p = 0.1799$

Table 3.1. ANOVA: Effects of ex*p*erimental conditions and/or populations on the Mitochondrial Respiration and Mitochondrial Damage in *Crassostrea virginica*. F ratios with the degrees of freedom for the factor effect and the error shown as a subscript, are given. Significant effects ($p < 0.05$) are highlighted in bold.

TABLE 3.2

Energy Storage Components - Pre- and Post- Hurricane Harker's Island

Parameters	**Tissue**	**Before/After (Season/year)**	**Habitat**	**Before/after X Habitat**
Protein Concentration	Hepatopancreas	$F_{3,77}$=30.0968 p < **0.0001***	$F_{1,77}$=2.6561 p = 0.1076	$F_{7,77}$=0.0667 p = 0.9774
Lipid Concentration	Hepatopancreas	$F_{3,75}$= 119.7873 p < **0.0001***	$F_{1,75}$= 0.0160 p = 0.8996	$F_{7,75}$= 0.2397 p = 0.8684
Glycogen/glucose	Hepatopancreas	$F_{3,71}$= 15.7190 p < **0.0001***	$F_{1,71}$= 0.9919 p = 0.3230	$F_{7,71}$ = 0.4975 p = 0.6853

Table 3.2. ANOVA: Effects of ex*p*erimental conditions and/or populations on the Energy Storage Components in *Crassostrea virginica*. F ratios with the degrees of freedom for the factor effect and the error shown as a subscript, are given. Significant effects ($p < 0.05$) are highlighted in bold.

TABLE 3.3

Sum of Energy Components – Harker's Island Pre- and Post-Hurricane

Parameters	**Tissue**	**Before/After (Season/year)**	**Habitat**	**Before/after X Habitat**
Sum of Energy Component (kJ)	Hepatopancreas	$F_{3,77}$= 40.3776 p < **0.0001***	$F_{1,77}$= 0.6633 p = 0.4193	$F_{7,77}$ = 9.75581 p = 0.7367

Table 3.3. ANOVA: Effects of ex*p*erimental conditions and/or populations on the Sum of Energy Components in *Crassostrea virginica*. F ratios with the degrees of freedom for the factor effect and the error shown as a subscript, are given. Significant effects ($p < 0.05$) are highlighted in bold.

TABLE 3.4

Cellular Component Damage - Pre- and Post- Hurricane Harker's Island

Parameters	**Tissue**	**Before/After (Season/year)**	**Habitat**	**Before/after X Habitat**
Carbonyl Concentration	Gills	$F_{3,75}$=19.6447 p < **0.0001***	$F_{1,75}$=3.7497 p = 0.0569	$F_{7,75}$=1.6046 p = 0.1962
HNE (Lipid Peroxidation)	Gills	$F_{3,59}$= 94.8410 p < **0.0001***	$F_{1,59}$= 1.1938 p = 0.2797	$F_{7,59}$=1.9898 p = 0.1272
DNA Damage	Hepatopancreas	$F_{3,65}$= 0.1254 p = 0.9447	$F_{1,65}$= 0.1809 p = - 0.6722	$F_{7,65}$= 1.4083 p = 0.2495

Table 3.4. ANOVA: Effects of ex*p*erimental conditions and/or populations on the Cellular Component Damage in *Crassostrea virginica*. F ratios with the degrees of freedom for the factor effect and the error shown as a subscript, are given. Significant effects ($p < 0.05$) are highlighted in bold.

FIGURE 3.1

Harker's Island Oyster Collection Site

Figure 3.1. Red stars show location of the Harker's Island oyster collection site. Yellow circle shows landfall location and approximate track of Hurricane Florence. Strong winds over washed the roadway from the east, dumping sand and debris on the oysters on the west side.

FIGURE 3.2

Mitochondrial Respiration – Harker's Island Pre- and Post- Hurricane

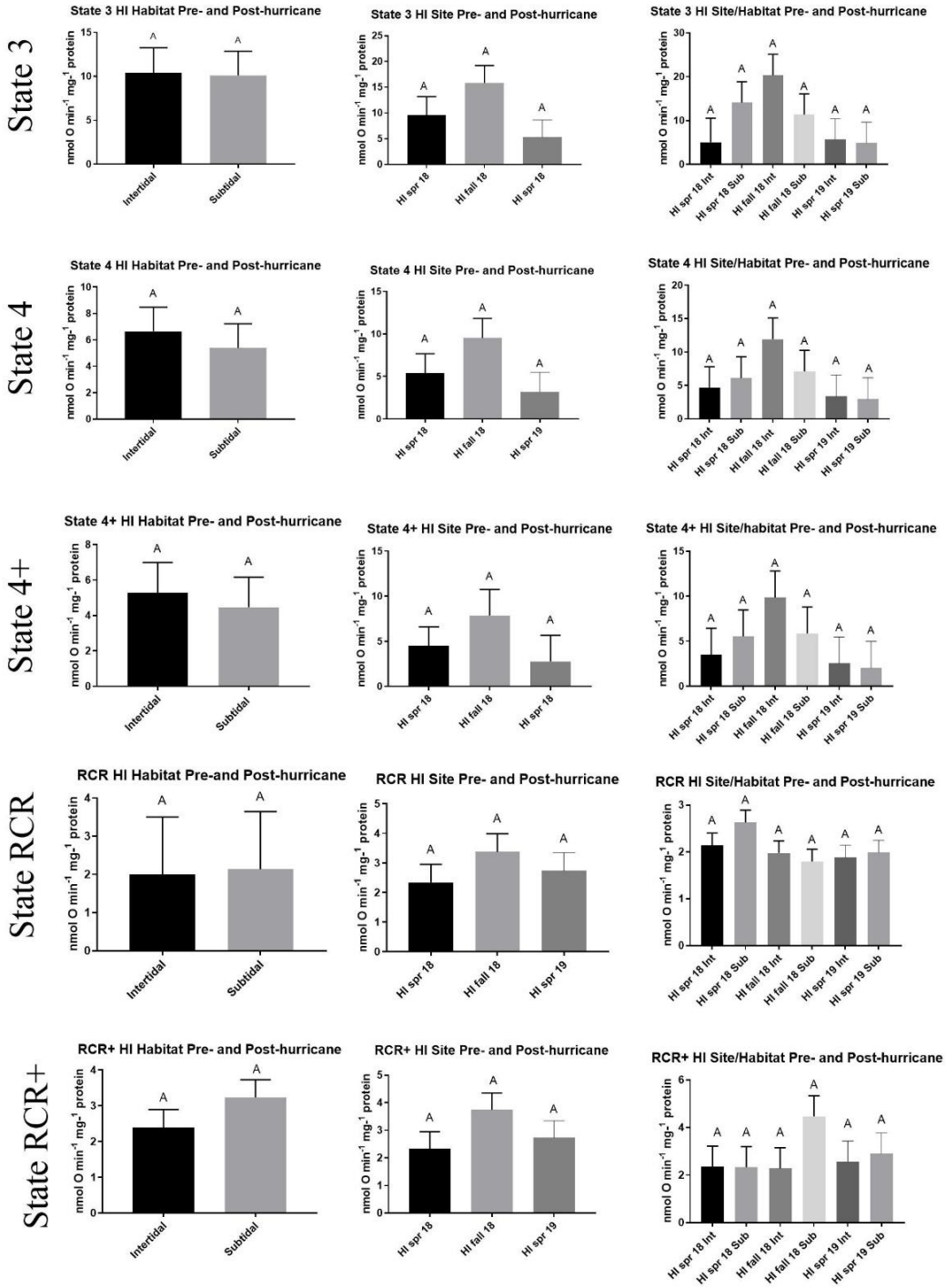

Figure 3.2. Different letters indicate the values that are significantly different among *C. virginica* from different zones ($p < 0.05$); if columns share a letter, the respective values are not significantly different ($p > 0.05$). Vertical bars represent the standard error of means.

FIGURE 3.3

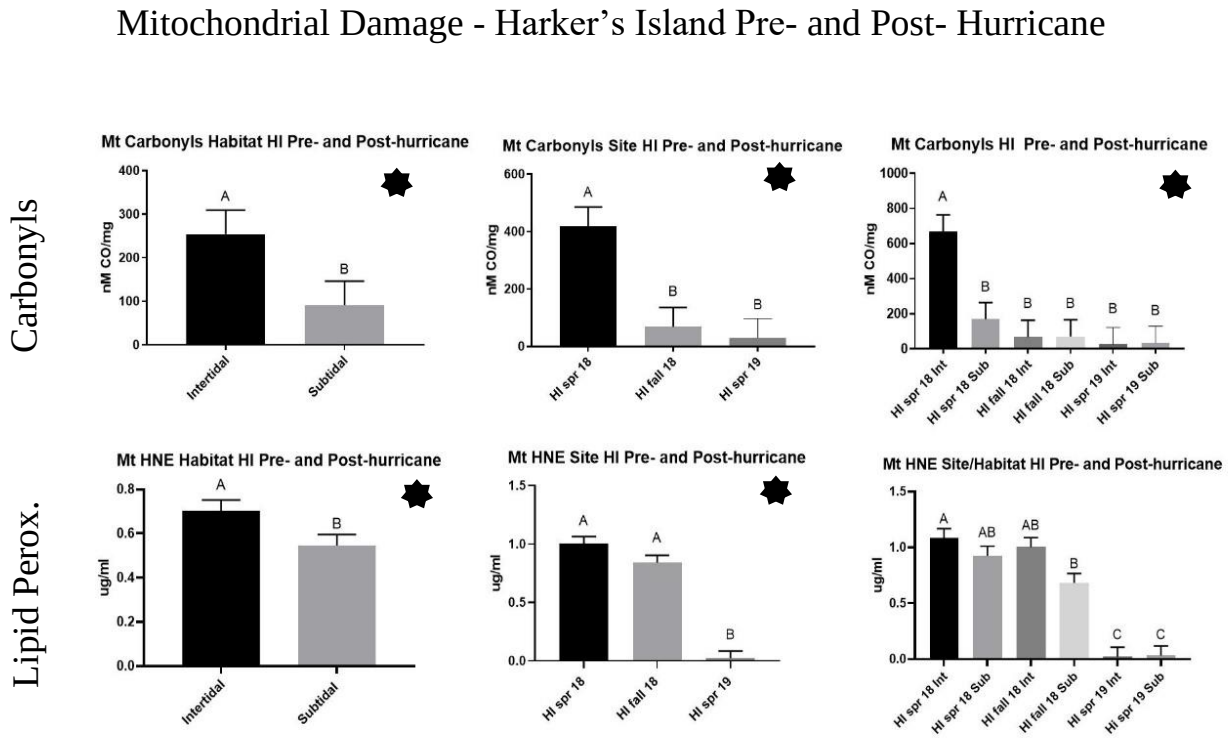

Figure 3.3. Different letters indicate the values that are significantly different among *C. virginica* from different zones ($p < 0.05$); if columns share a letter, the respective values are not significantly different ($p > 0.05$). Vertical bars represent the standard error of means. ✸ Indicates overall significance.

FIGURE 3.4

Energy Storage Components – Harker's Island Pre- and Post-hurricane

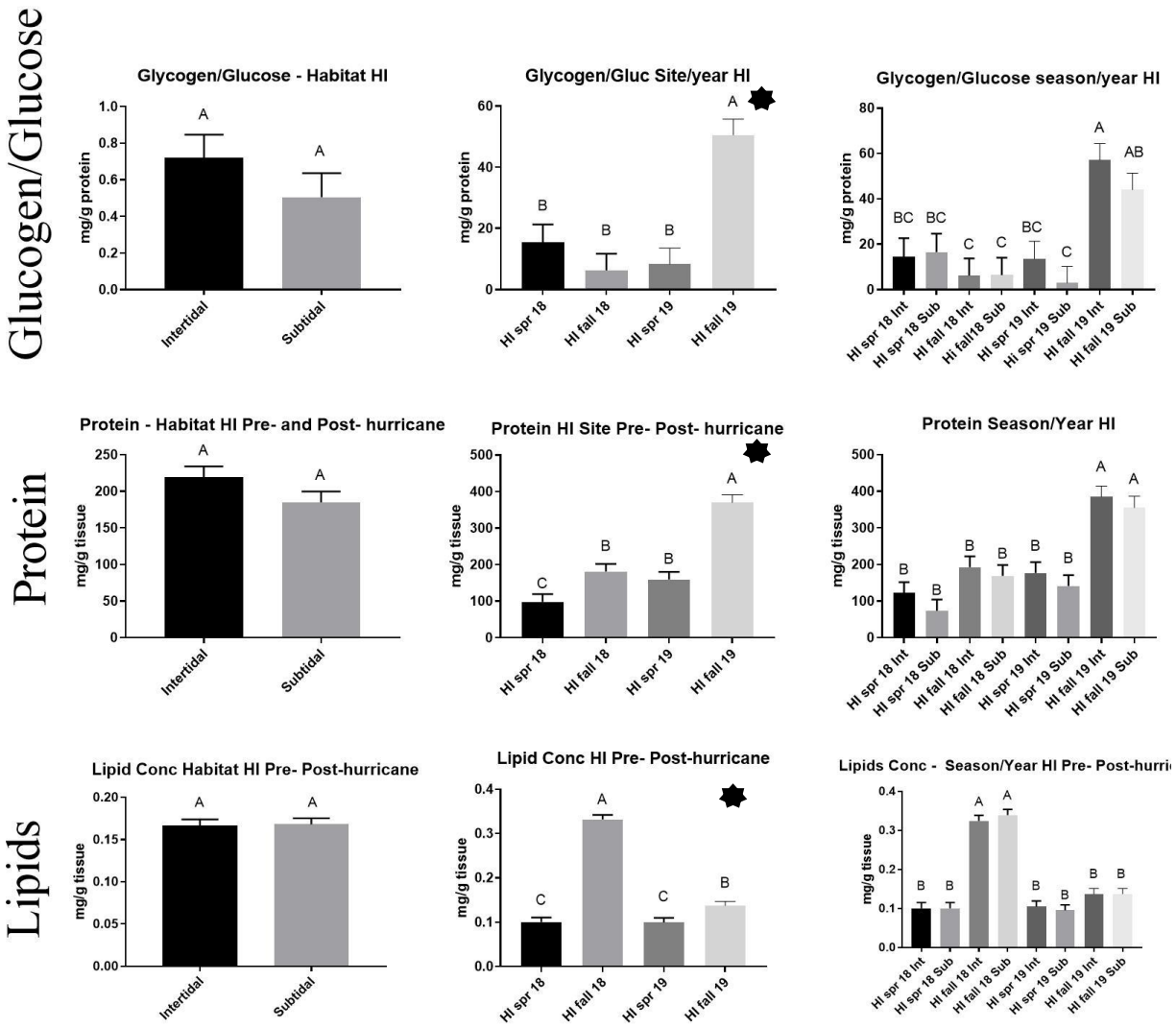

Figure 3.4. Different letters indicate the values that are significantly different among *C. virginica* from different zones ($p < 0.05$); if columns share a letter, the respective values are not significantly different ($p > 0.05$). Vertical bars represent the standard error of means. ✸ Indicates overall significance.

FIGURE 3.5

Sum of Energy Components – Harker's Island Pre- and Post- Hurricane

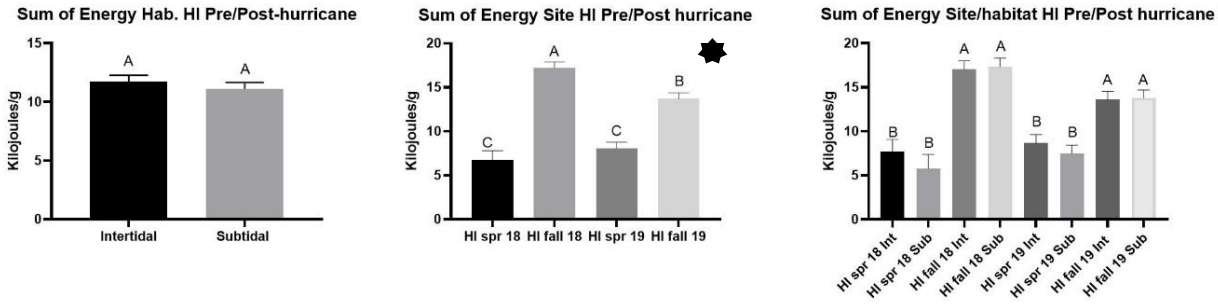

Figure 3.5. Different letters indicate the values that are significantly different among *C. virginica* from different zones ($p < 0.05$); if columns share a letter, the respective values are not significantly different ($p > 0.05$). Vertical bars represent the standard error of means. ✹ Indicates overall significance.

FIGURE 3.6

Cellular Oxidation Damage - Harker's Island Pre- and Post-hurricane

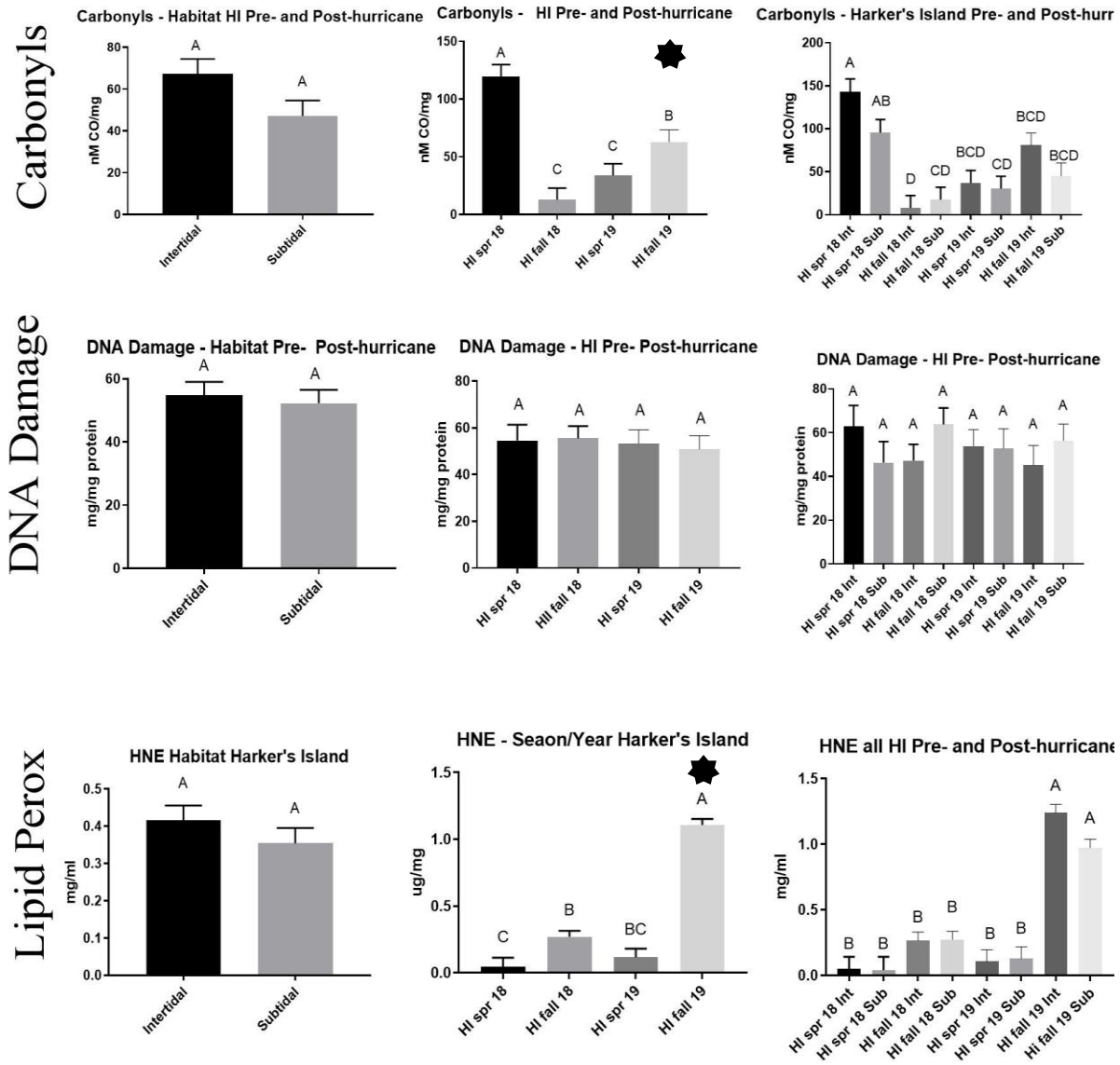

Figure 3.6. Different letters indicate the values that are significantly different among *C. virginica* from different zones ($p < 0.05$); if columns share a letter, the respective values are not significantly different ($p > 0.05$). Vertical bars represent the standard error of means. ✸ Indicates overall significance.

CHAPTER FOUR

PHYLOGENETICS AND IMMUNITY GENE EXPRESSION IN EASTERN OYSTERS OF NORTH AND SOUTH CAROLINA

(Furr, Denise; Reitzel, Adam; Ivanina, Anna)

ABSTRACT

Eastern oysters (*Crassostrea virginica*) have long been recognized as model organisms of extreme environmental tolerance, showing resilience to variation in temperature, salinity, hypoxia, and microbial pathogens. These phenotypic responses, however, show variability between geographic locations or tidal habitats. Physiological and genetic differences occur in populations throughout a species' geographical range, which may have been shaped by regional abiotic and biotic variations. Few studies of *Crassostrea virginica* have explored the combined factors of immunity gene expression and the genetic relationships of individuals between these locations. We measure innate immunity gene expression of hemocytes in different natural locations and habitats to compare basal expression and stress response in oysters. To characterize the genetic relationships of three locations of native oysters along the North Carolina and South Carolina coast, we sequenced a portion of cytochrome oxidase subunit I (COI) and a portion of the 16S gene. In wild oysters, expression of TNF (stress communication) and SRCR (tissue damage signaling) showed the strongest discrepancy between sites with extreme salinities. The gene expression results show a significant deficiency in cell damage signaling and stress communication in oysters in locations of their salinity tolerance extremes. The COI mismatch distributions are indicative of a gene flow along the coast with Harker's Island being the most likely to gain outside recruits, and 16S confirms the geographic position of these genotypes. These results are informative for understanding the range of physiological plasticity for stress responses in a native

oyster species, with implications for in the conservation effort to restore native oyster beds susceptible to salinity changes and rising pathogen loads.

INTRODUCTION

The innate immune system for Crassostrea virginica has been historically described as an innate immune system similar to other invertebrates. It has been assumed that invertebrates have no immunological memory with regards to pathogens (Wang et al. 2018). However, the oyster innate immune system has sophisticated forms of specificity which mimic vertebrate adaptive immunity; for instance, exposure to a pathogen can provide protection from that pathogen later through "innate immune-priming" with several mechanisms recognized (Wang et al. 2018). Several immune-related gene families have been greatly expanded in oysters associated with pathogen specificity (McDowell et al. 2016; Zhang et al. 2016).

Mucosal membranes of the gut and gills entrap and destroy pathogens before they can enter the oyster tissues, neutralizing most of them (Allam and Espinosa 2016). Mollusks can also increase production of protective mucoproteins in the presence of pathogens (Allam and Espinosa 2016). Oyster hemocytes, analogous to vertebrate white blood cells, stage the next defense against pathogens by recognizing and phagocytizing pathogens in the open circulatory system. Pattern Recognition Receptors (PRRs) bound to hemocytes can be very specific to particular pathogens or pathogen parts (Lv et al. 2018). PRRs such as Toll-like Receptors (TLRs) and Scavenger Receptors (SRCRs) are responsible for recognizing bacteria, but also function in the signaling and communicating pathways (Canesi and Pruzzo 2016; Song et al. 2010; Uematsu and Akira 2008). Immune effectors, those compounds that destroy the pathogen, in bivalves are highly diversified homologs of vertebrate immunity including cytokines, complement factors (like C3q), C-type

lectins, defensins and lysozymes (Zhang et al. 2016). For example, cytokines, like the Tumor Necrosis Factor (TNF). have diverse forms that not only signal the presence of a pathogen, but attack pathogens, including some fungi (Song et al. 2010). Finally, antioxidants play a huge role in the oysters' abilities to survive long term hypoxia and heat stress (Song et al. 2010).

Immunity factor gene expression

Oysters may have different responses to pathogens in different stages of life and location relative to the water. Intertidal and subtidal oysters experience different immunological challenges. It has been speculated that bacterial and viral pathogens are not as prevalent in the intertidal zone due to extremes of temperature. However, the reverse is true; intertidal oysters have been found to experience a higher load of *Perkinsus marinus* than subtidal oysters even though subtidal oysters have higher exposure due to longer periods of submersion (Malek and Byers 2017). Pathogens such as *Vibrio* sp. have been found in all salinity levels; however, oyster mortality due to a pathogen in oysters has been found to be substantially higher in low salinities (<10ppt.) (Li et al. 2022).

Immunity gene expression would be expected to differ between populations and tidal habitats due to differences in pathogen load. Salinity and temperature play a significant role in the amount of pathogen in the environment (Fleury et al. 2020). As oceans warm and shorelines rise, oysters face many challenges with extremes of temperature. Pathogens may spread into areas previously protected by cooler temperatures, such as was found in the increase in the prevalence of *Vibrio* species in the UK waters due to warming sea-surface temperature (Harrison et al. 2022).

We tested for mRNA expressed factors that may indicate a physiological or genetic advantage or disadvantage for oysters occupying a specific salinity or tidal elevation. A difference

in these factors would indicate resistance or susceptibility to pathogens for these regions as oysters mature. A higher morbidity to pathogens specific to the salinity or elevation may eliminate those oysters and produce a population of oysters with a more robust immunity in that location detectable by mRNA expression.

Oyster genetics

The species *Crassostrea virginica*, our common eastern oyster, ranges from Canada to Brazil in the Western Atlantic, and is still considered the same species. Oysters are difficult to identify to species morphologically due to the largely amorphic shell morphology (Guo et al. 2018), which may partially explain the historical lack of division of western Atlantic morphological species. Genetics has added credence to morphological data. The broad population genetics of the eastern oyster has been documented by allozyme, microsatellite and now, direct DNA analysis (Reeb and Avise 1990); however, *C. virginica* has remained one species thus far. A sister species, *Crassostrea gigas,* inhabits the Pacific Ocean, and both *C. virginica* and *C. gigas* genomes have been sequenced recently (Gómez-Chiarri et al. 2015; Zhang et al. 2012). The two species remain recognized species as originally described, although biogeographic clines have been reported in *C. virginica* by several authors (Hare and Avise 1996; Karl and Avise 1992; Reeb and Avise 1990) in spite of the highly dispersible planktonic larvae (Buroker 1983). Genetic work is still in progress with oysters, and cryptic species may still exist (Guo et al. 2018).

Previous studies have shown that populations of cultured oysters in the southeastern United States show a mixed genetic heritage by COI sequencing (Furr et al. 2021) (see Fig 5.4 in Chapter 5). These oysters are artificially seeded and raised in hatcheries by aquafarmers before being set out to grow in cages for the seafood market. It is no surprise that the heritage of these oysters is

mixed since hatcheries may use oyster larvae from different sources. Wild oysters disperse gametes into the water during spawning and were considered mostly homogenous due to wide larval dispersal. However, larval dispersal has been found to be uneven due to currents and temperature (Palumbi 1994). Large mortalities occur before recruitment. Due to the huge numbers of larvae spawned and juvenile recruitment risks, a variable genetic component for tidal elevation could exist within a recognized species. Because oyster settlement is hypothesized to be mostly random and opportunistic, oyster spat must find their recruitment suitable spot or they do not survive. Microhabitats such as the intertidal and subtidal zones may result in differential survival for a juvenile in the specific microhabitat upon which they land.

COI sequencing and gene expression was used in oysters from wild oyster beds to investigate the relationship between the wild oyster bed sites in North and South Carolina, as well as microhabitat phylogenetic differences in intertidal and subtidal microhabitats. It is hypothesized that location and microhabitat will both show significant evidence of genetic subdivision and differential gene expression.

MATERIALS AND METHODS

Animal Collection and Culture

Wild native oysters were field collected from three sites, two in North Carolina and one in South Carolina (Fig. 3). Both intertidal and subtidal oysters were taken at each site (see Chapter 2). The North Carolina sites were covered under N.C. Fisheries SEAP Permit Number 929729. Baruch Research Station in Georgetown, South Carolina, has issued a collection permit for that site. All oysters were collected in seafood safe zones. The Federal Point (FP), and Harker's Island (HI) oysters were collected in the Spring of 2018, and Baruch Research Station (BR) oysters were collected in the spring of 2019 for this study.

The three sites are in different macrohabitats as well as different salinities. HI oyster bed is beside a road which acts as a causeway between the mainland and Harker's Island proper. It is on an island in the sound serving as a base for the drawbridge. The oysters were on a rocky slope next to the road and along the edge of the beach-like area. Being in the open sound near an inlet keeps the salinity as high as the ocean (about 35 ppt). FP oysters were in a marsh, covered with marsh grass, near the parking area for the Wildlife Resources Commission Boating Access near Fort Fisher, NC. The Federal Point site is also in the middle of the Cape Fear River as it interacts with the ocean in tidal cycles, but approximately a mile from the mouth of the river, and so is highly influenced by freshwater outflow. BR, at the Baruch Institute of Marine Sciences, has a huge marsh accessible by boardwalk protected by barrier islands. It is mostly bare of grass, with beds of oysters in silty mud, and oysters were obtained from the open tidal marsh at the end of the boardwalk. Although the marsh salinity fluctuates with tides, it is consistently intermediate at around 25ppt.

At each site and date of collection at least ten oysters each were collected from the intertidal and subtidal zones at low tide. These were kept on ice overnight, then acclimated in aerated tanks in artificial sea water for 24 hours at native salinity and room temperature ($22\pm1^{o}C$). before dissection and collection of tissues. Optimum temperature for *Crassostrea virginica* has been determined experimentally to be $20\pm1^{o}C$ in other studies (Kurochkin et al. 2009); therefore, room temperature was considered near lowest stress level.

Immunity gene expression

Hemolymph is extracted from the individual oysters (n=10) from each location through collection with a sterile 10-ml syringe with a 21-gauge needle containing 1 ml ice-cold filtered

ASW to prevent aggregation of the hemocytes. Hemolymph samples are centrifuged for 10 min at 1000× *g*. The hemocyte pellet is washed once with ice-cold ASW and stored at −80 °C until RNA extraction. Total RNA is extracted from hemocytes using a RNA MiniPrep™ kit (Zymo Research, Irvine, CA, USA) according to the manufacturer instructions. RNA concentration is measured using NanoDrop 2000 spectrophotometer (Thermo Scientific, Pittsburg, USA) and expressed as μg RNA 10^{-6} cells. Cell count was determined by hemocytometer on a compound scope. Single-stranded cDNA was synthesized from 0.5 μg of the total RNA using 50 U μl^{-1} SMARTScribe™ Reverse Transcriptase (Clontech, Mountain View, CA, USA) and 20 μmol l^{-1} of oligo$(dT)_{18}$ primers.

Expression of target genes was determined with quantitative real-time PCR (qRT-PCR) using a 7500 Fast Real-Time PCR System (Applied Biosystems/Life Technologies, Carlsbad, CA, USA) and SYBR® Green PCR kit (Life Technologies, Bedford, MA, USA) according to the manufacturer protocol. The primer sequences are provided in Figure 4.2. The qRT-PCR reaction mixture consists of 7.5 μl of 2× SYBR® Green master mix, 0.3 μmol l^{-1} of each forward and reverse gene-specific primers, 1.5 μl of 10× diluted cDNA template and water to adjust to 15 μl. The reaction mixture is subjected to the following cycling: 15 s at 95 °C to denature DNA and activate Taq polymerase and 40 cycles of 15 s at 94 °C, 30 s at 55 °C (actin and C-type lectin); 58 °C (TLR2, TLR3, TLR4, Mannose Rec2 and TNF); or 62°C (SRCR) and 30 s at 72 °C. Serial dilutions of a cDNA standard are amplified in each run to determine amplification efficiency (Pfaffl 2001). Amplification efficiencies are 1.74-2.19 for all studied genes. A single cDNA sample from *Crassostrea virginica* hemocytes is used as an internal cDNA standard and included in each run to test for run-to-run amplification variability. The target gene mRNA expression is standardized relative to β-actin mRNA as described elsewhere (Ivanina et al. 2013; Pfaffl 2001;

Sanni et al. 2008). Gene expression data were calculated with the delta-delta Ct method that compares differential expression of the target gene and β-actin. Values are statistically evaluated using two-way ANOVA in JMP Pro 16 (SAS Institute, Cary, NC 2021) and graphed in GraphPad version 9 for Windows (GraphPad Software, San Diego, California USA, www.graphpad.com).

Oyster genetics of COI and 16S

Animal collection and preparation is done as described in Chapter 2 at three locations, FP, HI, and BR, and two microhabitats, intertidal and subtidal. Adductor muscle is dissected from each oyster, preserved in 100% ethanol and stored at -80^{o}C. Oyster COI sequencing has been done in the lab previously with cultured oysters (Furr et al. 2021) (see Chapter 5).

DNA sequences were analyzed from individual oysters from the three sites, representing three salinities. Intertidal and subtidal oysters from these sites were analyzed separately to determine differences between habitat as well as location. COI, a common genetic marker to determine population differences, was sequenced to determine the variation between location (and salinity) as well as microhabitat. DNA was extracted using a protocol developed specially for mollusks (see Appendix A.8). As determined in the previous study in Chapter 5, standard Folmer COI primers do not work with *Crassostrea virginica*, a common problem with mollusks. The COI gene is amplified with custom species-specific primer sequences (Cvi_F: 5'-TTGGGCAGTTTTAGCTGGGA-3'; Cvi_R: 5'-AAGGAGCATAGTAAGCCCGC-3'). A Q5 High Fidelity 2X Master Mix (New England Bio Labs) is used as a polymerase plus buffer for amplification. PCR results are confirmed by electrophoresis gel with a single band ~450bp, or gel purified, and then submitted for Sanger sequencing (Eurofins). Sequences are aligned with Muscle, phylogenies were constructed with maximum likelihood with bootstrap values using a Hasegawa-

Kishino-Yano model in MEGA11 (Tamura et al. 2021). Traces are corrected in SnapGene Software (www.snapgene.com). Variation within the species and pairwise comparisons are determined with DnaSP (Rozas et al. 2017).

The 16S gene is sequenced using mollusk specific primers as well. These were developed for land snails but worked well for oysters (see Chapter 6). The 16S primers used are 16SpolyF_5' GCCGCAGTACTTTGACTGTG-3' and 16SpolyR_5'-CCAACATCGAGGTCACAAAC-3'. A Q5 High Fidelity 2X Master Mix (New England Bio Labs) is used as a polymerase plus buffer for amplification as for COI. Phylogenic analysis in the same as for COI.

RESULTS

Immunity gene expression

Transcriptional profiles for genes involved in stress-sensing, stress-signaling and stress-response were obtained for oysters from the three locations. Five of the genes studied were stress-sensing genes (TLR2, TLR3, TLR4, MR2, and SRCR) involved in signaling tissue damage. A stress-communicating molecule, TNF, was also studied which is involved in communicating stress or pathogen recognition. Immune effectors (stress-response genes) C-type lectin, big-defensin, C3q, and lysozyme were also studied, which can neutralize pathogens (Wang et al. 2018).

In most immunity factors tested, there are no differences between the habitats, sites, or the interaction of habitat X site (see Table 4.1). Notable differences are TNF and SRCR, which shows significant variation with *P* values of $p = 0.0148$ and $p < 0.0001$ respectively between the sites, which differ mainly in salinity. Nearly no TNF was detected at extremes of salinity at FP (12ppt) and HI (35ppt). However, the intermediate site at Baruch Research Station (25ppt) has a high level of TNF. The exact same pattern was observed for SRCR, which is low in the salinity extremes,

but high at the intermediate salinity at BR. Big Defensin and lysozyme factors failed to amplify in the Baruch sample for unknown reasons, but there are no discernible differences in data from the other two sites. There is no significant difference between location or tidal elevation in the other immunity factors.

Oyster genetics of COI and 16S

Sequencing of the COI gene shows very similar sequences in all locations and tidal elevations with bootstrap values of close to zero for all but two tip clades (see Figure 4.3). Fifty-eight samples are sequenced with n = 9 to 10 from each location and tidal elevation. Four SNP locations (140, 141, 144, and 272 of 279 bases) have multiple haplotypes which may be informative. The other SNPs appear to be random one-offs, with 10 total haplotypes.

The COI distance statistics from DnaSP (Rozas et al. 2017) were not informative for population differentiation. Genetic distances are all zero and below, predictably (see Table 4.3). The Chi square value of genetic distances is not significant with a *P* value of $p = 0.5316$. Fu's F is strongly negative, -9.027and Tajima's D is also negative (-2.19425) and is significant ($p < 0.01$).

Mismatch distribution (Pairwise nucleotide comparison) showed correlation with the expected curve (which indicates a population in equilibrium and no expansion) for locations and tidal zones (see Table 4.2, Figures 4.4 – 4.6). In Figure 4.4, BR Station and FP are a close match to the expected curve with small deviations. HI, however, is strongly multimodal. In Figure 4.5, the multimodal state is shown to be somewhat present in all the populations when broken down by tidal zone, but most strongly in FP intertidal, HI subtidal and BR subtidal. When all tidal zone locations are examined together in Figure 4.6, the subtidal zone shows a marked difference in modality and raggedness, indicating more expansion in the population, and the intertidal oysters

closer to a constant and expected population dynamic (Harpending 1994). Smoothness of the curves indicates a large number of recruits from outside in all populations (Ray et al. 2003).

The 16S sequencing of *Crassostrea virginica* shows little difference in sequences of all three locations and two tidal zones. All bootstraps in the phylogeny (see Figure 4.7) except one were near zero, indicating nearly identical sequences. Only seven SNPs were found in the 55 sequences, and these appear to be unique mutations for single individuals except perhaps one clade that shows a bootstrap value of 67 on the phylogeny. These two specimens of FP intertidal oysters share one SNP in common at site 49 of the 215 bases in the 16S sequence. However, a known motif, 5'-GAAATTCTA-3", is found in the 16S sequence that places all the oysters in the southern region population.

DISCUSSION

Immunity factor gene expression

The immunity gene data showed significant differences in levels of TNF and SRCR, two stress and cell/tissue damage communication and signaling genes between locations. These factors have signaling functions, indicating localized tissue damage detection. The expression of these genes may be affected by the salinities of the different locations. The level of the gene expression of these signaling genes was lowest at the extremes of oyster salinity tolerance (12 ppt and 35 ppt) and highest in the intermediate salinity (25 ppt). It has been reported that oysters may or may not increase SRCR, and TNF actually decreased in response to the presence of pathogens (Furr et al. 2021)(see Chapter 5). Therefore, the presence of a pathogen is not a likely cause of the increase of expression of immunity genes in the intermediate salinity. Oysters in extremes of salinity (12 and 35 ppt) may be susceptible to pathogens that cause tissue damage due to impaired signaling response caused by a deficiency of these immunity factors.

These results of immunity gene expression are in contrast to that of Furr et al. (2021) where there was no significant variation between locations (under normalized conditions) of cultivated oysters with regard to TNF and SRCR (Furr et al. 2021); however, there were differences between locations in the levels of factors TLR2, Mannose Receptor-2 and lysozyme. The oysters of Furr et al. (2021) were of undetermined heritage from hatcheries and may have been reacting to different environmental cues than the hatchery where they were first grown, or they may be exhibiting a reaction to a specific cue in the particular current location. There is no evidence of significant response based on tidal zone habitat or the interaction of site and habitat in any of the genes expressed.

Oyster genetics of COI and 16S

Both COI and 16S mitochondrial genes are well conserved with little sequence variation in oysters as in most animals, except land snails (Thomaz et al. 1996). This research confirms there is very little variation in the COI gene and nearly zero in the 16S gene. However, the COI was variable enough for population comparisons, and a regional motif was found in the 16S gene, confirming an earlier study (Ó Foighil et al. 1995).

The COI sequences were used for mismatch distributions of pairwise nucleotide comparisons. All of the statistics for the mismatch distributions are non-significant, but the shape of the curve is indicates some differences between collection sites. The comparison of location, location and tidal zone, and just tidal zone showed some distinct differences in modality. All location/tidal zone charts showed some multimodality, indicating expansion and the influx of outsiders into the population, which is expected of a free spawning organism. Surprisingly, the FP intertidal and both BR and HI subtidal were strongly multimodal, which indicates expansion. The FP subtidal, BR and HI intertidal were close to expected, which indicates stability and equilibrium.

This may indicate that these close to expected are most stable and have less immigration than the multimodal groups. If the mismatch distribution of just tidal zone are compared, the subtidal zone has the most expansion from immigration, while the intertidal oysters are a very close match to the constant and expected population curve. In terms of location only, HI is showed the clearest multimodal pattern whereas the others are close to expected. This phenomenon at HI was driven by the subtidal, which experiences a large turnover. Constant submersion in high salinity may face predation and overgrowth that causes a high attrition rate, plus being open to the ocean is an opportunity for recruits from further down the coast.

There was no significance in the genetic distances (F_{ST} values), indicating common gene flow; however, the Fu's F and Tajima's D values were strongly negative and significant ($p<0.01$) indicating an expanding population, probably due to the outside recruitment. Overall, the oysters are dynamic populations well connected to others along the coast, especially at HI.

Ó Foighil et al. (1995) identified three distinct haplotypes based on the 16S gene of *Crassostrea virginica* on the Atlantic coast, a northern haplotype north of Cape Hatteras, a southern haplotype on the southeast coast, and another haplotype in the Gulf (Ó Foighil et al. 1995). These are distinguished by variation in a motif at his 288 - 296 site (166 - 174 in the sequences used in this study). The southern haplotype of the Southeast coast is identified by the motif 5'-GAAATTCTA-3" as opposed to the motif in the North of 5"-TAAATTCTA. The Gulf Coast haplotype is 5'-GAATTCTG-3'. Varney et al. (2016) found a mix of haplotypes on the North Carolina coast from the Pamlico Sound in the north to the SC state line with the majority (71%) being the southern haplotype. In their study of 16S gene in *Crassostrea virginica*, some of the specimens were collected north and around Cape Hatteras, which is considered a natural cline for oysters separating northern and southern populations. This may explain the number of northern

haplotypes in their samples. They also had 17 oysters (0.5%) that were of the Gulf Coast haplotype (Varney et al. 2009). Of the oysters in this study, 100% are the southern haplotype, regardless of location and tidal elevation. Gulf Coast oysters are not detected in this study. None of the seven SNPs in our alignment are located in the motif region.

The three localities are relatively close geographically, approximately 120 miles apart, on the south facing northern shore of the South Atlantic Bight. This section of coastline is in the direct path of the north flowing Gulf Stream. Our sample size was small compared to Varney et al (2016) which may have missed the Gulf oysters, and all locations used here were well south, nearly 100 miles of the Cape Hatteras cline, likely too far for infiltration of the northern population. The Gulf Stream current also likely has a strong influence on the cline and keeps northern larvae from being transported south. A larger sample size may be needed to discover any small inclusion of Gulf Coast oysters in the sampling. The tidal elevation is not a significant factor in oyster genetic relationships in this portion of their range.

CONCLUSION

The native oysters of southern North Carolina and South Carolina coast appear to be a homogenous population as shown by DNA analysis of COI and 16S genes. Similarly, expression of immunity genes was largely similar between locations and tidal heights. Only the TNF and SRCR immunity factors differed in locations, which also differ in salinity from a low to high extreme. The DNA analysis showed that the oysters are panmictic and probably share recruits. The DNA also demonstrates that tidal elevation does not result in differences in haplotype distribution. The eastern oyster, *Crassostrea virginca* is a highly versatile and phenotypically plastic organism that can survive in extremes of salinity and exposure. DNA regulation must drive a robust oyster

physiology that can adjust to extreme conditions. However, those extremes take a toll on the health of the organism as seen by the low values of the immunity signaling factors, which could affect the response to damaging pathogens on the edge of their salinity tolerance.

TABLE 4.1

Immunity Gene Expression in *Crassostrea virginica*

Parameters	**Tissue**	**Site**	**Habitat**	**Site X Habitat**
C-type Lectin	Hemocytes	$F_{2, 25}$=2.6161 p=0.0967	$F_{1,25}$=0.3856 p=0.5413	$F_{5,25}$=0.0528 p=0.0528
TLR2	Hemocytes	$F_{2,26}$= 0.7502 p= 0.4840	$F_{1,26}$ = 0.3084 p= 0.5843	$F_{5,26}$= 0.8163 p=0.4550
TLR3	Hemocytes	$F_{2,25}$= 1.5574 p = 0.2352	$F_{1,25}$= 1.6641 p = 0.2118	$F_{5,25}$= 1.6968 p = 0.2086
TLR4	Hemocytes	$F_{2,26}$= 0.1077 p = 0.8984	$F_{1,26}$= 0.6377 p = 0.4335	$F_{5,26}$= 0.3999 p = 0.6754
MR2	Hemocytes	$F_{2,25}$= 0.3081 p = 0.7382	$F_{1,25}$= 0.2985 p = 0.0993	$F_{5,25}$= 0.0142 p = 0.9829
TNF	Hemocytes	$F_{2,28}$= 5.0901 p = **0.0148***	$F_{1,28}$= 2.235 p = 0.1469	$F_{5,28}$= 2.1313 p = 0.1415
SRCR	Hemocytes	$F_{2,24}$= 16.6532 p < **0.0001***	$F_{1,24}$= 0.6106 p = 0.4442	$F_{5,24}$= 0.6164 p = 0.5508
Big Defensin	Hemocytes	$F_{2,17}$= 2.6107 p = 0.1284	$F_{1,17}$= 3.8451 p = 0.0701	$F_{3,17}$= 4.4169 p = 0.0542
C3q	Hemocytes	$F_{2,23}$= 1.3181 p = 0.2923	$F_{1,23}$= 0.4687 p = 0.5023	$F_{5,23}$= 0.5265 p = 0.5995
Lysozyme	Hemocytes	$F_{2,15}$= 0.1793 p = 0.6794	$F_{1,15}$= 0.2050 p = 0.6588	$F_{3,15}$= 1.4520 p = 0.2514

Table 4.1. ANOVA: Effects of experimental conditions and/or populations on the expression of immunity gene mRNAs in *Crassostrea virginica*. F ratios with the degrees of freedom for the factor effect and the error shown as a subscript, are given. Significant effects ($p < 0.05$) are highlighted in bold and with an asterisk (*).

Table 4.2

Primer sequences for Target Genes in *Crassostrea virginica*

Target	Accession number	Primer sequence	Tm, (°C)	Efficiency
TLR2	JH819194.1	Fw 5′-GCGCTTTATTGACGTTAGAC-3′	58	1.91
		Rev 5′-CGTAAACACATGAAACTGGT-3′		
TLR3	MGID92145	Fw 5′-TTTGGTTCAAGAACTGGGTT-3′	58	1.77
		Rev 5′-GATTAAGGCTCAACAATGGC-3′		
TLR4	MGID89881	Fw 5′-GCCTCCGACTGATTGATTTA-3′	58	1.78
		Rev 5′-ATACCTCTGAGGATAGGACG-3′		
Mannose Rec2	XM_011414451.2	Fw GTTCACTTTTACGTTCACCC-3′	58	1.76
		Rev 5′-TTTGTTGACATTTTGACGCA-3′		
SRCR	BG624783.1	Fw 5′-CACATGCGGCTTCTGTCTAA-3′	62	2.19
		Rev 5′-CGGTGATCGTGCTGGTATATG-3′		
TNF	MGID91531	Fw 5′-GCTTTGTAGGGTGTGATTTG-3′	58	1.94
		Rev 5′-GTTGTACTTGCCGATGACTT-3′		
Big defensin	CV133156	Fw 5′-TGGCAGCTGCTTACGGTATC-3′	60	1.78
		Rev 5′-CCCTGTTGTTGGCACAGCTA-3′		
C type lectin	CV088804.1	Fw 5′-ATTTGCTCAGCCTTGAATGG-3′	55	1.98
		Rev 5′-GTCCCTCCCACCCAGTAGTT-3′		
β-actin	X75894	Fw 5′-ACAGCCGCTTCCTCATCCTCC-3′	55	1.94
		Rev 5′-CGGCGGATTCCATACCAAGG-3′		

Table 4.2. Abbreviations: TLR-toll like receptor; Mannose Rec2-Mannose receptor 2; SRCR-Scavenger Receptor Cysteine Rich; TNF-tumor necrosis factor.

TABLE 4.3

Crassostrea virginica COI Mismatch Distribution Statistics

Location	Tidal Zone	n	MAE	r	R2	Pi
All Locations	all	58	0.1428	0.2720	0.0544	0.0047
Baruch Research Station	all	18	0.1208	0.3719	0.1571	0.0009
Federal Point	all	20	0.3068	0.0555	0.0735	0.0042
Harker's Island	all	20	0.3763	0.4146	0.1760	0.0049
Federal Point	intertidal	10	0.5558	0.0938	0.0981	0.0068
Federal Point	subtidal	10	0.1798	0.2222	0.2134	0.0022
Baruch Research Station	intertidal	9	0.1969	0.1798	0.2222	0.0024
Baruch Research Station	subtidal	9	0.4260	0.7037	0.3143	0.0018
Harker's Island	intertidal	10	0.1798	0.2222	0.2134	0.0043
Harker's Island	subtidal	10	0.6470	0.2854	0.2494	0.0044
All Locations	intertidal	29	0.1756	0.1500	0.0548	0.0059
All Locations	subtidal	29	0.1902	0.2527	0.1119	0.0023

Table 4.3. COI Mismatch Distribution Statistics. n - number of specimens in distribution; MAE – Mean Absolute Error; r – raggedness factor; R2 – R2 Statistic of correlation; Pi – nucleotide diversity. None are significant for P value $p<0.05$ by ANOVA.

TABLE 4.4

Crassostrea virginica COI Genetic Distance

POPULATION 1	POPULATION 2	F_{ST}	H_s
Fed_Pt_Intertidal	Fed_Pt_Subtidal	-0.0234	0.5222
Fed_Pt_Intertidal	Baruch_Intertidal	0.0313	0.4593
Fed_Pt_Intertidal	Baruch_Subtidal	0.0370	0.3556
Fed_Pt_Intertidal	Har_Isl_Intertidal	-0.0207	0.5222
Fed_Pt_Intertidal	Har_Isl_Subtidal	0.0023	0.4333
Fed_Pt_Subtidal	Baruch_Intertidal	-0.0769	0.3052
Fed_Pt_Subtidal	Baruch_Subtidal	0.0000	0.2015
Fed_Pt_Subtidal	Har_Isl_Intertidal	-0.0417	0.3778
Fed_Pt_Subtidal	Har_Isl_Subtidal	-0.0170	0.2889
Baruch_Intertidal	Baruch_Subtidal	0.0000	0.1111
Baruch_Intertidal	Har_Isl_Intertidal	0.0000	0.3052
Baruch_Intertidal	Har_Isl_Subtidal	0.0000	0.2104
Baruch_Subtidal	Har_Isl_Intertidal	0.0000	0.2015
Baruch_Subtidal	Har_Isl_Subtidal	0.0000	0.1067
Har_Isl_Intertidal	Har_Isl_Subtidal	-0.0606	0.2889

Supplemental 4.4. Genetic distances are not significant. Chi-square: F_{ST} – Genetic distance (fixation index); H_s – haplotype diversity; Chi^2: 43.594; P-value of Chi^2: 0.5316 not significant; (df = 45)

FIGURE 4.1

Immunity Gene Expression – Part 1

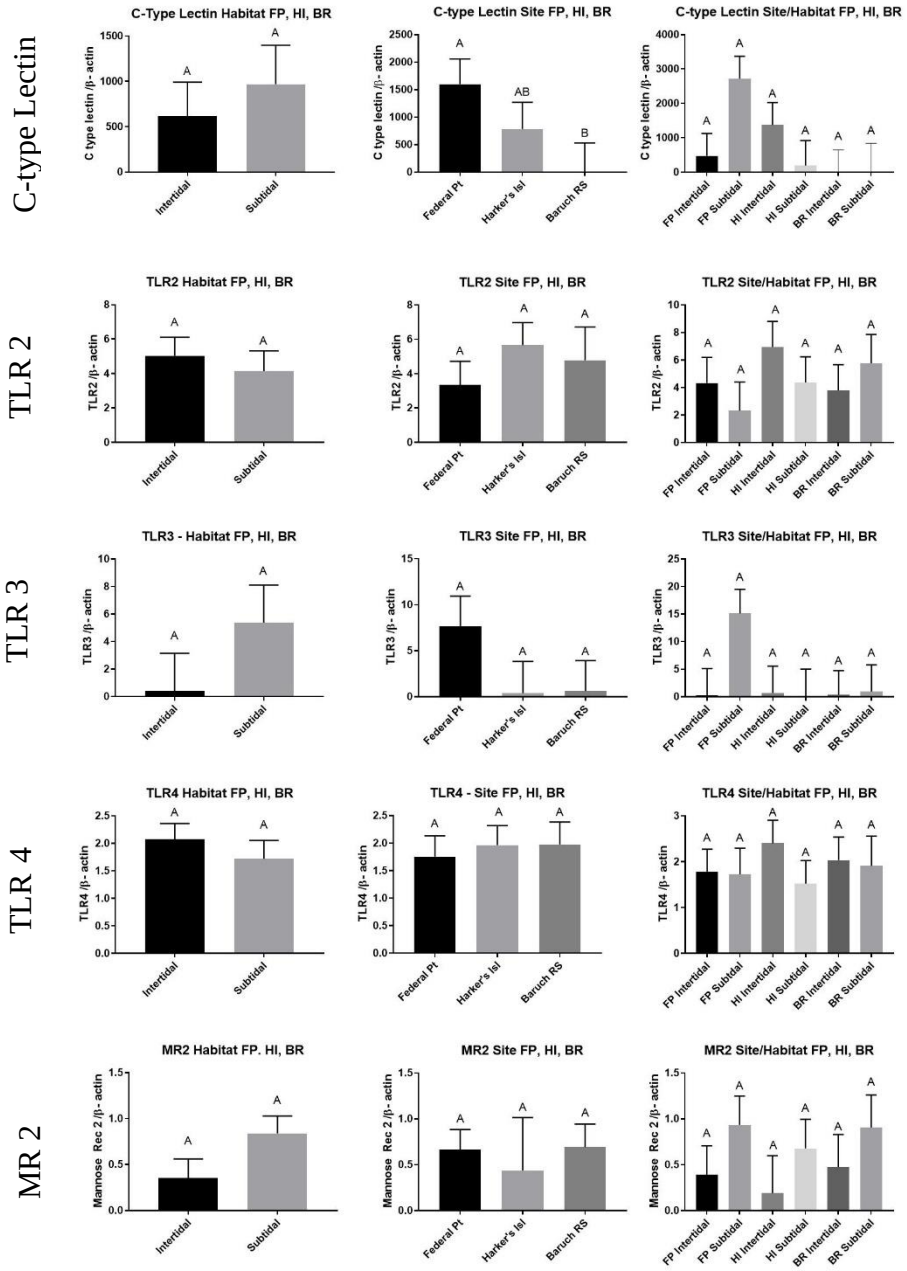

Figure 4.1. Level of expression of immunity molecules in HCs of *C. virginica* from different locations with different salinities. Different letters indicate the values that are significantly different among *C. virginica* from different zones ($p < 0.05$); if columns share a letter, the respective values are not significantly different ($p > 0.05$). Vertical bars represent the standard error of means.

FIGURE 4.2

Immunity Gene Expression – Part 2

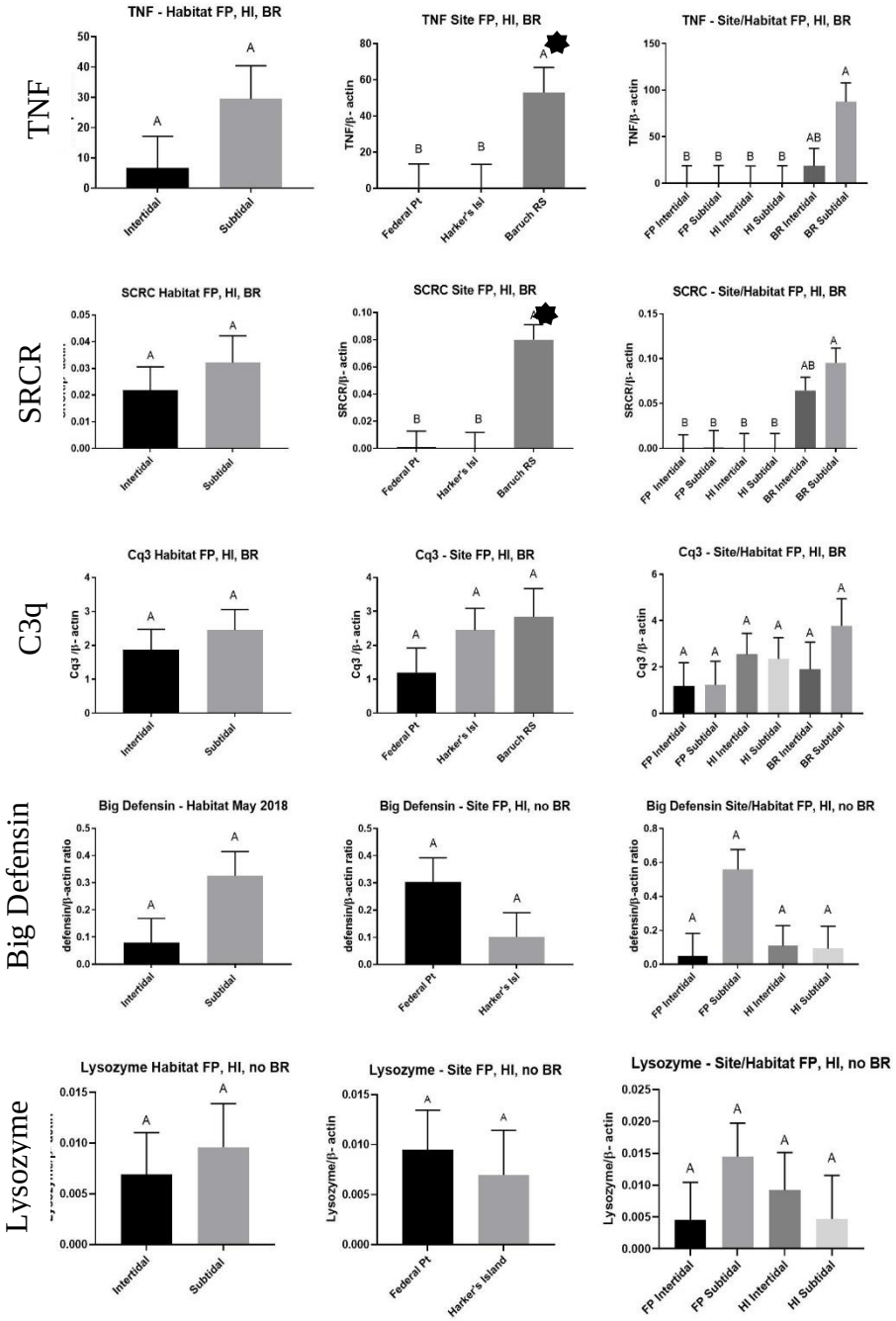

Figure 4.2. Gene expression of immunity factors in HCs of *C. virginica* from different locations with different salinities. Different letters indicate the values that are significantly different among *Crassostrea virginica* from different zones ($p < 0.05$); if columns share a letter, the respective values are not significantly different ($p > 0.05$). Vertical bars represent the standard error of means.

FIGURE 4.3

COI Phylogeny with Bootstrap Values

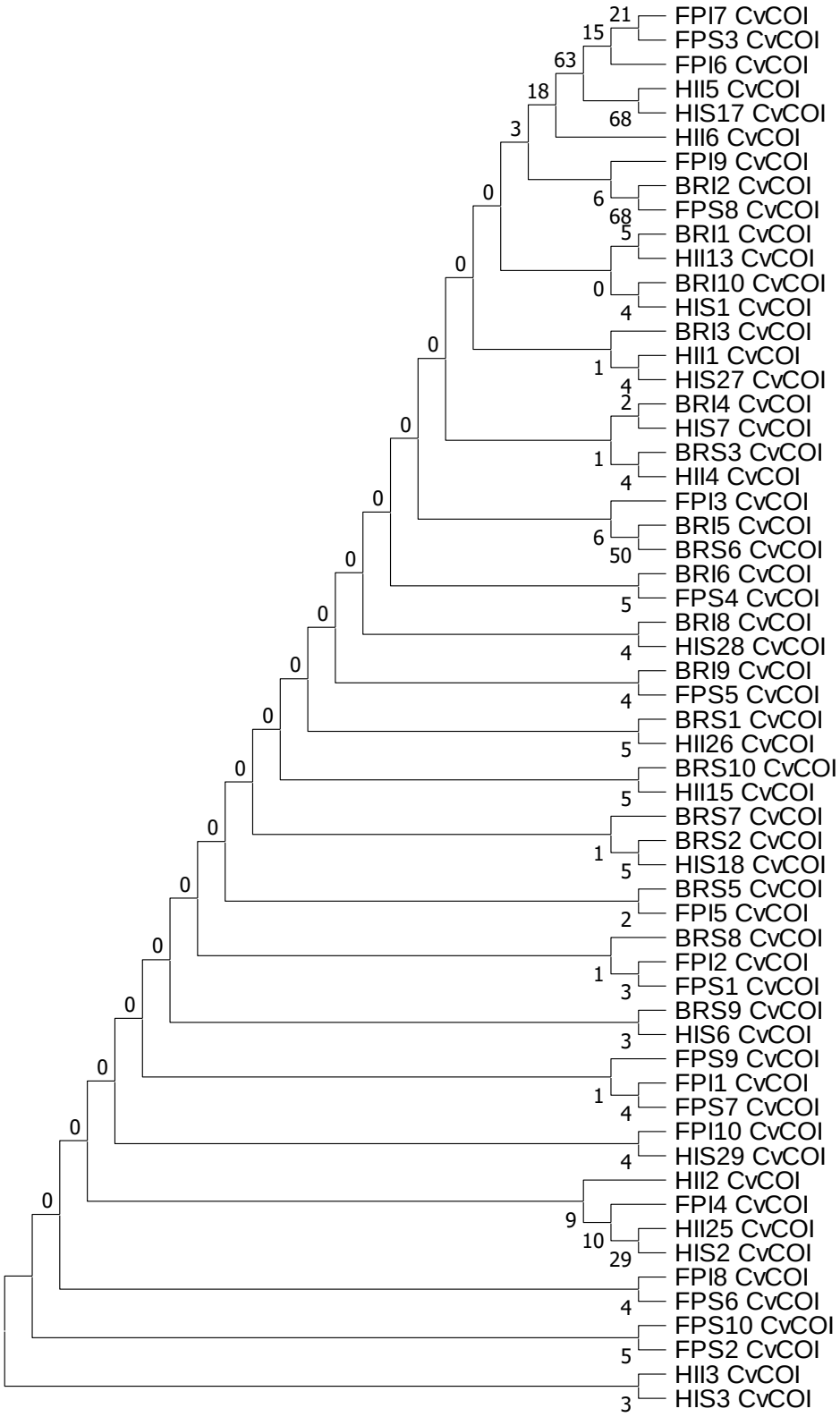

FIGURE 4.4

Crassostrea virginica COI Mismatch Distributions by Location

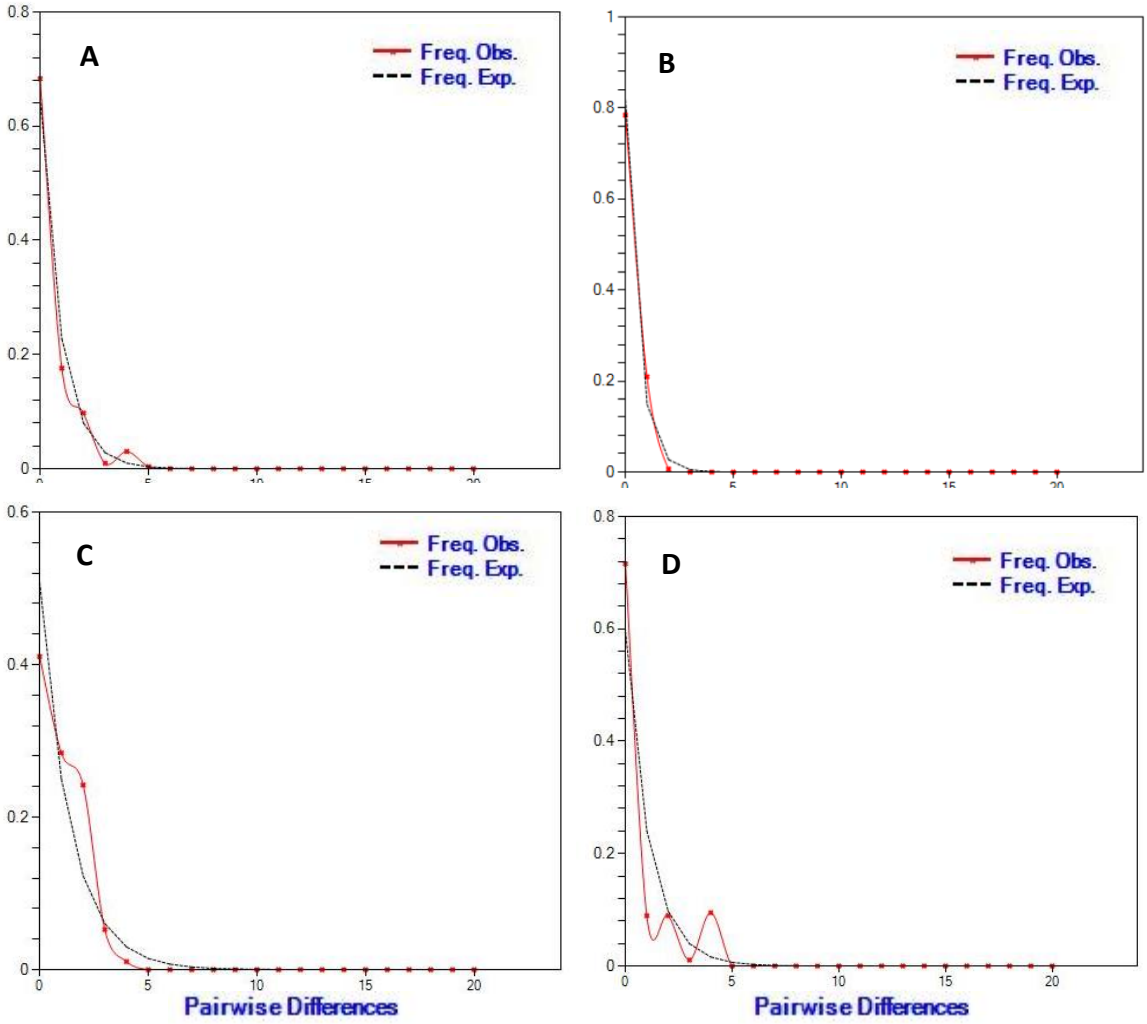

Figure 4.4. COI Mismatch Distributions. A) All locations; B) Baruch Research Station; C) Federal Point; D) Harker's Island. Statistics in Table 4.3.

FIGURE 4.5

Crassostrea virginica COI Mismatch Distributions by Location and Tidal Zone

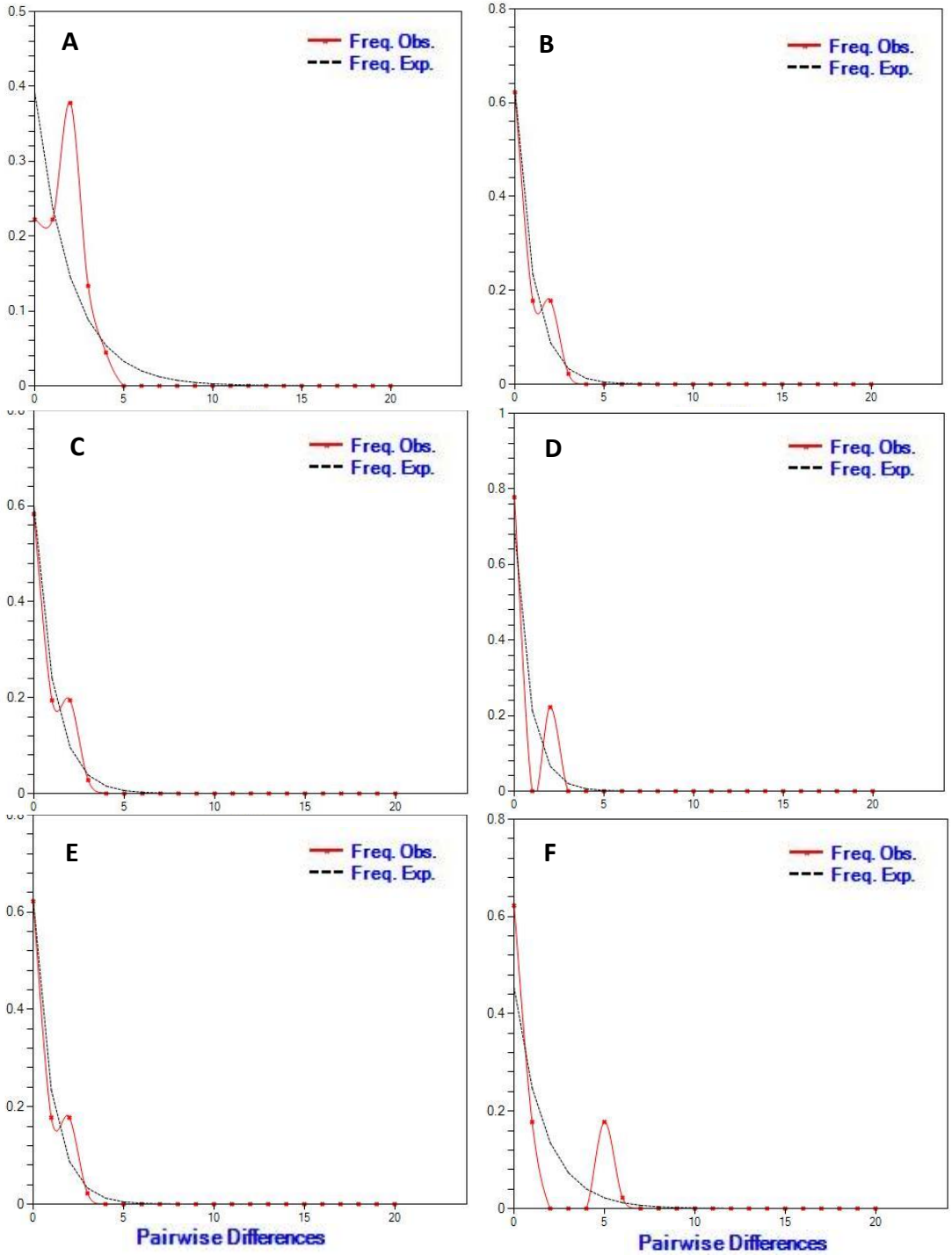

Figure 4.5. COI Mismatch Distributions. A) Federal Point Intertidal; B) Federal Point Subtidal; C) Baruch Research Station Intertidal; D) Baruch Research Station Subtidal; E) Harker's Island Intertidal; F) Harker's Island Subtidal. Statistics in Table 4.3.

FIGURE 4.6

Crassostrea virginica COI Mismatch Distributions by Tidal Zone

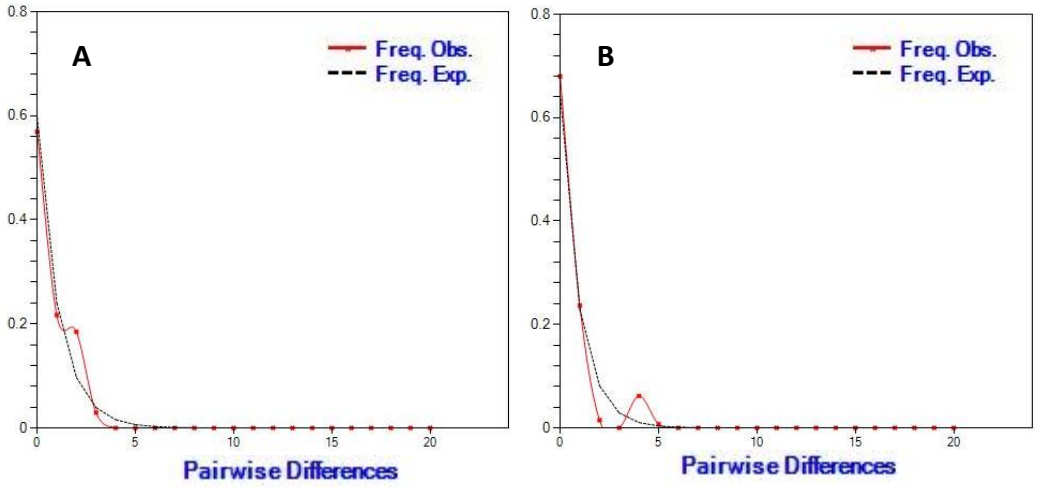

Figure 4.6. COI Mismatch Distributions. A) All locations intertidal; B) All locations subtidal. Statistics in Table 4.3.

FIGURE 4.7

DNA Analysis of 16S Gene with Bootstrap Values

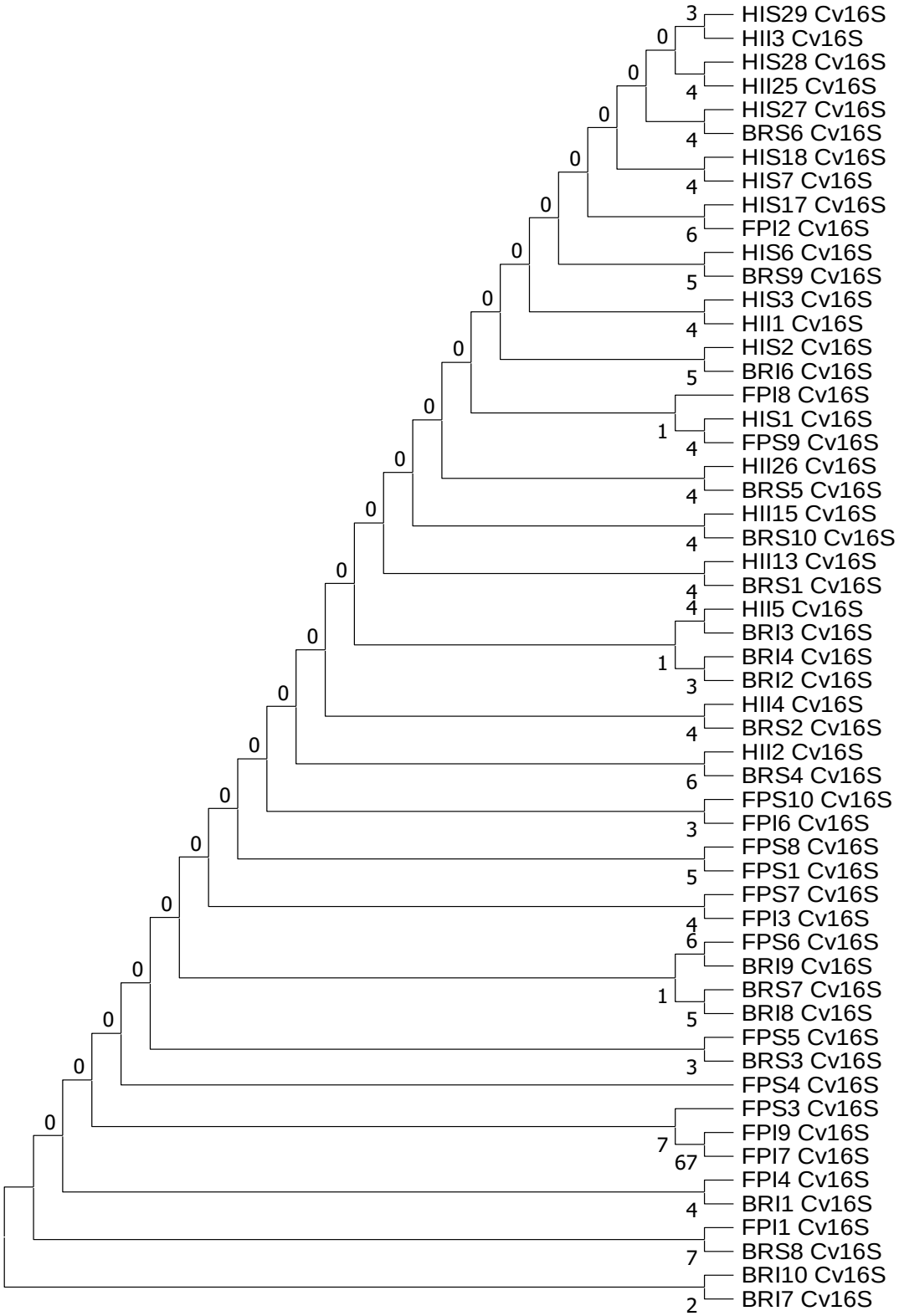

CHAPTER FIVE

PHYSIOLOGICAL VARIATION IN RESPONSE TO *VIBRIO* AND HYPOXIA BY AQUACULTURED EASTERN OYSTERS IN THE SOUTHEASTERN UNITED STATES

Furr, D., Ketchum, R. N., Phippen, B. L., Reitzel, A. M., and Ivanina, A. V. 2021. "Physiological Variation in Response to Vibrio and Hypoxia by Aquacultured Eastern Oysters in the Southeastern United States," Integrative and Comparative Biology (0), pp. 1-15.

ABSTRACT

Eastern oysters (*Crassostrea virginica*) have long been recognized as model organisms of extreme environmental tolerance, showing resilience to variation in temperature, salinity, hypoxia and microbial pathogens. These phenotypic responses, however, show variability between geographic locations or habitats (e.g., tidal). Physiological, morphological, and genetic differences occur in populations throughout a species' geographical range, which may have been shaped by regional abiotic and biotic variations. Few studies of *C. virginica* have explored the combined factors of physiological mechanisms of divergent phenotypes between locations and the genetic relationships of individuals between these locations. To characterize genetic relationships of four locations with aquacultured oysters along the North Carolina and Virginia coast, we sequenced a portion of cytochrome oxidase subunit I (COI) that revealed significant variation in haplotype distribution between locations. We then measured mitochondrial physiology and expression of the innate immunity response of hemocytes to lab acclimation and combined stress conditions (the pathogen *Vibrio vulnificus*, hypoxia) to compare basal expression and stress response in oysters between these locations. For stress sensing genes, toll-like receptors had the strongest location-specific response to hypoxia and *Vibrio*, whereas mannose receptor and a stress-receptor were specific to hypoxia and bacteria, respectively. The expression of stress response genes also showed

location-specific and stressor-specific changes in expression, particularly for big defensin and the complement gene C3q. Our results further suggested that genetic similarity of oysters from locations was not clearly related to physiological and molecular responses. These results are informative for understanding the range of physiological plasticity for stress responses in this commercially important oyster species, with implications in the oyster farming industry as well as the conservation efforts to restore native oyster beds susceptible to low oxygen and rising pathogen loads.

INTRODUCTION

Oysters are important ecosystem engineers, playing critical foundation roles in estuary ecosystems. Like other bivalves, they exert a strong influence on water quality, shore stability and habitat structure for other organisms (Gutiérrez et al. 2003). Many mollusks, including oysters, also serve as important fisheries and aquaculture resources providing substantial economic value for the coastal regions. Oysters of the genus *Crassostrea* are distributed worldwide and are the most common oyster in North America (NOAA 2005). Nearly 20 species in this genus are recognized, two of which – *C. virginica* and *C. gigas* - have broadly colonized the Atlantic and Pacific coasts of the United States, respectively (Hoover and Gaffney 2005).

Physiological differences between individuals from different geographic locations and/or habitats within the same locations are influenced by genetics and environmental conditions. Geographical differences and regional genetic clines have been reported for species within the genus *Crassostrea* (King et al. 1994). Multiple studies have shown that populations of *C. virginica* have strong phylogeographic structure over their large range (Hare and Avise 1996; Thongda et al. 2018; Varney et al. 2018). Although Atlantic oysters have a planktonic larval stage capable of

widespread dispersal, groups of *C. virginica* populations throughout their large geographical ranges vary in physiology and morphology (Conover and Schultz 1995; Hochachka 1988). Significant genetic structure has also been reported in both mitochondrial and nuclear DNA in *C. virginica* with two major clines: Atlantic (Gulf of St. Lawrence to Cape Canaveral) and Gulf Coast (Burford et al. 2014; Hare and Avise 1996; Reeb and Avise 1990). Transplant experiments in the southeastern Atlantic Bight have shown that *C. virginica* has clear genotype-environment interactions in growth and survival of oysters from North Carolina to Florida (Hughes et al. 2017). These phenotypic differences between populations are consistent with earlier comparisons of northern and southern *C. virginica* populations that have genetically-based differences in ciliary activity when reared in a common environment (Dittman 1997). Cultured oysters raised from hatchery spat of indeterminate heritage may exhibit these same genotype-environment interactions.

Determining variation in the physiological mechanisms for coping with environmental stressors is critical to determine growth and survival of individuals in an environment. For aquacultured species like *C. virginica*, any potential mismatching of the environment with oysters transplanted from other portions of the native range would impact yields from these fisheries. Recent research has also shown that oysters can vary genetically and physiologically on even limited spatial scales, including single estuaries (Eierman and Hare 2014; Eierman and Hare 2016; Varney et al. 2018). Oyster survival is influenced by co-variations in temperature, salinity, oxygen concentration and bacterial load (Bataller et al. 1999; Stanley and Sellers 1986). Determining how individual and combinations of environmental factors impact physiology and survival can be important for predicting how transplanted oysters for aquaculture will respond to new environments. For example, the relationships between salinity and oyster survival vary within and

among estuaries (Turner 2006; Wilber 1992). Furthermore, increased freshwater decreases oyster mortality rates due to reduced marine microbial load resulting from depressed salinity (Buzan et al. 2009; Livingston et al. 2000; Powell et al. 2003; Stanley and Sellers 1986).

Significant progress has been made towards our understanding of molluscan responses to stress, specifically the identification of gene-encoded elements related to biotic and abiotic stress sensing (Gestal et al. 2008; Gómez-Chiarri et al. 2015; Guo et al. 2015). Among 28,027 protein-coding genes identified in *Crassostrea gigas*, a congener of *C. virginica*, many are related to stress response (Zhang et al. 2012), including, for example, 1405 genes responsible for immune functions (Zhang et al. 2015). More recently, a *C. virginica* genome (NCBI BioProject PRJNA376014) has been released but a publication of gene content comparisons between these species has not been reported.

Oysters rely on their innate immune systems, specifically hemocytes (HC) in the hemolymph, to detect and respond to potential abiotic and biotic stressors, including microbes and viruses. Gene expression studies have uncovered highly conserved intracellular stress responses in oysters exposed to biotic or abiotic stresses (Li et al. 2017; McDowell et al. 2014; Raftos et al. 2016; Zhang et al. 2016). Those findings may be unexpected considering the heterogeneity of pathogen-associated molecular patterns (PAMPs) and damage-associated molecular patterns (DAMPs) that are able to activate an oyster's HC stress sensors, both in terms of biochemical structures (proteins, glycoproteins, glycolipids, polysaccharide, nucleic acids) but also in cellular compartmentalization (extracellular, intracellular cytoplasmic, intracellular endosomal compartment) (Song et al. 2010). Independent of the origin of the stress, HCs can produce inflammatory mediators providing positive feedback loops that further amplify the stress response. One family of inflammatory factors, the tumor necrosis factors (TNFs), are up-regulated in

response to elevated temperatures, *Vibrio spp*. or Herpes virus type-1 (OsHV-1) (Quistad and Traylor-Knowles 2016; Zhang et al. 2015). Through the synergistic activity of stress-sensing and inflammatory pathways, HCs can secrete antimicrobial cationic peptides (defensins) or complement proteins. Multiple defensins have been identified in this oyster in response to bacterial challenges (Rosa et al. 2011). Complement proteins are even more heterogeneous, with 337 sequences coding for C1q proteins contained in the *C. gigas* genome (Gerdol and Venier 2015). Defensins and complement proteins can exert direct antimicrobial activity through pathogen membrane destabilization; complement proteins can also act as opsonizing molecules promoting phagocytosis; stress-sensing and inflammatory pathways promote the oyster's HCs phagocytic activity (Guo and Ford 2017). For example, Cg-IFNLP proteins can promote HC phagocytosis of prokaryote and protozoan pathogens, but also modulate phenol-oxidase, lysozyme and other lysosomal anti-microbial peptide activities (Sun et al. 2014). Some mannose receptors, as C-type lectins, play a role in recognition of protozoan parasites, such as *P. marinus* (Vázquez-Mendoza et al. 2013). *P. marinus* have been shown to be especially harmful, sometimes killing 70-80% of harvestable oysters (Kern and Ford 2011) and elicits transcription and epigenetic responses in *C. virginica* (Johnson et al. 2020). Abiotic stresses, such as prolonged hypoxia or heavy metals, can also modulate HC phagocytic activity in an antagonistic fashion (Ivanina et al. 2014; Ivanina et al. 2016a).

The aim of our present study was to characterize variation in physiology and gene expression of diploid *C. virginica* oysters from different aquaculture operations in response to lab acclimation and abiotic and biotic stressors. We hypothesized that a combination of environmental (abiotic or biotic) factors and the location of origin of *C. virginica* may co-determine the eastern oyster's stress response. We focused our study on two types of physiological

responses: mitochondrial respiration and the stress sensing/response elements in hemocytes (HCs). To test these hypotheses, we determined haplotype diversity of four locations of *C. virginica* along North Carolina coast and Virginia. We exposed oysters from each location to abiotic (0.1% oxygen) or biotic (*Vibrio vulnificus*) stressors for 24 hours under laboratory conditions and measured their physiological responses.

MATERIAL AND METHODS

Animal collection and maintenance

Oysters (*C. virginica*) were purchased from local suppliers (Inland Seafood, Charlotte, NC, USA; Seaview Crab Company, Wilmington, NC, USA) in November 2017 from 4 different locations from North Carolina: New River, NC (zone C3), Queens Creek, NC (zone D2) and Sea Level (zone E9) and Virginia (Rappahannock River, VA) (Figure 1). Oysters from the three NC locations are referred to as C3, D2, and E9 based on the grow zones for each aquaculture. All four collection sites are routinely used for commercial oyster culture for human consumption. Oysters were shipped within 24–48 h to the University of North Carolina at Charlotte and placed in aerated tanks with recirculating artificial seawater (ASW) (Instant Ocean®, Kent Marine, Acworth, USA). In all experiments, selected acclimation temperatures and salinities were close to the temperature and salinity of the respective oyster habitats at the time of collections (within 1–3°C and 3–4‰, respectively; temperature and salinity values were from USGS databases for the date of collection from each location). For oysters from site C3, salinity and temperature were 24‰ and 22°C, for the oysters from site D2 30.5‰ and 18°C, animals from site E9 were acclimated at conditions: 30‰and 22°C and oysters from the VA site were kept at 15‰ and water temperature at 20°C. Oysters were allowed to acclimate for 2–3 weeks and fed *ad libitum* on alternate days with a

commercial algal blend (5 mL per 30 L tank) containing *Isochrysis* spp., *Pavlova* spp., *Thalassoisira weissflogii* and *Tetraselmis* spp. with 5–20 μm cells (Shellfish Diet 1800, Reed Mariculture, Campbell, CA, USA).

Genetic Variation

A portion of the adductor muscle was excised from 20 oysters from each geographic location and preserved in 100% ethanol at -20°C until processing. These tissue samples were from oysters from the same collection but were not matched with the specific oyster used for physiology and gene expression analyses. DNA was extracted from each sample using the DNeasy Blood and Tissue Kit (Qiagen) following the manufacturer's protocol for animal tissues. DNA quality and quantity were assessed for three randomly selected samples from each location using 1% agarose gel electrophoresis and spectrophotometry (NanoDrop), respectively.

A portion of cytochrome c oxidase 1 (COI) was amplified using species-specific primers (Cvi_F: 5-TTGGGCAGTTTTAGCTGGGA-3; Cvi_R: 5-AAGGAGCATAGTAAGCCCGC-3) designed from existing *C. virginica* COI sequences available at NCBI. PCRs attempted using the traditional COI primers (e.g., LCO_1490 and HCO_2198) did not result in an amplicon, which has been previously reported for other species in the genus *Crassostrea* (de Melo et al. 2010). PCR reactions were performed using Q5 High-Fidelity Polymerase Master Mix (New England Biolabs) with the following temperature profile: 95°C for 2 min, 35 cycles of 95°C for 30 sec, 30 sec at 57°C, and 1 min at 72°C, and a final hold at 4°C. PCR products were checked for a single product (~450 bp) on 1% agarose gels and then submitted for direct Sanger sequencing using the forward and reverse primer (Eurofins). Sequences were manually checked by eye for miscalls using

MEGA7 (Kumar et al. 2016) and then spliced together *in silico* for a complete COI sequence for each individual. These primer sequences are available in Supplemental S1.

COI sequences were aligned using MUSCLE in MEGA7. Analyses of population genetic structure, nucleotide and haplotype diversity, and haplotype distribution were completed using Arlequin v3.5 (Excoffier and Lischer 2010). Pairwise F statistics were calculated between all sites using haplotype frequencies and genetic distance. Analysis of molecular variance (Excoffier and Lischer 2010) was performed with 1000 permutations to assess how genetic variation was partitioned among the four geographic localities. For these analyses, we grouped locations using two strategies: 1) a three-group structure where site C3 and D2 were combined and 2) a two-group structure where C3 and D2 were combined as well as E9 and VA. This was used to determine if different group assignments influenced interpretation of partitioning of genetic diversity. The rationale for this grouping was based on overall genetic similarity determined from pairwise F_{ST} and relative geographic distance. A haplotype network for analysis of evolutionary relationships between haplotypes was generated using PopART 1.7 (Leigh et al. 2015). DnaSP v6.11.01 (Rozas et al. 2017) was used to annotate synonymous and nonsynonymous polymorphisms. Finally, we aligned the sequences generated from this study with previously published COI sequences (Genbank PopSet 406857474) to compare haplotypes from a wider geographic range.

Hypoxia exposure

To mimic hypoxic conditions, oysters were placed in plastic trays with lids (5 animals per 5 liters of ASW) containing water pre-equilibrated with nitrogen (Robert Oxygen, Charlotte, NC, USA) to achieve hypoxia (near–anoxia 0.04–0.1% O_2). Oysters were maintained under the hypoxic conditions for 24 h with continuous bubbling of the gas to maintain target O_2 levels. All exposures

were conducted at 18±1°C (D2 and C3) and 21±1°C (E9 and VA) at the same salinity used for the acclimated conditions (see above). Control animals were maintained under normoxic conditions (21% O_2) for the duration of the experiment. No mortality was observed during hypoxic exposure in any of the studied populations of oysters. From each population 20 animals were randomly assigned to a control or experimental group to have 10 animals per exposure.

Bacterial exposure - Bacterial strains and culture conditions

Vibrio vulnificus strain JDO-2 was utilized for this study as it can be identified from background bacteria when plated on Bacto Heart Infusion (HI) agar (BD Difco, Franklin Lakes, NJ, USA) with 2µg ml^{-1} chloramphenicol. For the duration of this study, the bacterium was stored at -80°C in Bacto Luria-Bertani broth (LB) (BD Difco, Franklin Lakes, NJ, USA) with 20% glycerol. For bacterial uptake experiments, cells were grown overnight in HI broth with antibiotic at 30°C with aeration in a rotary incubator.

Bacteria uptake experiments

Ten oysters from each location were randomly selected from maintenance tanks and placed in experimental tanks 24 hours before the experiment began. For bacterial challenges, overnight cultures of JDO-2 were washed three times in sterile 20‰ artificial sea water (ASW) and added to tanks at a concentration of 6 x 10^5 CFUs mL^{-1} under oxygenated conditions with bubbled air and fed to encourage uptake. After 24 hours, oysters were removed from the tanks and aseptically shucked using a flame-sterilized knife. Utilizing a modified homogenization protocol by Froelich et al. (Froelich et al. 2012), oysters were rinsed thoroughly with 20‰ ASW and placed in 50 ml conical tubes. Oysters were homogenized in 20 ‰ ASW at a 1:1 (wt/vol) ratio using sterile blender

cups (Waring, Torrington, CT) for 30 seconds, broken up into 10 second bursts. Samples were serially diluted and plated onto HI agar with chloramphenicol and *V. vulnificus*. CFUs g^{-1} oyster tissue were calculated.

Mitochondrial isolation and respiration

To determine how laboratory conditions and hypoxia exposure may differentially impact oysters from each studied location, mitochondria (n=5) were isolated from oysters exposed to normoxic and hypoxic conditions. Mitochondria were isolated from oyster gills pooled from two individuals per replicate and assayed using a method modified from Sokolova (Sokolova 2004). Briefly, gills (2–4 g) were homogenized with several passes of a Potter–Elvenhjem homogenizer and a loosely fitting Teflon pestle, centrifuged to remove cell debris, and then the supernatant was centrifuged again to obtain a mitochondrial pellet. The mitochondrial pellet was resuspended, washed with homogenization buffer, and resuspended in ice-cold assay medium. Oxygen uptake by mitochondria (MO_2) was measured in 1 ml water-jacked, temperature-controlled chambers using Clarke-type oxygen electrodes (Qubit Systems, Kingston ON, Canada) at 18°C. To test the effects of anoxia and reoxygenation on mitochondrial capacity, mitochondrial MO_2 was measured in the presence 10 mmol l^{-1} succinate.

Respiration with succinate was measured in the presence of 2.5 g ml^{-1} rotenone to inhibit the upstream complexes of the electron transport chain (Sokolova 2004). Mitochondrial MO_2 was measured at saturating O_2 concentrations according to the standard practice in mitochondrial physiology. All assays were completed within 2 hours of isolation of the mitochondria. State 3 (ADP-stimulated), state 4 (resting), and state 4ol (in the presence of 2.5 g ml^{-1} oligomycin) respiration rates were determined as described earlier (Sokolova 2004). State 3 of mitochondria

respiration was achieved by the addition of 100–150 mmol l^{-1} of ADP. States 4 and 4ol MO_2 represent uncoupled respiration when most (or all, in the case of state 4ol) energy of substrate oxidation is used to counteract the proton and cation cycles (collectively known as proton leak) across the mitochondrial membrane (Brand et al. 1994; Skulachev 1998). Respiratory control ratio (Harrison et al.) was calculated as the ratio of state 3 to state 4 respiration and used as an index of mitochondrial integrity (Estabrook 1967; Skulachev 1998). Mitochondrial respiration rates were corrected for the electrode drift and non-mitochondrial respiration and then converted into natom O min^{-1} mg^{-1} mitochondrial protein as described in Sokolova (Sokolova 2004). Protein concentrations in isolated mitochondria (treated with 0.1% Triton X-100 to solubilize mitochondrial membranes) were measured using the Bio-Rad protein assay (Bio-Rad Laboratories, Hercules, CA, USA).

Hemocyte collection and gene expression

After experimental treatments (i.e, normoxia, hypoxia or *V. vulnificus* exposure), hemolymph was extracted from the adductor muscle of individual oysters (n=5) from each population. Hemolymph was collected with a sterile 10-ml syringe with a 21-gauge needle containing 1 ml ice-cold filtered ASW to prevent aggregation of the hemocytes. Hemolymph samples were centrifuged for 10 min at 1000× *g*. The hemocyte pellet was washed once with ice-cold ASW and stored at −80 °C until RNA extraction. Total RNA was extracted from hemocytes using ZR RNA MiniPrep™ kit (Zymo Research, Irvine, CA, USA) according to the manufacturer instructions. RNA concentration was measured using NanoDrop 2000 spectrophotometer (Thermo Scientific, Pittsburg, USA) and expressed as μg RNA 10^{-6} cells. Single-stranded cDNA was

synthesized from 0.5 μg of the total RNA using 50 U μl^{-1} SMARTScribe™ Reverse Transcriptase (Clontech, Mountain View, CA, USA) and 20 μmol l^{-1} of oligo$(dT)_{18}$ primers.

Expression of target genes was determined with quantitative real-time PCR (qRT-PCR) using a 7500 Fast Real-Time PCR System (Applied Biosystems/Life Technologies, Carlsbad, CA, USA) and SYBR® Green PCR kit (Life Technologies, Bedford, MA, USA) according to the manufacturer instructions. The primer sequences are provided in Supplemental Table 1. The qRT-PCR reaction mixture consisted of 7.5 μl of 2× SYBR® Green master mix, 0.3 μmol l^{-1} of each forward and reverse gene-specific primers, 1.5 μl of 10× diluted cDNA template and water to adjust to 15 μl. The reaction mixture was subjected to the following cycling: 15 s at 95 °C to denature DNA and activate Taq polymerase and 40 cycles of 15 s at 94 °C, 30 s at 55 °C (actin and C-type lectin); 58 °C (TLR2, TLR3, TLR4, Mannose Rec2 and TNF); or 62°C (SRCR) and 30 s at 72 °C. Serial dilutions of a cDNA standard were amplified in each run to determine amplification efficiency (Pfaffl 2001). Amplification efficiencies were 1.74-2.19 for all studied genes. A single cDNA sample from *C. virginica* hemocytes was used as an internal cDNA standard and included in each run to test for run-to-run amplification variability. The target gene mRNA expression was standardized relative to β-actin mRNA as described elsewhere (Ivanina et al. 2013; Pfaffl 2001; Sanni et al. 2008). Gene expression data were calculated with the delta-delta Ct method that compared differential expression of the target gene and β-actin after hypoxia or bacterial exposure with unexposed oysters.

Statistical analyses

One-way ANOVA was used to test the effects of location on the measured traits. Prior to statistical analyses, data were tested for normality and homogeneity of variance by Kolmogorov-

Smirnoff and Levene's tests, respectively, and normalized as needed using Box-Cox common transforming method. Fisher's Least Significant Differences (LSD) tests were used for planned post-hoc comparisons of the differences between the pairs of means of interest. Differences were considered significant if the probability of Type I error was less than 0.05. The data are presented as means ± standard error of the mean (SEM) unless indicated otherwise.

RESULTS

Genetic Variation

The 440-bp portion of *C. virginica* cytochrome c oxidase 1 (COI) analyzed here revealed a total of 18 single nucleotide polymorphisms (SNPs) that resolved into 12 haplotypes. All SNPs were synonymous and were distributed throughout the amplified region. Comparison of these haplotypes with previously published COI sequences from *C. virginica* (Genbank PopSet: 406857474) showed these SNPs are present in oysters from other locations in the southeastern United States, particularly in South Carolina and Florida. Nucleotide diversity (π) was highest in VA at 6.01, followed by E9 (5.8), C3 (3.1), and D2 (0.58). There was significant genetic variation in pairwise comparisons between all populations except for C3 and D2. Population pairwise F-statistics calculated using haplotype frequencies (Supplemental 5.3) compared to pairwise differences (Supplemental 5.2) showed similar results, except when comparing E9 to VA. For this comparison haplotype frequency calculations were not significant while pairwise calculations were significant.

AMOVA analysis using a two-group structure, where site C3 and D2 were combined and E9 and VA were combined, showed that the percent variation among groups was 24.23%, among locations within groups was 8.61%, and within locations was 67.16%. When we used a three-group

structure (only C3 and D2 combined), the percent variation among groups was 31.31%, among locations within groups was -0.56%, and within locations was 69.25%. Thus, grouping had little impact on the distribution of genetic variation within and between locations, both of which showed the largest percentage within locations but at least a quarter between locations.

Consistent with the F_{ST} comparisons, the haplotype network analysis revealed the 12 haplotypes have an uneven geographic distribution between these locations (Figure 5.1). Two dominant haplotypes represented about two-thirds of the sampled oysters and contained 29 (haplotype 3) and 24 (haplotype 6) individuals (Supplemental 5.3). The next most common haplotypes contained nine and eight individuals, while the remaining haplotypes contained three or less individuals. There were seven population specific haplotypes, including haplotype 8 from nine VA oysters and haplotype 12 from eight individuals from E9.

Establishing normalized oyster husbandry condition

In order to determine if laboratory water conditions may impact an oyster's stress tolerance from each location, *C. virginica* was placed in husbandry conditions reflecting the environmental conditions at collection. 'Normalized' husbandry condition was used to maintain oysters from heterogeneous environments in similar/least stressful conditions (as defined by variation in metabolic rates) (Supplemental 5.4). Respiration rates (MO_2) of ADP-stimulated mitochondria respiration (State 3), resting (State 4) and proton leak (4ol) were not significantly different among all studied oyster locations although VA had consistently larger values (Supplemental 5.5). Respiratory control ratio (Harrison et al.) was not significantly different between locations.

Response to hypoxia: mitochondrial physiology

When exposed to hypoxia, oysters from each location showed significant differences in mitochondrial respiration depending on the location of origin and the specific state assayed (see Figure 5.2). E9 in North Carolina showed significant increases in State 3 as well as large, though not significant, increases in State 4. Oysters from the VA site, conversely, showed decreases in State 4 and significant increases in RCR. For C3 and D2 oysters, exposure to hypoxia did not significantly alter any of the physiological processes measured.

Crassostrea virginica gene expression in normalized husbandry condition

Transcriptional profiles for genes involved in stress-sensing, stress-signaling and stress-response were significantly different for oysters from these locations (see Supplemental 5.6). Out of five studied stress-sensing genes (TLR2, TLR3, TLR4, Mannose Rec2 and SRCR) only one (TLR4) had similar expression in all four studied locations of *C. virginica*. Expression of TLR2 was significantly higher in HCs of oysters from VA, where HCs of oysters from zone C3 and D2 had the lowest expression level. Expression of TLR3 was significantly higher (5.42-17.62 times) in oysters from zone C3 compared with the three other locations. Similarly, SRCR had the highest level of expression in oysters from zone C3 and D2 and significantly lower mRNA level in HCs of oysters from VA. In contrast, mRNA expression of MR2 was lowest in HCs of oysters from zones C3 and D2 and highest in oysters from VA. Expression of the stress-signaling molecule (TNF) was different between studied locations, with highest level of mRNA expression in oysters from zone E9 and lowest level of expression in oysters from zones C3 and D2.

Two of four studied stress-response genes, big defensin and C3q, had similar basal level of expression in HCs from all studied locations of *C. virginica*. mRNA level of lysozyme was

significantly lower in oysters from zone C3 and had similarly high level of expression in HCs of oysters from zone E9 and VA. C-type lectin expression was lowest in oysters from zone D2 and highest in oysters from zone E9.

Crassostrea virginica location comparison: hypoxia

To assess the effect of acute hypoxia on stress-sensing/response potential we measured expression of the same genes and compared expression in hypoxia vs. normalized conditions between locations. Expression of TLR2 was significantly lower in E9 and VA compared to C3 and D2, which showed essentially no change in expression (see Figure 5.2). HCs of oysters from all locations had decreased expression of TLR3 but these differences did not differ between locations (Figure 2B). Expression of TLR4 was decreased in comparison with normoxic conditions only in oysters from C3 and E9 (Figure 5.3). mRNA level of MR2 significantly decreased in oysters from zone E9 and VA and had no change in *C. virginica* from other zones. Oysters from only E9 had decreased expression of SRCR and TNF under hypoxic conditions.

Hypoxia had an inhibitory effect on mRNA expression of big defensin, lysozyme, C3q and C-type lectin depending on the location (Figure 5.3). HCs expressed less big defensin and C-type lectin transcripts in C3, E9, and VA when exposed to hypoxia, where expression was higher in D2. Lysozyme mRNA expression declined in all locations with no significant differences. C3q had significantly lower expression in C3 when compared with the other three locations.

Crassostrea virginica location comparison: bacteria

A 24-hour exposure to *Vibrio* led to an accumulation of *V. vulnificus* in oysters that varied between locations (Figure 5.4). *V. vulnificus* was the most abundant in oysters from zone VA

compared with other oyster populations. The least number of bacteria was accumulated in oysters sourced from zones C3 and E9. The exposure of oysters from each location to this bacterium resulted in significant differences in the expression of the surveyed innate immune genes (Figure 5.5). TLR2, which has a role in recognizing gram positive bacteria was slightly elevated in HCs of oysters from zone D2 and decreased in oysters from zone E9. Other genes involved in stress-sensing processes showed varied responses, from general lower expression for all locations (TLR3) to location specific decreases in expression (e.g., TLR4 and SRCR in E9). HCs of all studied populations decreased their ability for stress signaling (based on TNF expression) in the presence of *V. vulnificus*. Expression of stress response genes big defensin and C3q was significantly lower after bacterial exposure in C3 (Figure 5.6). Lysozyme and C-type lectin expression was inhibited in all studied locations.

DISCUSSION

The collective results from this study revealed significant differences in physiological and gene expression responses to acute biotic and abiotic stress of *Crassostrea virginica* from aquaculture sites in North Carolina and Virginia. Our data suggest that oysters from these locations vary genetically and phenotypically, which reveals potentially functional variation over a narrow portion of this species' broad geographic range in these aquaculture locations.

Physiological responses significantly differed in response to hypoxia in a location-dependent pattern. To compare location effects on oysters' physiological response, we first determined that mitochondrial functions under normalized conditions in lab show no significant differences in state 3, state 4 and state 4ol of mitochondrial respirations. Thus, laboratory conditions were able to normalize the metabolic physiology despite potential differences in

environmental conditions at each location of collection. However, when oysters from these locations are exposed to an acute hypoxia condition, these physiological responses differed substantially. Respiration rates increased under hypoxia conditions in mitochondria of oysters from VA. Notably, the increase in mitochondrial respiration for oysters from zone E9 was significant for state 3, where exposure to hypoxia had no effect on the basal metabolic rate of oysters from zone C3 and D2.

We focused our inquiry into potential location-based differences in the immune system by measuring the expression of the immune and stress sensing/response networks of *C. virginica* HCs. Oysters have a wide range of stress-sensing receptors to recognize and eliminate diverse forms of microorganisms. Stress sensing elements can recognize pathogen- and damage-associated molecular patterns. Our study showed that basal level of HC-expressed genes of stress-sensing, stress-communication and stress-response genes are different among the studied oysters. The ability to recognize gram positive bacteria, protozoan, and tissue damage (based on expression of TLR2, mannose rec 2 (MR2), scavenger receptor cysteine rich (SRCR), respectively) was considerably higher in oysters from zones E9 and VA as compared to the oysters from zones C3 and D2. Similarly, TNF (stress-communication) as well as C-type lectin and lysozyme (immune response) were also higher in E9 and VA. Conversely, the ability to potentially recognize viruses (as determined by expression of TLR3) was significantly higher in C3. This difference in basal gene expression of stress-sensing and elimination genes in different locations may determine differences in the capacity to fight and survive infections when oysters are raised in different locations for aquaculture.

When oysters from each location were exposed to acute hypoxia, we observed high heterogenicity in stress sensing and stress response genes between *C. virginica* from each location.

Hypoxia generally resulted in decreased expression of about half of the surveyed genes related to immune sensing in VA and E9. D2 showed little gene expression response after hypoxia exposure for most genes but with higher expression for two stress response genes (i.e., big defensin and C-type lectin).

We observed a similar heterogenous response in gene expression for oysters from each location exposed to pathogenic bacteria. Oysters are an important ecological niche for species of *Vibrio,* and they consume bacteria routinely that are associated with plankton. *V. vulnificus* is a gram negative, halophilic bacteria that is naturally present in the estuaries of North Carolina and Virginia (Oliver et al. 1983). Change in bacterial loads has been observed under different environmental conditions (e.g., change in oxygen, heavy metal presence, temperature, and salinity) (Froelich and Oliver 2013; Motes et al. 1998). We measured significant differences in bacterial accumulation when oysters from these locations were cultured under similar laboratory conditions. Among four studied locations, oysters from VA had a higher level of bacterial load (˜800-900 CFU/g tissue) followed by zone D2 (~650-700 CFU/g tissue). We detected no clear pattern for bacterial load and gene expression. Oysters from these locations differed in basal gene expression as well as responses after introduction of the bacteria. Thus, we observed no clear pattern for how gene expression may be predictive for bacterial accumulation.

Analysis of a portion of COI suggests that each location contains a genetically differentiated population of oysters and that haplotypes are not evenly distributed between locations. We did not genotype the oysters used for the physiology and gene expression study, so we are not able to connect genetic differences to the measured phenotypic responses. Because our oysters were from the field and acclimated to the lab, we also cannot account for the impact of potential epigenetic variation due to environmental history. Methylation varies more than genetic

variation in *C. virginica* (Johnson and Kelly 2020) and methylation is potentially important in the acclimation of oysters (Gavery and Roberts 2013; Gavery and Roberts 2017). Future research that explicitly compares genetic, epigenetic and phenotypic variation, in this region or elsewhere in *C. virginica*'s range, will be important to discern the impacts of each in oyster physiology and survival.

Effects of hypoxia and bacterial load are detrimental to the oyster industry at large. Hypoxia is associated with reduced oyster growth (Jeppesen et al. 2018). Infectious bacteria such as *Vibrio* can reduce production by impacting feeding activity of young oysters leading to economic losses (Travers et al. 2015), as well as produce serious human infections (Froelich and Oliver 2013). Oysters experiencing multiple stressors, such as hypoxia plus *Vibrio* exposure, harbor a higher bacterial load (Ivanina et al. 2011a). The cumulative effects of both stressors can be devastating to an already struggling industry. We have shown an environmental rather than genetic component for susceptibility to these common stressors, which needs to be taken into consideration in aquaculture planning.

TABLES 5.1

ANOVA: Effects of Experimental Conditions and/or Populations on the Expression of Studied mRNAs in *Crassostrea virginica*.

Trait	Po*p*ulations	Conditions	Po*p*ulations x Conditions
TLR2	$F_{3,65} = 7.32$ $P =$ **0.0003***	$F_{2,65} = 12.35$ $P <$ **0.0001***	$F_{6,65} = 4.22$ $P =$ **0.0015***
TLR3	$F_{3,64} = 5.34$ $P = 0.0027$	$F_{2,64} = 3.99$ $P = 0.0243$	$F_{6,64} = 2.44$ $P = 0.0374$
TLR4	$F_{3,65} = 1.19$ $P = 0.3220$	$F_{2,65} = 32.01$ $P <$ **0.0001***	$F_{6,65} = 2.18$ $P = 0.0588$
Mannose Rec2	$F_{3,59} = 4.85$ $P =$ **0.0050***	$F_{2,59} = 9.48$ $P =$ **0.0003***	$F_{6,59} = 3.25$ $P =$ **0.0092***
SRCR	$F_{3,65} = 2.39$ $P = 0.0785$	$F_{2,65} = 8.05$ $P =$ **0.0009***	$F_{6,65} = 2.23$ $P = 0.0538$
TNF	$F_{3,65} = 3.89$ $P = 0.0138$	$F_{2,65} = 14.31$ $P <$ **0.0001***	$F_{6,65} = 3.10$ $P =$ **0.0110***
Big Defensin	$F_{3,59} = 2.77$ $P = 0.0517$	$F_{2,59} = 10.26$ $P =$ **0.0002***	$F_{6,59} = 5.47$ $P =$ **0.0002***
C type lectin	$F_{3,61} = 0.47$ $P = 0.7056$	$F_{2,61} = 2.57$ $P = 0.0867$	$F_{6,61} = 1.52$ $P = 0.1896$
Complement component 3	$F_{3,51} = 0.75$ $P = 0.527$	$F_{2,51} = 2.64$ $P = 0.0836$	$F_{6,51} = 1.58$ $P = 0.1774$
Lysozyme	$F_{3,51} = 4.49$ $P =$ **0.008***	$F_{2,51} = 3.64$ $P =$ **0.0352***	$F_{6,51} = 1.05$ $P = 0.406$

Table 5.1. F ratios with the degrees of freedom for the factor effect and the error shown as a subscript, are given. Significant effects ($p < 0.05$) are highlighted in bold.

FIGURES 5.1

Collection Locations of Crassostrea virginica and Haplotype Network

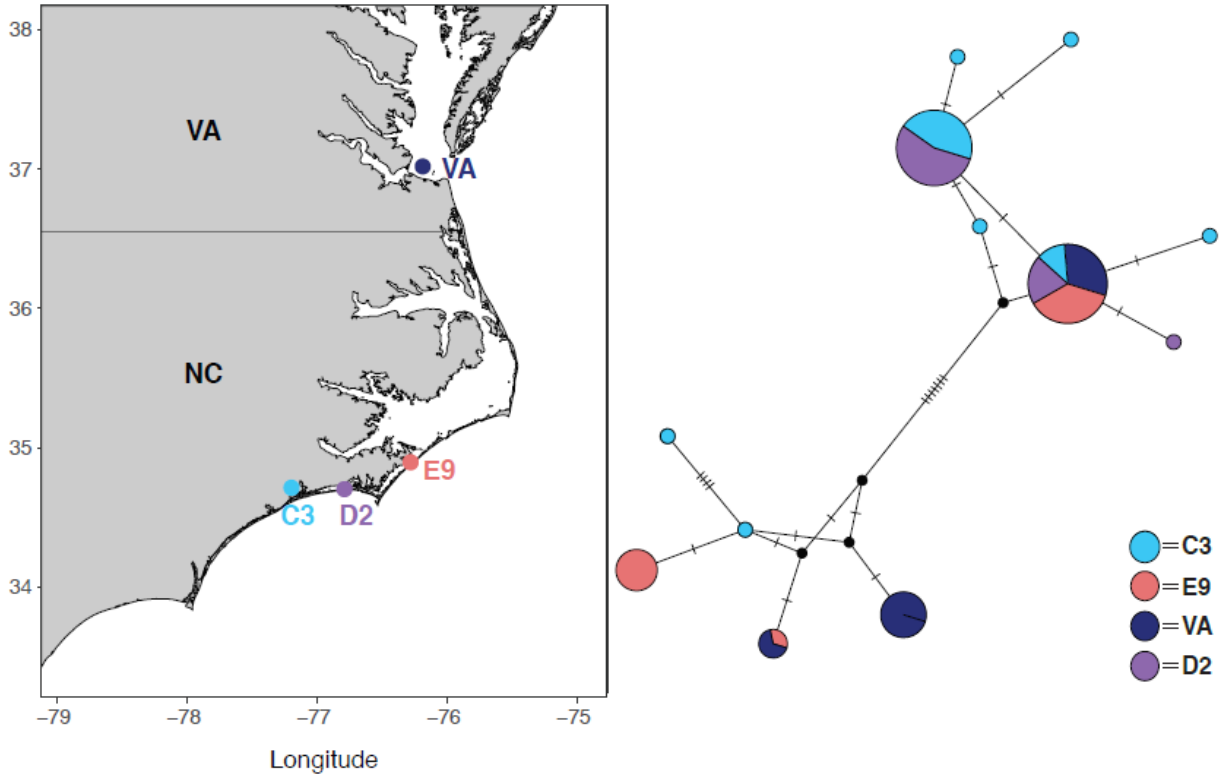

Figure 5.1. (Left) Map of four collection locations for *Crassostrea virginica* for this study. (Motes et al.) Haplotype network based on COI. Tick marks on branches indicate individual polymorphisms that differentiate the haplotypes. Size of the circle indicates number of individuals.

FIGURES 5.2

Stress-sensing Molecules under Hypoxia Stress

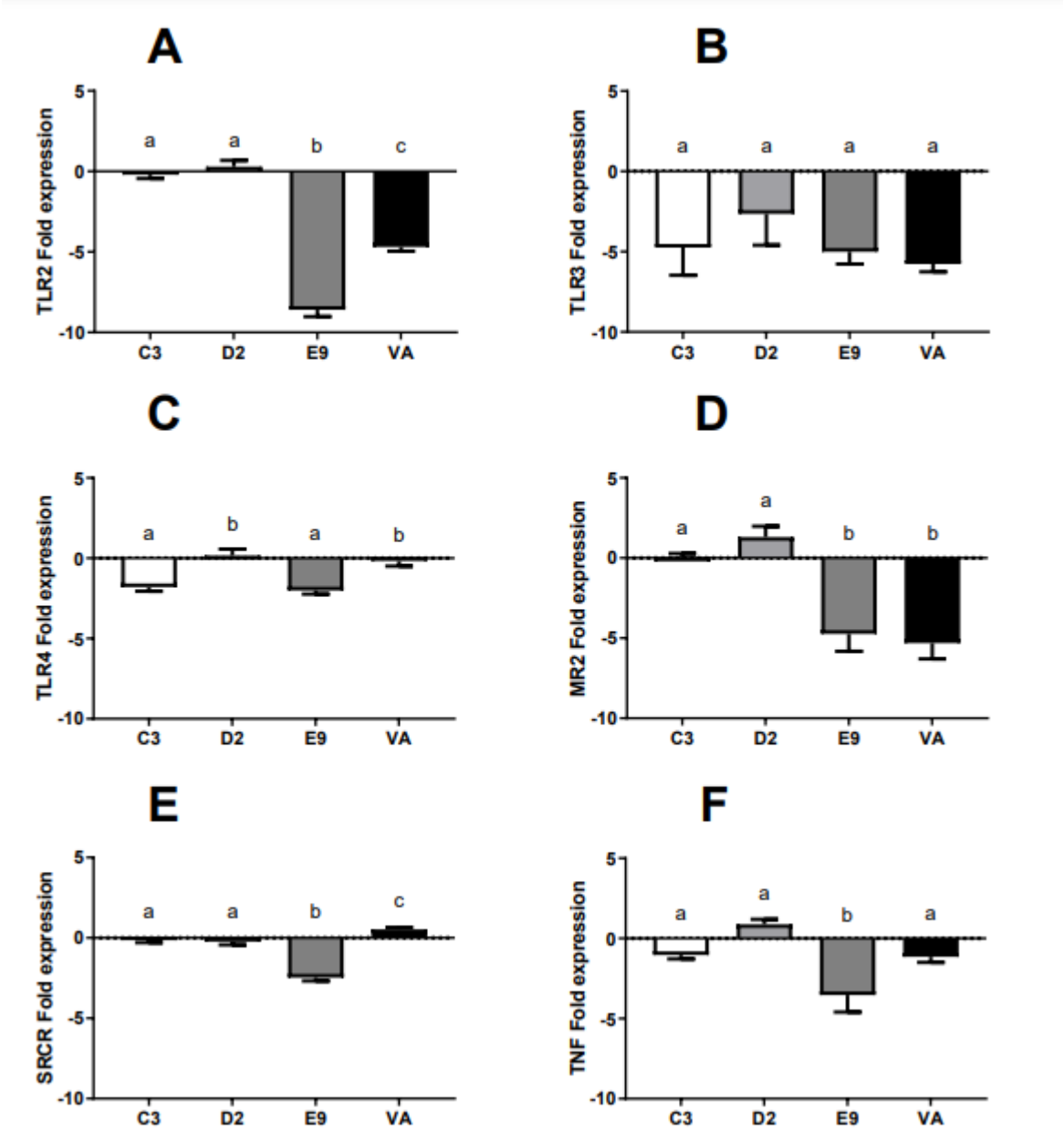

Figure 5.2. Level of expression of stress-sensing molecules in HCs of *C. virginica* from 4 different locations under hypoxia stress. (A) TLR2, (B) TLR3, (C) TLR4, (D) MR2, (E) SRCR and (F) TNF. Data presented as relative to normoxic control. Different letters indicate the values that are significantly different among *C. virginica* from different zones ($p < 0.05$); if columns share a letter, the respective values are not significantly different ($p > 0.05$). Vertical bars represent the standard error of means, N=5.

FIGURES 5.3

Expression of Stress-response under Hypoxia Stress

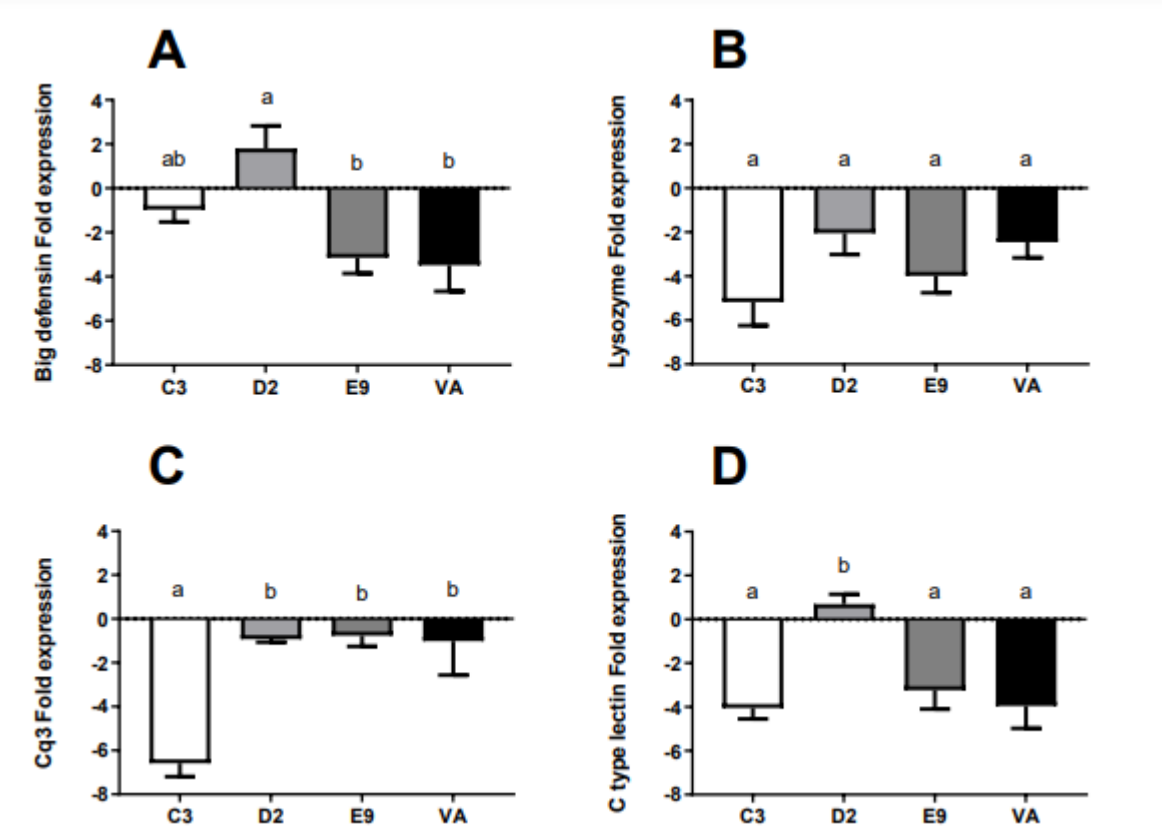

Figure 5.3. Level of expression of stress-response humoral molecules in HCs of *C. virginica* from 4 different locations under hypoxia stress. (A) Big defensin, (B lysozyme, (C) complement factor 3 C3q, (D)C-type lectin. Data presented as relative to normoxic control. Different letters indicate the values that are significantly different among *C. virginica* from different zones ($p < 0.05$); if columns share a letter, the respective values are not significantly different ($p > 0.05$). Vertical bars represent the standard error of means, N=5

FIGURES 5.4

Vibrio vulnificus Loads in Oyster Tissue under Normoxic Conditions

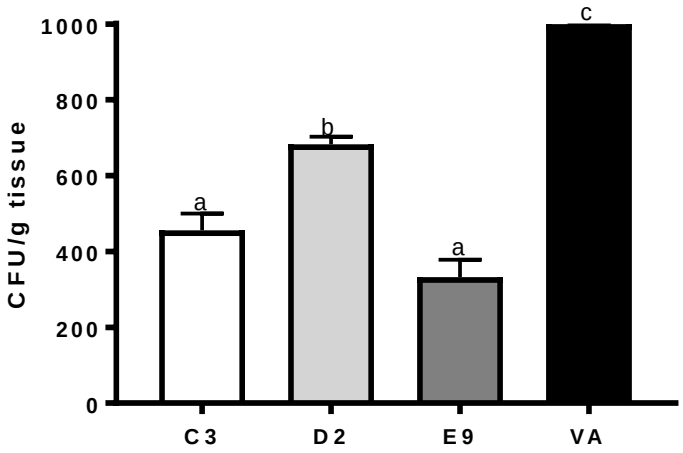

Figure 5.4. *Vibrio vulnificus* loads in oyster tissues under normoxic conditions (100% air saturation). Vertical bars represent standard errors. Columns that do not share the same letters represent significantly different values ($p < 0.05$). N=10.

FIGURES 5.5

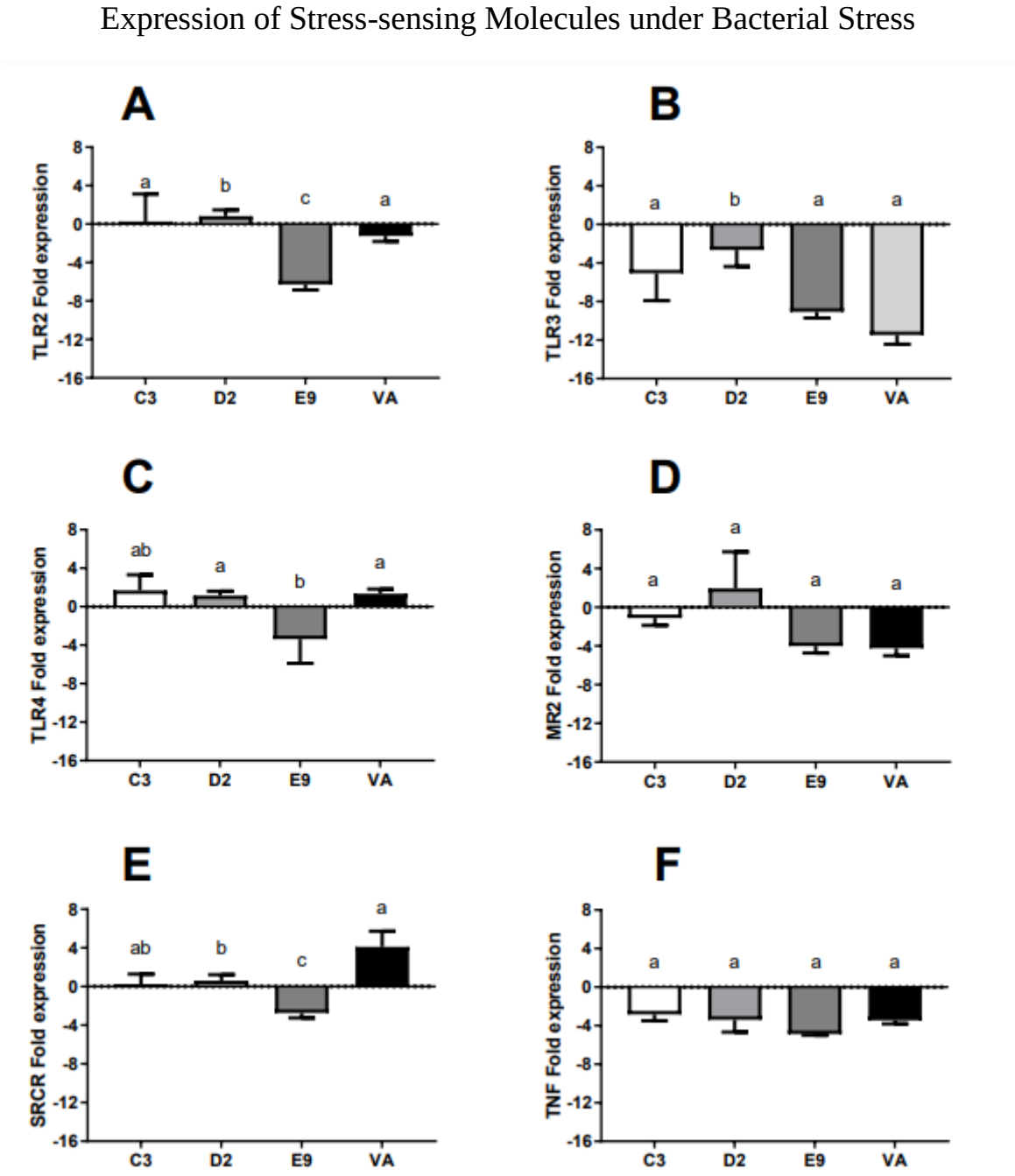

Figure 5.5. Level of expression of stress-sensing molecules in HCs of *C. virginica* from 4 different locations under bacterial stress. (A) TLR2, (B) TLR3, (C) TLR4, (D) MR2, (E) SRCR and (F) TNF. Data presented as relative to normoxic control. Different letters indicate the values that are significantly different among *C. virginica* from different zones ($p < 0.05$); if columns share a letter, the respective values are not significantly different ($p > 0.05$).Vertical bars represent the standard error of means, N=5.

FIGURES 5.6

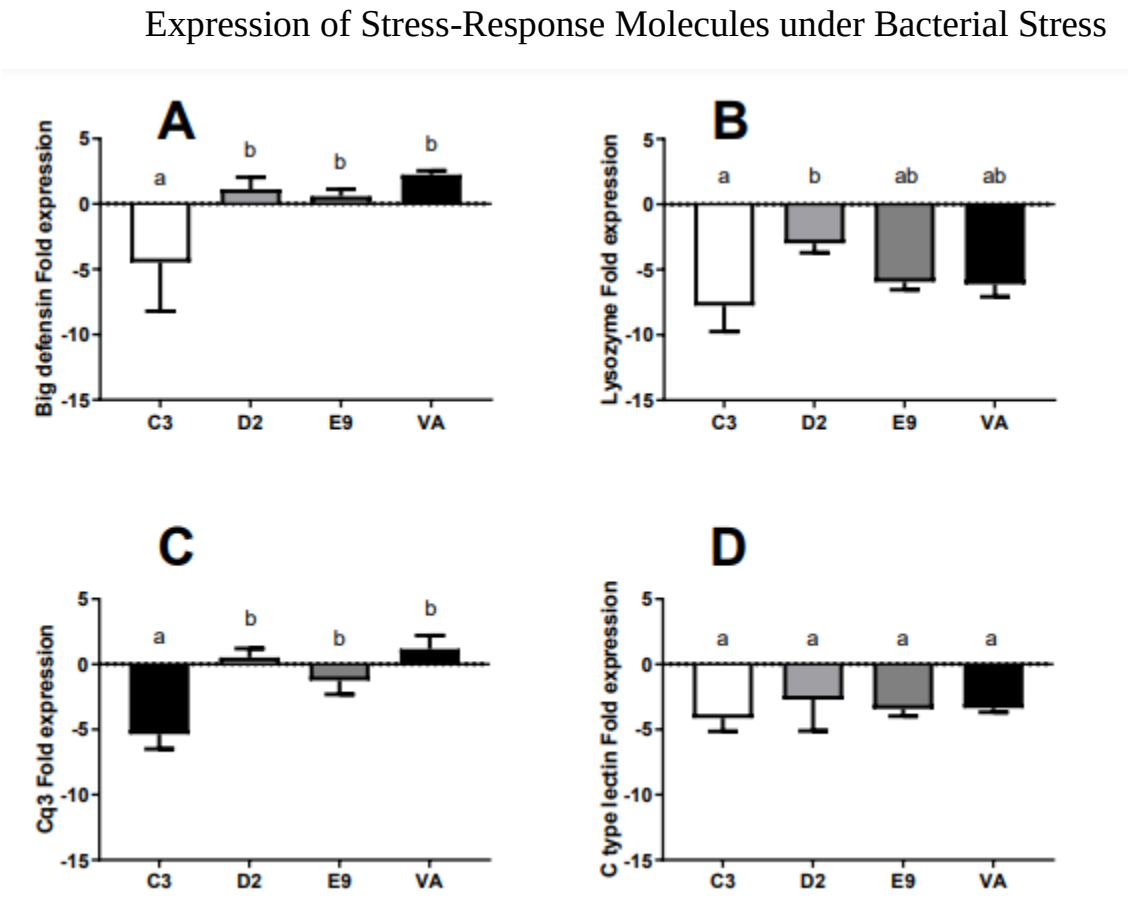

Figure 5.6. Level of expression of stress-response humoral molecules in HCs of *C. virginica* from 4 different locations under bacterial stress. (A) Big defensin, (B lysozyme, (C) complement factor 3 (C3q), (D) C-type lectin. Data presented as relative to normoxic control. Different letters indicate the values that are significantly different among *C. virginica* from different zones ($p < 0.05$); if columns share a letter, the respective values are not significantly different ($p > 0.05$). Vertical bars represent the standard error of means, N=5.

CHAPTER SIX

RELATIONSHIP OF MORPHOLOGY, PHYLOGENETICS, AND BIOGEOGRAPHY IN *TRIODOPSIS* RAFINESQUE, 1819 (STYLOMMATOPHORA, POLYGYRIDAE) LAND SNAILS

(Furr, Denise; Reitzel, Adam)

ABSTRACT

The *Triodopsis* genus of Stylommatophoran land snails has been confusing to malacologists for decades. Twenty-eight species have been described in the eastern and southern US, but some original descriptions are insufficient to correctly identify specimens, and misidentifications are common. Phylogenetic approaches have not been applied for species in this genus as the usual mitochondrial markers are extremely variable and difficult to sequence. DNA extraction is complicated by the presence of mucopolysaccharides. Therefore, a mollusk-specific DNA extraction protocol and custom primers are developed in this study to better facilitate genetic analysis of the family Polygyridae. *Triodopsis* genus phylogenies based on 16S, ITS2, and H3 genes are presented, with F_{ST} values suggesting a reduction in the number of named species. Three major groups have been recognized in the phylogeny, *Triodopsis fallax* (Say, 1825), *Triodopsis tridentata* (Say, 1817), and *Triodopsis fraudulenta* Pilsbry, 1894, and a stand-alone species, *Triodopsis burchi*, whose position is uncertain. Morphology is insufficient to delineate many of the recognized species, and geographic ranges overlap. We relate the phylogenetic clades to morphology and biogeography to attempt to better identify the recognized species and change the species status of some based on morphology measurements and overlapping distributions. An H3 molecular clock tree suggests a recent and rapid expansion in the family. New hypotheses are also presented that may explain the genetic variation in the Stylommatophoran mitochondrial genome,

as well as a possible explanation of the morphological variation within a clade that could still be undergoing rapid speciation after repeated isolation in refugia.

INTRODUCTION

The Stylommatophoran land snails

Land snails are usually environmental specialists and supposedly highly susceptible to extinction during extreme changes in environmental conditions (Barker et al. 2013). Stylommatophoran land snail populations have highly divergent mitochondrial genomes, even over short distances (Barker et al. 2013; Pinceel et al. 2005), possibly due to low dispersal or motility (Thomaz et al. 1996). Habitat specialists are reported to evolve rapidly, which may explain their rapid diversification (Avise 2004). Mitochondrial genes show high diversification (Thomaz et al. 1996); however, the same haplotype diversity is not seen in the nuclear genes.

Land snails are non-vagile (barely moving during a lifetime or under environmental stress), and populations either adapt to environmental changes or perish (Pfenninger et al. 2003). Dispersal of snails over geologic time is thought to occur by mostly passive means such as by other animals and water systems during floods. (Aubry et al. 2006; Sinclair 2010).

Eupulmonate gastropods (air breathing snails) diverged from aquatic superorder Hydrophila beginning around 160 mya, with the order Stylommatophora (truly terrestrial snails) emerging around 150 mya (Ayyagari and Sreerama 2020; Dayrat et al. 2011; Emberton 1994; Liu et al. 2021; Wade et al. 2006). Land invasion by mollusks likely occurred multiple times, probably with several habitat reversions (Holznagel et al. 2010). Just after the K-T boundary around 65 mya, as many other animals became extinct, the Stylommatophorans suddenly radiated into the many families (Liu et al. 2021) and genera living today (Emberton 1994). The sudden radiation of land

snail families has been speculated to correlate with a genome duplication in the Stylommatophora (Liu et al. 2021) made possible by hermaphroditic and/or self-fertilizing. The "extra" genes from the duplication may then have provided the genetic material for the development of many of the novelties that facilitated true terrestrial living, such as a true lung, a change in waste removal processes, and an enhanced immune system (Liu et al. 2021).

The Stylommatophora is now the most populous group of terrestrial mollusks and perhaps best adapted to a terrestrial habitat (Dayrat et al. 2011). The Polygyridae, a Stylommatophoran family, is hypothesized to have originated in the southern Appalachian Mountains and has radiated into genera and species throughout North and South America with the highest diversity in the southeastern United States (Emberton 1994). Generic radiation of Polygyrids has been measured by molecular clock at around 20 mya (Emberton 1995b; Liu et al. 2021), and speciation has continued to the present. Some land snails still have limited distributions and multiple similar sister species in the same habitat (Hubricht 1985), leading to questions of how speciation occurred in sympatry.

Genus *Triodopsis* has been separated into what is recognized as sister species by very subtle and sometimes ambiguous differences in shell morphology. Historically, land snails have been identified as morphological species first by shells, and later, anatomical characters such as genitalia. However, in many groups these are very similar characters that are not relevant to phylogeny (Emberton 1995b; Suvorov 2002). Qualitative rather than quantitative characters are used to describe species, such as "rounder" and "closer", as well as shades of color. Understandably, this use of non-quantitative characters is due to a lack of characters to quantify on a variable, rounded spiral shell and fluid body. In the Polygyridae family, the shell is barely useful in taxonomy in some genera due to convergence (Emberton 1995b). Even though the

Triodopsis species are identified by these subtle, and often variable, shell characters along with geographic distribution, few of the characters are consistently unique to species (Emberton 1995b; Goodfriend 1986) leading to many misidentifications. Members of this genus have a distinctive three "teeth" in the aperture of the shell (see Figure 6.1) and are well represented in the Southeast US; there are at least eight recognized species of *Triodopsis* found in Piedmont of North Carolina and 28 recognized species east of the Mississippi River (Dourson et al. 2013; Hubricht 1985; Pilsbry 1940). A list of recognized species in Eastern United States with authors is located in Table 6.4.

This research investigated the relationship of phylogenetic history inferred from the sequence data to the morphological species assignment in the *Triodopsis* genus. Other than studies to determine the phylogeny of genera and deeper taxa, little or no work has been done on relating phenotype and sympatric species radiation to genotype and none have full genomic sequences documented to date (Emberton 1995a; Liu et al. 2021). Emberton (1988) was the last known revision of the genus using allozymes and reproductive anatomy. Even though individuals are similar in reproductive anatomy, subtle differences in shell morphology have led malacologists to attempt to separate potential populations into unique species, even when collected at the same location (Emberton 1988). If snails are non-vagile, this implies that speciation occurred in sympatry (Emberton 1988), which is unlikely due to constant gene flow, or during some isolating event that now allows secondary contact.

The *Triodopsis* genus internal anatomy seems to contradict the Biological Concept of Species in that the physical structure of the reproductive structures is very similar between species (Emberton 1988). To complicate the issue further, cross-species hybridization has been reported (Emberton 1988; Grimm 1974; Vagvolgyi 1968). Interspecies mating has been observed, and

hybrids are reported to exist by observation of morphological intermediates (Emberton 1988; Grimm 1974) but have not been confirmed genetically. A study of apparent sympatric sister species is done here to determine the relationship between phenotypic and genetic variation among closely related and morphologically similar species.

History of Triodopsis Taxonomy and Research

Authors have disagreed on the taxonomy of the *Triodopsis* genus for nearly 100 years. Names have changed several times (Table 6.3), reflecting the difficulty in species identification. Morphology is misleading, and the definition of species in this group has not been established, especially in the *Triodopsis fallax* group. Many morphotypes with subtle differences are often found in the same location, and the morphological characters are variable within recognized species. Convergence is also a possibility since incidents of convergence have occurred multiple times in the family Polygyridae (Emberton 1995a).

Henry Pilsbry published a four-volume monograph in 1939 – 1948 that has been the most comprehensive collection of land snail descriptions for North America to this day. The *Triodopsis* genus is included in his monograph, but with far fewer species than are recognized today (Pilsbry 1940). Pilsbry recognized only 11 species and 9 subspecies.

In 1968, Joseph Vagvolgyi produced a comprehensive work on the evolution of the *Triodopsis* and a revision of the genus (Vagvolgyi 1968). His systematic treatment of the genus involved very detailed morphology keys and distribution maps, as well as ecological notes. He also postulated that hybridization was common, and distributions of the "species" were indistinct, refuting some of the described species and reporting them as hybrids or forms of existing species. The taxonomic revisions were especially true of the *T. fallax*-related species, most of which he

considered subspecies or hybrids. Vagvolgyi recognized 11 species and 6 subspecies, roughly the same as Pilsbry.

Wayne Grimm (1974) raised members of the *Triodopsis fallax* group in the laboratory and claimed that nearly all would freely interbreed in captivity. He considered the species *T. fallax*, *Triodopsis messana* Hubricht, 1952, *Triodopsis obsoleta* (Pilsbry, 1894), *Triodopsis soelneri* (J. B. Henderson, 1907), *Triodopsis vannostrandi* (Bland, 1876), *Triodopsis hopetonensis* (Shuttleworth, 1852), and *Triodopsis affinis* Hubricht, 1950, as populations and subspecies of *T. fallax.* (He did not study *Triodopsis palustris* (Hubricht, 1958)). He also recognized a southern population of *T. fallax* as species *Triodopsis alabamensis* (Pilsbry, 1902) and speculated that they were different waves of migrants to the east based on morphology. Overall, Grimm recognized 20 species of *Triodopsis* with 6 subspecies, but all the subspecies were of *T. fallax.*

It was not until Hubricht published *The Distributions of the Native Land Mollusks of the Eastern United States* (Hubricht 1985*)* that all the subspecies of *Triodopsis* were elevated to species status, including all those of the *T. fallax* group. These were listed as species in his monograph of distribution maps with no further explanation. The maps were incredibly useful to malacologists, and all taxa were commonly accepted as full species.

Kenneth Emberton (1988), publishing shortly after Hubricht's monograph of distributions, did not revise the genus, but did place Hubricht's list of species into groups, which he postulated should be the species level based on his study of genitalia and allozymes (Emberton 1988). Emberton formed nine groups with six subgroups from the 28 species recognized by Hubricht at the time, which strongly agree with Vagvolgyi (1968) and Pilsbry (1940). He also recognized two separate populations – a northern and a southern "race" - of *Triodopsis fallax* types which produced convergent morphological types as they migrated eastward into the coastal plain. The species

Triodopsis affinis was completely left out of Emberton's publication. It has since been considered a hybrid by malacologists and rarely recognized.

Emberton (1988) also dissected tribe Triodopsini genitalia and assigned a character state to 50 characters in the genitalia structure. Of these, only 18 characters are variable in all the *Triodopsis* in this study. Only those clades near the ancestral node show more than two- or three-characters difference in the matrix and many are identical. Emberton was the last to address the relationship between species in *Triodopsis* to date.

Based on authors other than Hubricht, the currently recognized number of species in the genus *Triodopsis* is likely over-inflated. Questions have emerged concerning the taxonomy of the *Triodopsis* land snails as malacologists struggle with identifications. First, this research plans to determine the criteria for species designation in *Triodopsis* based on morphological, phylogenetic, and biogeographical evidence; second, it intends to address the mitochondrial genetic diversity and its origins by examining the unusual reproduction of land snails; and third, it will explore the morphological variability of the *Triodopsis fallax* group by examining the environmental conditions during the family expansion and the subsequent effect on the speciation process. These aims will give insight into the roles for genetics and environmental history on the diverse yet overlapping phenotypes recognized as species in the *Triodopsis* genus.

The correlation of genomic markers with morphological phenotypes in the *Triodopsis* has not been previously studied. Traditional DNA barcode markers such as COI used by other researchers have been challenged to genetically separate similar mollusk species in this family due to high variation in the mitochondrial genome. This research will provide a much-needed correlation between mitochondrial genetic markers and morphological identities and will provide comments on the status of these species.

MATERIALS AND METHODS

Tissue procurement and collection

Most of the snail tissue used in this research was obtained from ethanol-preserved specimens contributed by curated collections at the Schiele Museum of Natural History (most of which were collected by the author personally). These were collected under North Carolina Resource Commission Collection License SC00369 and Endangered Species Permit ES00214 over the last 15 years. Other specimens were procured from the Schiele Museum, the North Carolina State Museum in Raleigh, Dr. Kathryn Perez at University of Texas of the Rio Grande Valley, the University of Florida Museum, Clemson University, and various independent malacology associates. At least 200 individual snails from 19 recognized species were used for DNA amplification and subsequent sequencing. All specimens used in phylogenies are listed in Supplemental 6.1. A strong attempt was made to use specimens collected from different geographic areas within their distribution range to test for variation between locations and likely populations. Individuals from type locations were used when available. However, since initial identifications are not considered in this study due to possible misidentifications in this difficult group, syntypes are not necessary and clades were matched to original descriptions.

Anatomical and morphological details were initially used as described by expert malacologists to identify the species. For those highly familiar with the genus, most individuals could be recognized as a member of a morphological taxon by an experienced eye. However, misidentifications are common, and morphological measurements show overlapping character traits for some species, especially those of the *Triodopsis fallax* group. Therefore, initial identifications were generally disregarded except to choose specimens for study. Species names

are ultimately assigned to genetic clades if in agreement with the morphology in the species description.

DNA extraction and PCR

A DNA extraction protocol has been customized for mollusks due to the high mucopoly-saccharide content and inhibitors in the tissue. This protocol (see Appendix A.8) was modified from a previous study (Sokolov 2000). SDS and protease K were used as emulsifiers and chloroform/isoamyl alcohol in DNA purification. DNA was precipitated with isopropanol and cold ethanol. This protocol is not only effective for *Triodopsis* but has also been used successfully with other Stylommatophoran mollusks used as outgroups and oysters in Chapter 4. No phenol or other high-risk chemicals are used in the protocol, and the protocol can be performed with minimal lab equipment making it useful for small institutions.

COI was found to be unsuitable for use in *Triodopsis* phylogeny, including the "universal" Folmer primers. Primers have not been found that amplify COI reliably for *Triodopsis* species. A high amount of degenerative bases would be required due to the large amount of variation in the land snail mitochondrial genome. Because of the indiscriminate nature of highly degenerate primers and the desire for species-level detail, COI was not used in this study. The 18S gene was found to be uninformative due to lack of variation in GenBank sequences of other Triodopsini genera, so was not used in *Triodopsis.*

The 16S rDNA gene was used in this research primarily for genus and species-level divisions. 16S primers used for other Triodopsini (Wilkinson 2020) produced inefficient amplification of *Triodopsis* 16S at an approximate 50% success rate. These primers were utilized to sequence 16S genes of other Triodopsini, such as *Neohelix*, but were not a good fit for

Triodopsis. The sequence of these first 16S trial primers were 16Sar_5'-CGCCTGTTTAHYAAAAACAT-3' and 16Sbr_5'-CCGGTCTGAACTCAGMTCAYGT-3', originally from Palumbi et al. (1991). Custom primers were then designed (Primer3) using sequence data acquired from these first primers.

The new 16S primers were designed from the few sequences amplified from the first primers and are 16SpolyF_5' GCCGCAGTACTTTGACTGTG-3' and 16SpolyR_5'-CCAACATCGAGGTCACAAAC-3'. The PCR protocol used for 16S is a step-up protocol modified from Thaewnon-ngiw et al (Thaewnon-ngiw et al. 2004) using Q5 High Fidelity 2X Master Mix (New England Bio Labs) with annealing temperatures of 45^{o}C (10X) and 60^{o}C (20X) (Wilkinson 2020). These primers and the optimized PCR protocol successfully amplified a 270 bp 16S sequence of all Polygyrid museum specimens tested if the tissue is not degraded, even with old museum specimens and dried tissue. This was a short segment, but highly variable.

ITS2 large subunit complex, including parts of 5.8S and 28S, of approximately 1200 bases was amplified and sequenced to complement the 16S rDNA sequence data for more genetic refinement. Primer sequences LSU-1_5'-CTAGCTGCGAGAATTAATGTGA-3' and LSU-3_5'-ACTTTCCCTCACGGTACTTG-3' were adapted from Wade and Mordan (2000). The PCR protocol used for ITS2 is a one-step PCR using Q5 High Fidelity 2X Master Mix (New England Bio Labs) with annealing temperature of 60^{o}C (30X). Due to intragenomic duplications in the ITS2 gene and lack of variation in 5.8S and 28S portions, a smaller portion of primarily ITS2 of approximately 400 bases within the larger subunit that appeared free of conflicting traces was used. This is referred to in this study as the ITS2 gene.

H3 primers and thermocycler conditions from (Wilkinson 2020), H3F_5'-ATGGCTCGTACCAAGCAGACVGC-3' and H3R_5'-ATATCCTTRGGCATRATRGTGAC-

3', were also used for generation of additional sequence data from the nuclear genome. A PCR protocol and step-up temperature profile is adapted for use with Q5 High Fidelity 2X Master Mix (New England Bio Labs) from a previous study (Thaewnon-ngiw et al. 2004) with annealing temperatures of 45^{o}C (10X) and 60^{o}C (20X). H3 PCR products of 230 bp required further purification with a gel purification kit (GeneJet) due to multiple fragments.

Outgroups of the genus *Mesodon* A. Férussac, 1821 (tribe Mesodontini), *Neohelix* Ihering, 1892 (tribe Triodopsini, same as *Triodopsis*), and members of a sister family, Helicidae (*Cantareus aspertus* (Born, 1778) and *Helix pomatia* Linnaeus, 1758) are used to establish the position of *Triodopsis* in the family Polygyridae. Some of these sequences were available on GenBank and additional sequence data were generated by this author. More distant roots from GenBank (Supplemental 6.2) in addition to the ones above are used for ITS2 and H3, and a non-Stylommatophoran mollusk was used in the molecular clock tree to reference the emergence of Stylommatophora. Amplified DNA was shipped for Sanger sequencing by an external vendor (Eurofins). Traces are corrected in SnapGene (www.snapgene.com) and/or MEGA11 (Tamura et al. 2021). Alignments for each locus was preformed using Muscle in MEGA11.

Phylogeny tree construction

Phylogenies were constructed using maximum likelihood and bootstrapped using MEGA11 using the Hasegawa- Kishino-Yano model and 100 replications. Other models gave essentially the same results. Duplicates at the same location and exact sequence were removed. Concatenation of 16S and ITS2 sequences and subsequent phylogeny were also built with MEGA11. The tree is bootstrapped with the same parameters as the other trees. The molecular clock tree was produced in MEGA11, and genetic distance statistics were calculated in DnaSP

(Rozas et al. 2017). Haplotype network for the concatenated 16S/ITS2 gene was constructed in Network 10.2.0.0 (fluxus-engineering.com). The population statistics of the 16S gene and population statistics (pairwise comparisons and population growth estimates) were calculated for all data as well as subsets of the data corresponding to identified clades were calculated with DnaSP.

H3 tree was constructed MEGA11 from H3 sequences and also with the same parameters. The molecular clock tree was produced using the H3 gene sequences and phylogeny file of *Triodopsis* and various other Stylommatophoran groups from GenBank. The tree was run as a RelTime – ML clock with a member of the Hydrophila as an outgroup (Hydrophila is a sister superorder to the Eupulmonata, which includes the Stylommatophora). The divergence of Stylommatophora at 150mya (Wade et al. 2006) was entered as a constraint and the default analysis settings accepted.

Morphology measurements and biogeography maps

Morphology measurements of the *Triodopsis fallax* group were made by stereomicroscope (Amscope) with an eyepiece reticle, and anatomy is measured as shown in Figure 6.1. Spire height (a.) is from the penultimate suture to the tip of the spire to avoid different body whorl shapes, width (b) is the widest dimension including lip, height (c.) is the highest dimension with top of whorls level, and umbilicus width (d.) is from the closest part of the lip through the middle of the umbilicus which is always offset in *Triodopsis*. Whorl count is from the tip of the embryonic whorl out to the periphery and the decimal fraction to the lip edge is estimated. Photos by author of extremes of *Triodopsis fallax* group morphology are represented in Figure 6.1 e. and f. Some

specimens not used in the final trees due to duplicate sequences are included in the morphological data.

Clades 1,2,3,7 were measured and plotted to find a unique character for identification of clades. Morphological data (see Supplemental 6.3, Figures 6.2 – 6.5) calculated from all measurements (width, height, umbilicus size, spire height and number of whorls), showed a high degree of overlap in all *Triodopsis fallax* group clades. Since in a spherical object such as a shell, size in one direction is not independent of size in another, two-variable PCA plots were created in R (R_Core_Team 2023) with overlapping polygons representing the four clades by color – clade 1 red, clade 2 blue, clade 3 green, and clade 7 purple.

Box plot graphs were constructed by (JMP Pro 16 by SAS Institute, Cary, NC 2021) (see Figures 6.4 – 6.5). In Figure 6.5, we determine any two-variable effect of the characters by plotting ratios of width/height, width/umbilicus size and width/spire height versus clade. Data were tested with two-factor ANOVA (JMP), with several plots showing significance overall.

Biogeographical maps (see Figures 6.16 – 6.18) were produced in Google maps with specimens used in sequencing. Numbers are based on clades produced by the 16S phylogeny. Geographic locations were provided with the specimens as standard provenience or confirmed on Google Earth for self-collected specimens.

RESULTS

Triodopsis genus 16S phylogeny

16S in land snails has a high amount of variability and was used for species level phylogeny (see Figures 6.6 – 6.8). The ITS2 nuclear gene provides some distinction between *Triodopsis* groups, but not enough resolution for the inferred species level (see Figure 6.9). The H3 nuclear

gene had some variability and provided resolution at the family and genus level, (see Figure 6.11) but is not informative at the species level. It is, however, used in the molecular clock determination (see Figure 6.12) and is useful when used for comparison at the order/family taxonomic level. These three genes provide a hierarchical level means of separating the Polygyridae snails genetically – H3 at the family level, ITS2 at a generic/subgeneric level, and 16S at a finer species level, allowing a more complete picture of the evolutionary divergence of this rapidly diverging taxon. The specifics of each tree are discussed below.

In the *Triodopsis* phylogeny tree (see Figure 6.6), major clades are numbered, and specimens are numbered at the beginning of their label as to the clade they into which they fall in the 16S rDNA tree. This grouping was used to reflect consistent membership in clades in the 16S tree despite the low bootstrap values and variation in relationship of these clades with respect to one another. The 16S numbered clades, being more specific to species level, are used as a reference comparison to the morphological characters. These clade numbers stay consistent as part of the name throughout the other trees constructed from sequence for other loci to show the difference in clade composition between the genes. Specimen names in other genera include the taxonomic identification given by malacologists who identified the specimen.

Clades were identified as to species by matching the morphology of the specimens in the clade to species descriptions in Pilsbry (1940) and original authors' publications when possible. Except for the *Triodopsis fallax* group, species names are generally straightforward to assign to clades. In the *T. fallax* group, morphology is indeterminate as to species, so the clades remain as numbered clades only.

All trees have very low bootstrap values in nodes for the internal nodes resulting in instability in the arrangement of the clades near the base. The numbered clades, however, were

consistent and are considered largely stable when using 16S. All three major groups and *Triodopsis burchi* are nearly in a polytomic relationship, even in the 16S phylogeny, likely due to a recent rapid divergence. The two largest clades, the *Triodopsis fallax* group and the *Triodopsis tridentata* group were consistently separated. Even though the bootstrap values are low with 24% and 41% bootstrap values respectively, they are relatively high compared to other clades. The 16S total Triodopsis tree has 122 sequences and 259 base pairs with total number of mutations 170. There are 95 haplotypes, giving a haplotype diversity of 0.99 – nearly every sequence is different. Average number of nucleotide differences is 24.1. F_{ST}'s of different clades are in Table 6.2.

The Triodopsis fallax group 16S phylogeny

The 16S tree of just the *Triodopsis fallax* group (see Figure 6.7) consists of clades 1,2,6, and 7. These clade numbers were assigned for their affinity to stay together, but with low bootstrap values, sometimes they move as seen by specimen 02_NCSM64950 appearing in the middle of Clade 1. Clade 6 (a single specimen) usually stands alone, but in this particular tree, it has another member from Clade 7 with it. Clades 3 and 7 are always closest to the ancestral node and are the furthest south and west of all the clades except Clade 1, which overlaps all other clades on the biogeography map. Clade 4, with good support of a bootstrap of 86%, always forms a stable clade, but in this case, it is inside Clade 2. Clade 2 perhaps should be divided into multiple clades, but low bootstrap values mean tips of Clade 2 recombine. None of these clades have distinct morphology except Clade 4, which is a named species, *Triodopsis obsoleta*. The *Triodopsis fallax* group branch has 60 sequences with 84 polymorphic sites and 41 haplotypes with a haplotype diversity of 0.97. Average number of nucleotide differences is 19.1.

The Triodopsis fraudulenta and Triodopsis tridentata group 16S tree

The tree of *Triodopsis fraudulenta* and *Triodopsis tridentata* (see Figure 6.8) shows good support for most of the clades, but the basal nodes have low bootstrap values. *Triodopsis fraudulenta* (clade 11) and *Triodopsis vulgata* (clade 10) are well supported, but *Triodopsis pendula* (clade 12) is polyphyletic in this instance, showing its close relationship to *T. fraudulenta*.

The *Triodopsis fraudulenta* group (clades 10,11,12) has 11 sequences, 78 polymorphic sites per 259 bases and total mutations of 115. There are 11 haplotypes in 11 sequences with a haplotype diversity of 1.00. The average number of nucleotide differences is 34.3.

Triodopsis burchi (clade 13) is a clade with a bootstrap of 99%. This clade of one species is always stand-alone. It is a well-supported species but its position in the tree is indefinite.

The *Triodopsis tridentata* group, with a relatively high bootstrap value of 41%, always includes *Triodopsis tennesseensis/complanata* (clades 21,22), *Triodopsis fulciden* (clade 14), *Triodopsis tridentata* (clades 15,16,17, 18) and *Triodopsis juxtidens* (clade 19). The *T. tenneessensis/complanata* clade is a solid clade with nearly full support (99%); however, the two "species" are not always separate clades, as is shown in Figure 6.8. *Triodopsis fulciden* (clade 14) is a definite species with 100% bootstrap support. *T. tridentata* and *T. juxtidens* are a mixture of clades, even though *T. juxtidens* (clade 19) is always separate from those of *T. tridentata* (clades 15, 16 17, 18). The entire clade of *Triodopsis tridentata* is not well supported as a single species and needs more work. *T. tridentata* has well supported clades within the main clade that were numbered because they were constantly separate and well supported. *T. juxtidens* also has several clades with good support within the main clade. Clade 16, inside the *T. tridentata* clade, is a named species, *Triodopsis anteridon*, that is not supported in the phylogram as a separate clade but is morphological distinct. It should be noted that specimens of *T. tridentata* and *T. juxtidens* that

were available for this study were from the southern part of their large range only, and most were from permafrost-free areas during the last glacial period. The *Triodopsis tridentata/juxtidens* couplet is a terminal clade that resembles the mixtures of clades of the *Triodopsis fallax* group with low bootstrap values and inconsistent clade structure; however, a significant difference is that the morphology of many of these clades is distinct, but without the phylogeny support. Together, the *Triodopsis tridentata* group has 47 sequences, 76 polymorphic sites and 43 haplotypes at a haplotype diversity of 0.995. The number of mutations is 130 and the average number of nucleotide differences is 23.6.

Population Statistics

Evidence for population expansion was explored by graphing pairwise differences as mismatch distributions of all *Triodopsis* and as separate major groups, comparing observed differences to those expected of constant population size (see Figure 6.14). A large deviation from expected was evident, with an R^2 value of 0.1330 and a mean absolute error of 1.0477 for all clades showing expanding populations. The *Triodopsis fallax* clade had a high peak at lower nucleotide values than the *Triodopsis tridentata* or *Triodopsis fraudulenta* clades, indicating smaller nucleotide number differences are prevalent. The *Triodopsis fallax* clade was also multimodal, whereas the other groups were unimodal. The *Triodopsis tridentata* clade curve was smooth, whereas the other groups have a high raggedness factor, potentially due to lower number of sequences used in the analysis.

Fu's F and Tajima's D of 16S clades were non-significant (see Figure 6.13) and close to zero. However, Clade 2, 13, 15/16/17, 19 and 21/22 are all negative, indicating a population expansion. In Clade 1 and particularly Clade 14, the values are net positive indicating a contracting

population. Clades 3,4,10, and 12 had neutral values, with populations near equilibrium. Clades 11 and 4 had too few species to determine these statistics. Clade 6 with one member was excluded from the calculation, and there is no 5, 8, or 9.

ITS2 and *16S/ITS2 Concatenation*

The ITS2 tree (see Figure 6.9) is unremarkable in that there is little resolution of tip clades and even groups identified in 16S are not distinct. The genera in the tribe, however, were separated with reasonable support, and Tribe Mesodontini appears as a sister to other members of the Tribe Triodopsini. This may be accurate as Perez et al. (2014) found Triodopsini to be polyphyletic.

Concatenation of 16S and ITS2 produces a slightly different structure from the 16S, with two main terminal groups, *Triodopsis fallax* group and *Triodopsis tridentata* group, and the *Triodopsis fraudulenta* group as an ancestral clade. *Triodopsis burchi* (clade 13) is a separate clade, but an ancestral clade in the *Triodopsis fallax* group. Fewer specimens were used for this tree because not all specimens amplified or sequenced well in both ITS2 and 16S. A total of 35 *Triodopsis* sequences were used and was 452 bp in length. There were 134 polymorphic sites with 240 mutations. There were 35 haplotypes with a haplotype diversity of 1.00. Average number of nucleotide differences were 41.1.

A haplotype network (Network 10.2.00) is produced from the concatenation of 16S and ITS2 (see Figure 6.15) that shows an unusual circular shape with a connection between the two major groups at Clades 19 (*Triodopsis juxtidens*) and Clade 3 (*Triodopsis fallax* group). Another connection between major groups occurs between Clade 10 (*Triodopsis pendula*) and Clade 7 (*Triodopsis fallax* group). Other loops occur within the *Triodopsis tridentata* group and the *Triodopsis fallax* group. This is similar to a reticulated haplotype network where gene flow is

occurring between branches rather than a bifurcating tree. Clade 10 (*Triodopsis vulgata*) and Clade 11 (*Triodopsis fraudulenta*) in the Triodopsis fraudulenta group are closest to the root. *Neohelix albolabris*, also in the tribe Triodopsini and ancestral to *Triodopsis*, is used as the root (R).

H3 phylogeny and molecular clock

The H3 tree has little resolution at the species or group level due to the relative lack of variation in the sequences. There were few SNPs in the sequences that would differentiate those clades at the subgenus level. Genera seem to be separate clades; however, bootstraps are very low. There were 58 sequences with 38 polymorphic sites. Total mutations were 39. Number of haplotypes were 21 with a haplotype diversity of 0.62, much lower than other trees. The average number of nucleotide differences is 1.99.

Other Stylommatophorans and a non-Stylommatophoran from GenBank were added to the H3 phylogeny for the molecular tree. The molecular clock tree (fig. 6.12) approximated the evolutionary history of the Stylommatophora from 150mya from Wade et al (2006). Other dates were supported by the molecular clock scale – the K-T Extinction and diversification of Stylommatophora at 64mya (Liu et al. 2021), and the emergence of the Polygyridae at 20mya (Emberton 1994). The Triodopsini and Mesodontini tribes are in a large polytomy at nearly time 0mya, indicating a rapid and recent divergence much less than 20 mya. The Last Glacial Maximum occurred about 20 thousand years ago (Woodward 2014) with a warming trend since.

Morphology measurements and biogeography maps

The graphs show the overlap in characters in the four largest clades in the *Triodopsis fallax* group. In Figures 6.2 and 6.3, only outliers were unique characters, but the middle range of nearly

all the character comparisons is overlapping. Clade 7 is the only clade that is nearly separate in whorls/width (see Figure 6.3,A), but there is still overlap with Clade 3.

The graphs in Figures 6.4 and 6.5 represent the data above a little differently. Single characters and ratios of the characters were tested. Several of the characters were significantly different overall between clades (with two-factor ANOVA, $p < 0.005$), but they were not unique characters that could define a species.

Biogeographical maps (see Figures 6.16) of *Triodopsis fallax* species' ranges showed overlaps in distribution with all clades in the *Triodopsis fallax* group. As with the morphological data, no clade had a unique distribution that excludes all others. Clade 7, ranging from Alabama to just south of the North Carolina line, overlapped only slightly with Clades 2 and 3. Clade 3 covers much of the Piedmont of North and South Carolina and includes Clade 6. Clade 2 covered the Piedmont of the Carolinas and north to New Jersey. However, Clade 1 overlapped all other clades from Texas to New Jersey and across the mountains into Tennessee. The distributions published by Hubricht (1985) indicate that the species included in this clade cover the same territory as Clade 1 but further north to northern Pennsylvania and south to northern Florida.

Maps of the *Triodopsis fraudulenta* group and *Triodopsis burchi* (Clade 13) (see Figure 6.17) show Clades 10, 11, 12, and 13 as separate geographic ranges, closely approximating their proximity in the mountain area. Clade 10 is much larger than the specimen range in this study, but there is very little overlap between clades.

Maps of the *Triodopsis tridentata* group (see Figure 6.18) indicate that the ranges of Clades 17 and 19 are much larger than the range of specimen in this study. Even though there is little overlap of these two distributions in North Carolina, they overlap substantially in West Virginia and north. Several small clades are embedded in the Clade 17 in the southern Appalachians.

DISCUSSION

The 16S gene in land snails has a high amount of variability and works well for species level phylogeny. The ITS2 nuclear gene provides some distinction between *Triodopsis* groups, but not enough resolution for the inferred species level. The H3 nuclear gene had limited variability and provided resolution at the family and genus level but is not informative at the species level. It is, however, used in the molecular clock determination and is useful when used for comparison at the order/family taxonomic level. These three genes provide a hierarchical level means of separating the Polygyridae snails genetically – H3 at the family level, ITS2 at a generic/subgeneric level, and 16S at a finer species level, allowing a more complete picture of the evolutionary divergence of this rapidly diverging and difficult taxon.

Triodopsis 16S phylogeny

The 16S mitochondrial gene was chosen for phylogenetics because it amplified consistently and separated species-level clades well. A 16S phylogeny tree (see Figure 6.6) of all *Triodopsis* in this research shows a divergence of two main subgroups of the *Triodopsis* genus – the *Triodopsis fallax* group and the *Triodopsis tridentata* group, named by the oldest original description. A few other clades that diverged close to the ancestral node were separate from these two groups. One of these is the *Triodopsis fraudulenta* group and includes *Triodopsis fraudulenta* (Clade 11), *Triodopsis vulgata* Pilsbry 1940 (Clade 10), and *Triodopsis pendula* Hubricht, 1952 (Clade 12), as recognized by their morphology. The other, *Triodopsis burchi* (Clade 14), consistently stood alone in the different phylogenies, suggesting that it does not belong to a group. Bootstrap values are very low in nearly all nodes near the ancestral base node of the clade, likely reflecting the recent and rapid divergence of this genus and the short, very variable gene segments

sequenced. More sequence data would likely improve bootstrap scores in the future. Genome wide datasets with a balance of variable and conserved sites may be needed to distinguish these cryptic clades. Whole genome sequencing is needed in this difficult taxon, and none is published to date. This problem with bootstrap values and rapid divergence is likely to be common in other Stylommatophora radiations, since multiple genera have numbers of sympatric sister species in the Southeast US, reflecting the high diversity and high rate of divergence of the land snails there. The high genetic variation is seen in the high number of haplotypes (95) and haplotype diversity (0.99) in the 259 base pairs.

The Triodopsis fallax group

The specimens in the *Triodopsis fallax* group (Clades 1, 2, 3, 4, 6, and 7) are grouped by clade number in the phylogeny (see Figure 6.7) and generally stay in the same clade, despite the low support at the base. Several smaller clades appear in the group with strong support but generally are grouped within the numbered clades. Only one clade in the group is identifiable by morphology. Clade 4 is a stable clade with high support and has been described as *Triodopsis obsoleta* due to highly reduced apertural armature. The other clades could not be identified by morphology to species due to variability of characters and the lack of unique characters to define a species.

It is likely that all *Triodopsis fallax* group clades represent different populations from vicariance during glacial refugia and are in various states of admixture with other clades. Since gene flow between them is apparent from the F_{ST} values between at least adjacent clade ranges, it appears that these are all one species with multiple morphotypes. These morphotypes can even have individual distributions, as they likely were isolated together at one time, and as such, have

been named individual species. After multiple glacial periods, the group is thoroughly mixed, but still retains reproductive compatibility. It is also possible that a longer 16S gene segment would delineate these clades further.

The widespread and expanding Clade 1 may have acquired some invasive characteristics, and further studies to look for multiple duplications of transposable elements may show a genetic signature recognized in other invasive mollusks (Liu et al. 2021). It seems to be easily spread anthropogenically and thrives around buildings and in landscaping in urbanized settings.

The Triodopsis fraudulenta group and Triodopsis burchi

The node nearest the base of the divergence of the genus *Triodopsis* was unstable with low bootstrap values. The *Triodopsis fraudulenta* group, including *Triodopsis vulgata* Pilsbry, 1940 (Clade 10), *Triodopsis fraudulenta* (Clade 11), and *Triodopsis pendula* Hubricht, 1952 (Clade 12), can appear in either main branch depending on the tree iteration. These clades are close to an ancestral *Triodopsis* species and form essentially a polytomy with the other two main groups and *Triodopsis burchi* Hubricht, 1950. The clades in the *Triodopsis fraudulenta* group are recognizable as species by morphology and separate distribution. Even though *Triodopsis pendula* has been misunderstood for many years due to Hubricht's vague description, it can be recognized more easily since genetic analysis helps to clarify the morphological characters. Hubricht's description in 1952 described the shell as the "basal tooth blunt, set transversely on the lip callus" (Hubricht 1952). Without an image, this description was vague and could be applied to many of the *Triodopsis* forms. The members of Clade 12 have a distinctive basal "tooth" that appears to sit not only sideways but protrudes backward into the aperture in a distinctive hook-like shape (see Figure 6.1g). The distribution of this clade also matches Hubricht's limited distribution for *T. pendula*

(Hubricht 1985), and one of the specimens was from the type location of *T. pendula*. Since the rest of Hubricht's description fits, this clade is assumed to be true *Triodopsis pendula*.

Triodopsis fraudulenta and *Triodopsis pendula* are close clades with low bootstrap values that sometimes mix, raising the question of whether they are complete species. The F_{ST} value is just over 0.5. The geographic distribution of the two are disjunct but adjacent and separated by a mountain ridge, which may indicate an evolutionary division that is very recent. The fact that they are recognizable morphologically, genetically, and biogeographically indicates a species-level designation, albeit a potentially a young species. Future analyses with more samples would be likely confirm these hypothesized incipient species. *Triodopsis vulgata* is a close relative but is always separate from the other two.

Triodopsis burchi (Clade 13) also lies near the *Triodopsis* ancestral node. Like the *Triodopsis fraudulenta* group, *T. burchi* groups in various parts of the tree depending on the analysis. It is a Piedmont species in northern North Carolina and southern Virginia and was once thought to be a subspecies of *Triodopsis tennesseensis* (B. Walker & Pilsbry, 1902) because of its shape, but it seems to stand alone in the phylogeny. Its distinctive morphology makes it easy to recognize (highly reduced apertural lip teeth), and the F_{ST} values verify that *T. burchi* is a separate species. Its closest relative has yet to be determined although it should likely branch at the base of the *Triodopsis* tree.

The Triodopsis tridentata group

The group with perhaps the most distinct morphological distinction between species is the *Triodopsis tridentata* group. This group ironically includes some of the largest and the smallest of the recognized *Triodopsis* species. The clade closest to the ancestral node is the largest *Triodopsis*

in this study, *Triodopsis tennesseensis* (Clade 22) and *Triodopsis complanata* (Pilsbry, 1898) (Clade 21). These are in a distinct clade together; however, the limited number of specimens tend to shuffle between separate and mixed within the clade. The morphological descriptions also vary only by slight differences in shell surface structure and geography, so these are clearly closely related. The low number of specimens prevents statistical analysis to determine the F_{ST} value within the clades. Only one *Triodopsis complanata* specimen is included in this study, but it was collected at the type location in Pulaski County, KY, making it a credible representative of the species. The *Triodopsis tennesseensis* specimen from Greene Co., TN is also a syntype. According to other records of geographical distribution of these species, the ranges overlap considerably in eastern Kentucky and Tennessee (Dourson 2010). The two species have changed names several times since Pilsbry (1940), who considered them both *Triodopsis tridentata* (Pilsbry 1940). Since Grimm (1974), they have been considered separate species. More specimens should be sequenced to verify, but in this phylogeny, it appears they may not be separate species.

Triodopsis tridentata sensu stricto (clade 17) is a common species in the mountains and western Piedmont. This species ranges further north than the *Triodopsis fallax* group and has spread to Canada and Michigan. *Triodopsis tridentata* is the type species of the genus and is usually recognizable, with a triangular, symmetrical aperture. Several sister clades to *Triodopsis tridentata* are distinct morphologically. *T. juxtidens* resembles the *Triodopsis fallax* group in size and aperture armature but also retains some *T. tridentata* characters such as the shape of the aperture. Vagvolgyi (1968), Grimm (1974), and Emberton (1988) considered *T. juxtidens* to be a separate species with its own subspecies, but it is genetically part of a clade with *T. tridentata*. Grimm also reported finding them with *T. tridentata* without sign of hybridization. However, statistics show that reproductive isolation may not be complete, even though the clade has

recognizable unique characters; the F_{ST} is only 0.3 between *T. juxtidens* and *T. tridentata* indicating probable gene flow.

Triodopsis juxtidens (Pilsbry, 1899) (Clade 19) appears to be a predominately Piedmont offshoot of *T. tridentata* in the Carolinas but has also spread at least to the Canadian border on the coast and northern mountains. This could be an edge effect where populations on the margins of ranges tend to have less diversity and lower gene flow with the main population, eventually leading to new species if they remain isolated (Dempsey et al. 2020). Spread north of the North Carolina state line must have been from expansion since the Last Glacial Maximum and permafrost, so the original ranges in the Carolinas were in a separate region and habitat. It is not known if they are actually interbreeding in the northern part of their range, or if they just still share ancestral polymorphisms. It is possible that *T. tridentata* and *T. juxtidens* only recently spread into each other's range after many years separated. Sequencing of other genes and specimens from the northern part of their ranges will be needed to determine the status of these two closely related clades. Meanwhile, the definite difference in morphology and separate southern ranges justify leaving them as species pending further work on the northern range of the distribution.

Interestingly, a recognized species, *Triodopsis anteridon* Pilsbry, 1940, (Clade 16) has appeared in the middle of the *Triodopsis tridentata* clade and is collected in the same geographic range. This is best supported as a localized form of *Triodopsis tridentata* and not a separate clade according to 16S, although more specimens are needed to calculate an F_{ST} value. Even though it has a recognized morphology and a distribution that encompasses several counties, it should not be considered a subspecies of *T. tridentata* because of biogeographic overlap and tight phylogeny.

Several other small clades of *T. tridentata* consistently separated from the main clade, namely Clades 15 and 18. These are not morphologically different from *T. tridentata* but seem to

be localized distinct populations within the geographic distribution of *T. tridentata*. More specimens need to be sequenced to investigate these subclades further. Since these land snails tend to create localized forms in isolated habitats, subclades should be considered as such and not subspecies or separate species if within the larger geographic distribution.

Finally, the smallest of the genus, *Triodopsis fulciden* Hubricht, 1952 (Clade 14), falls in a separate clade within the *Triodopsis tridentata* group. This tiny species, only 6-8mm, is located in the foothills of the mountains in North Carolina with a distribution of only 4-5 counties, the center of which is a monadnock called South Mountain. It appears to have become a true species with F_{ST} values high in pairwise comparison with all other clades but is most closely related to the *Triodopsis tennesseensis/complanata* clade in the 16S phylogeny. This is a potential example of the complete speciation of a population in an isolated habitat whose distinctive morphology may have stemmed from a bottleneck effect and is now likely reproductively isolated. The small size may have been a reproductive isolating mechanism as well.

Triodopsis population statistics

The aligned 16S sequences of clades with more than two members have been evaluated with DnaSP (Rozas et al. 2017) to determine if the clades of *Triodopsis*, especially those of the *Triodopsis fallax* group are separate statistically in terms of genetic distance (F_{ST}) and variability. The variability was determined by percentage of nucleotide differences (K_s) in the total number of bases in the 16S segment (var = K_s/259 X 100). Variability between the sequences is high in all clades. Hebert et al. suggests 3% variation in nucleotide sequence to be delimiting between clades for barcoding distinctive species with mitochondrial genes in lepidopteran insects (Hebert et al. 2003). This is obviously an unrealistic cut-off for land snails (Davison et al. 2009), as variation as

high as 21% has been found (Pinceel et al. 2005). Between these *Triodopsis* clades, the percent variation is in the 1.2 – 8.1% range. However, this pairwise variation is mathematically dependent on the individual clade variation, which can vary considerably in *Triodopsis*, and is not a good indicator of speciated clades in land snails.

A better indicator of speciation is the fixation index, F_{ST}, based on allele frequency. All the *Triodopsis* clades show a relatively high F_{ST} value with all values above 0.3 and most above 0.5. This is higher than most other animal species; however, due to the high variability in Stylommatophoran snails, a higher threshold for species delineation is needed for 16S, although more sampling would perhaps lower the F_{ST} values by distributing the variation. In Table 6.2, values of F_{ST} less than 0.4 are marked with an asterisk and are considered the least likely to be separate species based on morphological data in addition to F_{ST}. Most of these are *Triodopsis fallax* group clades – clades 1, 2, 3, 4, and 7 - and are likely to be the same species. Clades 15,16,17 and 19 in the *Triodopsis tridentata* group also show a low F_{ST} of 0.3. *Triodopsis tridentata* (clade 15-17) and *Triodopsis juxtidens* (clade 19) are sister clades. Even though these two clades are morphologically distinct, they may be subspecies of *Triodopsis tridentata* based on F_{ST} values and their branching patterns in the phylogeny. However, only those in the southern part of their distributions have been sequenced, and those in the northern states are needed to determine species status.

The mismatch distribution shown in pairwise comparisons of nucleotide variation in 16S showed a unimodal and general Poisson shape in the *Triodopsis tridentata* group, a sign of a recent population expansion (Harpending 1994; Ray et al. 2003). This type of mismatch distribution indicates a starlike phylogeny, which may explain the low bootstrap values and near polytomies (Ray et al. 2003). The *Triodopsis fallax* and *Triodopsis fraudulenta* groups, however, were

multimodal, a sign of population stability and equilibrium. Raggedness was apparent in all groups, but especially the *Triodopsis fallax* group, reflecting the high diversity of nucleotides in the sequences and a stationary population (Grant 2015; Harpending 1994; Ray et al. 2003). This all signals that *Triodopsis fallax* is a stable population with an ancient expansion, and *Triodopsis tridentata* is a currently expanding population. The *Triodopsis fraudulenta* group likely has too few members to be accurately portrayed, but it resembles the *Triodopsis fallax* group in raggedness, indicating stability.

Overall, the mismatch distributions of the *Triodopsis* genus showed evidence of a population expansion in the past, which agrees with the molecular clock and phylogenies. The *T. fallax* group is a highly diverse population that is currently in equilibrium. *Triodopsis tridentata*, on the other hand, has a smoother curve and appears to be currently expanding. Its spread to Canada since the last ice sheets covered the North is physical evidence of this expansion. The northern and Piedmont spread of *Triodopsis tridentata* may have only recently overlapped *Triodopsis juxtidens*, an earlier isolated subgroup, which overlaps *T. tridentata* in the North Carolina foothills and in the Appalachian Mountains of West Virginia and Virginia.

Statistical tests, Fu's Fs and Tajima's D can be used to infer a population stability from variation in the sequences of a population. Statistically, the values are all nonsignificant, but the sign of the value (positive or negative) is important to predict stability. A negative Fu's Fs indicates a larger than expected number of haplotypes, which is a sign of expansion. A negative Tajima's D indicates a larger than expected number of low-frequency polymorphisms, which also signals expansion. The chart in Figure 6.13 shows relative values of these two tests in clades. *Triodopsis tridentata* had a large negative value and appears to be currently expanding which agrees with the mismatch distribution. However, several individual clades (3, 7, 10, 12, 14) have positive Fu's Fs

values and negative Tajima's D, which tend to balance out. In Clade 1, they were both positive but close to zero, indicating near equilibrium or slightly contracting. (Clades 4 and 11 had too few sequences to run the tests.) Clade 14, *Triodopsis fulciden*, was strongly positive, indicating possible contraction of its small range. This could be a concern for this species that is listed as threatened in the 2015 North Carolina Wildlife Action Plan (https://www.ncwildlife.org), giving credibility to the protection status and ongoing remediation efforts.

In summary, the mismatch distribution and population stability tests agree that the *Triodopsis tridentata* group is currently expanding, but the *Triodopsis fallax* and *Triodopsis fraudulenta* groups are near equilibrium and stable, or slightly expanding in some clades. *Triodopsis fulciden* is the only concern for a possible declining population at the moment.

ITS2 and H3 gene sequencing

The ITS2 gene distinguishes genera of tribe Triodopsini but did not produce enough resolution to be informative at the species level. Concatenation of the 16S and ITS2 sequences produced a tree similar to 16S with group separation; however, the *Triodopsis fraudulenta* group clade is ancestral to other *Triodopsis,* and *Triodopsis burchi* is part of the *Triodopsis fallax* group. This is a likely arrangement as the placement of the base of the *Triodopsis fraudulenta* group was unstable within the 16S phylogeny. It also supports Emberton's consensus tree based on allozymes and the genital character matrix, which shows the *Triodopsis tridentata* and *Triodopsis fallax* groups as sister clades with identical reproductive anatomy and that of the *Triodopsis fraudulenta* group as ancestral (Emberton 1988). Bootstrap values are still low, however, and the group placement is still uncertain. The phylogeny from the concatenated data does demonstrate that the *Triodopsis fraudulenta* group is likely the closest to the *Triodopsis* ancestor. *Triodopsis burchi*

remains an enigma and the exact placement of this species is yet to be determined. F_{ST} statistics show more typical values in this tree. A threshold of 0.2 is closer to that of other organisms. With this threshold, *Triodopsis fallax* group clades are still below the threshold except for Clade 1, which appears differentiated from the other clades in this group (See Table 6.3). Mismatch Distributions, however, (Figure 6.16) are very similar to the ones for 16S except more raggedness due to fewer specimens being compared.

The haplotype network from concatenated 16S and ITS2 sequences shows an unusual circular shape similar to reticulated networks with closed loops and the root (R) at the base of the network. Clades 3 and 7 (*Triodopsis fallax* group) have loops and connections with other groups in the 16S/ITS2 haplotype network. This network makes sense when Emberton's (1988) study of genitalia structures and allozymes are considered. The haplotype network shows a connection between the *Triodopsis tridentata* group and the *Triodopsis fallax* group, of which Emberton found had identical genitalia in 50 characters. Hybridization within the genus in the laboratory and intergrades in the field have been reported by Grimm (1974), including limited hybridization between groups as defined here. The F_{ST} values (see Table 6.3) for the connecting Clades 7 and 12, and 3 and 17, are low, below 0.35 when the cut-off for this study for possibly the same species is 0.2. For clades in different major groups, this is very unusual and may be further evidence of hybridization. It is possible that gene flow is common in the genus, much like other organisms such as amphibians, known for widespread hybridization and interspecies gene flow, but not precluding the formation of separate species (Nadachowska-Brzyska 2010).

The only difference in Emberton's consensus tree and the 16S/ITS2 tree is the position of *Triodopsis pendula*. Emberton has it as a sister to *Triodopsis juxtidens*, which is highly unlikely

based on these genetics. What is more likely is the confusion over the morphology of *T. pendula* led to a misidentification and mischaracterization of the species in Emberton's (1988) paper.

The phylogenies resulting from the H3 gene were less informative at the subgenus level. Families, tribes, and genera are distinct clades, but large subgeneric clades and species are not totally resolved; however, the H3 gene is good for deeper splits in the studied species. The molecular clock calculation uses H3 sequences to measure the time of divergence of *Triodopsis* and the family Polygyridae. A steep curve shown in the molecular clock data indicates that a rapid diversification within the Polygyridae likely occurred (and may still be occurring) in the past 20 million years, perhaps as recently as the Last Glacial Maximum (LGM). The tree is incapable of enough resolution to date the exact emergence of the *Triodopsis* genus. However, it has been previously determined that Triodopsini and Mesodontini are at the tip of the Polygyridae lineage, and the youngest of the genera in the family (Perez et al. 2014). These two tribes are shown in a polytomy in the molecular clock tree in a recent expansion.

The Mesodontini appears as a sister clade of the *Triodopsis* within the Triodopsini in some trees, making the tribe polyphyletic. This agrees with Perez et al. (2014) where the Mesodontini is also a sister to the *Triodopsis*, splitting the Triodopsini tribe. The bootstrap values indicate that this may need further study to determine the exact placement. From this research, it appears the two tribes evolved rapidly and nearly simultaneously.

The molecular clock corresponds to other authors' estimates of the divergence of the family based on other criteria like morphology (Emberton 1994), and Stylommatophoran emergence and expansion (Liu et al. 2021). It also explains the low bootstrap values in the basal nodes of phylogenetic trees since genes underwent rapid mutations and potentially had unsorted polymorphisms. It is likely that the genus is still undergoing rapid change, and speciation is not

complete in many forms, making it difficult to assign a species name to entities that may still be speciating.

Relationship of Morphology and 16S phylogenetics

In the *Triodopsis fallax* group phylogeny, even though many clades are numbered (1, 2, 3, 4, 6, 7), few are assigned a proper taxonomic species name due to the uncertain identification. The specimens are highly variable morphologically, and clades include several morphotypes described as different species by authors. This group includes the recognized species *Triodopsis fallax, Triodopsis hopetonensis, Triodopsis obsoleta, Triodopsis messana, Triodopsis affinis, Triodopsis palustris, Triodopsis vannostrandi, Triodopsis alabamensis,* and a Texas form, *Triodopsis henriettae* (Mazÿck, 1878) as identified by morphology. This uncertainty in taxonomy agrees with past authors; the *Triodopsis fallax*-related clades were always considered subspecies since Pilsbry (1940) until Hubricht's distribution monograph in 1985 (Emberton 1988; Grimm 1974; Hubricht 1985; Pilsbry 1940; Vagvolgyi 1968) (see Table 6.4). Grimm (1974) has observed all the species in the *T. fallax* group freely interbreed and produce fertile offspring with the exception of *T. palustris* (not studied by Grimm) and *T. henriettae*. He considered these taxa, as well as *Triodopsis soelneri* (J. B. Henderson, 1907) (not included in this study), to be subspecies of *T. fallax*.

The *Triodopsis fallax* group similarity was also reflected in morphological measurements. Even though some of the measurements are statistically significant overall ($p < 0.05$), there is no single unique character for any clade when considered individually. For example, one specimen cannot be assigned one and only one clade based on any of these characteristics. Clade 7 is the more southern clade and specimens could be classified as *Triodopsis alabamensis* at the extreme

end of the whorl number (approaching six whorls). However, the entire clade was not always discernible from other clades, especially Clade 3, at lower whorl numbers.

Often *Triodopsis fallax* group snails found in the same population have been identified by morphology as different species despite living in close proximity. Morphology measurements indicate that it may be impossible to separate these as species based on morphology. Populations may very well consist of multiple morphology types and be genetically identical, leading to the current confusion over *Triodopsis fallax* group species and speculation of sympatric speciation.

Only one in the *Triodopsis fallax* group clade has distinct apertural structure. *Triodopsis obsoleta* (clade 4) can be recognized as a form that could be distinct. This species has only one apertural structure, referred to as "teeth", making it easy to identify. The F_{ST} values did not support the complete speciation of *Triodopsis obsoleta*, however. The accepted definition of a subspecies is a distinct population separated by geographical distribution from the parent species (Avise 2004; Patten and Unitt 2002). *T. obsoleta* is not geographically separated from the other clades, so is considered a localized form of the major clade. This phenomenon also occurs in the other clades of *Triodopsis.* The apertural structure of other clades in the *T. fallax* group is highly variable and has been found unsuitable for definitive species identification.

All clades in the *Triodopsis fallax* group appear to be the same according to the F_{ST} values with values less than 0.4 between clades, the bootstrap values between clades in the phylogeny are low, and morphology is indistinct. With no morphological, biogeographical, or genetic separation, they all appear to be the same species with variable morphotypes. Thus, there is no basis for a subspecies designation.

Extreme mitochondrial genome variation in Polygyridae

The extreme mitochondrial genome variation in the Polygyridae is not easily explained. This variation in the land snail genome has been documented previously several times by other authors (Pinceel et al. 2005; Thomaz et al. 1996; Zając et al. 2020). Even though the 16S gene is quite variable in land snails, the COI gene has an even larger amount of variation, to the extent of making it difficult to amplify with standard primers or too variable to design custom primers. This leads to the question of how mitochondrial genes in this taxon can accrue this much variability and maintain function. COI primers have been used successfully for other Stylommatophorans (Harl et al. 2014; Salvador et al. 2020; Zhou et al. 2017), but Polygyrids appear to have more variation than some, requiring degenerate primers. A much lesser degree of variation is found in the Polygyrid nuclear DNA, making this phenomenon limited to mitochondrial genomes. Haase (2013) attributes high COI variability in the snail *Arianta* (Linnaeus, 1758) (Helicidae) as due to Pleistocene glacial survival in refugia in Europe, but doesn't give a genetic mechanism for the variation.

Several theories have been proposed to explain this high mtDNA variation. Long isolated subpopulations that eventually connect is one possible reason for this variation (Avise 2000) in agreement with the refugia scenario. A potential source of mutation could be impaired mitochondrial DNA damage repair, as is suspected in hydra (Barve et al. 2021), which causes rapid accumulation of mutations leading to high genetic variation. This could be a source of the mutations, but mating habits could maintain each non-lethal mutation in the population.

A theory that may explain this phenomenon takes into account that nearly all land snails are hermaphroditic and most engage in reciprocal fertilization (Barker 2001). All snails in a lineage can pass on their haplotype since all could take the female role and lay eggs (Barker 2001). In

reciprocal fertilization, there are two egg clutches laid from each mating, assuming each is successfully fertilized (see Figure 6.19). In terms of mitochondrial genomes, this means that since both snails act as a female (and simultaneously, both as a male), their haplotype, only being passed to the next generation in the egg, is passed on by both snails equally to their offspring. Whereas a haplotype would be lost in male offspring in dioecious animals, it has the potential to be passed on by all offspring in hermaphrodites with reciprocal fertilization. The only way the haplotype is lost is if a snail does not successfully reproduce. This means that every haplotype that is created by random viable mutation has the potential to persist in a population, leading to a high population haplotype diversity. Reciprocal fertilization potentially increases the variation two-fold, with each mating producing two broods of eggs. These are large clutch sizes and have high attrition, but if any survive from the two clutches, the haplotype diversity is maintained.

Is this level of mutation in the mitochondrial genes affecting the function of electron transport and other critical mitochondrial functions? It either has not, or snails have developed alternative functions that allow alterations of critical mitochondrial genes. This phenomenon should be explored to determine if functionality is affected by the high variation in the Polygyrid mitochondrial genome.

Other Stylommatophorans that reproduce by reciprocal fertilization should also be studied, for example, Limacoid and Arionoid slugs. Pinceel (2005) has documented the extreme mtDNA diversity of Arionid slugs and listed several possible reasons but did not consider reciprocal fertilization as a factor. Philomycid slugs also have shown the same type of genetic variation in preliminary data (this author, unpublished). The extreme variation in the mitochondrial genome is further evidence of unusual relationships among land snail populations, making land snails a unique future study in population genetics.

Phylogeography and Speciation in Triodopsis

The two main *Triodopsis* groups, *fallax* and *tridentata*, appear to have different phenotypic reactions to their environment. The *Triodopsis fallax* group has multiple stable clades in its phylogeny, but variable morphologies that do not correspond to the clades. The *Triodopsis tridentata* group has distinct morphologies that correspond nicely to clades in the phylogeny, even if not completely speciated. It appears genetic change came first in one group, and morphology change in the other. A possible theory of the difference in morphology correlation to genetics between the *Triodopsis fallax* group and the *Triodopsis tridentata* group may be based on climate history and phylogeography.

If the *Triodopsis* genus arose during the last 20 million years, it did so during a volatile climate period of repeated and numerous glaciation events every 20 – 40 thousand years (Hewitt 2000). Ice sheets did not reach what is now the eastern Coastal Plain south of Pennsylvania, but the changing climate resulted in repeated temperature fluctuations and uninhabitable regions throughout the Piedmont and Coastal Plain during multiple glacial periods. Cold, dry, windy conditions reduced populations of animals to refugia clusters (Walker et al. 2009). Refugia were located south of the ice sheet and permafrost, which extended nearly to North Carolina (Hewitt 2000).

Climate refugia identified for other animal species have been broad areas, such as the Appalachian Mountains or the Gulf Coast (Waltari et al. 2007). It is suspected that snails require a much smaller area of refugia than larger animals, micro-refugia such as sheltered ravines and rocky hillsides. Years of collecting in North Carolina has shown that the diversity of snails is highest on the north side of Piedmont monadnocks, the small remnant mountains such as Bakers Mountain, Spencer Mountain, Morrow Mountain and South Mountain in the North Carolina

Piedmont (Furr, unpublished data). Isolated subgroups may have been reduced to small populations on the north side of these small mountains and acquired deme-like specific mutations, much like those of Lepidoptera (Vandewoestijne and Van Dyck 2010). Mixtures of these "demes" were repeatedly reduced to these mountain mini-refugia during each glaciation and then dispersed with secondary contact during every interglacial period. It is speculated this may have contributed to the mixture of morphological phenotypes in the primarily Piedmont and coastal *Triodopsis fallax* group. These microrefugia are close enough together to allow land snails to redistribute nearly completely during each interglacial period. During warmer, wetter conditions, the populations likely outgrew the small monadnocks and spread, mixing with other populations until the next glacial period restricted a few survivors to the refugia again. Snails can spread over large geographic areas during interglacial periods, just as *Triodopsis tridentata* has reached Canada since the Last Glacial Maximum, even with passive transport.

For the potential incipient species that has not achieved reproductive isolation, this secondary contact could result in many integrations and genetic swapping, producing a mosaic of intergrades and hybrids, primarily in the Piedmont and Coastal Plain. Here is a taxon that has appeared to have diverged into numerous separate species sympatrically; however, when the phylogeography and past climate conditions are considered, refugia have provided the isolation to allow diversification of the group into separate morphotypes. These would have eventually become biological-concept species, except conditions changed, and secondary contact occurred before the process was complete.

There has been little research on invertebrates in this area of study except for large millipedes, genus *Narceus* Rafinesque, 1820, which incidentally occupy a habitat similar to woodland snails (Walker et al. 2009). Glacial period refugia for the millipede has been suggested

to include the Appalachian Mountains and Gulf Coast. The same diversity is also shown in the *Narceus* millipede, and the phylogeny trees are strikingly similar (Walker et al. 2009), even to the many morphologically cryptic polytomic clades at the phylogeny tip. The authors found the same rapid diversification and variable mitochondrial genome occurred in the millipede as reported here for these snails. This could help explain the extreme COI gene variation (Haase et al. 2013).

The *Triodopsis tridentata* group is primarily centered along the Appalachian Mountains, already in what is considered refugia territory (Walker et al. 2009). This group did not experience the same conditions as those in the Piedmont and Coastal Plain endured. The speciation was able to progress to completion in some cases, and the species were able to remain relatively stable, protected from secondary contact by the elevations and valleys of the mountains. *Triodopsis tridentata* and *Triodopsis juxtidens* seem to have greatly expanded distribution since the last ice sheets, perhaps overlapping in some areas only relatively recently.

Emberton has postulated that the *Triodopsis* has southern Appalachian origins (Emberton 1994), and our phylogeography shows the deepest ancestral clade, the *Triodopsis fraudulenta* group, to have a distribution centered in the Appalachians, supporting his theory. *Triodopsis vulgata* also has a different genitalia structure than others of the genus, although hybridization with tip species has been reported (Emberton 1988). It and *Triodopsis fraudulenta* are also the closest to the root, *Neohelix albolabris*, labeled R in the haplotype network, which was chosen due to its ancestral position in other trees. This evidence leads us to believe that these are the closest living species to the ancestral *Triodopsis* of these studied so far.

More work needs to be done in this area to better understand the phylogeographic distribution of land snails during this period. This could provide important insight into the

ramifications of climate change and the need to preserve refugia areas as habitats for future glacial periods and/or climate warming.

CONCLUSION

The question of what a species is has been controversial since Linnaeus. There appears to be no universal answer for all groups of organisms. Three species concepts have been proposed in the past - biological, phylogenetic, and morphological. All concepts must be considered, but a perfectly good species may not fit all three. Such is the case in the *Triodopsis* genus of land snails. Adherence to any of the concepts has been difficult to determine in these animals.

The premise of the biological concept is reproductive isolation or lack of gene flow. Emberton (1988) showed the similarity of the reproductive anatomy of *Triodopsis* snails. They are also hermaphroditic with reciprocal fertilization, the ability to self-fertilize, and have been known to store sperm for indeterminate amounts of time (Barker 2001), making it difficult to determine gene flow empirically. Many in this taxon have overlapping distributions that rule out biogeographical isolation. In many cases, the complete distributions of snails are not fully known.

Phylogenetic separation is difficult as mitochondrial genes most often used for species determination are extremely variable in *Triodopsis* even within clades. The 16S gene has been the most useful for species definition, but low bootstraps on the ancestral nodes make relationships between major clades uncertain. Many clades cannot be matched to a described species. There is evidence of possible gene flow from sequence data, even between well delineated clades considered species. Hybridization between species and major groups has been recorded (Grimm 1974), and the haplotype network reveals evidence of interbreeding.

Morphology is uncertain, as at least one major clade in *Triodopsis* is a morphological mixture of described forms that are genetically similar. Morphology can be environmentally induced and prone to high variation in some of these snails. In others, morphology matches phylogeny and biogeography quite well. Again, it is only evidence that must be considered, and once confirmed, can be used by taxonomists as a tool.

With the concepts taken together, there may be enough clues to reasonably determine which clades are distinct enough to name them confidently. After all, a species name is purely a human construct, speciation is a process, and populations in the process of speciation may not be at a point where they can be uniquely named to species level, or they may not fit our definition of species.

This research has provided genetic markers for different taxon levels for the Polygyridae, and one that works well at species-level clades. It has also outlined a protocol that works well with Polygyrid land snails to extract DNA with high yields for single-gene sequencing which has previously been notoriously difficult. A correlation between morphological description and genetic sequence of the 16S gene has been established here for many *Triodopsis* species, and yet failed to distinguish established species in a substantial number, which leads to a reassessment of the number of species in the genus. The recommended changes for *Triodopsis* species names are included in Table 6.4.

A full *Triodopsis* genus revision needs to be completed to define all the species and subspecies. Unfortunately, a total revision of the genus is not possible at this time since all the recognized species are not included in this study. A total of 19 of the 28 recognized species are included here. Missing are some of the northern, mid-west, and Texas-area species that could not be located in time, including *Triodopsis claibornensis* Lutz, 1950, *Triodopsis picea* Hubricht,

1952, *Triodopsis platysayoides* (Brooks, 1932), *Triodopsis rugosa* Brooks& MacMillan, 1940, *Triodopsis cragini* Call, 1886, *Triodopsis vultuosa* (A. Gould, 1848), *Triodopsis discoidea* (Pilsbry, 1904), and *Triodopsis neglecta* (Pilsbry, 1899). Also missing is an eastern North Carolina species, *Triodopsis soelneri* (J. B. Henderson, 1907), which is federal and state listed as threatened. Some included clades need more representatives to confirm phylogenetic positions.

In addition, this study provides a novel hypothesis on the effect of climate on the phenotype and genetics of small non-vagile invertebrates, as well as a hypothesis of the cause of the extreme mitochondrial variation and haplotype diversity in the Polygyrid snails. Reciprocal fertilization has not been previously recognized as a factor in mitochondrial genetic variation.

Divergence into species with gene flow with discordances between morphology and phylogeny is not unique to land snails. It is common in amphibians as well (Nadachowska-Brzyska 2010). To determine the evolutionary history of taxa that hybridize freely, a single genetic marker may not be sufficient. Multilocus approaches are necessary to investigate not only gene phylogeny, but also species phylogeny, which may not agree due to incomplete lineage sorting and introgression. This research will continue and will investigate other phylogenetic techniques to help resolve this difficult taxon.

Phylogeography research should also be a priority in land snails and all woodland invertebrates as much can be learned from the survival and distribution of these organisms during climatic events. Genetic sequencing of these animals will help to better define species, determine distributions, and access the need for protection status of habitat and individual populations. The land snails in the family Polygyridae are currently understudied and need more focus in the future.

TABLE 6.1

Key to *Triodopsis* 16S Clade Numbers Used In Phylogenies
(Currently Recognized Species Names)

<u>*Triodopsis fallax* Group</u>	
Clades 1, 2, 3, 6, 7	*Triodopsis fallax/hopetonensis/palustris/ alabamensis/vannostrandi*
Clade 4	*Triodopsis obsoleta*
<u>*Triodopsis fraudulenta* Group</u>	
Clade 10	*Triodopsis vulgata*
Clade 11	*Triodopsis fraudulenta*
Clade 12	*Triodopsis pendula*
<u>*Triodopsis burchi* Group</u>	
Clade 13	*Triodopsis burchi*
<u>*Triodopsis tridentata* Group</u>	
Clade 14	*Triodopsis fulciden*
Clade 15	*Triodopsis tridentata* (west of Appalachians)
Clade 16	*Triodopsis anteridon*
Clade 17	*Triodopsis tridentata* (east of Appalachians)
Clade 18	*Triodopsis tridentata* (Polk County, NC)
Clade 19	*Triodopsis juxtidens*
Clade 21	*Triodopsis complanata*
Clade 22	*Triodopsis tennesseensis*

TABLE 6.2

16S Pairwise Polymorphism Statistics of All *Triodopsis* Clades

POP 1	POP 2	F_{ST}	Hs	Ks	% var
Clade_1	Clade_2	*0.349	0.908	9.610	3.710
Clade_1	Clade_3	0.473	0.868	8.503	3.283
Clade_1	Clade_4	0.490	0.850	6.764	2.612
Clade_1	Clade_7	0.516	0.877	8.052	3.109
Clade_1	Clade_10	0.586	0.868	7.363	2.843
Clade_1	Clade_11	0.791	0.863	6.231	2.406
Clade_1	Clade_12	0.674	0.868	7.815	3.017
Clade_1	Clade_13	0.855	0.868	5.664	2.187
Clade_1	Clade_14	0.872	0.831	5.578	2.154
Clade_1	Clade_15_16_17	0.665	0.921	9.831	3.796
Clade_1	Clade_19	0.688	0.897	8.619	3.328
Clade_1	Clade_21_22	0.793	0.862	6.248	2.412
Clade_2	Clade_3	*0.327	0.988	16.282	6.286
Clade_2	Clade_4	*0.328	0.968	14.168	5.470
Clade_2	Clade_7	*0.290	0.990	15.014	5.797
Clade_2	Clade_10	0.495	0.988	14.676	5.666
Clade_2	Clade_11	0.656	0.988	13.406	5.176
Clade_2	Clade_12	0.517	0.988	15.312	5.912
Clade_2	Clade_13	0.754	0.988	12.282	4.742
Clade_2	Clade_14	0.772	0.933	12.160	4.695
Clade_2	Clade_15_16_17	0.554	0.992	14.297	5.520
Clade_2	Clade_19	0.556	0.987	14.173	5.472
Clade_2	Clade_21_22	0.650	0.973	12.806	4.944
Clade_3	Clade_4	0.446	0.889	18.381	7.097
Clade_3	Clade_7	*0.320	1.000	19.147	7.393
Clade_3	Clade_10	0.420	1.000	19.250	7.432
Clade_3	Clade_11	0.595	1.000	16.095	6.214
Clade_3	Clade_12	0.434	1.000	21.000	8.108

Clade_3	Clade_13	0.642	1.000	12.667	4.891
Clade_3	Clade_14	0.646	0.750	12.333	4.762
Clade_3	Clade_15_16_17	0.418	0.996	15.456	5.967
Clade_3	Clade_19	0.426	0.989	15.912	6.144
Clade_3	Clade_21_22	0.563	0.940	13.963	5.391
Clade_4	Clade_7	0.437	0.933	14.533	5.611
Clade_4	Clade_10	0.579	0.889	13.333	5.148
Clade_4	Clade_11	0.752	0.833	8.667	3.346
Clade_4	Clade_12	0.634	0.889	15.333	5.920
Clade_4	Clade_13	0.808	0.889	5.810	2.243
Clade_4	Clade_14	0.833	0.556	5.429	2.096
Clade_4	Clade_15_16_17	0.602	0.981	13.717	5.296
Clade_4	Clade_19	0.632	0.960	13.115	5.064
Clade_4	Clade_21_22	0.739	0.842	8.125	3.137
Clade_7	Clade_10	0.438	1.000	15.613	6.028
Clade_7	Clade_11	0.626	1.000	12.756	4.925
Clade_7	Clade_12	0.469	1.000	17.013	6.569
Clade_7	Clade_13	0.691	1.000	10.347	3.995
Clade_7	Clade_14	0.743	0.833	10.080	3.892
Clade_7	Clade_15_16_17	0.489	0.997	14.463	5.584
Clade_7	Clade_19	0.488	0.991	14.349	5.540
Clade_7	Clade_21_22	0.624	0.957	11.618	4.486
Clade_10	Clade_11	0.570	1.000	11.048	4.266
Clade_10	Clade_12	0.488	1.000	16.583	6.403
Clade_10	Clade_13	0.711	1.000	8.250	3.185
Clade_10	Clade_14	0.667	0.750	7.917	3.057
Clade_10	Clade_15_16_17	0.447	0.996	14.147	5.462
Clade_10	Clade_19	0.542	0.989	13.833	5.341
Clade_10	Clade_21_22	0.584	0.940	10.037	3.875
Clade_11	Clade_12	0.568	1.000	13.048	5.038
Clade_11	Clade_13	0.891	1.000	3.524	1.361

Clade_11	Clade_14	0.865	0.667	3.143	1.214
Clade_11	Clade_15_16_17	0.632	0.996	13.101	5.059
Clade_11	Clade_19	0.666	0.988	12.115	4.677
Clade_11	Clade_21_22	0.794	0.925	6.125	2.365
Clade_12	Clade_13	0.725	1.000	10.000	3.861
Clade_12	Clade_14	0.737	0.750	9.667	3.732
Clade_12	Clade_15_16_17	0.515	0.996	14.666	5.662
Clade_12	Clade_19	0.504	0.989	14.657	5.659
Clade_12	Clade_21_22	0.600	0.940	11.593	4.476
Clade_13	Clade_14	0.950	0.750	1.333	0.515
Clade_13	Clade_15_16_17	0.696	0.996	12.196	4.709
Clade_13	Clade_19	0.730	0.989	10.735	4.145
Clade_13	Clade_21_22	0.866	0.940	4.185	1.616
Clade_14	Clade_15_16_17	0.611	0.953	12.098	4.671
Clade_14	Clade_19	0.698	0.912	10.578	4.084
Clade_14	Clade_21_22	0.843	0.740	3.889	1.502
Clade_15_16_17	Clade_19	*0.303	0.993	13.846	5.346
Clade_15_16_17	Clade_21_22	0.516	0.984	12.630	4.876
Clade_19	Clade_21_22	0.487	0.969	11.491	4.437

Chi^2: 1416.00; $p = 0.0000$; (df = 1104) (DnaSP)

Table 6.2 Pairwise comparisons of all major clades in the *Triodopsis* as computed with 16S sequences. F_{ST} – Fixation Index; Hs – Haplotype Diversity; Ks - # nucleotide differences. (DnaSP). Percent variation is calculated as Ks/259 (number of bases in sequence) X 100. F_{ST} values that round to less than 0.4 are marked with an (*). (DnaSP) A key to clade numbers is in Table 6.1.

TABLE 6.3

16S/ITS2 Pairwise Polymorphism Statistics of All *Triodopsis* Clades

POP 1	POP 2	Fst	Hs	Ks	% var
T_fallax_group	T_fraudulenta_group	0.2295	1.0000	36.1281	0.0547
T_fallax_group	T_tridentata_group	0.2661	1.0000	33.1987	0.0503
T_fraudulenta_group	T_tridentata_group	0.2719	1.0000	31.3649	0.0475
Clade_7	Clade_17	0.3656	1.0000	25.3125	0.0384
Clade_7	Clade_19	0.2987	1.0000	28.8333	0.0437
Clade_7	Clade_2	*0.1243	1.0000	33.6667	0.0510
Clade_7	Clade_1	0.3808	1.0000	23.6667	0.0359
Clade_7	Clade_3	*0.1306	1.0000	38.8333	0.0588
Clade_7	Clade_12	0.3414	1.0000	28.4762	0.0431
Clade_7	Clade_21_22	0.4499	1.0000	25.0000	0.0379
Clade_17	Clade_19	0.3527	1.0000	19.9375	0.0302
Clade_17	Clade_2	0.4516	1.0000	23.5625	0.0357
Clade_17	Clade_1	0.6485	1.0000	16.0625	0.0243
Clade_17	Clade_3	0.3483	1.0000	27.4375	0.0416
Clade_17	Clade_12	0.5532	1.0000	20.6482	0.0313
Clade_17	Clade_21_22	0.5414	1.0000	17.0625	0.0259
Clade_19	Clade_2	0.3789	1.0000	26.5000	0.0402
Clade_19	Clade_1	0.6396	1.0000	16.5000	0.0250
Clade_19	Clade_3	0.3552	1.0000	31.6667	0.0480
Clade_19	Clade_12	0.4953	1.0000	22.3333	0.0338
Clade_19	Clade_21_22	0.4309	1.0000	17.8333	0.0270
Clade_2	Clade_1	0.2558	1.0000	21.3333	0.0323
Clade_2	Clade_3	*0.1909	1.0000	36.5000	0.0553
Clade_2	Clade_12	0.3993	1.0000	26.4762	0.0401
Clade_2	Clade_21_22	0.5189	1.0000	22.6667	0.0343
Clade_1	Clade_3	0.3657	1.0000	26.5000	0.0402
Clade_1	Clade_12	0.6661	1.0000	17.9048	0.0271
Clade_1	Clade_21_22	0.7299	1.0000	12.6667	0.0192
Clade_3	Clade_12	0.3818	1.0000	30.9048	0.0468
Clade_3	Clade_21_22	0.4519	1.0000	27.8333	0.0422
Clade_12	Clade_21_22	0.5900	1.0000	19.0476	0.0289

Table 6.3 Pairwise comparisons of all major clades in the *Triodopsis* as computed with 16S sequences. F_{ST} – Fixation Index; Hs – Haplotype Diversity; Ks - # nucleotide differences. (DnaSP). Percent variation is calculated as Ks/259 (number of bases in sequence) X 100. F_{ST} values that round to less than 0.2 are marked with an (*). (DnaSP) A key to clade numbers is in Table 6.1.

TABLE 6.4 A History of the *Triodopsis* genus Nomenclature
(modified from Emberton, 1988)

Currently Recognized Triodopsis Species	Pilsbry, 1940	Vagvolgyi, 1960	Grimm, 1974	Hubricht, 1985	Emberton, 1988*	Furr and Reitzel - this research	16S Clades
Triodopsis fallax (Say, 1825)	*T. fallax*	*T. fallax*	*T. fallax fallax*	*T. fallax*	*T. fallax/fallax*	***Triodopsis fallax***	1,2,3,4,6,7
Triodopsis messana Hubricht, 1952	-	*T. fallax (hybrid)*	*T. fallax messana*	*T. messana*	*T. fallax/fallax*		?
Triodopsis palustris (Hubricht, 1958)	-	*T. fallax obsoleta*	-	*T. palustris*	*T. fallax/fallax*		?
Triodopsis obsoleta (Pilsbry, 1894)	*T. hopetonensis*	*T. fallax obsoleta*	*T. fallax obsoleta*	*T. obsoleta*	*T. fallax/fallax*		4
Triodopsis alabamensis (Pilsbry, 1902)	*T. vannostrandi*	*T. fallax alabamensis*	*T. fallax alabamensis*	*T. alabamensis*	*T. fallax/alabamensis*		?
Triodopsis vannostrandi (Bland, 1876)	*T. vannostrandi*	*T. fallax (hybrid)*	*T. fallax vannostrandi*	*T. vannostrandi*	*T. fallax/alabamensis*		?
Triodopsis hopetonensis (Shuttleworth, 1852)	*T. hopetonensis*	*T. fallax (hybrid)*	*T. fallax hopetonensis*	*T. hopetonensis*	*T. fallax/alabamensis*		?
Triodopsis henriettae (Mazyck, 1878)	*T. vultuosa*	*T. copei (hybrid)*	*T. henriettae*	*T. henriettae*	*T. cragini*	*Triodopsis henriettae* ◊	?
Triodopsis affinis (Hubricht, 1954)*	-	-	*T. fallax affinis*	*T. affinis*	-	*Triodopsis fallax*	?
Triodopsis vulgata Pilsbry, 1940	*T. fraudulenta*	*T. neglecta vulgata*	*T. vulgata*	*T. vulgata*	*T. vulgata/vulgata*	*Triodopsis vulgata*	10
Triodopsis fraudulenta Pilsbry, 1894	*T. fraudulenta*	*T. fraudulenta*	*T. fraudulenta*	*T. fraudulenta*	*T. vulgata/fraudulenta*	*Triodopsis fraudulenta*	11
Triodopsis pendula Hubricht, 1952	-	*T. pendula*	-	*T. pendula*	*T. juxtidens/neglecta*	*Triodopsis pendula*	12
Triodopsis burchi Hubricht, 1950	-	*T. burchi*	*T. burchi*	*T. burchi*	*T. burchi*	*Triodopsis burchi*	13
Triodopsis fulciden Hubricht, 1952	-	*T. fulciden*	-	*T. fulciden*	*T. rugosa(?)*	*Triodopsis fulciden*	14
Triodopsis anteridon Pilsbry, 1940	*T. rugosa*	*T. rugosa*	*T. tridentata anteridon*	*T. anteridon*	*T. tridentata*	***Triodopsis tridentata***	16
Triodopsis tridentata (Say, 1817)	*T. tridentata*	*T. tridentata*	*T. tridentata*	*T. tridentata*	*T. tridentata*		15,17,18
Triodopsis juxtidens (Pilsbry, 1899)	*T. tridentata*	*T. juxtidens juxtidens*	*T. juxtidens*	*T. juxtidens*	*T. juxtidens/juxtidens*	*Triodopsis juxtidens* ◊	19
Triodopsis tennesseensis (Walker&Pilsbry, 1902)	*T. tridentata*	*T. complanata*	*T. tennesseensis*	*T. tennesseensis*	*T. tennesseensis*	*Triodopsis tennesseensis* ◊	22
Triodopsis complanata (Pilsbry, 1898)	*T. tridentata*	*T. complanata*	*T. complanata*	*T. complanata*	*T. complanata*	*Triodopsis complanata* ◊	21
Triodopsis claibornensis Lutz, 1950	-	*T. neglecta vulgata*	-	*T. claibornensis*	*T. vulgata/claibornensis*	Not studied	
Triodopsis picea Hubricht, 1952	-	*T. fraudulenta*	-	*T. picea*	*T. vulgata/fraudulenta*	Not studied	
Triodopsis platysayoides (Brooks, 1932)	*T. platysayoides*	*T. complanata platysayoides*	*T. platysayoides*	*T. platysayoides*	*T. platysayoides*	Not studied	
Triodopsis rugosa Brooks&MacMillan, 1940	*T. rugosa*	*T. rugosa*	-	*T. rugosa*	*T. rugosa*	Not studied	
Triodopsis cragini Call, 1886	*T, cragini*	*T. copei cragini*	*T. cragini*	*T. cragini*	*T. cragini*	Not studied	
Triodopsis vultuosa (A. Gould, 1848)	*T. vultuosa*	*T. copei (hybrid)*	*T. vultuosa*	*T. vultuosa*	*T. cragini*	Not studied	
Triodopsis soelneri (J.B.Henderon, 1907)	*T. soelneri*	*T. soelneri*	*T. soelneri*	*T. soelneri*	*T. fallax/fallax*	Not studied	
Triodopsis discoidea (Pilsbry, 1904)	*T. tridentata*	*T. juxtidens discoidea*	*T. juxtidens discoidea*	*T. discoidea*	*T. juxtidens/juxtidens*	Not studied	
Triodopsis neglecta (Pilsbry, 1899)	*T. neglecta*	*T. neglecta neglecta*	-	*T. neglecta*	*T. juxtidens/neglecta*	Not studied	

Table 6.4. *Emberton's list is of groups and subgroups – he did not officially change species names.◊ Insufficient specimens for determination of status. Names and authors are as listed at Molluscabase.org. Name changes in bold.

FIGURE 6.1

Triodopsis Shell Morphology

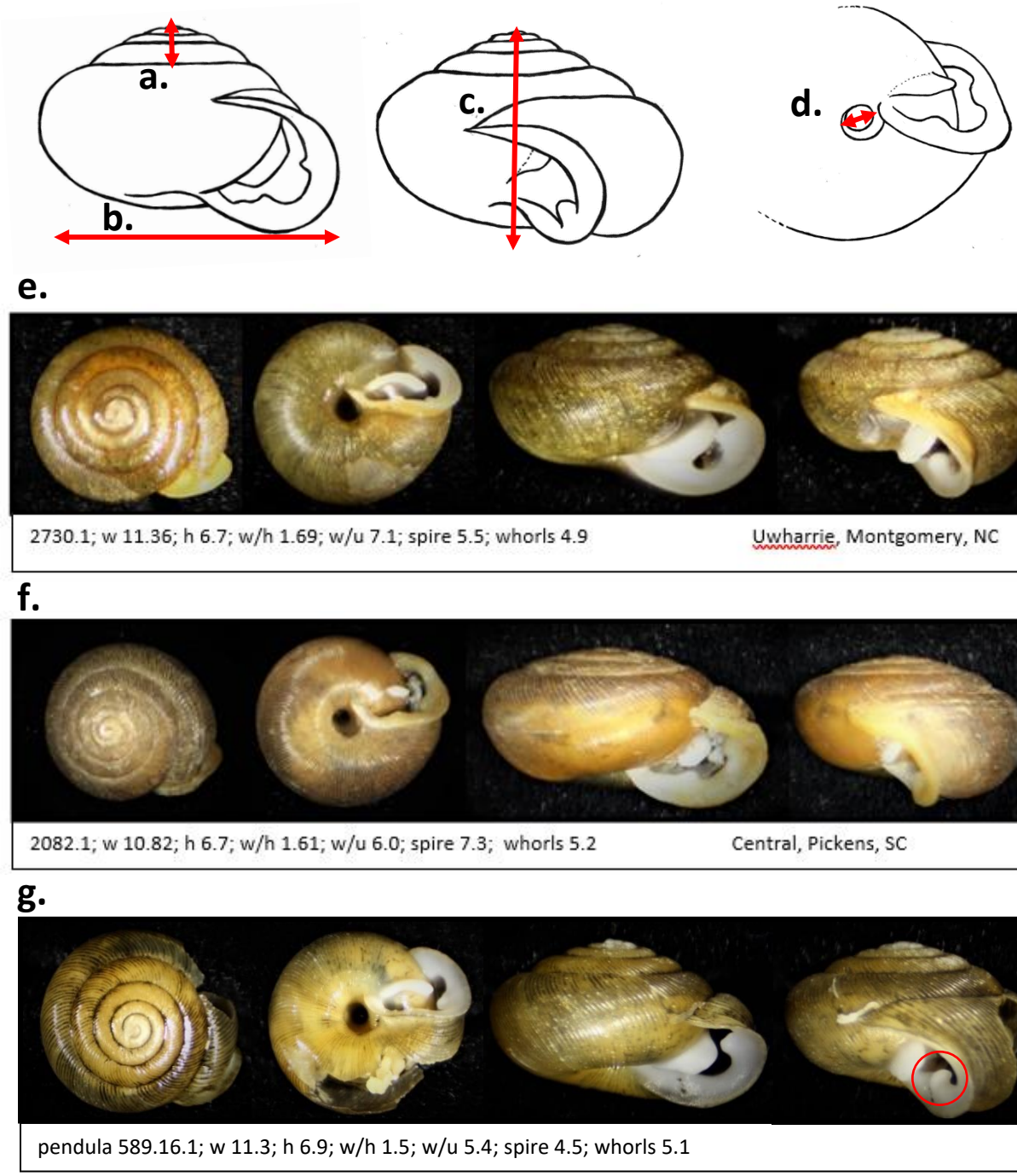

Figure 6.1. Measuring *Triodopsis* shell morphology (all measurements in mm), a.) spire height, b.) width, c.) height, d.) width of umbilicus, e. – f.) Extremes of *Triodopsis fallax* group morphology, e. has larger "teeth" and a crowded opening, g) *Triodopsis pendula* with hook-like basal tooth circled. Tissue can be seen inside f. Drawings and photos by author.

FIGURE 6.2

Triodopsis Morphology Two-Variable Measurement Graphs – Part 1

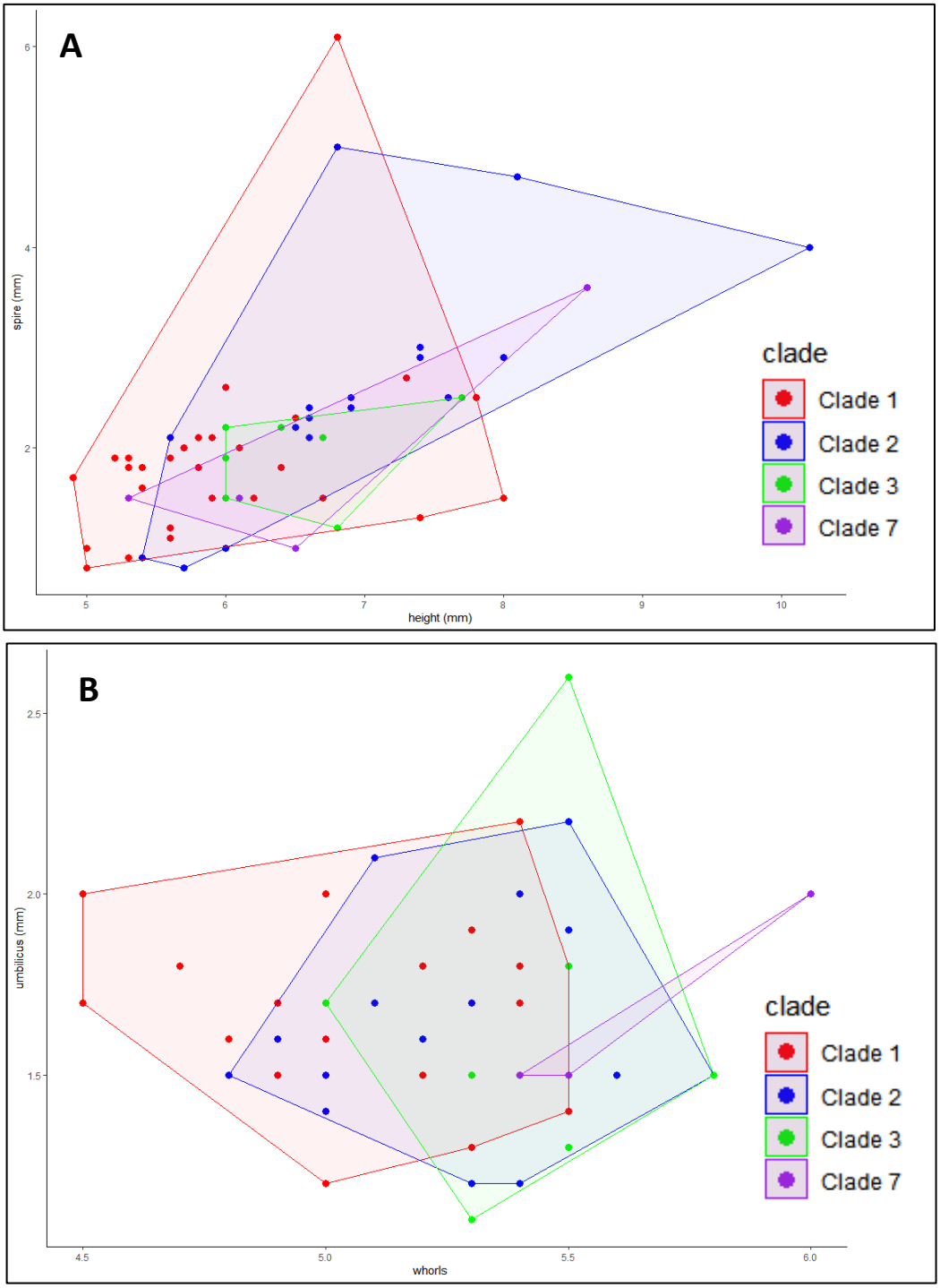

Figure 6.2. Graphs comparing two variables in clades in the *Triodopsis fallax* group. A) Height vs. Spire height, B) Whorls vs. Umbilicus width. A key to clade numbers is in Table 6.1 (R).

FIGURE 6.3

Triodopsis Morphology Two-Variable Measurement Graphs – Part 2

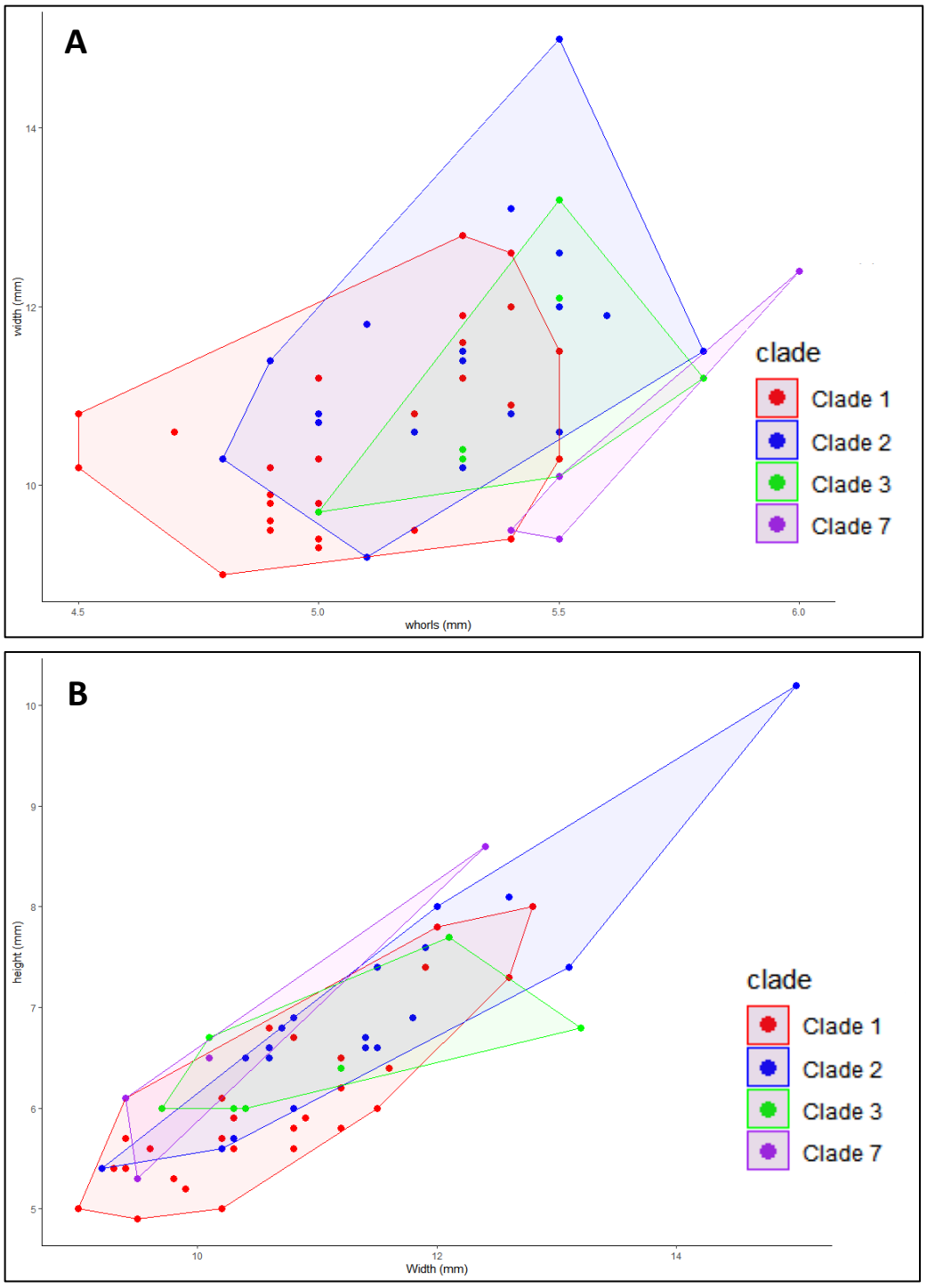

Figure 6.3. Graphs comparing two variables in clades in the *Triodopsis fallax* group. A) Whorls vs. Width, B) Width vs. Height. A key to clade numbers is in Table 6.1. (R)

FIGURE 6.4

Morphological measurements of *Triodopsis fallax* Group Clades – Part 1

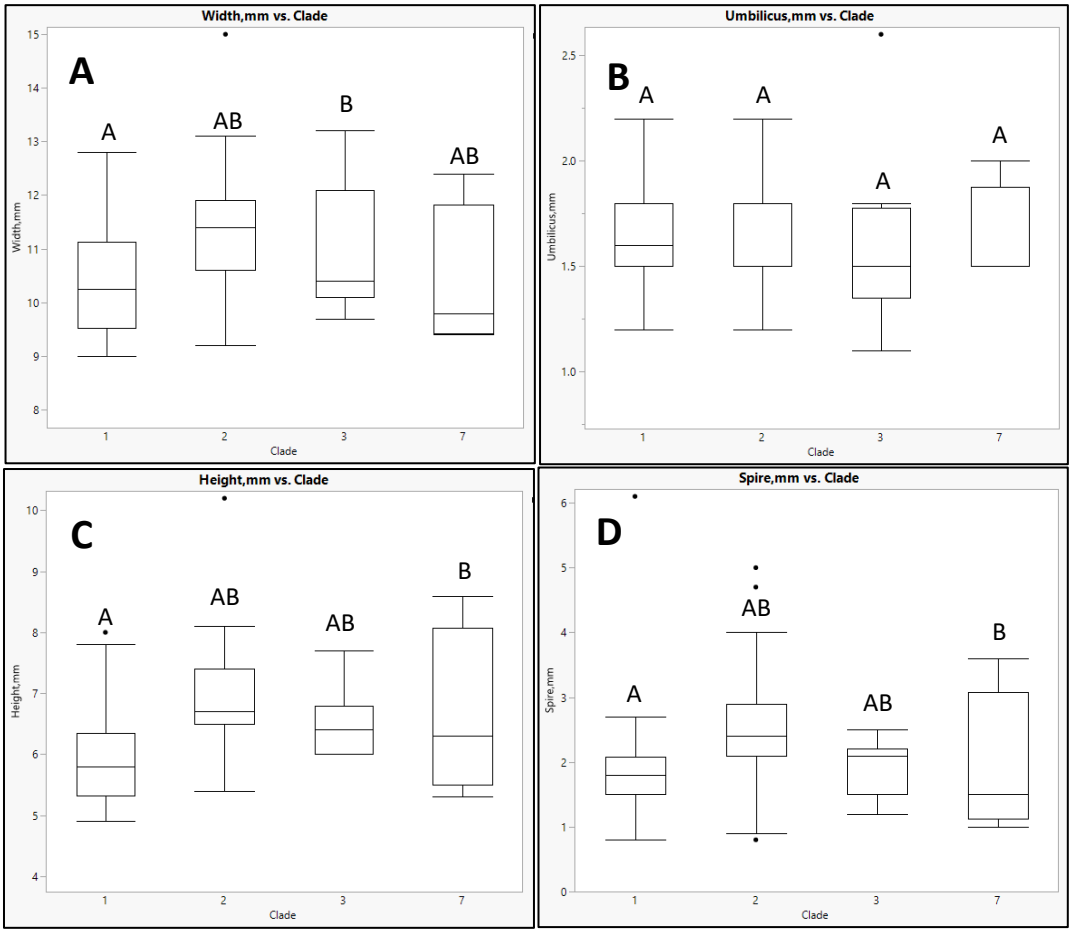

Figure 6.4. Character measurement comparisons in the *Triodopsis fallax* group, clades 1, 2, 3, and 7 by ANOVA and Student's T, by JMP Pro 16 (SAS Institute, Cary, NC 2023). A) Width, mm, df=3, p=0.0283*; B) Number of whorls, df=3, p=0.9877; C) Height, mm, df=3, p=0.0071*; D) Width/spire ratio, df=3, p=0.1359. A key to clade numbers is in Table 6.1.

FIGURE 6.5

Morphological measurements of *Triodopsis fallax* Group Clades – Part 2

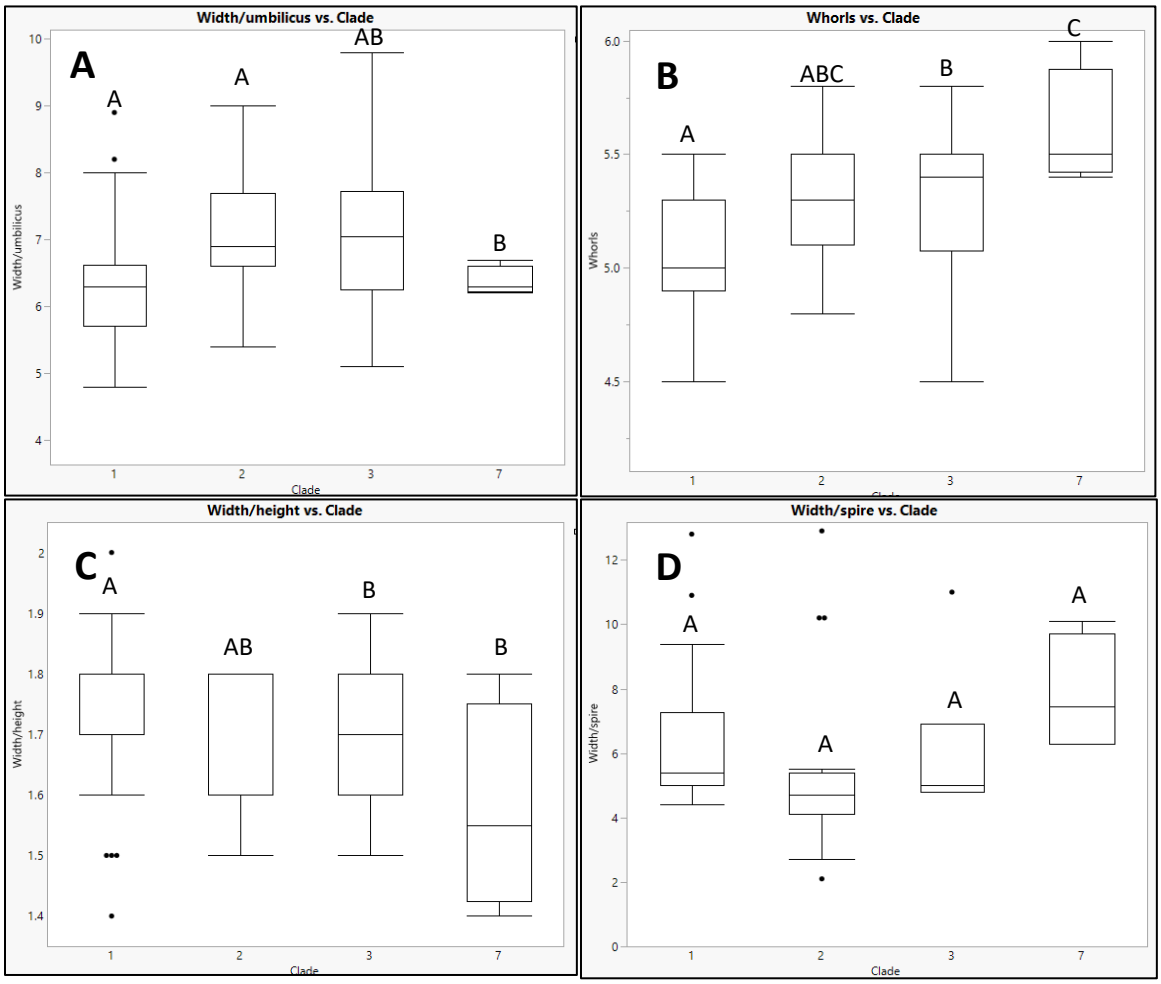

Figure 6.5. Character measurement comparisons in the *Triodopsis fallax* group, clades 1, 2, 3, and7 by ANOVA and Student's T, by JMP Pro 16 (SAS Institute, Cary, NC 2023). A) Width/umbilicus ratio, df=3, p=0.0285*; B) Number of whorls, df=3, p=0.0026*; C) Width/height ratio, df=3, p=0.0492*; D) Width/spire ratio, df=3, p=0.2344. A key to clade numbers is in Table 6.1.

FIGURE 6.6

16S Phylogeny of All *Triodopsis* and other Polygyridae

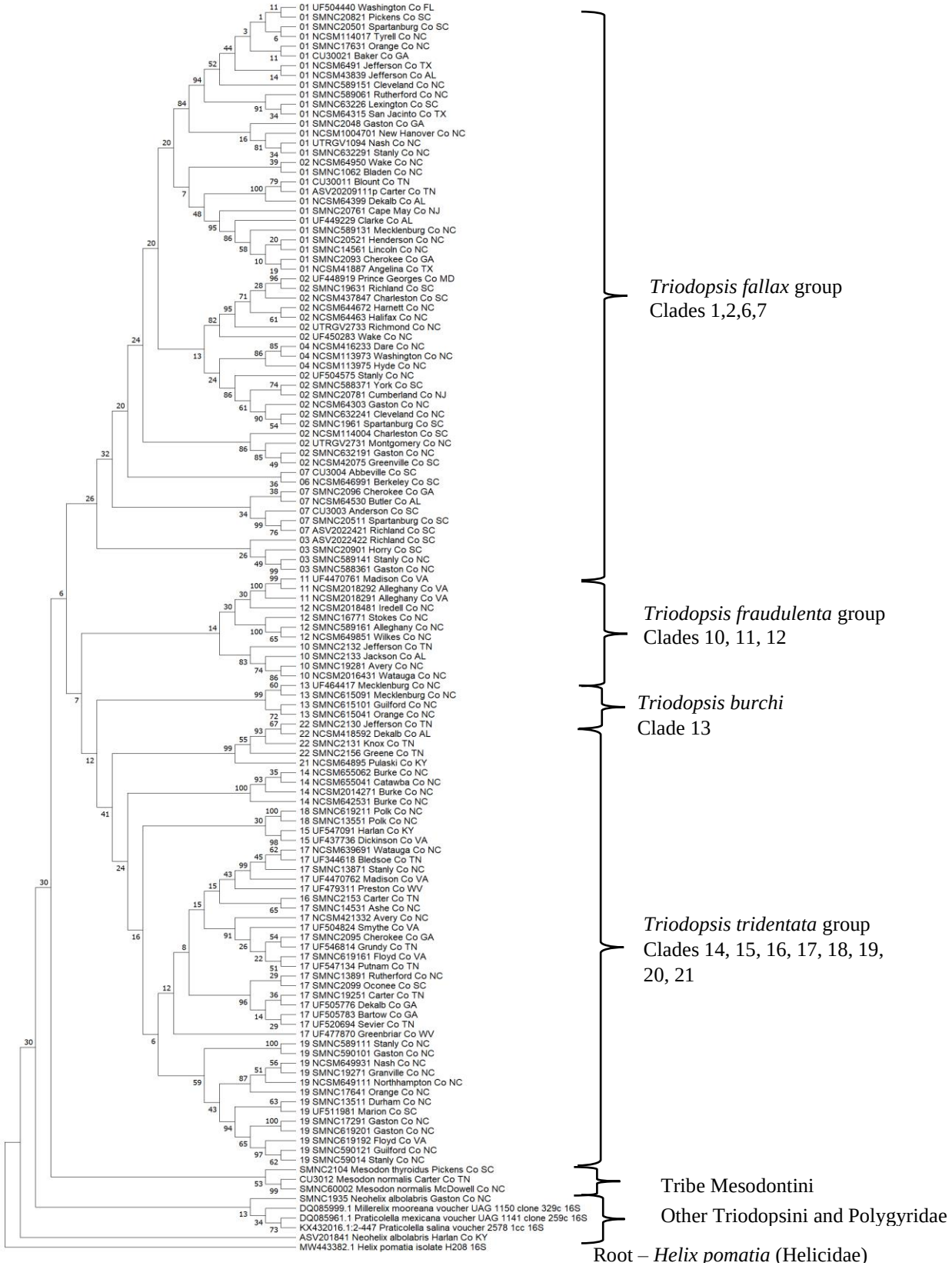

FIGURE 6.7

16S Phylogeny of *Triodopsis fallax* group only

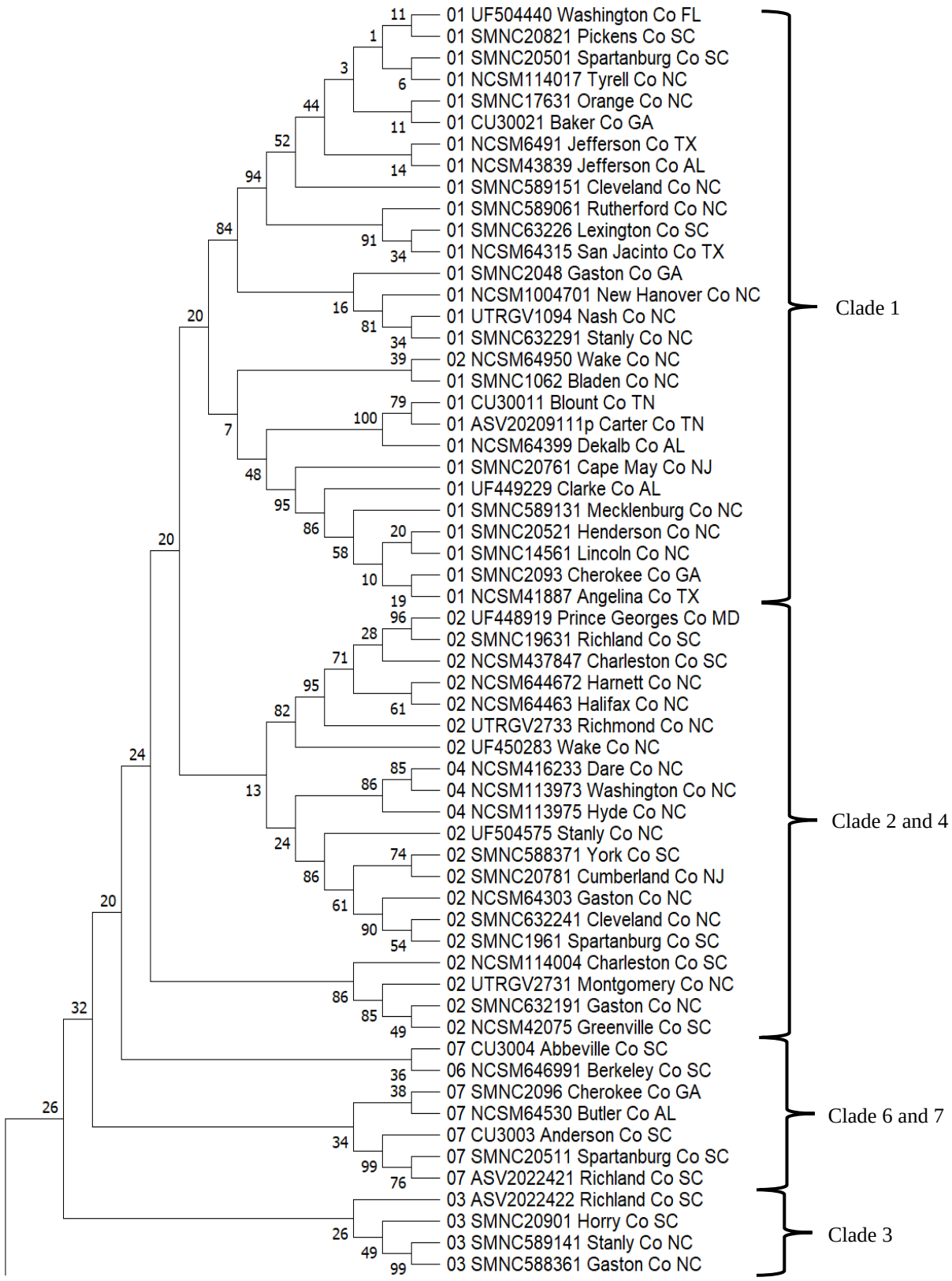

FIGURE 6.8

16S Phylogeny of *Triodopsis fraudulenta* and *tridentata* groups only

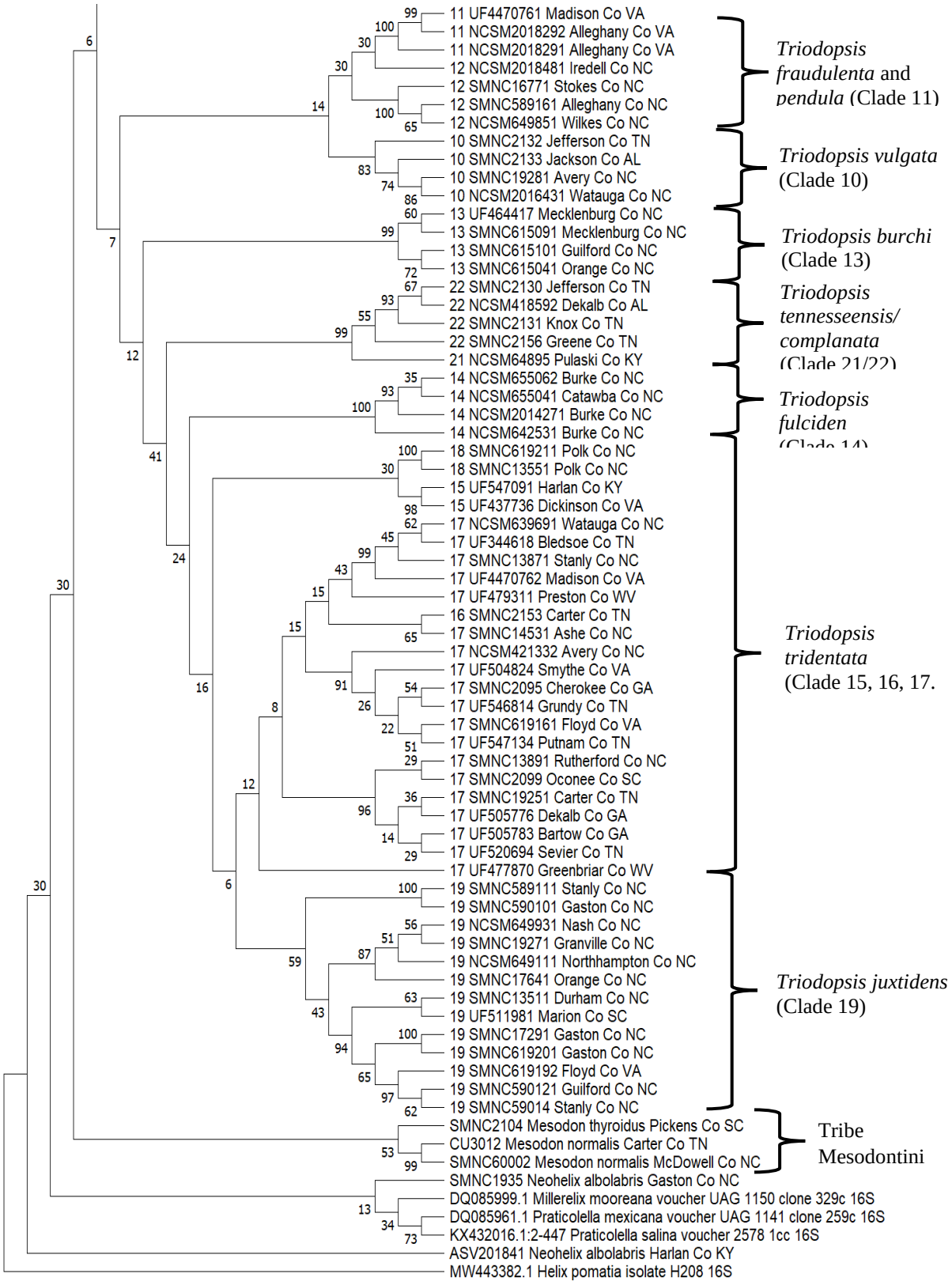

FIGURE 6.9

ITS2 Phylogeny of *Triodopsis*, Others in Triodopsini and Mesodontini

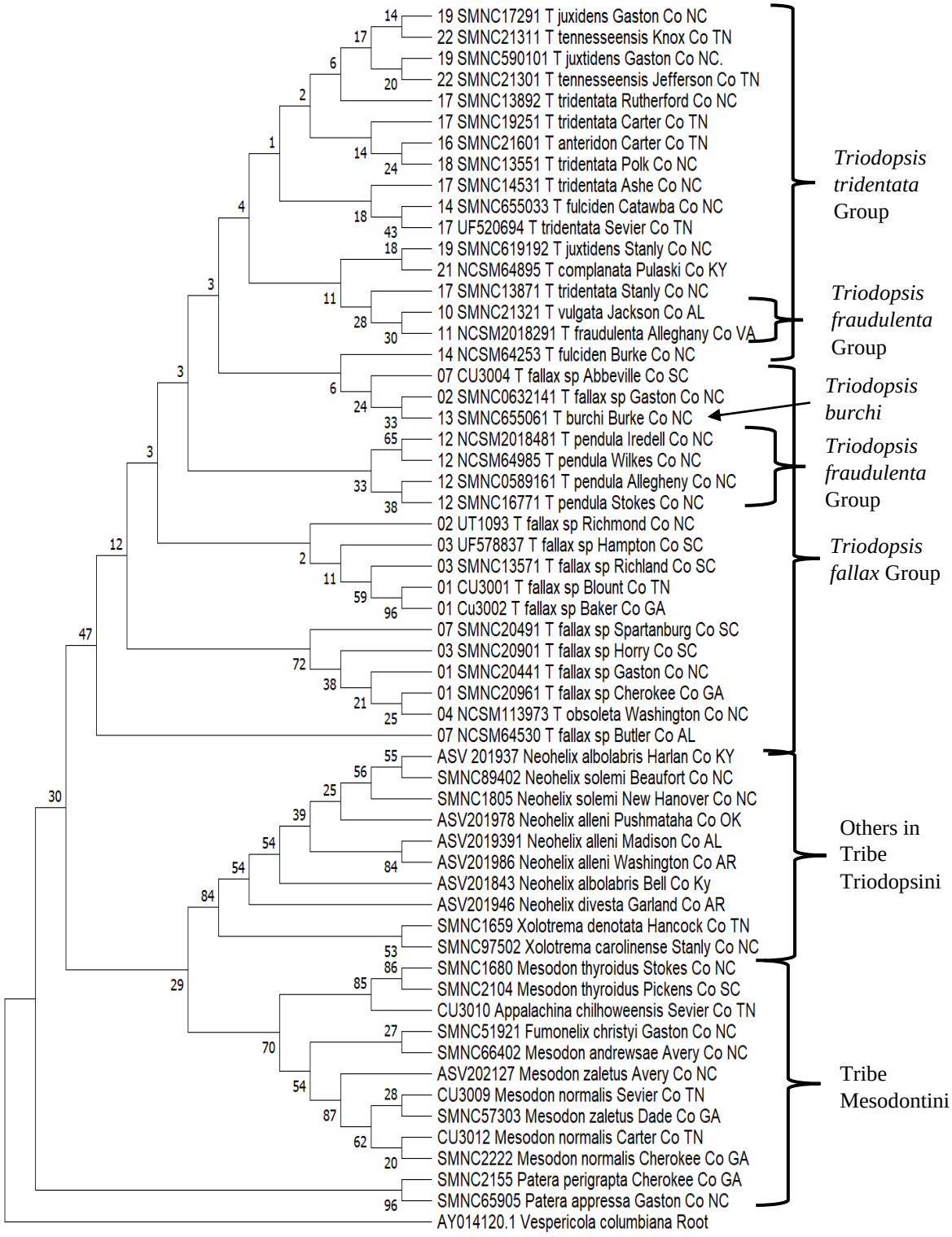

FIGURE 6.10

Concatenation of *Triodopsis* 16S and ITS2 Genes

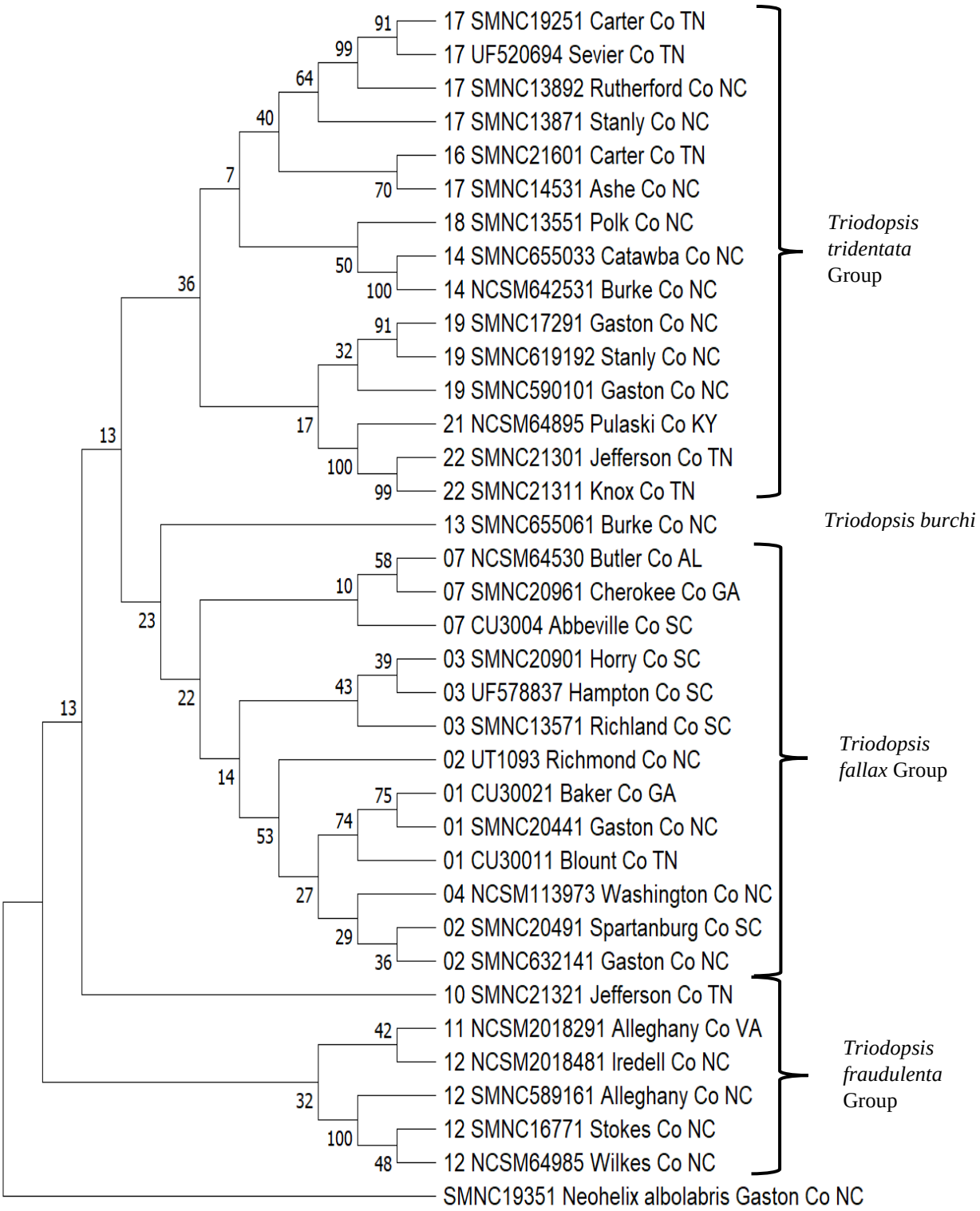

FIGURE 6.11

H3 Phylogeny for *Triodopsis*, Stylommatophora, and Outgroups

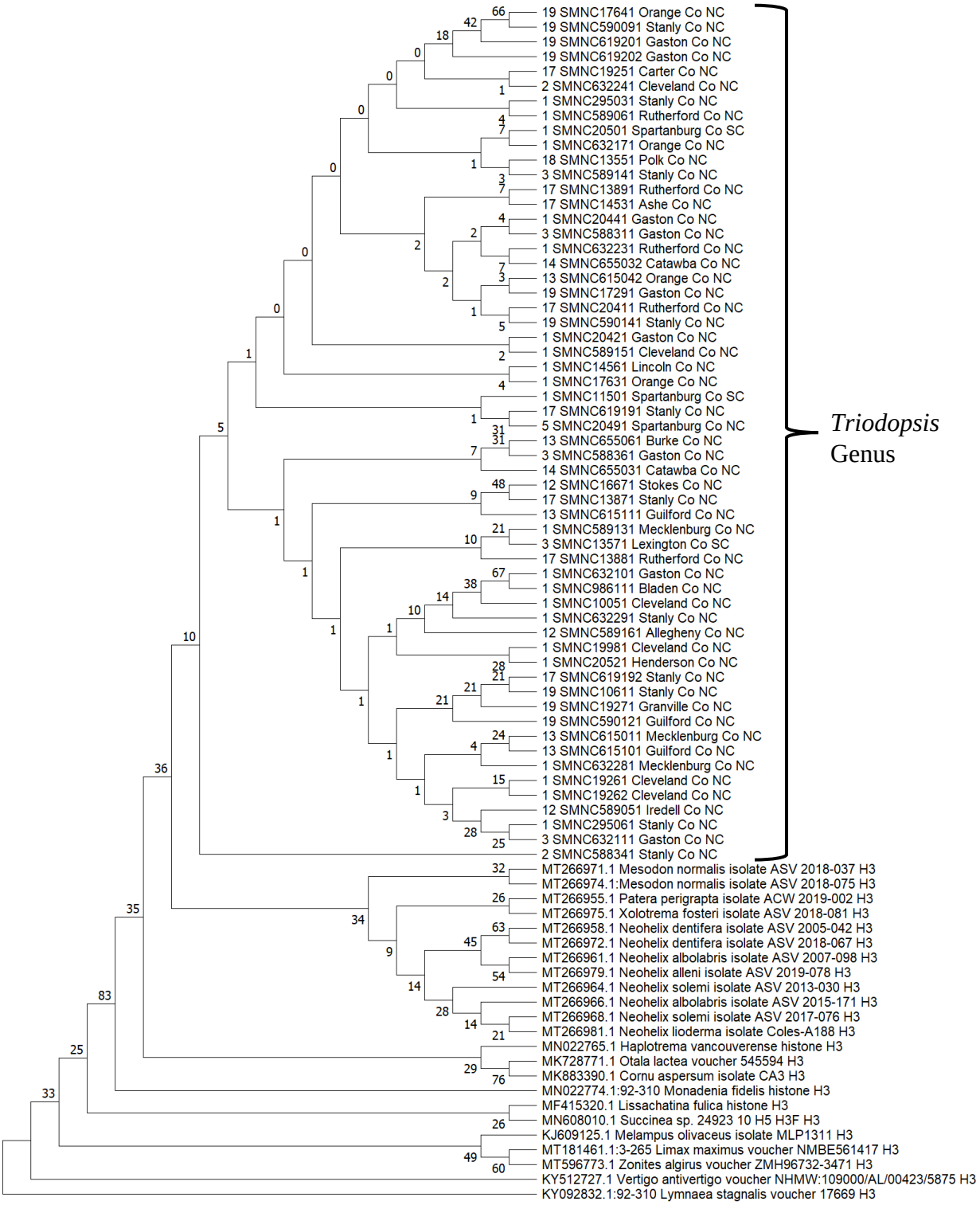

FIGURE 6.12

H3 *Triodopsis* Molecular Clock Tree

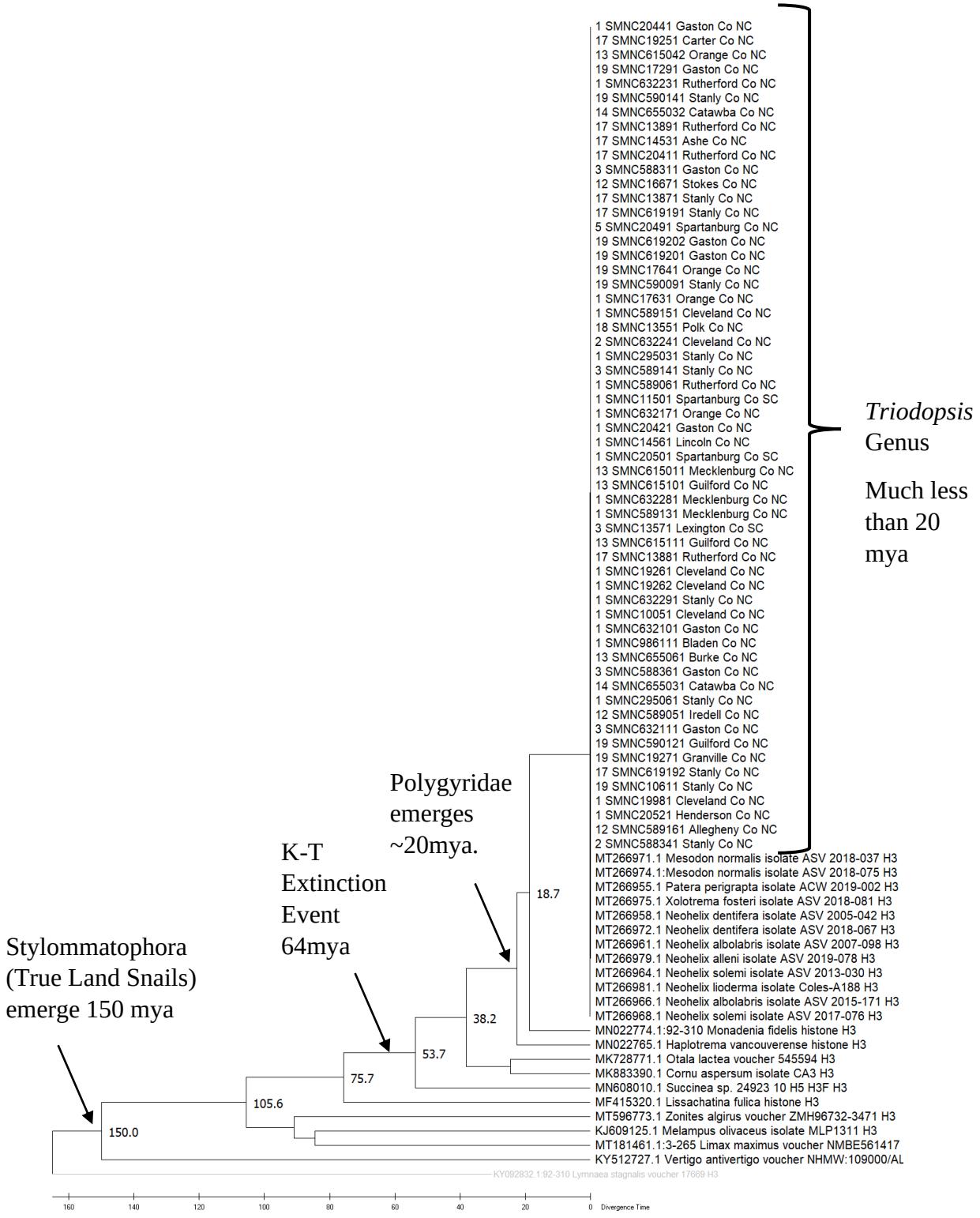

FIGURE 6.13

Population Stability in *Triodopsis* Clades

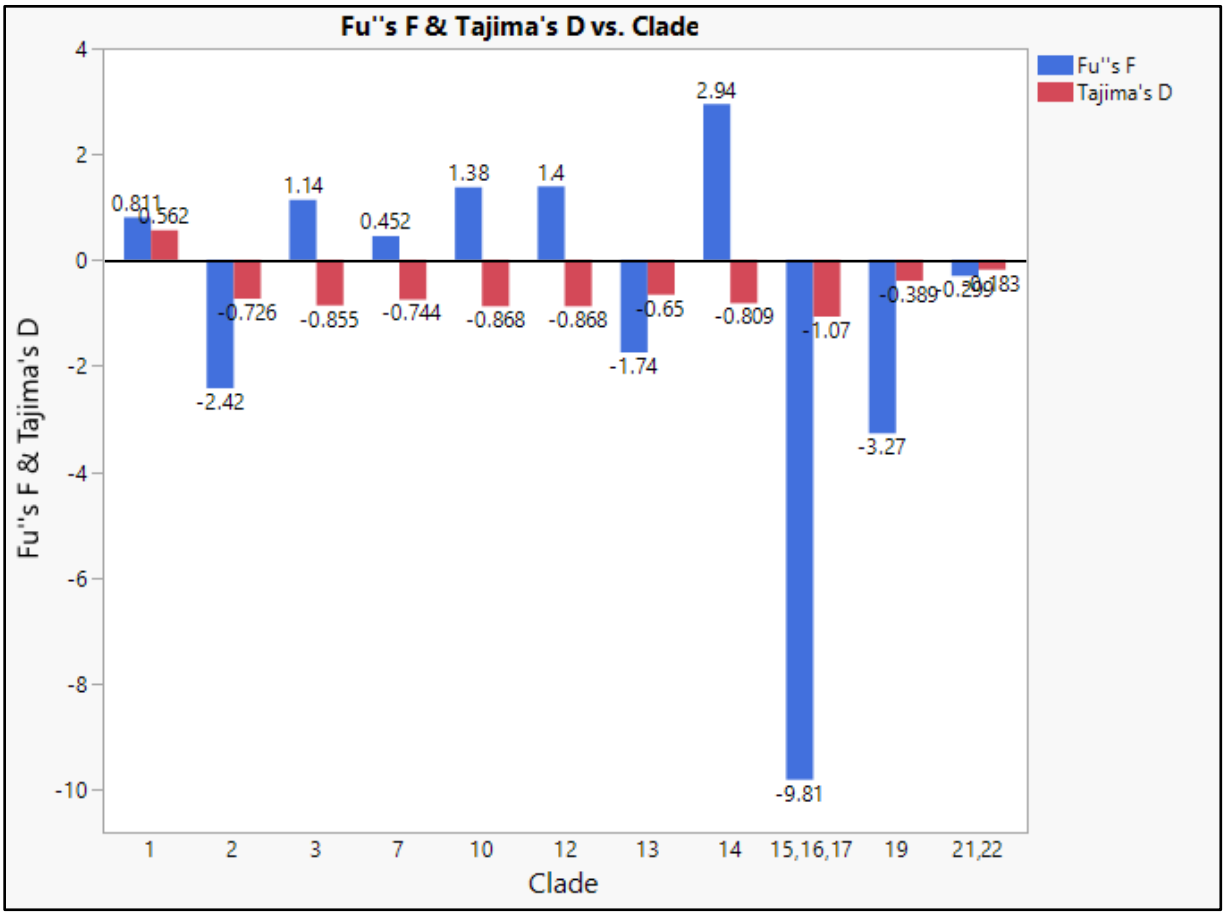

Figure 6.13. Groups and clades on the right identify values of Fu's Fs and Tajima's D. Negative values indicate expansion of the populations, and positive values indicate populations in equilibrium. Main expanding clades are the *Triodopsis tridentata* species (15, 16, 17) and *Triodopsis juxtidens* (clade 19), contributing to the large expansion of the *Triodopsis tridentata* group. The *Triodopsis fallax* group (1,2,3,7) is expanding overall, but the large negative value is driven mostly by clade 2 and variation within the group. Clade 14, *Triodopsis fulciden*, seems to be contracting. The huge negative value of the entire genus is mainly due to variation between clades. A key to clade numbers is in Table 6.1. Values are not significantly different ($p \leq 0.050$).

FIGURE 6.14

Expected 16S Genetic Differentiation Estimates -
Population Size vs. Observed in *Triodopsis* Genus

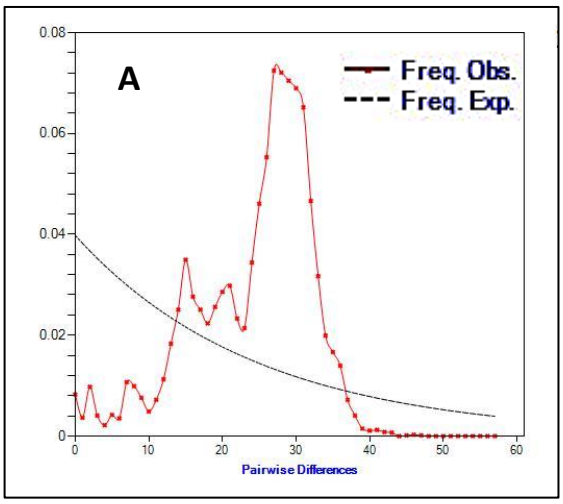

MAE = 1.0675; R^2 = 0.1356; Raggedness= 0.0020 (DnaSP)

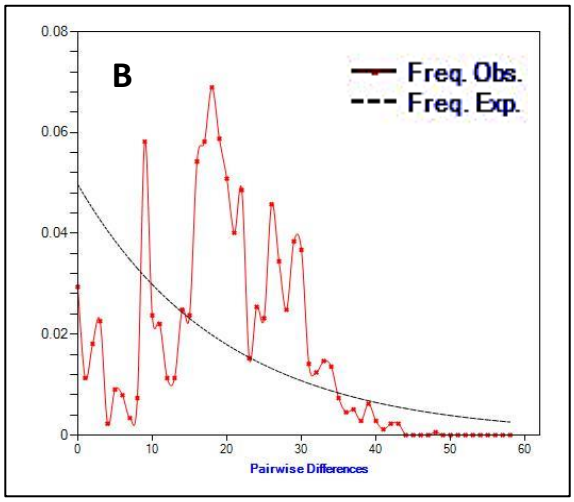

MAE = 0.8642; R^2 = 0.1062; Raggedness= 0.091 (DnaSP)

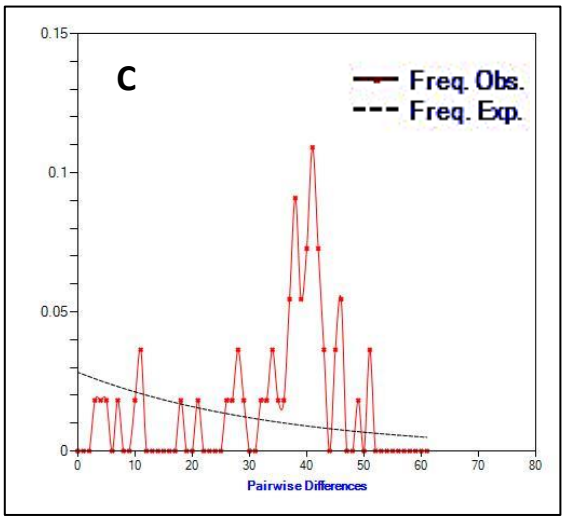

MAE = 1.2595; R^2 = 0.1787; Raggedness= 0.0245 (DnaSP)

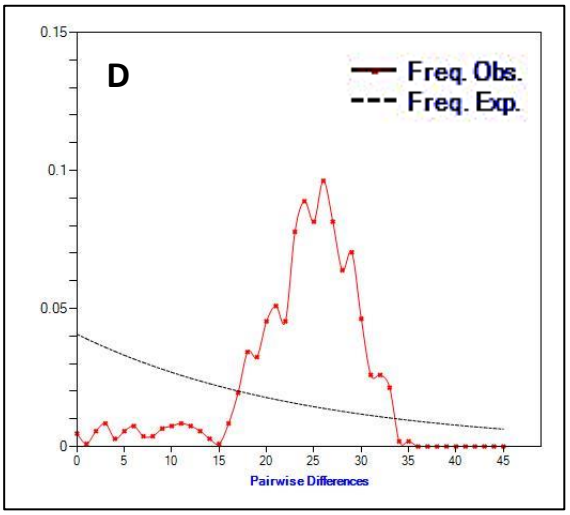

MAE = 1.3145; R^2 = 0.1484; Raggedness=0.0042 (DnaSP)

Fig. 6.14 Expected Values for Constant Population Size vs. Observed. shows a huge increase in differences in 20 – 30 bases, signaling a rapid recent population expansion. MAE, Mean Absolute Error. A) Overall *Triodopsis.* B) *Triodopsis fallax* group only, C) *Triodopsis fraudulenta* group only, D) *Triodopsis tridentata* group only (excluding *Triodopsis burchi*).

FIGURE 6.15

Statistical Parsimony Haplotype Network with *Triodopsis* 16S and ITS2

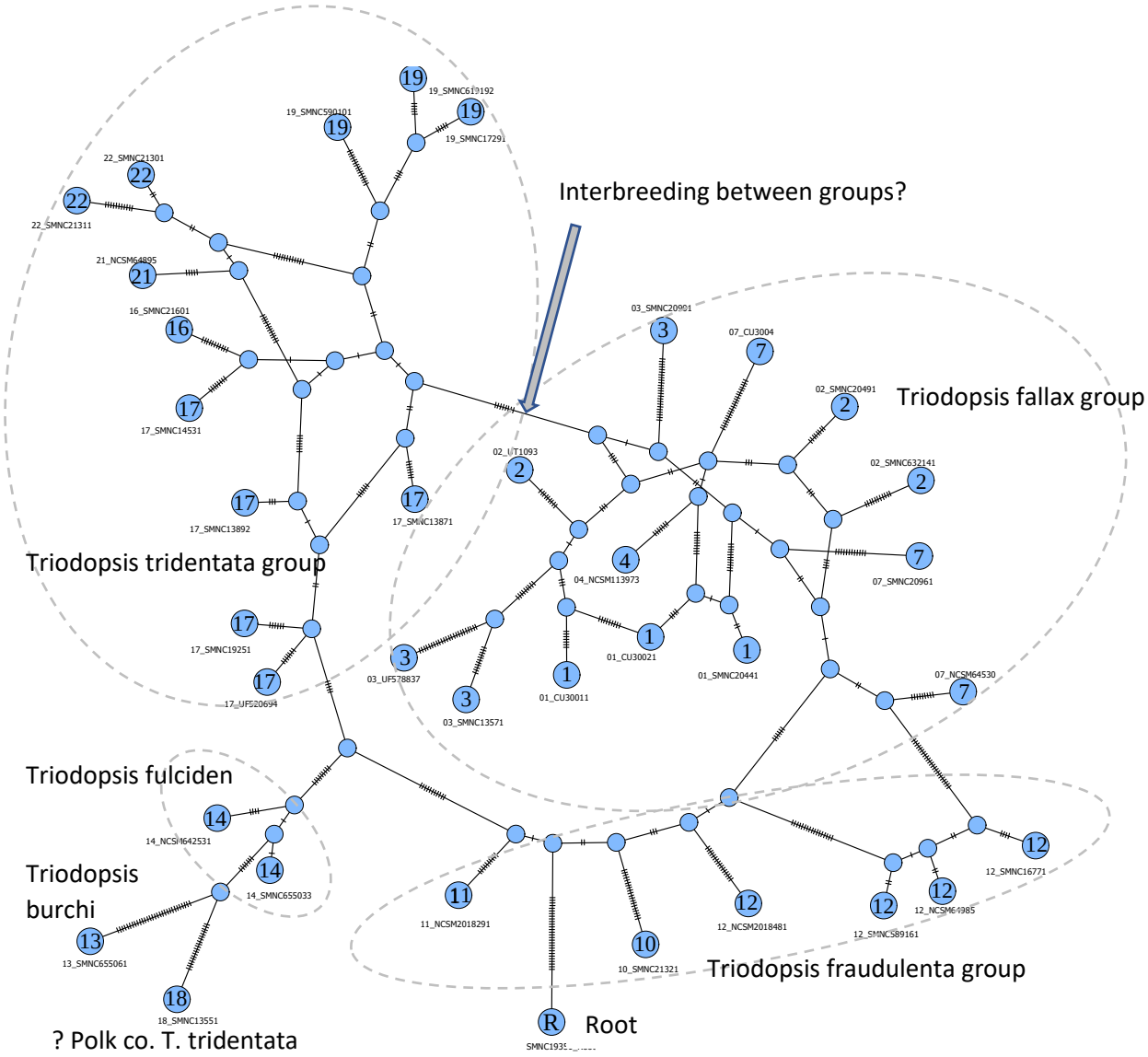

Figure 6.15. Statistical parsimony (TCS) haplotype network with concatenated Triodopsis 16S and ITS2 sequences and Neohelix root (R). For this network, Tajima's D = 0.849, p = 0.4105. A key to clade numbers is in Table 6.1. The Root (R) is *Neohelix albolabris*.

FIGURE 6.16

Expected 16S/ITS2 Genetic Differentiation Estimates -
Population Size vs. Observed in *Triodopsis* Genus

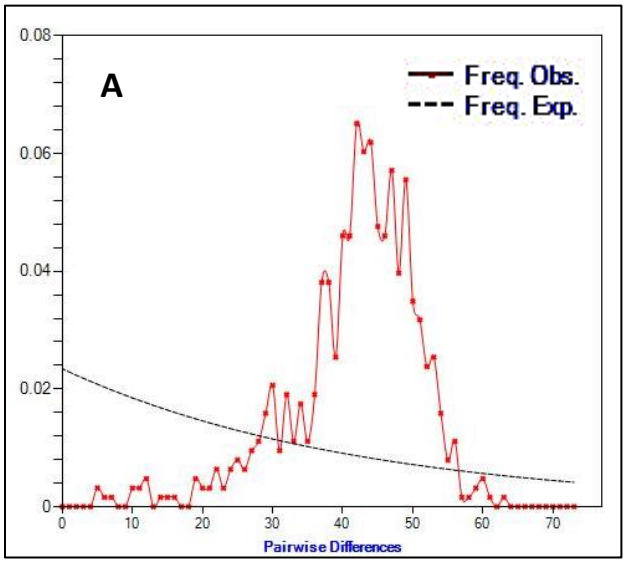

R2: 0.1386; Raggedness: 0.0036; MAE: 1.3187

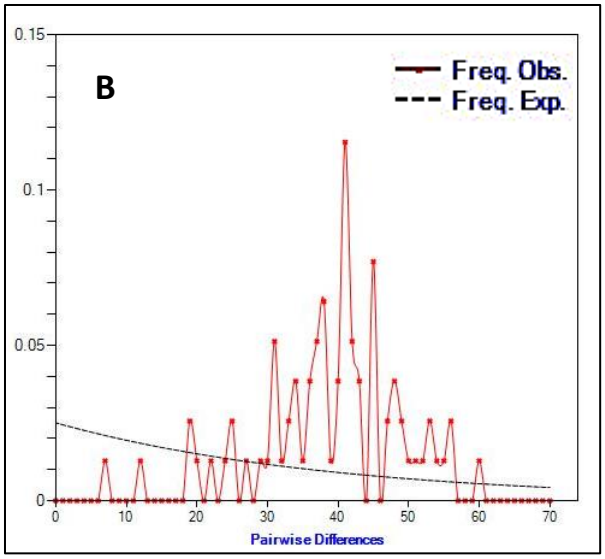

R2: 0.1556; Raggedness: 0.0378; MAE: 1.3081

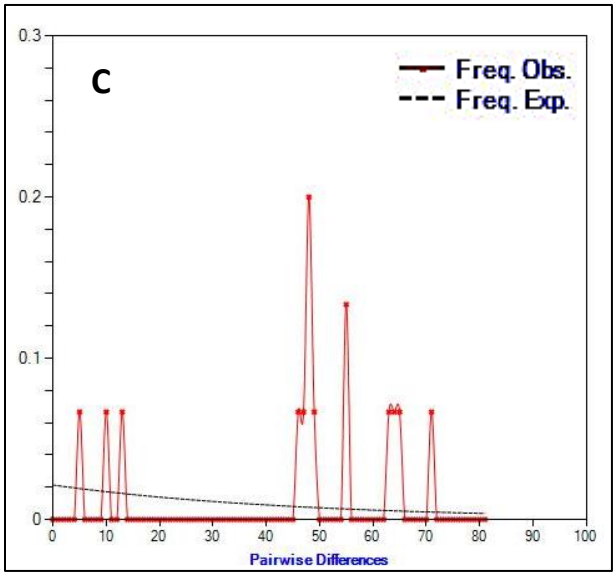

R2; 0.1319; Raggedness: 0.0276; MAE; 1.2563

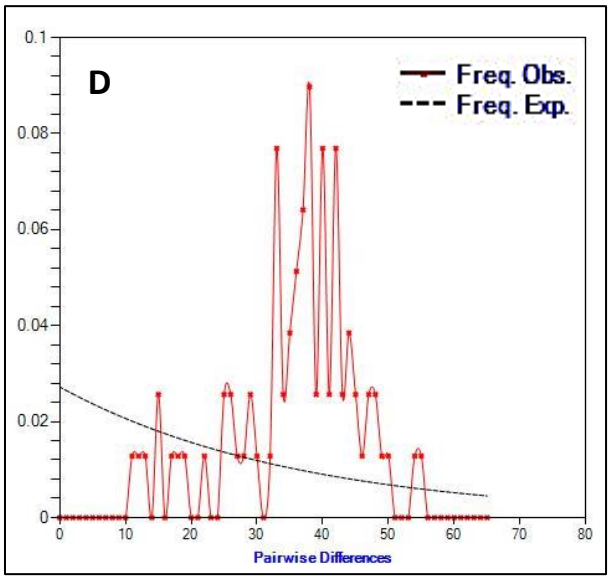

R2: 0.1319; Raggedness: 0.0276; MAE: 1.2563

Fig. 6.16 Expected 16S/ITS2 Values for Constant Population Size vs. Observed. shows a huge increase in differences in 20 – 30 bases, signaling a rapid recent population expansion. MAE, Mean Absolute Error. A) Overall *Triodopsis.* B) *Triodopsis fallax* group only, C) *Triodopsis fraudulenta* group only, D) *Triodopsis tridentata* group only (excluding *Triodopsis burchi*).

FIGURE 6.17

Triodopsis fallax Group Distributions

Clades 1 and 4

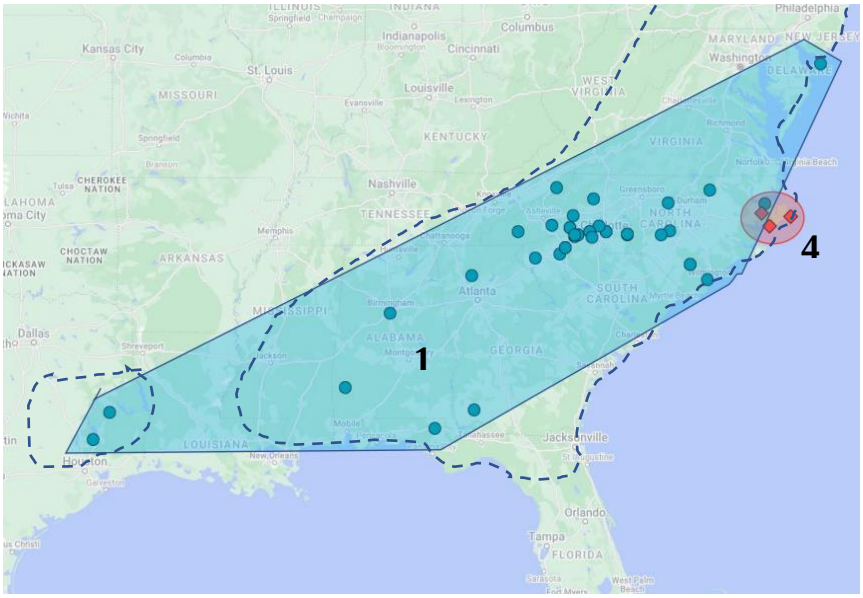

Clades 2,3,6 and 7

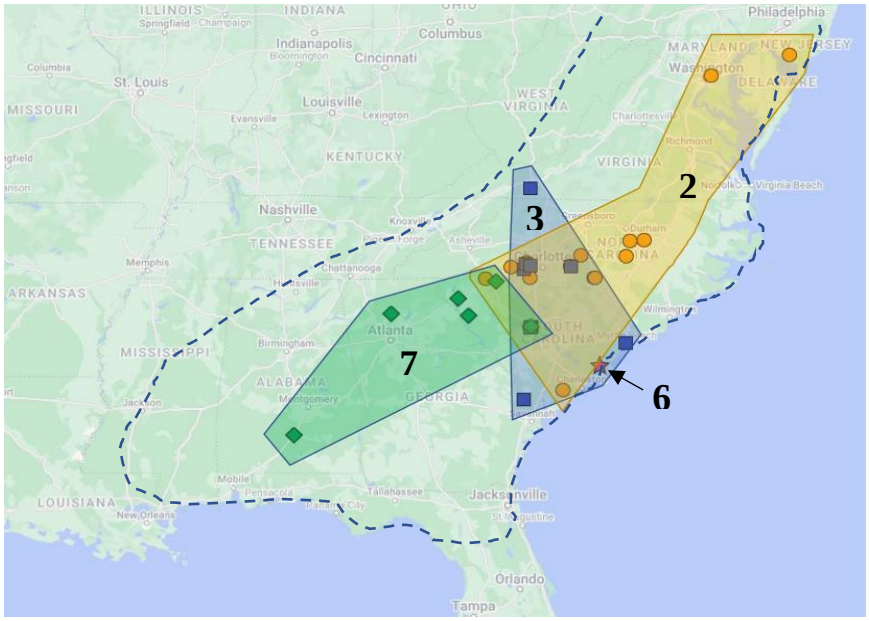

Fig. 6.17. Distributions of the major clades of the *Triodopsis fallax* group show overlapping ranges with a few isolated coastal entities. Clade one is suspected to be invasive and spreading anthropogenically. *Dashed lines indicate approximate distributions for all species studied in this group from Hubricht, 1985. Northern range to Pennsylvania-New York line.* A key to clade numbers is in Table 6.1.

FIGURE 6.18

Triodopsis fraudulenta Group Distributions

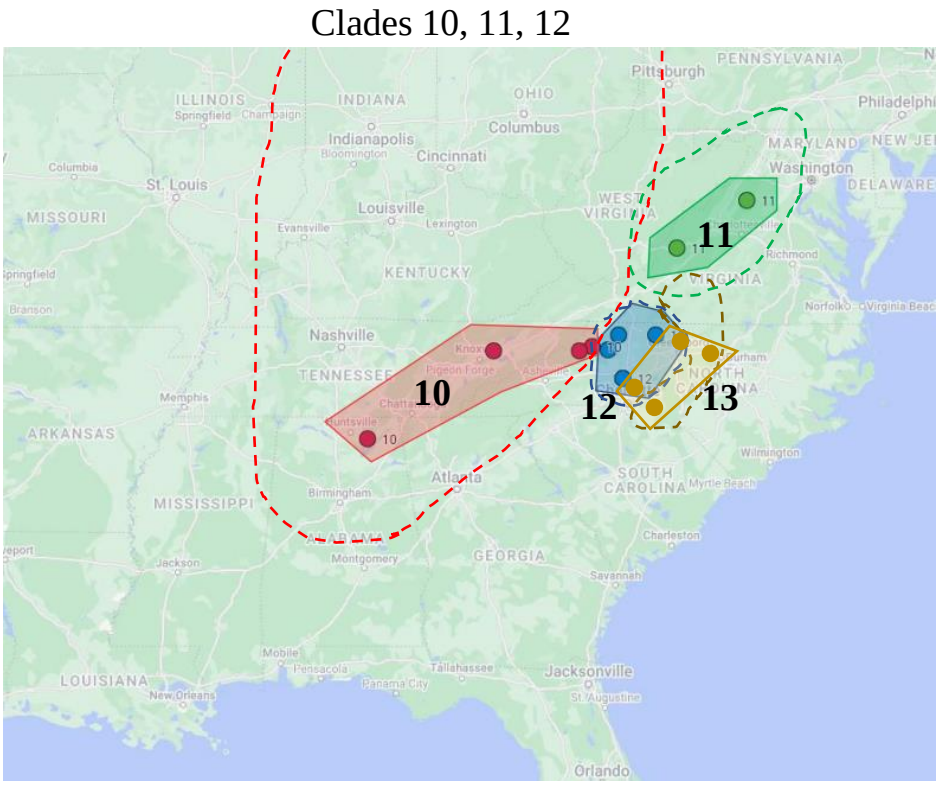

Fig. 6.18. The *Triodopsis fraudulenta* group (clades 10 – 12) and *Triodopsis burchi* (clade 13), which are closest to the ancestral *Triodopsis* node, consist of very distinct species populations that are nevertheless closely related. These straddle the Appalachian Mountains, which may have influenced their speciation. *Dashed lines indicate approximate distributions for this species from Hubricht, 1985. Northern range to Great Lakes for Clade 10.* A key to clade numbers is in Table 6.1.

FIGURE 6.19

Triodopsis tridentata Group Distributions

Clades 15, 16, 17, 18, 19

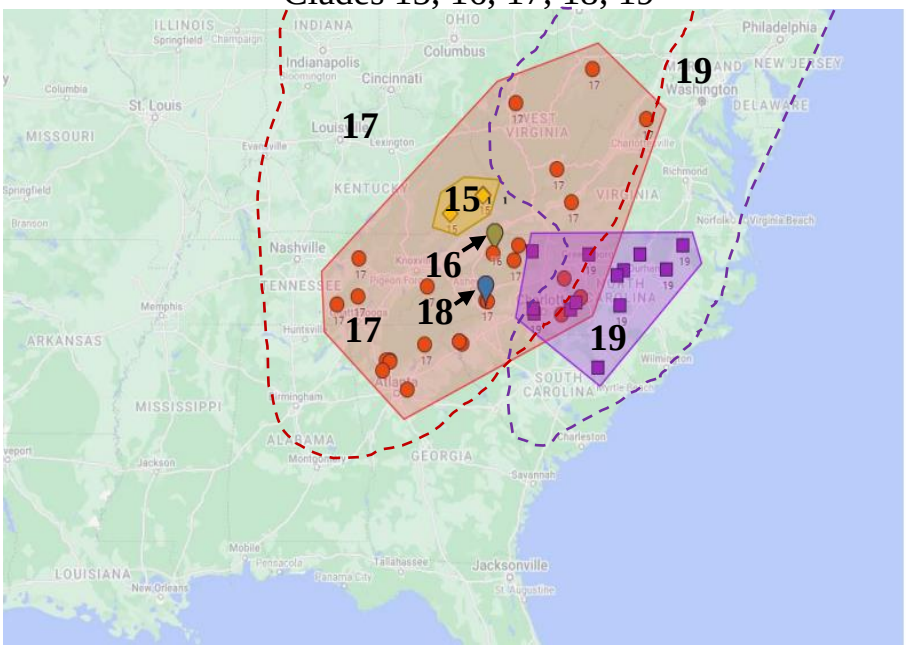

Clades 14, 21, 22

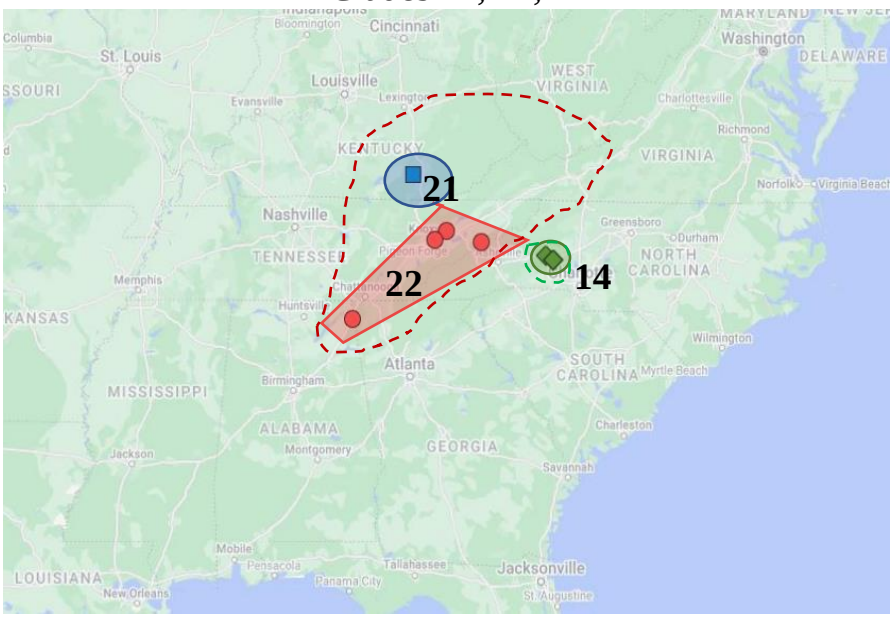

Fig. 6.19. Distributions of the *Triodopsis tridentata* group show distinct divisions except in *Triodopsis tridentata* clade 17, which has several clades within it which may be localized forms. Triodopsis juxtidens (clade 19) is the only clade that is primarily Piedmont. *Dashed lines indicate approximate distributions for this species from Hubricht, 1985. Northern range for Clades 17 and 19 at least to Canadian border.* A key to clade numbers is in Table 6.1.

FIGURE 6.20

Reciprocal Fertilization Creates Mitochondrial Haplotype Diversity

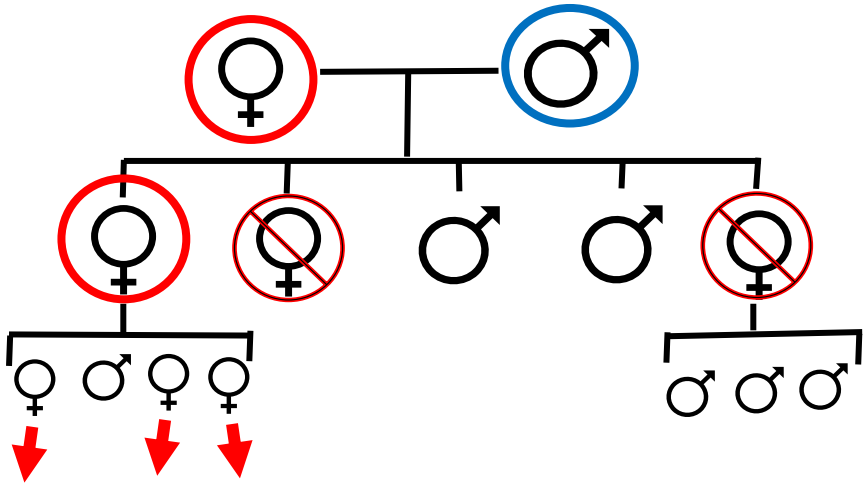

Dioecious Organism

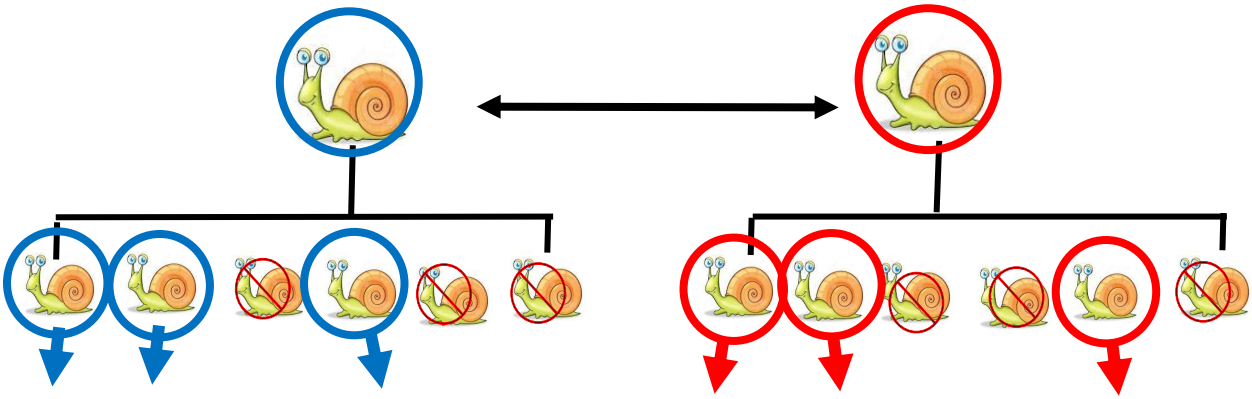

Hermaphroditic Organism with Reciprocal Fertilization

Figure 6.20. The difference in the haplotype transfer to offspring between a dioecious organism and a hermaphroditic organism with reciprocal fertilization. Fewer haplotypes are lost in the hermaphroditic organism as all snails lay eggs. The only ones that do not pass on their haplotype are the ones that do not reproduce due to attrition. All haplotypes have the possibility of staying in circulation, creating a high diversity in the population.

CHAPTER SEVEN

OVERALL CONCLUSION

This thesis has examined the relationship between phenotype and genetics in two groups of mollusks – one species from the ancient group of bivalves, and one relatively recently diverged genus of Stylommatophoran land snails. The eastern oyster, *Crassostrea virginica*, is a wide-spread species of bivalve with a variable morphology conforms to its spatial limits, and therefore, physiology was used to determine differences in phenotype. Oysters live in an environment of constant changing conditions but are essentially one genotype with a phenotypically plastic physiology. In the *Triodopsis* land snails, many morphological types have been described as species, and the challenge is to determine truly isolated forms with little or no gene flow to use to compare phylogenic differences. Land snails live in a relatively constant environment, but occupy small niches, with many mitochondrial haplotypes in one population, and morphology can follow genetic phylogeny, or not.

In this research, I have addressed the different forms of phenotypic plasticity in mollusks. For Aim 1, I investigated the physiological differences between locations, salinities, and the microhabitats of *C. virginica* in Chapter 2. This was determined by tests of mitochondrial respiration and damage, cellular component damage due to oxidative products, and the amount of energy storage compounds in different conditions. Salinity differences of the three locations was was most likely the prominent variable resulting in differences between oysters from each location. At the extremes of salinity, oyster population survival was potentially threatened due to reduced reproductive abilities. Tidal zone comparisons, on the other hand, showed no difference as oysters well adapted to both subtidal and intertidal habitats. A serendipitous event of a hurricane making landfall close to one of the study sites, discussed in Chapter 3, resulted in an opportunity to measure

oysters both before and after this weather event. Subsequent studies of the site for the next year found that this climatic event exacerbated the effects of the high salinity at the site, making it unlikely that the oysters spawned the following year. Cellular damage and energy storage compounds were directly affected.

In Chapter 4, I address Aim 2 and study the genetics of oysters in both the mRNA expression of immunity genes and the DNA analysis of COI and 16S. There are no significant differences in the immunity gene expression except in signaling and damage recognition. These are again different between locations, i.e., salinity ranges, with extremes showing extremely low levels of these compounds. These extremes of salinity may affect the oysters' ability to recognize and signal the attack of a pathogen, and therefore make them more susceptible to disease. The DNA analysis shows the stability of this species as there are little or no variation in the sequences of either COI or 16S. I identified the haplotype of the oysters present in all three sites as being the southern population from the presence of specific 16S motifs recognized by previous studies. This is expected since they are all from populations south of Cape Hatteras.

In Chapter 5, components of Aims 1 and 2 are applied to a study of cultured *Crassostrea virginica* in North Carolina and Virginia, which were challenged with hypoxia and a pathogen. This study is conducted in collaboration with other lab mates, Whitney Leach and Remi Ketchum, and has been published in the journal Integrative and Comparative Biology. In the publication, mitochondrial respiration, immunity gene expression, and DNA analysis have been tested in the oyster cultures of four sites and compared in both hypoxia and *Vibrio* infection and combinations of the two conditions. There are significant effects on immunity gene expression between locations and conditions in four of the immunity factors, which show a synergistic effect with multiple

abiotic and biotic challenges in an oyster population. The DNA analysis shows a mixture of haplotypes from the four locations, not surprising for cultured oysters.

Chapter 6 is a study of land snail morphology and phylogenies of the 16S, ITS2 and H3 gene, the topic of Aim 3. The confusing species status in this genus made it a challenge to identify the specimens for the study. Eventually, I relied on the 16S phylogeny to dictate the clades, and I was able to match the clades to a species by morphology for many. However, the members of the *Triodopsis fallax* clade, a total of 9 species, could not be distinguished by matching morphology to the clades inferred from DNA sequence data. Statistics of the morphological measurements show no significant differences between these clades. These are considered all one species, and assigned the oldest species name, *Triodopsis fallax*. Another species in the *Triodopsis tridentata* clade, *Triodopsis anteridon*, is determined to not be a valid species. Others will require more work to determine species status. A phylogram of the 16S gene shows the uncertainty of the ancestral nodes in the tree, a sign of a recent and rapid diversification and incomplete speciation of many of the morphotypes. A molecular clock tree from the H3 sequences shows the genus rapidly expanding within the last 20 million years, and possibly since the last glacial event. A haplotype network of the concatenated 16S and ITS2 genes revealed a reticulated network, possibly reflecting the inbreeding between clades from incomplete reproductive isolation. Statistics indicate that many of the clades in the *Triodopsis* genus are still expanding, especially *Triodopsis tridentata*, which has spread as far as Canada since the last glacial maximum.

The contrast between *Crassostrea* and *Triodopsis* is evident. The marine oyster is a generalist population which has a robust physiology adapted to extremes in its environment. Eastern oysters are a nearly homogeneous species that has survived hundreds of millions of years in the same type of environment with variable conditions and habitats and can tolerate all of them

to an extent. The *Triodopsis* land snail is a relatively young genus that has evolved during extreme climatic fluctuations and is still in the speciation process. Land snails are specialists, adapting by changing morphology and speciating in micro-refugia by genetic drift or in response to subtle cues of environment. The land snails have extreme genetic variability in their mitochondria genome and many clades of diverging populations, possibly due to their reproductive methods.

This dissertation opens the door for more investigations on the effect of micro-habitat on the adaptation of mollusks to their environment. The future of oysters is challenged by sea level changes, warming and acidifying oceans, and human intrusion into their habitats. *Triodopsis* land snails have an unusually variable mitochondrial genome that still needs investigation to determine functionality. The complexity of their speciation state also needs more work to include the remaining members of the genus and establishment of complete distribution ranges. Hopefully, this research will help to further the knowledge of this highly diverse phylum.

REFERENCES

Abele, D., Philipp, E., Gonzalez, P. M., and Puntarulo, S. 2007. "Marine Invertebrate Mitochondria and Oxidative Stress," *Frontiers in Bioscience* (12), pp. 933-946.

Allam, B., and Espinosa, E. P. 2016. "Bivalve Immunity and Response to Infections: Are We Looking at the Right Place?," *Fish & Shellfish Immunology* (53), pp. 4-12.

Aubry, S., Labaune, C., Magnin, F., Roche, P., and Kiss, L. 2006. "Active and Passive Dispersal of an Invading Land Snail in Mediterranean France," *The Journal of animal ecology* (75), pp. 802-813.

Avise, J. C. 2000. *Phylogeography: The History and Formation of Species*. Cambridge, Massachusetts: Harvard University Press.

Avise, J. C. 2004. *Molecular Markers, Natural History, and Evolution, 2nd Edition*. Sunderland, Massachusetts: Sinauer Associates.

Ayyagari, V. S., and Sreerama, K. 2020. "Molecular Phylogeny and Evolution of Pulmonata (Mollusca: Gastropoda) on the Basis of Mitochondrial (16s, Coi) and Nuclear Markers (18s, 28s): An Overview," *Journal of Genetics* (99), pp. 1-14.

Bacca, H., Huvet, A., Fabioux, C., J.-Y., D., Delaporte, M., Poureau, S., Van Wormhoudt, A., and Moal, J. 2005. "Molecular Cloning and Seasonal Expression of Oyster Glycogen Phosphorylase and Glycogen Synthase Genes," *Comparative Biochemistry and Physiology Part B* (140), pp. 635-646.

Barker, G. M. 2001. "Gastropods on Land: Phylogeny, Diversity and Adaptive Morphology," in *The Biology of Terrestrial Mollusks*, G.M. Barker (ed.). Wallingford, NY: CABI, pp. Pp. 1-146.

Barker, N. P., Fearon, J. L., and Herbert, D. G. 2013. "Moisture Variables, and Not Temperature, Are Responsible for Climate Filtering and Genetic Bottlenecks in the South African Endemic Terrestrial Mollusc Prestonella (Orthalicoidea)," *Conservation Genetics* (14:5), pp. 1065-1081.

Bartol, I. K., Mann, R., and Luckenbach, M. 1999. "Growth and Mortality of Oysters (Crassostrea Virginica) on Constructed Intertidal Reefs: Effects of Tidal Height and Substrate Level," *Journal of Experimental Marine Biology and Ecology* (237), pp. 157-184.

Barve, A., Galande, A. A., Ghaskadbi, S. S., and Ghaskadbi, S. 2021. "DNA Repair Repertoire of the Enigmatic Hydra," *Frontiers in Genetics* (12).

Bataller, E. E., Boghen, A. D., and Burt, M. D. B. 1999. "Comparative Growth of the Eastern Oyster *Crassostrea Virginica* (Gmelin) Reared at Low and High Salinities in New Brunswick, Canada," *Journal of Shellfish Research* (18), pp. 107-114.

Bayne, B. 2017. *Biology of Oysters*, (First Edition ed.). Ellsevier, Academic Press.

Berthelin, C., Kellner, K., and Mathieu, M. 2000. "Storage Metabolism in the Pacific Oyster (*Crassostrea Gigas*) in Relation to Summer Mortalities and Reporductive Cycle (West Coast of France)," *Comparative Biochemistry and Physiology Part B* (125), pp. 359-369.

Bester, M. J., Potgieter, H. C., and Vermaak, W. J. 1994. "Cholate and Ph Reduce Interference by Sodium Dodecyl Sulfate in the Determination of DNA with Hoechst," *Anal Biochem* (223:2), pp. 299-305.

Bishop, M., and Peterson, C. H. 2006. "Direct Effects of Physical Stress Can Be Counteracted by Indirect Benefits: Oyster Growth on a Tidal Elevation Gradient," *Oecologia* (147), pp. 426-433.

Bishop, M. J., Rivera, J. A., Irlandi, E. A., Ambrose, W. G., and Peterson, C. H. 2005. "Spatio-Temporal Patterns in the Mortality of Bay Scallop Recruits in North Carolina: Investigation of a Life History Anomaly," *Journal of Experimental Marine Biology and Ecology* (315:2), pp. 127-146.

Boyd, J. N., and Burnett, L. E. 1999. "Reactive Oxygen Intermediate Production by Oyster Hemocytes Exposed to Hypoxia," *The Journal of Experimental Biology* (202), pp. 3135-3143.

Bradford, M. M. 1976. "A Rapid and Sensitive Method for the Quantitation of Microgram Quantities of Protein Utilizing the Principle of Protein-Dye Binding," *Anal Biochem* (72), pp. 248-254.

Brand, M. D., Chien, L.-F., Ainscow, E. K., Rolfe, D. F. S., and Porter, R. K. 1994. "The Causes and Functions of Mitochondrial Proton Leak," *BBA - Bioenergetics* (1187:2), pp. 132-139.

Burford, M., Scarpa, J., Cook, B. J., and Hare, M. P. 2014. "Local Adaptation of a Marine Invertebrate with a High Dispersal Potential: Evidence from a Reciprocal Transplant Experiment of the Eastern Oyster Crassostrea Virginica," *Mar. Ecol. Prog. Ser.* (505), pp. 161-175.

Buroker, N. E. 1983. "Population Genetics of the American Oyster Crassostrea Virginica Along the Atlantic Coast and the Gulf of Mexico," *Marine Biology* (75:1), pp. 99-112.

Buzan, D., Lee, W., Culbertson, J., Kuhn, N., and Robinson, L. 2009. "Positive Relationship between Freshwater Inflow and Oyster Bundance in Galveston Bay, Texas," *Estuaries and Coasts* (32:1), pp. 206-212.

Canesi, L., and Pruzzo, C. 2016. "Specificity of Innate Immunity in Bivalves: A Lesson from Bacteria," in *Lessons in Immunity: From Single-Cell Organisms to Mammals*, L. Ballarin and Commarata (eds.). Cambridge, MA: Elsevier Inc.

Casas, S. M., Filgueira, R., Lavaud, R., Comeau, L. A., La Peyre, M. K., and La Peyre, J. F. 2018. "Combined Effects of Temperature and Salinity on the Physiology of Two Geographically-Distant Eastern Oyster Populations," *Journal of Experimental Marine Biology and Ecology* (506), pp. 82-90.

Conover, D. O., and Schultz, E. T. 1995. "Phenotypic Similarity and the Evolutionary Significance of Countergradient Variation," *Trends in Ecology & Evolution* (10:6), pp. 248-252.

Criscione, F., and Kohler, F. 2016. "Snails in the Desert: Assessing the Mitochondrial and Morphological Diversity and the Influence of Aestivation Behavior on Lineage Differentiation in the Australian Endemic *Granulomelon* Iredale, 1933 (Stylommatophora: Camaenidae)," *Molecular Phylogenetics and Evolution* (94), pp. 101-112.

Csala, M., Kardon, T., Legeza, B., Lizák, B., Mandl, J., Margittai, É., Puskás, F., Száraz, P., Szelényi, P., and Bánhegyi, G. 2015. "On the Role of 4-Hydroxynonenal in Health and Disease," *Biochimica et Biophysica Acta (BBA) - Molecular Basis of Disease* (1852:5), pp. 826-838.

Davison, A., Blackie, R. L., and Scothern, G. P. 2009. "DNA Barcoding of Stylommatophoran Land Snails: A Test of Existing Sequences," *Mol Ecol Resour* (9:4), pp. 1092-1101.

Dayrat, B., Conrad, M., Balayan, S., White, T. R., Albrecht, C., Golding, R., Gomes, S. R., Harasewych, M. G., and de Frias Martins, A. M. 2011. "Phylogenetic Relationships and Evolution of Pulmonate Gastropods (Mollusca): New Insights from Increased Taxon Sampling," *Molecular Phylogenetics and Evolution* (59:2), pp. 425-437.

de Melo, A. G. C., Varela, E. S., Beasley, C. R., Schneider, H., Sampaio, I., Gaffney, P. M., Reece, K. S., and Tagliaro, C. H. 2010. "Molecular Identification, Phylogeny and Geographic

Distribution of Brazilian Mangrove Oysters (Crassostrea)," *Genetics and molecular biology* (33:3), pp. 564-572.
Dempsey, Z. W., Goater, C. P., and Burg, T. M. 2020. "Living on the Edge: Comparative Phylogeography and Phylogenetics of Oreohelix Land Snails at Their Range Edge in Western Canada," *BMC Evolutionary Biology* (20:1), p. 3.
DeSalle, R., and Goldstein, P. 2019. "Review and Interpretation of Trends in DNA Barcoding," *Frontiers in Ecology and Evolution* (7:302).
Dickinson, G. H., Ivanina, A. V., Matoo, O. B., Portner, H. O., Lannig, G., Bock, C., Beniash, E., and Sokolova, I. M. 2012. "Interactive Effects of Salinity and Elevated Co_2 Levels of Juvenile Eastern Oysters, Crassostrea Virginica," *Journal of Experimental Biology* (215:1), pp. 29-43.
Dittman, D. E. 1997. "Latitudinal Compensation in Oyster Ciliary Activity," *Functional ecology* (11:5), pp. 573-578.
Dourson, D. C. 2010. *Kentucky's Land Snails and Their Ecological Communities*. Bakersville, North Carolina, USA: Goatslug Publications.
Dourson, D. C., Langdon, K., and Dourson, J. 2013. *Land Snails of the Great Smoky Mountains National Park and Southern Appalachians, Tennessee & North Carolina*. Bakersville, North Carolina, USA: Goatslug Publications.
Eierman, L. E., and Hare, M. P. 2014. "Transcriptomic Analysis of Candidate Osmoregulatory Genes in the Eastern Oyster Crassostrea Virginica," *BMC genomics* (15:1), pp. 503-503.
Eierman, L. E., and Hare, M. P. 2016. "Reef-Specific Patterns of Gene Expression Plasticity in Eastern Oysters (Crassostrea Virginica)," *The Journal of heredity* (107:1), pp. 90-100.
Emberton, K. C. 1988. "The Genitalic, Allozymic, and Conchological Evolution of the Eastern North American Triodopsinae (Gastropoda: Pulmonata: Polygyridae)," *Malacologia* (28), pp. 159-273.
Emberton, K. C. 1994. "Polygyrid Land Snail Phylogeny: External Sperm Exchange, Early North American Biogeography, Iterative Shell Evolution," *Biological Journal of the Linnean Society* (52:3), pp. 241-271.
Emberton, K. C. 1995a. "Sympatric Convergence and Environmental Correlation between Two Land-Snail Species," *Evolution* (49:3), pp. 469-475.
Emberton, K. C. 1995b. "When Shells Do Not Tell: 145 Million Years of Evolution in North American Polygyrid Land Snails, with a Revision and Conservation Priorities," *Malacologia* (37), pp. 69-110.
Estabrook, R. W. 1967. "Mitochondrial Respiratory Control and the Polarographic Measurement of Adp : O Ratios," *Methods in Enzymology* (10), pp. 41-47.
Excoffier, L., and Lischer, H. E. L. 2010. "Arlequin Suite Ver 3.5: A New Series of Programs to Perform Population Genetics Analyses under Linux and Windows," *Molecular ecology resources* (10:3), pp. 564-567.
Fleury, E., Barbier, P., Petton, B., Normand, J., Thomas, Y., Pouvreau, S., Daigle, G., and Pernet, F. 2020. "Latitudinal Drivers of Oyster Mortality: Deciphering Host, Pathogen and Environmental Risk Factors," *Scientific Reports* (10:1), p. 7264.
Folch, J., Lees, M., and Sloane Stanley, G. H. 1957. "A Simple Method for the Isolation and Purification of Total Lipides from Animal Tissues," *J Biol Chem* (226:1), pp. 497-509.
Froelich, B., and Oliver, J. D. 2013. "The Interactions of *Vibrio Vulnificus* and the Oyster *Crassostrea Virginica*," *Microbial Ecolology* (65:4), pp. 807-816.

Froelich, B. A., Williams, T. C., Noble, R. T., and Oliver, J. D. 2012. "Apparent Loss of *Vibrio Vulnificus* from North Carolina Oysters Coincides with a Drought-Induced Increase in Salinity," *Applied and Environmental Microbiology* (78:11), pp. 3885-3889.

Fuhrmann, M., Delisle, L., Petton, B., Corporeau, C., and Pernet, F. 2018. "Metabolism of the Pacific Oyster, Crassostrea Gigas, Is Influenced by Salinity and Modulates Survival to the Ostreid Herpesvirus Oshv-1," *Biol Open* (7:2).

Furr, D., Ketchum, R. N., Phippen, B. L., Reitzel, A. M., and Ivanina, A. V. 2021. "Physiological Variation in Response to Vibrio and Hypoxia by Aquacultured Eastern Oysters in the Southeastern United States," *Integrative and Comparative Biology* (0), pp. 1-15.

Gao, J.-X., Zhang, Y.-Y., Huang, X.-H., Liu, R., Dong, X.-P., Zhu, B.-W., and Qin, L. 2021. "Comparison of Amino Acid, 5′-Nucleotide and Lipid Metabolism of Oysters (Crassostrea Gigas Thunberg) Captured in Different Seasons," *Food Research International* (147), p. 110560.

Gavery, M. R., and Roberts, S. B. 2013. "Predominant Intragenic Methylation Is Associated with Gene Expression Characteristics in a Bivalve Mollusc," *PeerJ* (1), p. e215.

Gavery, M. R., and Roberts, S. B. 2017. "Epigenetic Considerations in Aquaculture," *PeerJ* (5), p. e4147.

Geller, J., Meyer, C., Parker, M., and Hawk, H. 2013. "Redesign of Pcr Primers for Mitochondrial Cytochrome C Oxidase Subunit I for Marine Invertebrates and Application in All-Taxa Biotic Surveys," *Mol Ecol Resour* (13:5), pp. 851-861.

Gerdol, M., and Venier, P. 2015. "An Updated Molecular Basis for Mussel Immunity," *Fish & Shellfish Immunology* (46:1), pp. 17-38.

Gestal, C., Roch, P., Renault, T., Pallavicini, A., Paillard, C., Novoa, B., Oubella, R., Venier, P., and Figueras, A. 2008. "Study of Diseases and the Immune System of Bivalves Using Molecular Biology and Genomics," *Reviews in fisheries science* (16:sup1), pp. 133-156.

Gilchrist, G. W. 1995. "Specialists and Generalists in Changing Environments. I. Fitness Landscapes of Thermal Sensitivity," *The American Naturalist* (146:2), pp. 252-270.

Gómez-Chiarri, M., Warren, W. C., Guo, X., and Proestou, D. 2015. "Developing Tools for the Study of Molluscan Immunity: The sequencing of the Genome of the Eastern Oyster, Crassostrea virginica," *Fish & Shellfish Immunology* (46:1), pp. 2-4.

Goodfriend, G. A. 1986. "Variation in Land-Snail Shell Form and Size and Its Causes: A Review," *Systematic Biology* (35:2), pp. 204-223.

Grant, W. S. 2015. "Problems and Cautions with Sequence Mismatch Analysis and Bayesian Skyline Plots to Infer Historical Demography," *Journal of Heredity* (106:4), pp. 333-346.

Grieshaber, M. K., Hardewig, I., Kreutzer, U., and Portner, H. O. 1994. "Physiological and Metabolic Responses to Hypoxia in Invertebrates," *Rev. Physiol. Biochem. Pharmacol.* (125), pp. 43-147.

Grimm, F. W. 1974. "Speciation within the Triodopsis Fallax Group (Pulmonata: Polygyridae) - a Preliminary Report," *Bulletin of the American Malacological Union*), pp. 23-29.

Guo, X., and Ford, S. E. 2017. "Infectious Diseases of Marine Molluscs and Host Responses as Revealed by Genomic Tools," *Philosophical Transcation of the Royal Society B* (371).

Guo, X., He, Y., Zhang, L., Lelong, C., and Jouaux, A. 2015. "Immune and Stress Responses in Oysters with Insights on Adaptation," *Fish & shellfish immunology* (46:1), pp. 107-119.

Guo, X., Li, C., Wang, H., and Xu, Z. 2018. "Diversity and Evolution of Living Oysters," *Journal of Shellfish Research* (37:4), pp. 755-771, 717.

Gutiérrez, J. L., Jones, C. G., Strayer, D. L., and Iribarne, O. O. 2003. "Mollusks as Ecosystem Engineers: The Role of Shell Production in Aquatic Habitats," *Oikos* (101:1), pp. 79-90.

Haase, M., Esch, S., and Misof, B. 2013. "Local Adaptation, Refugial Isolation and Secondary Contact of Alpine Populations of the Land Snail Arianta Arbustorum," *Journal of Molluscan Studies* (79), pp. 241-248.

Hare, M. P., and Avise, J. C. 1996. "Molecular Genetic Analysis of a Stepped Multilocus Cline in the American Oyster (Crassostrea Virginica)," *Evolution* (50:6), pp. 2305-2315.

Harl, J., Páll-Gergely, B., Kirchner, S., Sattmann, H., Duda, M., Kruckenhauser, L., and Haring, E. 2014. "Phylogeography of the Land Snail Genus Orcula(Orculidae, Stylommatophora) with Emphasis on the Eastern Alpine Taxa: Speciation, Hybridization and Morphological Variation," *BMC Evolutionary Biology* (14:1), p. 223.

Harpending, H. C. 1994. "Signature of Ancient Population Growth in a Low-Resolution Mitochondrial DNA Mismatch Distribution," *Human Biology* (66:4), pp. 591-600.

Harrison, J., Nelson, K., Morcrette, H., Morcrette, C., Preston, J., Helmer, L., Titball, R. W., Butler, C. S., and Wagley, S. 2022. "The Increased Prevalence of Vibrio Species and the First Reporting of Vibrio Jasicida and Vibrio Rotiferianus at Uk Shellfish Sites," *Water Res* (211), p. 117942.

Hebert, P. D., Cywinska, A., Ball, S. L., and deWaard, J. R. 2003. "Biological Identifications through DNA Barcodes," *Proc Biol Sci* (270:1512), pp. 313-321.

Heilmayer, O., Digialleonardo, J., Qian, L., and Guritno, R. 2008. "Stress Tolerance of a Subtropical Crassostrea Virginica Population to the Combined Effects of Temperature and Salinity," *Estuarine, Coastal and Shelf Science* (79:2008), pp. 179-185.

Hellberg, M., Burton, R., Neigel, J., and Palumbi, S. R. 2002. "Genetic Assessment of Connectivity among Marine Populations," *Bulletin of Marine Science* (701 (Supplement S)), pp. 273-290.

Hewitt, G. 2000. "The Genetic Legacy of the Quaternary Ice Ages," *Nature* (405:6789), pp. 907-913.

Hochachka, P. W. 1988. "The Nature of Evolution and Adaptation: Resolving the Unity-Diversity Paradox," *Canadian journal of zoology* (66:5), pp. 1146-1152.

Hochachka, P. W., and Somero, G. N. 2002. *Biochemical Adaptation: Mechanism and Process in Physological Evolution*. NY: Oxford University Press.

Holznagel, W. E., Colgan, D. J., and Lydeard, C. 2010. "Pulmonate Phylogeny Based on 28s Rrna Gene Sequences: A Framework for Discussing Habitat Transitions and Character Transformation," *Mol Phylogenet Evol* (57:3), pp. 1017-1025.

Hoover, C. A., and Gaffney, P. M. 2005. "Geographic Variation in Nuclear Genes of the Eastern Oyster, *Crassostrea Virginica* Gmelin," *Journal of Shellfish Research* (24), pp. 103-112.

Hubricht, L. 1952. "Three New Species of Triodopsis from North Carolina," *The Nautilus* (65:3), pp. 80-82.

Hubricht, L. 1985. *The Distributions of the Native Land Mollusks of the Eastern United States*. Chicago :: Field Museum of Natural History.

Hughes, A. R., Hanley, T. C., Byers, J. E., Grabowski, J. H., Malek, J. C., Piehler, M. F., and Kimbro, D. L. 2017. "Genetic by Environmental Variation but No Local Adaptation in Oysters (Crassostrea Virginica)," *Ecology and evolution* (7:2), pp. 697-709.

Ivanina, A. V., Beniash, E., Etzkorn, M., Meyers, T. B., Ringwood, A. H., and Sokolova, I. M. 2013. "Short-Term Acute Hypercapnia Affects Cellular Responses to Trace Metals in the Hard Clams *Mercenaria Mercenaria*," *Aquatic toxicology* (140-141), pp. 123-133.

Ivanina, A. V., Ellers, S., Kurochkin, I. O., Chung, J. S., Techa, S., Piontkivska, H., Sokolova, E. P., and Sokolova, I. M. 2010. "Effects of Cadmium Exposure and Intermittent Anoxia on Nitric Oxide Metabolism in Eastern Oysters, Crassostrea Virginica Gmelin," *J. Exp. Biol.* (213:3), pp. 433-444.

Ivanina, A. V., Froelich, B., Williams, T., Sokolova, E. P., Oliver, J. D., and Sokolova, I. M. 2011a. "Interactive Effects of Cadmium and Hypoxia on Metabolic Responses and Bacterial Loads of Eastern Oysters *Crassostrea Virginica* Gmelin," *Chemosphere* (83:3), pp. 377-389.

Ivanina, A. V., Froelich, B., Williams, T., Sokolova, E. P., Oliver, J. D., and Sokolova, I. M. 2011b. "Interactive Effects of Cadmium and Hypoxia on Metabolic Responses and Bacterial Loads of Eastern Oysters *Crassostrea Virginica* Gmelin," *Chemosphere`* (83:3), pp. 377-389.

Ivanina, A. V., Hawkins, C., and Sokolova, I. M. 2014. "Immunomodulation by the Interactive Effects of Cadmium and Hypercapnia in Marine Bivalves Crassostrea Virginica and Mercenaria Mercenaria," *Fish & shellfish immunology* (37:2), pp. 299-312.

Ivanina, A. V., Hawkins, C., and Sokolova, I. M. 2016a. "Interactive Effects of Copper Exposure and Environmental Hypercapnia on Immune Functions of Marine Bivalves Crassostrea Virginica and Mercenaria Mercenaria," *Fish & shellfish immunology* (49), pp. 54-65.

Ivanina, A. V., Kurochkin, I. O., Leamy, L., and Sokolova, I. M. 2012. "Effects of Temperature and Cadmium Exposure on the Mitochondria of Oysters (Crassostrea Virginica) Exposed to Hypoxia and Subsequent Reoxygenation," *Journal of Experimental Biology* (215), pp. 3142-3154.

Ivanina, A. V., Nesmelova, I., Leamy, L., Sokolova, E. P., and Sokolova, I. M. 2016b. "Intermittent Hypoxia Leads to Functional Reorganization of Mitochondria and Affects Cellular Bioenergetics in Marine Molluscs," *Journal of Experimental Biology*).

Ivanina, A. V., and Sokolova, I. M. 2013. "Interactive Effects of Ph and Metals on Mitochondrial Functions of Intertidal Bivalves *Crassostrea Virginica* and *Mercenaria Mercenaria*," *Aquatic toxicology* (144-145), pp. 303-309.

Iverson, S. J., Lang, S. L., and Cooper, M. H. 2001. "Comparison of the Bligh and Dyer and Folch Methods for Total Lipid Determination in a Broad Range of Marine Tissue," *Lipids* (36:11), pp. 1283-1287.

Jeppesen, R., Rodriguez, M., Rinde, J., Haskins, J., Hughes, B., Mehner, L., and Wasson, K. 2018. "Effects of Hypoxia on Fish Survival and Oyster Growth in a Highly Eutrophic Estuary," *Estuaries and Coasts* (41:1), pp. 89-98.

Johnson, K. M., and Kelly, M. W. 2020. "Population Epigenetic Divergence Exceeds Genetic Divergence in the Eastern Oyster Crassostrea Virginica in the Northern Gulf of Mexico," *Evolutionary Applications* (13:5), pp. 945-959.

Johnson, K. M., Sirovy, K. A., Casas, S. M., La Peyre, J. F., and Kelly, M. W. 2020. "Characterizing the Epigenetic and Transcriptomic Responses to Perkinsus Marinus Infection in the Eastern Oyster Crassostrea Virginica," *Frontiers in Marine Science* (7:598).

Karl, S. A., and Avise, J. C. 1992. "Balancing Selection at Allozyme Loci in Oysters: Implications from Nuclear Rflps," *Science* (256:5053), pp. 100-102.

Keppler, D., and Decker, K. 1981. "Glycogen," in *Methods of Enzymatic Analysis*, H. Bergmeyer (ed.). Weinheim, Germany: Verlag Chemie, pp. 11-18.

Kern, F., and Ford, S. E. 2011. " Dermo Disease of Oysters Caused by *Perkinsus Marinus* - Ices Identification Leaflets for Diseases and Parasites of Fish and Shellfish." Copenhagen, Denmark: International Council for the Exploration of the Sea, p. 5.

King, T. L., Ward, R., and Zimmerman, E. G. 1994. "Population Structure of Eastern Oysters (Crassostrea Virginica) Inhabiting the Laguna Madre, Texas, and Adjacent Bay Systems," *Canadian journal of fisheries and aquatic sciences* (51:S1), pp. 215-222.

Kirby, M. X. 2004. "Fishing Down the Coast: Historical Expansion and Collapse of Oyster Fisheries Along Continental Margins," *Proceedings of the National Academy of Sciences* (101:35), pp. 13096-13099.

Kumar, S., Stecher, G., and Tamura, K. 2016. "Mega7: Molecular Evolutionary Genetics Analysis Version 7.0 for Bigger Datasets," *Molecular biology and evolution* (33:7), pp. 1870-1874.

Kurochkin, I. O., Ivanina, A. V., Eilers, S., Downs, C. A., May, L. A., and Sokolova, I. M. 2009. "Cadmium Affects Metabolic Responses to Prolonged Anoxia and Reoxygenation in Eastern Oysters (*Crassostrea Virginica)*," *Am. J. Physiol. Regulatory Integrative Comp Physiol.* (297), pp. R1262-R1272.

La Peyre, M. K., Eberline, B. S., Soniat, T. M., and La Peyre, J. F. 2013. "Differences in Extreme Low Salinity Timing and Duration Differentially Affect Eastern Oyster (Crassostrea Virginica) Size Class Growth and Mortality in Breton Sound, La," *Estuarine, Coastal and Shelf Science* (135), pp. 146-157.

Leigh, J. W., Bryant, D., and Nakagawa, S. 2015. "Popart: Full-Feature Software for Haplotype Network Construction," *Methods in ecology and evolution* (6:9), pp. 1110-1116.

Letendre, J., Leboulenger, F., and Durand, F. 2012. "Oxidative Challenge and Redox Sensing in Mollusks: Effects of Natural and Anthropic Stressors," in *Oxidative Stress in Vertebrates and Invertebrates: Molecular Aspects of Cell Signaling, First Edition,* T. Farooqui and A.A. Farooqui (eds.). John Wiley & Sons, Inc. .

Levine, R. L. 2002. "Carbonyl Modified Proteins in Cellular Regulation, Aging, and Disease," *Free Radic Biol Med* (32:9), pp. 790-796.

Levine, R. L., Wehr, N., Williams, J. A., Stadtman, E. R., and Shacter, E. 2000. "Determination of Carbonyl Groups in Oxidized Proteins," *Methods Mol Biol* (99), pp. 15-24.

Li, J., Zhang, Y., Mao, F., Tong, Y., Liu, Y., Zhang, Y., and Yu, Z. 2017. "Characterization and Identification of Differentially Expressed Genes Involved in Thermal Adaptation of the Hong Kong Oyster Crassostrea Hongkongensis by Digital Gene Expression Profiling," *Frontiers in Marine Science* (4).

Li, X., Yang, B., Shi, C., Wang, H., Yu, R., Li, Q., and Liu, S. 2022. "Synergistic Interaction of Low Salinity Stress with Vibrio Infection Causes Mass Mortalities in the Oyster by Inducing Host Microflora Imbalance and Immune Dysregulation," *Frontiers in immunology* (13), pp. 859975-859975.

Li, Y., Qin, J. G., Abbott, C. A., Li, X., and Benkendorff, K. 2007. "Synergistic Impacts of Heat Shock and Spawning on the Physiology and Immune Health of Crassostrea Gigas: An Explanation for Summer Mortality in Pacific Oysters," *Am J Physiol Regul Integr Comp Physiol* (293:6), pp. R2353-2362.

Liu, C., Ren, Y., Li, Z., Hu, Q., Yin, L., Wang, H., Qiao, X., Zhang, Y., Xing, L., Xi, Y., Jiang, F., Wang, S., Huang, C., Liu, B., Liu, H., Wan, F., Qian, W., and Fan, W. 2021. "Giant African Snail Genomes Provide Insights into Molluscan Whole-Genome Duplication and Aquatic–Terrestrial Transition," *Molecular Ecology Resources* (21:2), pp. 478-494.

Liu, M., and Guo, X. 2017. "A Novel and Stress Adaptive Alternative Oxidase Derived from Alternative Splicing of Duplicated Exon in Oyster Crassostrea Virginica," *Scientific Reports* (7), p. 10785.

Livingston, R. J., Lewis, F. G., Woodsum, G. C., Niu, X. F., Galperin, B., Huang, W., Christensen, J. D., Monaco, M. E., Battista, T. A., Klein, C. J., Howell, R. L., and Ray, G. L. 2000. "Modelling Oyster Population Response to Variation in Freshwater Input," *Estuarine, coastal and shelf science* (50:5), pp. 655-672.

Lv, Z., Qiu, L., Wang, M., Jia, Z., Wang, W., Xin, L., Liu, Z., Wang, L., and Song, L. 2018. "Comparative Study of Three C1q Domain Containing Proteins from Pacific Oyster Crassostrea Gigas," *Dev Comp Immunol* (78), pp. 42-51.

Madeira, P. M., Chefaoui, R. M., Cunha, R. L., Moreira, F., Dias, S., Calado, G., and Castilho, R. 2017. "High Unexpected Genetic Diversity of a Narrow Endemic Terrestrial Mollusc," *PeerJ*).

Malek, J. C., and Byers, J. E. 2017. "The Effects of Tidal Elevation on Parasite Heterogeneity and Co-Infection in the Eastern Oyster, Crassostrea Virginica," *Journal of Experimental Marine Biology and Ecology* (494), pp. 32-37.

Malhi, Y., Franklin, J., Seddon, N., Solan, M., Turner, M. G., Field, C. B., and Knowlton, N. 2020. "Climate Change and Ecosystems: Threats, Opportunities and Solutions," *Philosophical Transactions of the Royal Society B: Biological Sciences* (375:1794), p. 20190104.

McDowell, I. C., Modak, T. H., Lane, C. E., and Gomez-Chiarri, M. 2016. "Multi-Species Protein Similarity Clustering Reveals Novel Expanded Immune Gene Families in the Eastern Oyster Crassostrea Virginica," *Fish & Shellfish Immunology* (53), pp. 13-23.

McDowell, I. C., Nikapitiya, C., Aguiar, D., Lane, C. E., Istrail, S., and Gomez-Chiarri, M. 2014. "Transcriptome of American Oysters, *Crassostrea Virginica*, in Response to Bacterial Challenge: Insights into 0otential Mechanisms of Disease Resistance," *PLOS ONE* (9:8), p. e105097.

Meng, J., Wang, T., Li, L., and Zhang, G. 2018. "Inducible Variation in Anaerobic Energy Metabolism Reflects Hypoxia Tolerance across the Intertidal and Subtidal Distribution of the Pacific Oyster *(Crassostrea Gigas)*," *Marine environmental research* (138), pp. 135-143.

Meng, J., Wang, W., Li, L., Yin, Q., and Zhang, G. 2017. "Cadmium Effects on DNA and Protein Metabolism in Oyster (Crassostrea Gigas) Revealed by Proteomic Analyses," *Scientific reports* (7:1), pp. 11716-11716.

Mihalas, B. P., De Iuliis, G. N., Redgrove, K. A., McLaughlin, E. A., and Nixon, B. 2017. "The Lipid Peroxidation Product 4-Hydroxynonenal Contributes to Oxidative Stress-Mediated Deterioration of the Ageing Oocyte," *Scientific Reports* (7:1), p. 6247.

Miller, L. S., Peyre, J. L., and Peyre, M. L. 2017. "Suitability of Oyster Restoration Sites Along the Louisiana Coast: Examining Site and Stock X Site Interaction," *Journal of Shellfish Research* (36:2), pp. 341-351.

Motes, M. L., Depaola, A., Cook, D. W., Veazey, J. E., Hunsucker, J. C., Garthright, W. E., Blodgett, R. J., and Chirtel, S. J. 1998. "Influence of Water Temperature and Salinity on Vibrio Vulnificus in Northern Gulf and Atlantic Coast Oysters *(Crassostrea Virginica)*," *Applied and environmental microbiology* (64:4), pp. 1459-1465.

Müller, M., Mentel, M., van Hellemond, J. J., Henze, K., Woehle, C., Gould, S. B., Yu, R.-Y., van der Giezen, M., Tielens, A. G. M., and Martin, W. F. 2012. "Biochemistry and Evolution

of Anaerobic Energy Metabolism in Eukaryotes," *Microbiology and Molecular Biology Reviews* (76:2), pp. 444-496.
Nadachowska-Brzyska, K. 2010. "Divergence with Gene Flow - the Amphibian Perspective," *The Herpetological Journal* (20), pp. 7-15.
Nicolai, A., and Ansart, A. 2017. "Conservation at a Slow Pace: Terrestrial Gastropods Facing Fast-Changing Climate," *Conservation Physiology* (5), pp. 1-17.
NOAA. 2005. "Eastern Oyster." *Species Directory*, from https://www.fisheries.noaa.gov/species/eastern-oyster
Ó Foighil, D., Gaffney, P. M., and Hilbish, T. J. 1995. "Differences in Mitochondrial 16s Ribosomal Gene Sequences Allow Discrimination among American [Crassostrea Virginica (Gmelin)] and Asian [C. Gigas (Thunberg) C. Ariakensis Wakiya] Oyster Species," *Journal of Experimental Marine Biology and Ecology* (192:2), pp. 211-220.
Olive, P. L. 1988. "DNA Precipitation Assay: A Rapid and Simple Method for Detecting DNA Damage in Mammalian Cells," *Environmental and Molecular Mutagenesis* (11:4), pp. 487-495.
Olive, P. L., Chan, A. P. S., and Cu, C. S. 1988. "Comparison between the DNA Precipitation and Alkali Unwinding Assays for Detecting DNA Strand Breaks and Cross-Links," *Cancer Research* (48:22), p. 6444.
Oliver, J. D., Warner, R. A., and Cleland, D. R. 1983. "Distribution of *Vibrio Vulnificus* and Other Lactose-Fermenting Vibrios in the Marine Environment," *Applied and Environmental Microbiology* (45:3), pp. 985-998.
Palumbi, S., University of Hawaii. Department of, Z., and University of Hawaii. Kewalo Marine, L. 1991. *The Simple Fool's Guide to Pcr : Version 2.0, Saturday, July 27, 1991*. Honolulu: Department of Zoology and Kewalo Marine Laboratory.
Palumbi, S. R. 1994. "Genetic Divergence, Reproductive Isolation, and Marine Speciation," *Annu. Rev. Ecol. Syst.* (25), pp. 547-572.
Pannunzio, T. M., and Storey, K. B. 1998. "Antioxidant Defenses and Lipid Peroxidation During Anoxia Stress and Aerobic Recovery in the Marine Gastropod Littorina Littorea," *Journal of Experimental Marine Biology and Ecology* (221:2), pp. 277-292.
Parker, L. M., Scanes, E., O'Connor, W. A., and Ross, P. M. 2021. "Transgenerational Plasticity Responses of Oysters to Ocean Acidification Differ with Habitat," *Journal of Experimental Biology* (224:12).
Patten, M. A., and Unitt, P. 2002. "Diagnosability Versus Mean Differences of Sage Sparrow Subspecies," *The Auk* (119:1), pp. 26-35.
Perez, K. E., deFreitas, N., Slapcinsky, J., Minton, R. L., Anderson, F., and Pearce, T. A. 2014. "Molecular Phylogeny, Evolution of Shell Shape, and DNA Barcoding in Polygyridae (Gastropoda: Pulmonata), an Endemic North American Clade of Land Snails."
Pfaffl, M. W. 2001. "A New Mathematical Model for Relative Quantification in Real-Time Rt-Pcr," *Nucleic Acids Research* (29:9), p. e45.
Pfenninger, M., Posada, D., and Magnin, F. 2003. "Evidence for Survival of Pleistocene Climatic Changes in Northern Refugia by the Land Snail Trochoidea Geyeri (Soós 1926) (Helicellinae, Stylommatophora)," *BMC Evolutionary Biology* (3), pp. 8 - 8.
Pilsbry, H. A. 1940. *Land Mollusca of North America (North of Mexico)*. Philadelphia: The Academy of Natural Sciences of Philadelphia.

Pinceel, J., Jordaens, K., and Backeljau, T. 2005. "Extreme Mtdna Divergences in a Terrestrial Slug (Gastropoda, Pulmonata, Arionidae): Accelerated Evolution, Allopatric Divergence and Secondary Contact," *J Evol Biol* (18:5), pp. 1264-1280.

Powell, E. N., Klinck, J. M., Hofmann, E. E., and McManus, M. A. 2003. "Influence of Water Allocation and Freshwater Inflow on Oyster Production: A Hydrodynamic–Oyster Population Model for Galveston Bay, Texas, USA," *Environmental Management* (31:1), pp. 0100-0121.

Puckett, B. J., and Eggleston, D. B. 2012. "Oyster Demographics in a Network of No-Take Reserves: Recruitment, Growth, Survival Adn Density Dependence," *Marine and Coastal Fisheries: Dynamics, Management and Ecosystem Science* (4), pp. 605-627.

Quistad, S. D., and Traylor-Knowles, N. 2016. "Precambrian Origins of the Tnfr Superfamily," *Cell death discovery* (2:1), pp. 16058-16058.

R_Core_Team. 2023. "R: A Language and Environment for Statistical Computing," in: *R Foundation for Statistical Computing*. Vienna, Austria.

Raftos, D. A., Melwani, A. R., Haynes, P. A., Muralidharan, S., Birch, G. F., Amaral, V., Thompson, E. L., and Taylor, D. A. 2016. "The Biology of Environmental Stress: Molecular Biomarkers in Sydney Rock Oysters (*Saccostrea Glomerata*)," *Environmental science--processes & impacts* (18:9), pp. 1129-1139.

Ray, N., Currat, M., and Excoffier, L. 2003. "Intra-Deme Molecular Diversity in Spatially Expanding Populations," *Mol Biol Evol* (20:1), pp. 76-86.

Reeb, C. A., and Avise, J. C. 1990. "A Genetic Discontinuity in a Continuously Distributed Species: Mitochondrial DNA in the American Oyster, Crassostrea Virginica," *Genetics* (124:2), pp. 397-406.

Rosa, R. D., Santini, A., Fievet, J., Bulet, P., Destoumieux-Garzón, D., and Bachère, E. 2011. "Big Defensins, a Diverse Family of Antimicrobial Peptides That Follows Different Patterns of Expression in Hemocytes of the Oyster *Crassostrea Gigas*," *PloS one* (6:9), pp. e25594-e25594.

Rozas, J., Ferrer-Mata, A., Sánchez-DelBarrio, J. C., Guirao-Rico, S., Librado, P., Ramos-Onsins, S. E., and Sánchez-Gracia, A. 2017. "Dnasp 6: DNA Sequence Polymorphism Analysis of Large Data Sets," *Molecular biology and evolution* (34:12), pp. 3299-3302.

Salmon, T. B., Evert, B. A., Song, B., and Doetsch, P. W. 2004. "Biological Consequences of Oxidative Stress-Induced DNA Damage in Saccharomyces Cerevisiae," *Nucleic acids research* (32:12), pp. 3712-3723.

Salvador, R. B., Brook, F. J., Shepherd, L. D., and Kennedy, M. 2020. "Molecular Phylogenetic Analysis of Punctoidea (Gastropoda, Stylommatophora)," *Zoosystematics and Evolution* (96:2), pp. 397-410.

Sanni, B., Williams, K., Sokolov, E. P., and Sokolova, I. M. 2008. "Effects of Acclimation Temperature and Cadmium Exposure on Mitochondrial Aconitase and Lon Protease from a Model Marine Ectotherm, *Crassostrea Virginica*," *Comparative biochemistry and physiology. Toxicology & pharmacology* (147:1), pp. 101-112.

Sauer, J., and Hausdorf, B. 2012. "A Comparison of DNA-Based Methods for Delimiting Species in a Cretan Land Snail Radiation Reveals Shortcomings of Exclusively Molecular Taxonomy," *Cladistics* (28:3), pp. 300-316.

Saupe, E. E., Qiao, H., Hendricks, J. R., Portell, R. W., Hunter, S. J., Soberón, J., and Lieberman, B. S. 2015. "Niche Breadth and Geographic Range Size as Determinants of Species

Survival on Geological Time Scales," *Global Ecology and Biogeography* (24:10), pp. 1159-1169.
Sinclair, C. S. 2010. "Surfing Snails: Population Genetics of the Land Snail Ventridens Ligera (Stylommatophora: Zonitidae) in the Potomac Gorge," *American Malacological Bulletin* (28:2), pp. 105-112, 108.
Skulachev, V. P. 1998. "Uncoupling: New Approaches to an Old Problem of Bioenergetics," *BBA - Bioenergetics* (1363:2), pp. 100-124.
Söderhäll, K. 2010. "Invertebrate Immunity," K. Söderhäll (ed.). New York: Springer Science+Business Media, LLC; Landes Bioscience, p. 338.
Sokolov, E. P. 2000. "An Improved Method for DNA Isolation from Mucopolysaccharide-Rich Molluscan Tissues," *Journal of Molluscan Studies* (66:4), pp. 573-575.
Sokolova, I. M. 2004. "Cadmium Effects on Mitochondrial Function Are Enhanced by Elevated Temperatures in a Marine Poikilotherm, Crassostrea Virginica Gmelin (Bivalvia: Ostreidae)," *Journal of experimental biology* (207:Pt 15), pp. 2639-2648.
Sokolova, I. M., Bock, C., and Pörtner, H. O. 2000. "Resistance to Freshwater Exposure in White Sea Littorina Spp. I: Anaerobic Metabolism and Energetics," *J Comp Physiol B* (170:2), pp. 91-103.
Sokolova, I. M., Sukhotin, A. A., and Lannig, G. 2012. "Stress Effects on Metabolism and Energy Budgets in Mollusks," in *Oxidative Stress in Aquatic Ecosystems*, D. Abele, V.-M.J. P. and T. Zenteno-Savin (eds.). West Sussex, UK: Wiley-Blackwell.
Song, L., Wang, L., Qiu, L., and Zhang, H. 2010. "Bivalve Immunity," in *Invertebrate Immunity*, K. Söderhäll (ed.). Boston, MA: Springer US, pp. 44-65.
Souza-Shibatta, L., Kotelok-Diniz, T., Ferreira, D. G., Shibatta, O. A., Sofia, S. H., de Assumpção, L., Pini, S. F. R., Makrakis, S., and Makrakis, M. C. 2018. "Genetic Diversity of the Endangered Neotropical Cichlid Fish (Gymnogeophagus Setequedas) in Brazil," *Front Genet* (9), p. 13.
Stanley, J. G., and Sellers, M. A. 1986. "Species Profiles. Life Histories and Environmental Requirements of Coastal Fishes and Invertebrates (Gulf of Mexico). American Oyster."
Sun, S. e., Li, Q., Kong, L., and Yu, H. 2017. "Limited Locomotive Ability Relaxed Selective Constraints on Molluscs Mitochondrial Genomes," *Scientific Reports* (7).
Sun, Y., Zhou, Z., Wang, L., Yang, C., Jianga, S., and Song, L. 2014. "The Immunomodulation of a Novel Tumor Necrosis Factor (Cgtnf-1) in Oyster Crassostrea Gigas," *Developmental and comparative immunology* (45:2), pp. 291-299.
Suvorov, A. N. 2002. "Prospects for Studies of Morphological Variability of Land Pulmonate Snails," *Biology Bulletin of the Russian Academy of Sciences* (29:5), pp. 455-467.
Tamura, K., Stecher, G., and Kumar, S. 2021. "Mega11: Molecular Evolutionary Genetics Analysis Version 11," *Molecular biology and evolution* (37), pp. 1237-1239.
Thaewnon-ngiw, B., Klinbunga, S., Phanwichien, K., Sangduen, N., Lauhachinda, N., and Menasveta, P. 2004. "Genetic Diversity and Molecular Markers in Introduced and Thai Native Apple Snails (Pomacea and Pila)," *Journal of biochemistry and molecular biology* (37 4), pp. 493-502.
Thomaz, D., Guiller, A., and Clarke, B. C. 1996. "Extreme Divergence of Mitochondrial DNA within Species of Pulmonate Land Snails," *Proceedings of the Royal Society of London. Series B: Biological Sciences* (263:1368), pp. 363-368.
Thongda, W., Zhao, H., Zhang, D., Jescovitch, L. N., Liu, M., Guo, X., Schrandt, M., Powers, S. P., and Peatman, E. 2018. "Development of Snp Panels as a New Yool to Assess the

Genetic Diversity, Population Structure, and Parentage Analysis of the Eastern Oyster (*Crassostrea Virginica*)," *Marine Biotechnology* (20:3), pp. 385-395.
Travers, M. A., Boettcher Miller, K., Roque, A., and Friedman, C. S. 2015. "Bacterial Diseases in Marine Bivalves," *Journal of Invertebrate Pathology* (131), pp. 11-31.
Turner, R. E. 2006. "Will Lowering Estuarine Salinity Increase Gulf of Mexico Oyster Landings?," *Estuaries and coasts* (29:3), pp. 345-352.
Uematsu, S., and Akira, S. 2008. *Toll-Like Receptors (Tlrs) and Their Ligands*. Berlin, Heidelberg: Springer-Verlag.
Vagvolgyi, J. 1968. "Systematics and Evolution of the Genus Triodopsis (Mollusca: Pulmonata: Polygyridae)," *Bulletin of the Museum of Comparative Zoology at Harvard College.* (136), pp. 145-254.
Vandewoestijne, S., and Van Dyck, H. 2010. "Population Genetic Differences Along a Latitudinal Cline between Original and Recently Colonized Habitat in a Butterfly," *PLoS One* (5:11), p. e13810.
Varney, R. L., Galindo-Sánchez, C. E., Cruz, P., and Gaffney, P. M. 2009. "Population Genetics of the Eastern Oyster *Crassostrea Virginica* (Gmelin, 1791) in the Gulf of Mexico," *Journal of Shellfish Research* (28:4), pp. 855-864, 810.
Varney, R. L., Watts, J. C., and Wilbur, A. E. 2018. "Genetic Impacts of a Commercial Aquaculture Lease on Adjacent Oyster Populations," *Aquaculture* (491), pp. 310-320.
Vázquez-Mendoza, A., Carrero, J. C., and Rodriguez-Sosa, M. 2013. "Parasitic Infections: A Role for C-Type Lectins Receptors," *BioMed research international* (2013), pp. 456352-456311.
Wade, C. M., Mordan, P. B., and Naggs, F. 2006. "Evolutionary Relationships among the Pulmonate Land Snails and Slugs (Pulmonata, Stylommatophora)," *Biological Journal of the Linnean Society* (87:4), pp. 593-610.
Walker, M. J., Stockman, A. K., Marek, P. E., and Bond, J. E. 2009. "Pleistocene Glacial Refugia across the Appalachian Mountains and Coastal Plain in the Millipede Genus Narceus: Evidence from Population Genetic, Phylogeographic, and Paleoclimatic Data," *BMC Evol Biol* (9), p. 25.
Waltari, E., Hijmans, R. J., Peterson, A. T., Nyári, A. S., Perkins, S. L., and Guralnick, R. P. 2007. "Locating Pleistocene Refugia: Comparing Phylogeographic and Ecological Niche Model Predictions," *PLoS One* (2:6), p. e563.
Wang, L., Song, X., and Song, L. 2018. "The Oyster Immunity," *Developmental and Comparative Immunology* (80), pp. 99-118.
Wanninger, A., and Wollesen, T. 2018. "The Evolution of Molluscs," *Biological Review*), pp. 1-14.
Weihe, E., and Abele, D. 2008. "Differences in the Physiological Response of Inter- and Subtidal Antarctic Limpets *Nacella Concinna* to Aerial Exposure," *Aquatic biology* (4), pp. 155-166.
Whitehill, E. A. G., and Moran, A. L. 2012. "Comparative Larval Energetics of an Ophiuroid and an Echinoid Echinoderm," *Invertebrate biology* (131:4), pp. 345-354.
Wilber, D. H. 1992. "Associations between Freshwater Inflows and Oyster Productivity in Apalachicola Bay, Florida," *Estuarine, coastal and shelf science* (35:2), pp. 179-190.
Wilkinson, A. C. 2020. "Shell Convergence: An Interspecific Molecular Phylogeny of *Neohelix* (Gastropoda: Polygyridae)," in: *Department of Biology*. Appalachian State University.

Woodward, J. 2014. *The Ice Age: A Very Short Introduction*. United Kingdom: Oxford University Press.

Zając, K. S., Proćków, M., Zając, K., Stec, D., and Lachowska-Cierlik, D. 2020. "Phylogeography and Potential Glacial Refugia of Terrestrial Gastropod Faustina Faustina (Rossmässler, 1835) (Gastropoda: Eupulmonata: Helicidae) Inferred from Molecular Data and Species Distribution Models," *Organisms Diversity & Evolution* (20:4), pp. 747-762.

Zhang, G., Fang, X., Guo, X., Li, L., Luo, R., Xu, F., Yang, P., Zhang, L., Wang, X., Qi, H., Xiong, Z., Que, H., Xie, Y., Holland, P. W. H., Paps, J., Zhu, Y., Wu, F., Chen, Y., Wang, J., Peng, C., Meng, J., Yang, L., Liu, J., Wen, B., Zhang, N., Huang, Z., Zhu, Q., Feng, Y., Mount, A., Hedgecock, D., Xu, Z., Liu, Y., Domazet-Loso, T., Du, Y., Sun, X., Zhang, S., Liu, B., Cheng, P., Jiang, X., Li, J., Fan, D., Wang, W., Fu, W., Wang, T., Wang, B., Zhang, J., Peng, Z., Li, Y., Li, N., Wang, J., Chen, M., Yan, H., Tan, F., Song, X., Zheng, Q., Huang, R., Yang, H., Du, X., Chen, L., Yang, M., Gaffney, P. M., Wang, S., Luo, L., She, Z., Ming, Y., Huang, W., Zhang, S., Huang, B., Zhang, Y., Qu, T., Ni, P., Miao, G., Wang, J., Wang, Q., Steinberg, C. E. W., Wang, H., Li, N., Qian, L., Zhang, G., Li, Y., Yang, H., Liu, X., Wang, J., Yin, Y., and Wang, J. 2012. "The Oyster Genome Reveals Stress Adaptation and Complexity of Shell Formation," *Nature (London)* (490:7418), pp. 49-54.

Zhang, G., Li, L., Meng, J., Qi, H., Qu, T., Xu, F., and Zhang, L. 2016. "Molecular Basis for Adaptation of Oysters to Stressful Marine Intertidal Environments," *Annual review of animal biosciences* (4:1), pp. 357-381.

Zhang, L., Li, L., Guo, X., Litman, G. W., Dishaw, L. J., and Zhang, G. 2015. "Massive Expansion and Functional Divergence of Innate Immune Genes in a Protostome," *Scientific reports* (5:1), pp. 8693-8693.

Zhong, H., and Yin, H. 2015. "Role of Lipid Peroxidation Derived 4-Hydroxynonenal (4-Hne) in Cancer: Focusing on Mitochondria," *Redox biology* (4), pp. 193-199.

Zhou, W., Yang, H., Ding, H., Yang, S., Lin, J., and Wang, P. 2017. "Population Genetic Structure of the Land Snail Camaena Cicatricosa (Stylommatophora, Camaenidae) in China Inferred from Mitochondrial Genes and Its2 Sequences," *Scientific Reports* (7).

APPENDIX A.1

Lipid determination

Modified after Folch and Iverson (Folch et al. 1957; Iverson et al. 2001)

1 Tare each 2ml tube before adding tissue.

2 Grind tissue sample to powder in liquid nitrogen.

3 Place no more than 50 mg of ground tissue powder into a tared and marked 2 ml Eppendorf tube and record tissue weight on worksheet. (More than 50 mg requires more liquid than the capacity of the tube in later steps.)

4 Add solvent (Chloroform/Methanol mixture, 2:1 v/v) in a proportion 1:20 (tissue to solvent, w/v). (Tissue, mg * 20 = solvent, ul).

5 Sonicate the sample for 1 min. then vortex vigorously for 2 min.

6 Centrifuge the sample at room temperature at 13000 x g for 5 min.

7 Remove supernatant into a new marked 2 ml Eppendorf tube. Add 0.5 ml of fresh solvent to the pellet.

8 Sonicate the sample for 1 min.

9 Vortex vigorously for 2 min.

10 Centrifuge the sample at room temperature at 13000 g for 5 min.

11 Add supernatant to the tube with previous supernatant of the same sample.

12 Take tube with supernatants, add H_2O in the amount of ¼ of the total volume of supernatant. (Chloroform: Methanol: Water ratio is 8:4:3) (if you have 1600 ul of supernatants take 400 ul of water).

13 Vortex vigorously for 2 min.

14 Centrifuge the sample at room temperature at 13000 g for 5 min.

15 Transfer the lower phase (chloroform) in a weighed tube and evaporate chloroform, overnight if necessary.

16 Weigh tube with lipids residue. (This gives better estimate of lipids, than weighing de-fatted tissues, because there are substances other than lipids that are extracted by chl:met,-like pigments. They are left in water-methanol phase).

APPENDIX A.2

Glucose/Glycogen Assay
(Keppler and Decker 1981)

Reactions:

$$\text{Glycogen} + H_2O \xrightarrow[\text{pH 4.8}]{\text{Glucoamylase}} \text{alpha-glucosyl} + \text{Glucose}$$

$$\text{Glucose} + \text{ATP} \xrightarrow[\text{pH 7.5}]{\text{Hexokinase}} \text{Glucose-6-Phoaphate} + \text{ADP}$$

$$\text{Glucose-6-Phosphate} + NADP^+ \xrightarrow{\text{G6P-DH}} \text{6-P-glucono-1,5-lactone} + NADPH + H^+$$

Reagent	Stock Conc.	Amount	To Make:	Comments
Perchloric acid (Souza-Shibatta et al.)(70%)	0.6M	5.2ml	100ml	Dilute with H_2O. On shelf
Potassium hydrogen carbonate ($KHCO_3$)	1 M	2g	20ml	Dilute with H_2O. In frig
Acetate Buffer:				
Acetic Acid 96% Sodium acetate	96%	4.8ml 9.75g	1000ml	Dilute with H_2O. In frig.
Glucoamylase solution:				
Glucoamylase or amyloglucosidase	$\geq$ 10 kU/mg protein	20mg	20ml	Dilute with acetate buffer. Stored frozen at -20C.
TAE/ATP/NADP/ G-6-PDH Master Mix:				
TAE $MgSO_4$-$7H_2O$ KOH	 1 M	5.6g 100mg 12ml	100ml	Check pH & adjust to pH 7.5 if necessary. Make up to 100ml with water. In frig.
ATP-Na_2H_2-$3H_2O$ NADP G6P-DH	100mM 100mM $\geq$ 700 U/l	100ul 90ul 50ul	10ml (for 48 wells)	Dilute with TAE Buffer to 10ml; **Make immediately before using.** Calculate how much is needed based on sample number – 200ul/well
Hexokinase:				
Hexokinase (HK) ($\geq$ 280 kU/l)	$\geq$ 140 U/mg protein	Undiluted		At 25°C. In frig.

Tissue Homogenization (or use PCA Extraction Protocol for Adenylates):

1. Add PCA to frozen sample at 5:1 by weight and homogenize. Sample must stay a pH 4 – 5 and can be stored in the cold for several days.
2. After homogenization, pipette 0.2ml suspension into a centrifuge tube and keep in on ice. Remainder in perchloric acid is centrifuged and used for glucose determination.

Glycogen and Free Glucose Determination:

For Glycogen Determination:

Use *Glycogen Hydrolysis* step and sub-aliquot of homogenization sample above. Continue with *Glucose Determination*.

For Free-glucose Determination:

Use PCA sample prepared in Tissue Homogenization above or in Adenylate prep.

Do not use the hydrolysis step. Continue with *Glucose Determination*.

Both values from this assay and PCA worksheet are needed for Glycogen/Free Glucose Calculations.

Glycogen Hydrolysis:

3. Pipette into centrifuge tube: (Can use less homogenate, if needed. Adjust reagents, including PCA in #5. Disadvantage – difficult to adjust pH in step 6 because of small volume.)

	Large volume	Small volume	Conc. In mixture
Homogenate	25ul	10ul	Up to 2g/l (glucose)
$KHCO_3$	12.5ul	5ul	43mM
Glucoamylase sol.	250ul	100ul	Enzyme 8.7kU/ acetate 174mM
PCA in step 5	*125ul*	*50.88ul*	*210mM*

4. Stopper tube, incubate at 40°C for 2 hours.
5. Add Perchloric Acid 0.6M – 125ul **(Adjust to appropriate volume for changes of step 3)**
6. Check pH and adjust to 7.0 – 7.5 as for PCA homogenization. Record volumes.
7. Mix, centrifuge for 10 min at maximum speed, then use supernatant for glucose determination or store at -80°C.

.

Make Glucose Standards:

8. Dilute 500 mM Glucose (Dextrose) stock to 50 mM Glucose. Make Glucose Standard:

Conc. in well (211 µL)	Conc. of Standard	50mM Glucose (µL)	Di H_2O (µL)	Vol of Standard (µL)
0.284mM	6mM	12.0	88	100
0.237mM	5mM	10.0	90	100
0.190mM	4mM	8.00	92	100
0.142mM	3mM	6.00	94	100
0.095mM	2mM	4.00	96	100
0.047mM	1mM	20.0	980	1000
0.024mM	0.5mM	10.0	990	1000
0.000mM	0.0mM	0.00	100	100

Continued

Glucose Determination:

9. Pipette successively into wells:

		Conc. In well	
Standard or Sample (deproteinized)	10ul	Up to 0.4 mM (glucose)	
ATP/NADP/G6P-DH/buffer	200ul	ATP	1mM
		NADP	0.9mM
		TAE	285mM
		$MgSO_4$	4mM
		G6P-DH	0.7kU/l

10. Mix thoroughly and allow to sit for at least 5 minutes, then read A_1 340 nm (background).
11. Add 1 ul HK suspension and incubate for 30 minutes at 37ºC.
12. Read A_2 at 340 nm. Use $A_2 - A_1 = A$ for calculation. The change in absorbance due to the addition of HK suspension can be neglected.

Calculations – (PCA worksheet information is needed for calculations.)

1. Determine the average absorbance values for each standard and sample.
2. Subtract the background absorbance values from each.
3. Subtract the absorbance of the free glucose samples from the absorbance of hydrolyzed glycogen samples.
4. Determine the standard curve for each plate and calculate the concentration of each sample based on the standard curve.
5. Using data from the PCA worksheet, adjust the values of free glycose and glycogen for volume on the **Glucose Glycogen Calculation** worksheets.

Terms:

TAE	Buffer of Tris base, acetic acid and EDTA
Tris	Trisaminomethane
$MgSO_4$-$7H_2O$	Magnesium sulfate
KOH	Potassium hydroxide
ATP-Na_2H_2-$3H_2O$	Adenosine 5-triphosphate disodium salt
NADP	Nicotinamide adenine dinucleotide phosphate
G6P-DH	Glucose 6-phosphate
NADPH	Reduced form of NADP
PCA	Perchloric acid
HK	Hexakinase
$KHCO_3$	Potassium carbonate
ATP	Adenosine triphosphate
ADP	Adenosine diphosphate
kU	Kilounits
mM	millimolar

APPENDIX A.3

DNA Degradation Protocol
(Olive 1988)

Prepare Stock Reagents:

1. For Tris-EDTA Homogenizing Buffer #1: Make from powdered reagents (Step 1):

Reagent stocks	To make 28 ml	To make 50 ml	Final Conc.	Notes:
Tris FW-121.14 g/M	169.96 mg	303.5 mg	50mM	Adjust pH to 8.0 with HCl. Dilute with DI water.
EDTA 0.5M stock FW- 372.2 g/M	5.6 ml	10 ml	100mM	
SDS (Sodium laurel sulfate) FW- 288.37 g/M	140 mg	250 mg	0.5%	

2. 10mM Tris-EDTA + 40mM NaOH + 2% SDS Buffer #2: Make these 3 solutions individually. Mix together immediately before use. (Step 2)

	Reagent stocks	To make 10 ml	To make 50 ml	Final Conc.	Conc. In sample
1.	Tris EDTA 0.5M stock	20 mg 340 ul	100 mg 1.7 ml	17mM 17mM	10mM 10mM
2.	NaOH	-	400 mg	200mM	40mM
3.	SDS (Sodium laurel sulfate)	-	500 mg	10%	2%

3. 0.24 M KCl #3 (Step 3)

KCl	134 mg	0.893g
H_2O	Up to 7.5 ml	Up to 50 ml

(Add 125ul of 0.24 M KCl to sample)

4. 0.2M Tris + 0.8M NaCl + 8 mM sodium cholate #4, pH 9.0 (Step 8)

Tris	290.4mg	1.210 g	
NaCl	561.6mg	2.340 g	(FW: 58.44 g/M)
Sodium cholate	41.34mg	0.172 g	(FW: 430.56 g/M)
H_2O	Up to 12ml	Up to 50 ml	

5. 10mM Tris + 1mM EDTA Buffer #5, pH 8.0: (For DNA working stock)

Tris	12mg	0.06 g
EDTA (0.5M stock)	20 ul	100 ul
H_2O	Up to 10ml	Up to 50 ml

6. 0.1M Tris + 0.4M NaCl Buffer #6, pH 9.0 (For DNA and Standards and Hoescht Dye):

Tris	290.4 mg	1.21 g
NaCl	561.6 mg	2.34 g
H_2O	Up to 12 ml	Up to 50 ml

Tubes:
Prepare two 1.5ml tubes for each sample homogenate (one for this protocol and one for protein determination) and two 1.5ml tubes for each sample for supernatant and pellet aliquots. **Total: 4 tubes per sample**. Plus, prepare one tube per DNA standard concentration, one for DNA working solution, one for dye dilution and Buffer #2 Master Mix.

Procedure for preparing samples:

1. Take about 50 ug of each sample tissue and homogenize in 1/10 parts of Tris-EDTA Homogenizing Buffer #1. Add 250ul homogenate to a sample tube. Save extra homogenate for Bradford protein determination.

2. Heat Di water to 65^{o}C for later use.

3. Add 250 ul of Master Mix of 10mM Tris-EDTA-NaOH Buffer #2 to each tube. Make Master Mix of the three solutions in #2 immediately before use.

Reagent stocks	1X	8X	10X	12X	Final Conc.
Tris-EDTA 17/17 mM stock	150ul	1200ul	1500ul	1800ul	10 mM
NaOH 0.2 M stock	50ul	400ul	500ul	600ul	40 mM
SDS 10% stock	50ul	400ul	500ul	600ul	2%
Total	250ul	2000ul	2500ul	3000ul	

4. Incubate for 1 minute. Add 125 ul of 0.2 M KCl #3 to reaction mixture and incubate at 60^{o}C for 10 minutes.

5. Precipitate DNA associated with proteins by cooling the mixture at -20^{o}C for 20 minutes, followed by centrifuging at 6000 g for 15 minutes at 4^{o}C.

6. Pipette 250ml of supernatant into new labeled tubes. Discard the rest of the supernatant.

7. Dissolve the pellet in 1ml hot Di H_2O (65^{o}C), mix thoroughly and take an aliquot of dissolved pellet (250 ul) into a new labeled tube.

8. Mix each aliquot (250 ul) of supernatant or pellet solution with 750 ul of 0.2M Tris + 0.8M NaCl + 8 mM sodium cholate #4 (pH 9). Add 200ul to each well. Half will be blanks and half will have dye. Four wells are needed for each supernatant and four for each pellet sample (with duplicates) – 8 per tissue sample. See worksheet for example plate configuration.

Make DNA Standards:

1. Make DNA working solution for calibration curve:
   DNA Stock - Commercial salmon sperm DNA (1mg) diluted in 1ml of 10mM Tris + 1mM EDTA #5.
   Working stock - 100 ul of stock solution (100 ug DNA) to 900 ul of 10 mM Tris + 1 mM EDTA Buffer #5.

2. Dilute standards with 0.1M Tris + 0.4M NaCl Buffer #6.

Standards:

DNA level in sample, ng/ml	DNA working stock solution, ul	Tris-NaCl Buffer #6, ul	Standard volume, ul In well
0.0	0	600	200
2.5	15	585	200
5	30	570	200
10	60	540	200
15	90	510	200
20	120	480	200
25	150	450	200
50	300	300	200

Load plate with Standards and Samples:

1. Measure the level of protein-free DNA in the supernatant and the DNA in pellet solution using Hoechst dye in the presence of 0.1 M Tris, 0.4 M NaCl, and 4 mM sodium cholate (pH 9) to reduce the possible traces of SDS in the supernatant (Bester et al. 1994). Each sample has four wells – blank supernatant, supernatant, blank pellet and pellet, plus duplicates if desired.

2. Prepare plate for RFU determination**:** 200 ul in each well, plus dye if added.

	DNA Standard	Unknown Supernatant Blank	Unknown Supernatant	Unknown Pellet Blank	Unknown Pellet Solution
Amount in well (ul)	200	200	200	200	200
Hoescht dye (diluted) (ul)	2	None	2	None	2

3. Add 2 ul diluted **Bisbenzimide (Hoechst Dye 33258)**. Stock – 1 mg in 1ml of K-phosphate Buffer (as received). Immediately before use, make dye dilution. Makes enough for 50 wells.
   0.1M Tris and 0.4M NaCl Buffer #6 90 ul
   Hoescht Dye Stock 10 ul

4. The content is allowed to react in darkness for 15 minutes.

5. Determine the amount of DNA in each fraction fluorometrically using microplate reader or spectrophotometer set at an excitation wavelength of 350/360 nm and an emission wavelength 450/465 mm and a gain of 63.

6. Determine the percentage of protein-free DNA in supernatant by dividing the RFU (reflective fluorescence unit) in the supernatant by the total of the RFU in the pellet plus supernatant and multiplying by 100.

$$\frac{RFU_S}{RFU_P + RFU_S} \times 100 = \text{\% protein-free DNA}$$

7. Determine protein concentration with Bradford method to determine amount of DNA damage per unit of protein.

Terms:

Tris	Tris(hydroxymethyl)aminomethane
EDTA	Ethylenediaminetetraacetic acid
NaOH	Sodium hydroxide
SDS	Sodium dodecyl sulfate, sodium lauryl sulfate
KCl	Potassium chloride
NaCl	Sodium chloride
RFU	Reflective fluorescence units
FW	Formula weight
Nm	Nanometers
Di	Deionized

APPENDIX A.4

Carbonyl Groups (aldehydes and ketones) in Oxidized Proteins

Modified after Levine (Levine et al. 2000)

This version of the technique is for very small samples or for mitochondria. For mitochondria, start the procedure at step 7 after mitochondria are isolated.

Chemicals:

For Homogenization:

Homogenization buffer, adjust to pH 7.4:

50mM HEPES	0.3g/25ml
125mM KCl	0.238g/25ml

Add to buffer immediately before using:

PMSF (Protease inhibitor)	87ul/25ml buffer
EDTA 0.5M (Chelation agent)	0.0102ul/25ml buffer
$MgSO_4$ 0.6Mm	0.00365g/25ml buffer

2M HCl (165ml HCl cc filled up to 1000ml)

10 mM 2,4 Dinitrophenylhydrazine (DNP) in 2M HCl (0.099g/50ml) MW 198.1

100% Trichloroacetic Acid (TCA) (w/v) (10g in 10ml H_20)(in +4^{o}C Frig)

6M Guanidine HCl in 20mM KH_2PO_4; pH 2.5 adjusted with TCA, molecular weight: 95.5, 286.5g/500ml

20mM KH_2PO_4, molecular weight 136.09, 1.36g/500ml, 2.04g/750ml

Ethanol:Ethyl acetate (EtOH:EtAc) (50:50)

Streptomycin sulfate 10% stock solution in KH_2PO_4:

10% Streptomycin sulfate, powdered (in -20^{o}C freezer) (100mg/10ml KH_2PO_4)

Homogenize tissue:

1. Keep tissue frozen in liquid nitrogen until weighed.
2. Take about 0.100 - 0.050g frozen tissue, add to homogenizer tube.
3. Add 10x Prepared Homogenized Buffer (w/PMSF, EDTA, Mg) (0.0500g – 500ml buffer).
4. Homogenize, transfer to labeled tube. Keep tissue sample on ice.
5. Centrifuge at maximum speed for 15min. at +4^{o}C.
6. Transfer supernatant to labeled tubes.

For mitochondria, start here, for homogenate, continue:

7. Incubate with Streptomycin Sulfate (1%) in sample for 15 min. room temperature (10ul 10% stock/100ul sample).
8. Spin 6000g 10 min. at +4^{o}C.
9. Pipette super-aliquot into 2 tubes – 50ul (replicate) and 50ul (blank).
10. Add 175ul 10mM DNP (replicate) or 175ul 2M HCL (blank) to 50ul sample.
11. Vortex for one minute at room temperature every 15 min. 4 times.
12. Add 25ul 100% TCA.
13. Spin at 11000g for 3 minutes.
14. Wash pellets at least 3-4 times with 125ul EtOH:EtAc until supernatant is no longer yellow. Pellet will be solid but light and may come loose.
15. Air dry pellets completely in tubes under hood.

16. Add 125ul Guanidine HCL, vortex and sonicate about 10 sec.
17. Keep overnight at +4^{o}C.
18. Next day: spin 5 min. at 11000g at room temperature.
19. Prepare plate sheet. There is not enough sample to make duplicates, only replicate and blank!
20. Load samples 100ul/well into 96 well slide. GUANIDINE BUBBLES! Load slowly and carefully; bubbles are next to impossible to remove. Run Spectrophotometry at 360 nm wavelength.
21. Store plate at -20^{o}C to determine protein concentration later.

Calculations:

$$\text{Nmol CO/mg proteins} = \frac{\text{Abs} * \text{Vol (Guanidine in ml)} * 10^{9}}{\varepsilon * 1000 * \text{proteins (mg/ml)}}$$

$$(\varepsilon = 22{,}000\ cm^{-1} * M^{-1})$$

Terms:

Abs	absorbance
Vol	volume
HEPES	4-(2-hydroxyethyl)-1-piperazineethanesulfonic acid buffer
KCl	potassium chloride
PMSF	phenylmethylsulfonyl fluoride – protease inhibitor
EDTA	ethylenediaminetetraacetic acid
$MgSO_4$	magnesium sulfate
HCl	hydrogen chloride (hydrochloric acid)
DNP	2,4 Dinitrophenylhydrazine - chelator
TCA	Trichloroacetic Acid buffer
KH_2PO_4	potassium dihydrogen phosphate
EtOH:EtAc	Ethanol:Ethyl Acetate

APPENDIX A.5

ELISA protocols for HNE Determination

List of materials

a. NUNC Maxisorp plates 300 ul
b. Phoenix research low retention tubes and tips (10 ul and 300 ul)

List of reagents

a. Fisher scientific 10x PBS, diluted to 1x

PBS Buffer if made from scratch:

PBS (1X)	1 liter
NaCl	8g
KCl	0.2g
Na_2HPO_4(HNa_2O_4P)	1.44g
KH_2PO_4	0.24g

b. Homogenization Buffer:

PBS 1X	50 ml
Aprotinin, 10mg/ml	25 ul (or use 2X PMSF)
PMSF, 20mM	100ul

c. Stock and Reduced BSA. Make fresh each time.

Sigma BSA, essentially gamma-globulin free

Stock 1 - 500mg BSA + 50 ml 1X PBS → BSA 10 mg/ml

Stock 2 - Dilute stock 1 1000X in 1X PBS: 10ul in 10ml PBS → 10ug/ml reduced BSA

d. PBS-Tween solution: 1X PBS with 0.05% of tween-20 (0.5ml/1000ml PBS)
e. Blocking solution: 3 ml BSA Stock 1 (10mg/ml) + 27ml 1X PBS for ELISA step 4 → BSA (1mg/ml)
f. Stop solution is 2M sulfuric acid (be careful!)
g. Carbonate - bicarbonate buffer 1M, pH 9.5

Anhydrous sodium carbonate (Na_2CO_3)	-	31 g
Sodium bicarbonate ($NaHCO_3$)	-	13.78 g
Sodium azide	-	0.2 g

Dissolve in 1000 ml distilled water after adjusting the pH to 9.5

c. Thermo ULRTA-TMB ELISA substrate

Standards (Use low retention tubes and tips)

HNE standard: prepare 10ug/ml of HNE-BSA by diluting the 1mg/ml HNE-BSA stock in 1X PBS:
5ul HNE/496ul 1X PBS (tubes prepared with 5ul)

Serial dilution of HNE-BSA standards:

	HNE-BSA (ug/ml)	10ug/ml HNE-BSA	1X PBS
1.	10	500ul	0 ul
2.	5	250ul of #1	250 ul
3.	2.5	250ul of #2	250 ul
4.	1.25	250ul of #3	250 ul
5.	0.625	250ul of #4	250 ul
6.	0.313	250ul of #5	250 ul
7.	0.156	250ul of #6	250 ul
8.	0.0	0	250 ul

Sample preparation

1. Prepare homogenization buffer.
   In 50 ml of buffer – PBS 1x 50 ml, aprotinin 10 mg/ml 25 ul, PMSF 20 mM 100 ul. Cool down to 4^{o}C. Homogenization must be done on ice.
2. Cut approximately 100 mg of tissue and homogenize it in 1/10 ice-cold using tight glass homogenizer at 500 RPM. Alternatively, samples can be frozen in liquid nitrogen and processed later. Store frozen samples at -80^{o}C.
3. Centrifuge extracts at 15000 for 10 minutes.
4. Transfer supernatant to new tubes.
5. Determine protein concentration using Bradford assay. Usually this lies in the range from 1 to 2.5 mg of protein per 1ml.
6. Aliquot and store at -80^{o}C

General protocol of indirect ELISA

1. Coat the plate using diluted antigen in the concentration no more than 10 ug per ml.
   Determine the protein concentration of samples first. Use that number to put 10 ug of protein to each well. Make standards. Add 100 ul of diluted sample or standard in each well in duplicates or triplicates.
2. Wrap plate with film or put in plastic zip bag. Allow to stand overnight at 4^{o}C.
3. Wash each well 2 times with 300 ul of 1X PBS.
4. Add 300 ul of 1 mg/ml reduced BSA in 1X PBS (blocking solution).
5. Incubate on orbital shaker for 2h at 37^{o}C.
6. Wash 5 times with PBS-Tween (PBS with 0.05% of Tween-20).
7. Add 100 ul of primary antibody diluted in blocking solution in desired concentration (usually from 1:1000 to 1:10000) to each well (for HNE 1:4 000). Make 16ml: HNE – 4ul/16ml.
8. Incubate at room temperature for 1 hour on orbital shaker.
9. Repeat step 6.
10. Add 100 ul of diluted in blocking solution secondary antibody, (anti-rabbit conjugated with HRP horseradish peroxides) in desired concentration (1:16 000).
11. Incubate at room temperature for 1 hour on orbital shaker.
12. Repeat step 6.
13. Add ELISA substrate 100 ul in each well. Wait for color to develop, then stop reaction.
14. Stop reaction with 100 ul stop solution – 2M H_2SO_4.
15. Read the plate using microplate reader 450 nm.

Terms:

1	ELISA	Enzyme-linked immunoassay	7	Na_2CO_3	Sodium carbonate
2	PBS	Phosphate-buffered saline	8	$NaHCO_3$	Sodium bicarbonate
3	NaCl	Sodium chloride – table salt	9	HNE	4-hydroxynonenal
4	KCl	Potassium chloride	10	HRP	Horse radish peroxidase
5	KH_2PO_4	Potassium dihydrogen phosphate	11	Nm	Nanometers
6	BSA	Bovine Serum Albumin	12	H_2SO_4	Sulfuric acid
13	Na_2HPO_4 or (HNa_2O_4P)	Disodium phosphate			

APPENDIX A.6

Protein Extraction and Determination by Bradford Dye
(Bradford 1976)

Make Protein Extraction Buffer, if necessary:

For 500ml:

100 mM Tris	6.059g
100 mM NaCl	2.922g
0.5% deoxycholate	2.5g

Add 400ml DI water, then add:

1 mM EDTA	0.186g (1 ml of 0.5M stock solution)
1 mM EGTA	0.1902g (1 ml of 0.5M stock solution)
1% Triton-X	5 ml
10% Glycerol	50 ml
0.1% SDS	0.5g (add last, suds)

Stir; adjust to 7.4 pH with NaOH or HCL.

Adjust volume to 500 ml.

Immediately before assay, add a protease inhibitor to buffer:

PMSF	40ul/10ml PE Buffer (ice cold) (10 samples)

Bradford Protein Stain (Dilute Stock Bradford 1 part to 4 parts water [30ml:120ml])

Homogenize frozen tissue: (If using mitochondria samples, see modifications below.)

1. Add PMSF (40ul/10ml Buffer) to buffer.
2. Measure frozen tissue – try to select size up to 100 mg for small homogenizer.
3. Add buffer: 100mg:1000ul (1:10 weight: volume ratio) to homogenizer and homogenize IN ICE until liquefied. Keep tissue and buffer cold!
4. Transfer to labeled tube.
5. Sonicate 3 times for 10 sec. each. Keep samples on ice between sonications.
6. Centrifuge on 10,000g for 10 min. at 4^{o}C.
7. Transfer supernatant to a newly labeled tube. Keep on ice for the further measurement or at
   -80°C for storage. Homogenate usually requires at least a 10/1 dilution with water for the Bradford assay. Use 10ul in each well.

Make BSA Standard:

1. Make 10mg/ml (100mg/10ml) with DI water.
2. Dilute to 1mg/ml with DI water (or buffer* of sample). (DO NOT SHAKE)
   *Use water when using Protein Isolation Buffer because the SDS interferes with copper. When using Tris or any other buffer without SDS, use the buffer for dilution.
3. Make series of concentrations of sample with DI water* (or buffer*) (example: 70%, etc.)
4. Load a 96 well plate with 10 ul of sample/or standard per well.
5. Add 200 ul of Bradford reagent to each well. Incubate minimum 5 min, but no longer then 1h.
6. Measure absorbance at 595nm on plate reader.

If reusing a Carbonyl plate:

Use same sample wells.

Make new standard series (BSA) with guanidine instead of water and use the same protocol.

For Mitochondria samples: (do not vortex Triton – bubbles)

1. Digest mitochondria by adding 1ul 1% Triton to 9ul mitochondria (to make 0.1% Triton in solution).
2. Sonicate for 10 seconds, three times.
3. Use mitochondrial assay medium (Mito AM) to dilute mitochondria 50/1 (2ul mt/ 98ul Mito AM).
4. Make BSA standards as above using Mito AM as dilution medium.
5. Load plate and Bradford dye as above.

Terms:

Tris	Tris(hydroxymethyl)aminomethane
NaCl	Sodium chloride
DI	Deionized
EDTA	Ethylenediaminetetraacetic acid
EGTA	Egtazic acid, an aminopolycarboxylic acid
SDS	Sodium dodecyl sulfate, sodium lauryl sulfate
PMSF	Phenylmethylsulfonyl fluoride – protease inhibitor

APPENDIX A.7

Perchloric Acid Extracts of Tissues for Carbohydrates

Based on Sokolova (Sokolova et al. 2000)

1. For extraction, use 0.6 M of ice-cold perchloric acid (Souza-Shibatta et al.) + 15 mM ethylenediaminetetraacetic acid (EDTA). Add EDTA to PCA immediately prior to the extractions; otherwise, it will precipitate. Add 30ml of 1M PCA, 1.5ml 0.5M EDTA, and dilute with DI water to make 50ml PCA/EDTA, later called PCA in the protocol. Keep on ice. (No protease inhibitor needed because proteins precipitate out.) PCA precipitates proteins; EDTA chelates calcium and magnesium ions. Use PCA worksheet to record weights.

2. Prepare 2 – 2ml tubes and 4 – 0.65ml tubes per sample. WEIGH THE 2ML TUBES AND RECORD THE WEIGHT. Take a 2 ml tube and add 500 µl of 0.6 M of ice-cold PCA + 15 mM EDTA (Souza-Shibatta et al.).

3. Weigh the tube with PCA on the analytical balances, RECORD THE WEIGHT.

4. Freeze the microcentrifuge tube with PCA in liquid nitrogen and place the tube on ice.

5. Pour some liquid nitrogen (carefully and using a ladle) into a clean mortar with pestle. Let the mortar and pestle cool, add liquid nitrogen as needed. DO NOT ALLOW THE NITROGEN TO COMPLETELY EVAPORATE, it will lead to water condensation in the mortar.

6. Place a piece of tissue under the liquid nitrogen and grind it with a pestle under the liquid nitrogen. Add more nitrogen as needed.

7. Take ca. 50 - 100 mg of tissue powder with a small steel spoon pre-cooled in liquid nitrogen and place in the tube with frozen PCA. WEIGH AND RECORD THE WEIGHT.

8. Add 250ul of ice-cold PCA. WEIGH AND RECORD THE WEIGHT.

9. Homogenize on ice using a sonicator set at 10 for 3 times, 10 sec each, with 20 sec intervals between sonications. Incubate 5 min on ice.

10. For future glycogen assay, save 50ul in a separate 0.65ml tube at this stage. RECORD NEW WEIGHT.

11. Centrifuge the sample for 2 min at maximum speed and 4°C. Collect supernatant (=liquid) into a new clean 2 ml tube, tared on the scale. Do not disturb the pellet. WEIGH AND RECORD THE WEIGHT.

12. Check pH with an indicator strip. Take a drop of the liquid with a plastic stick and touch the indicator paper. If pH is between 7 and 7.5, no further addition of potassium hydroxide (Criscione and Kohler) is needed – proceed to step 16. If pH is below 7, proceed to step 14. If pH is above 7.5, proceed to step 15.

13. Add small volumes of 1 M KOH (10 µl at a time), mix and check pH after each addition until you get pH of 7-7.5. RECORD VOLUME OF KOH ADDED!

14. Add small volumes of 1 M hydrochloric acid (HCl) (5 µl at a time), mix and check pH after each addition until you get pH of 7-7.5. RECORD VOLUME OF HCl ADDED!

15. Place on ice and incubate for 10 min.

16. Centrifuge for 10 min at maximum speed and 4°C.

17. Collect supernatant (=liquid) without disturbing the pellet, split into 5 roughly equal volumes (ca. 250-300 µl) into 3 clean 0.65ml tubes. WRITE NUMBER OF THE SAMPLE ON EACH TUBE.

18. Place tubes in a box and store in a freezer at -80°C.

APPENDIX A.8

DNA Extraction Method with SDS for Museum Specimens in Alcohol

Modified from Sokolov (Sokolov 2000)

Collection of tissue:

1. Mince 25 - 50mg of tissue from alcohol preserved specimens on clean surface with sterile tools.
2. Weigh in 1½ ml tube. Wash tissue in DI water before using lysis buffer if specimens are in alcohol.
3. Add 500ul SDS Lysis buffer.

SDS Lysis Buffer, make 50 ml and store in refrigerator, warm to dissolve before use:			
	Concentration	Stock	Amount in 50ml
Tris-HCl pH 8.0	50 mM	1M	2.5ml
NaCl	100mM	1M	5ml
EDTA	10mM	1M	500ul
SDS	1% w/v	----	0.5g
Add Molecular Grade Water to 50ml			

4. Add 30ul of 20mg/ml Proteinase K (20mg/ml) immediately before use.
5. Incubate at 60^{o}C for at least 2 hours in shaking incubator, or overnight at 40^{o}C, inverting occasionally for first hour.
6. Remove from heat and add salt – 50ul of saturated KCl.
7. Chill on ice for 15 minutes.
8. Centrifuge at 10,000g for 15 minutes.
9. Transfer supernatant to a clean tube. Repeat step 8 in clean tube if supernatant is not clean or is hard to remove.

DNA Purification:

1. Add equal volume (500ul) of chloroform:isoamyl alcohol (24:1). Invert tube for 15 seconds to mix.
2. Incubate for 10-15 minutes at room temperature.
3. Centrifuge at 10,000g for 15 minutes.
4. Remove aqueous layer (top) into clean tubes, avoiding the interface. 400 ul is enough.
5. Repeat this section at least once more, maybe twice, until aqueous layer is transparent (may still be yellowish).

DNA Precipitation:

1. Precipitate nucleic acids by adding 0.7-0.8 volumes (about 300ul) of room temperature anhydrous isopropanol. Mix by inversion.
2. Incubate for 15 minutes at room temperature.
3. Centrifuge 15 minutes at 10,000g.

4. Decant supernatant carefully. The pellet may not be visible and is easily dislodged.
5. Wash pellet with 500ul of ice cold 80% ethanol, diluted with Molecular Grade Water. Centrifuge again to reset pellet. Decant and discard supernatant.
6. Repeat the wash with ethanol. No need to centrifuge again. Decant and discard alcohol.
7. Allow pellet to air dry. Air flow in a hood or with a fan helps it dry within 30 minutes.
8. Resuspend DNA in 50 or 100ul Molecular Grade Water.
9. Incubate at 37^{o}C for 30-60 minutes to dissolve pellet.
10. Store at -20^{o}C.

Terms:

Tris	Tris(hydroxymethyl)aminomethane
NaCl	Sodium chloride
EDTA	Ethylenediaminetetraacetic acid
SDS	Sodium dodecyl sulfate, sodium lauryl sulfate
DNA	Deoxyribonucleic Acid

SUPPLEMENTAL 5.1

Chapter 5 Primer sequences for target genes in *Crassostrea virginica*

Target	Accession number	Primer sequence	Tm, (°C)	Efficiency
TLR2	JH819194.1	Fw 5′-GCGCTTTATTGACGTTAGAC-3′	58	1.91
		Rev 5′-CGTAAACACATGAAACTGGT-3′		
TLR3	MGID92145	Fw 5′-TTTGGTTCAAGAACTGGGTT-3′	58	1.77
		Rev 5′-GATTAAGGCTCAACAATGGC-3′		
TLR4	MGID89881	Fw 5′-GCCTCCGACTGATTGATTTA-3′	58	1.78
		Rev 5′-ATACCTCTGAGGATAGGACG-3′		
Mannose Rec2	XM_011414451.2	Fw GTTCACTTTTACGTTCACCC-3′	58	1.76
		Rev 5′-TTTGTTGACATTTTGACGCA-3′		
SRCR	BG624783.1	Fw 5′-CACATGCGGCTTCTGTCTAA-3′	62	2.19
		Rev 5′-CGGTGATCGTGCTGGTATATG-3′		
TNF	MGID91531	Fw 5′-GCTTTGTAGGGTGTGATTTG-3′	58	1.94
		Rev 5′-GTTGTACTTGCCGATGACTT-3′		
Big defensin	CV133156	Fw 5′-TGGCAGCTGCTTACGGTATC-3′	60	1.78
		Rev 5′-CCCTGTTGTTGGCACAGCTA-3′		
C type lectin	CV088804.1	Fw 5′-ATTTGCTCAGCCTTGAATGG-3′	55	1.98
		Rev 5′-GTCCCTCCCACCCAGTAGTT-3′		
β-actin	X75894	Fw 5′-ACAGCCGCTTCCTCATCCTCC-3′	55	1.94
		Rev 5′-CGGCGGATTCCATACCAAGG-3′		

Supplemental 5.1. Abbreviations: TLR-toll like receptor; Mannose Rec2-Mannose receptor 2; SRCR-Scavenger Receptor Cysteine Rich; TNF-tumor necrosis factor.

SUPPLEMENTAL 5.2

Population pairwise F-Statistics by Haplotype and Distance

Supplemental 5.2a. Population pairwise F-statistics calculated by haplotype frequencies. Asterisks denote significant F_{ST} values ($p < 0.05$).

	E9	**C3**	**VA**	**D2**
E9	0	-	-	-
C3	0.31450*	0	-	-
VA	0.21141*	0.29730*	0	-
D2	0.35708*	-0.00859	0.34895*	0

Supplemental 5.2b. Population pairwise F-statistics calculated by the distance method, pairwise difference. Asterisks denote significant F_{ST} values ($p < 0.05$).

	E9	**C3**	**VA**	**D2**
E9	0	-	-	-
C3	0.26585*	0	-	-
VA	0.05132	0.31369*	0	-
D2	0.43045*	-0.02534	0.48134*	0

SUPPLEMENTAL 5.3

Haplotype distribution from Four Locations of Oysters

Haplotype	Total number of individuals within haplotype	Location Composition
1	1	C3
2	1	D2
3	29	9 VA, 3 C3, 6 D2, 11 E9
4	1	C3
5	1	C3
6	24	11 C3, 13 D2
7	1	C3
8	9	9 VA
9	3	1 E9, 2 VA
10	1	C3
11	1	C3
12	8	8 E9

Supplemental 5.3. Haplotype distribution from the four locations of oysters. The total number of individual oysters and the locations where each haplotype was sourced are shown for the 12 recovered haplotypes.

SUPPLEMENTAL 5.4

Effect of Acclimation Husbandry Conditions on Mitochondrial Respirations

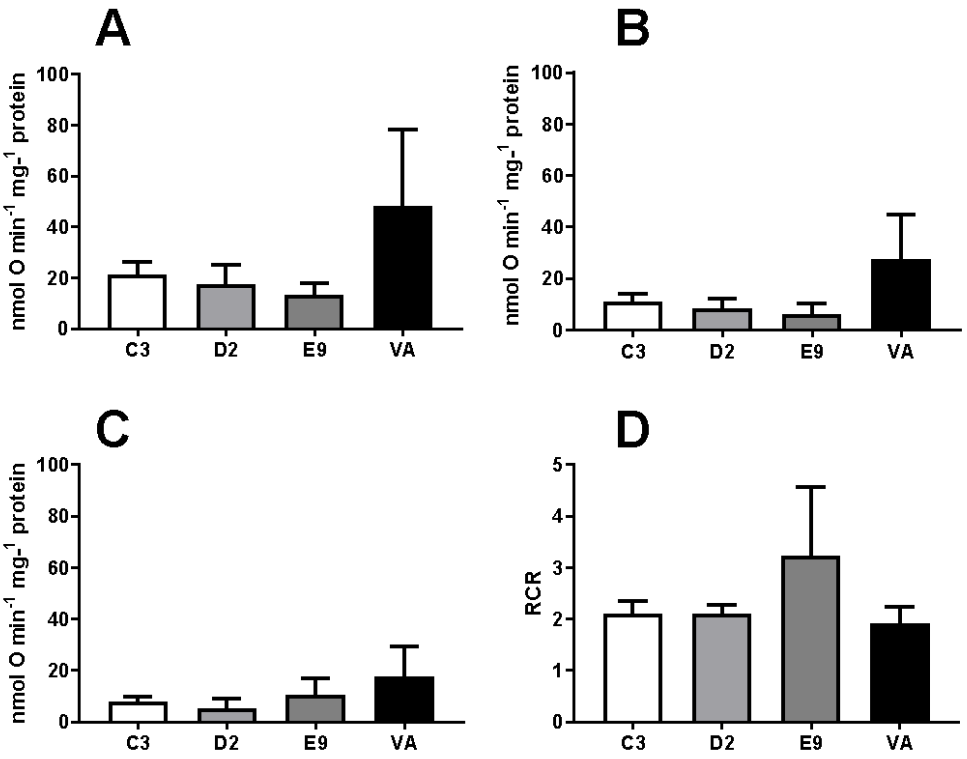

Supplemental 5.4. Effect of acclimation husbandry conditions on mitochondrial respirations of oysters from different locations. (A) State 3 of mitochondrial respiration, (B) State 4 of mitochondrial respiration, (C) State 4ol of mitochondrial respiration. (D) RCR (respiratory control ratio) of mitochondria. Vertical bars represent the standard error of means. No significant differences were observed for any comparison of locations.

SUPPLEMENTAL 5.5

Effect of Hypoxia Conditions on Mitochondrial Respirations

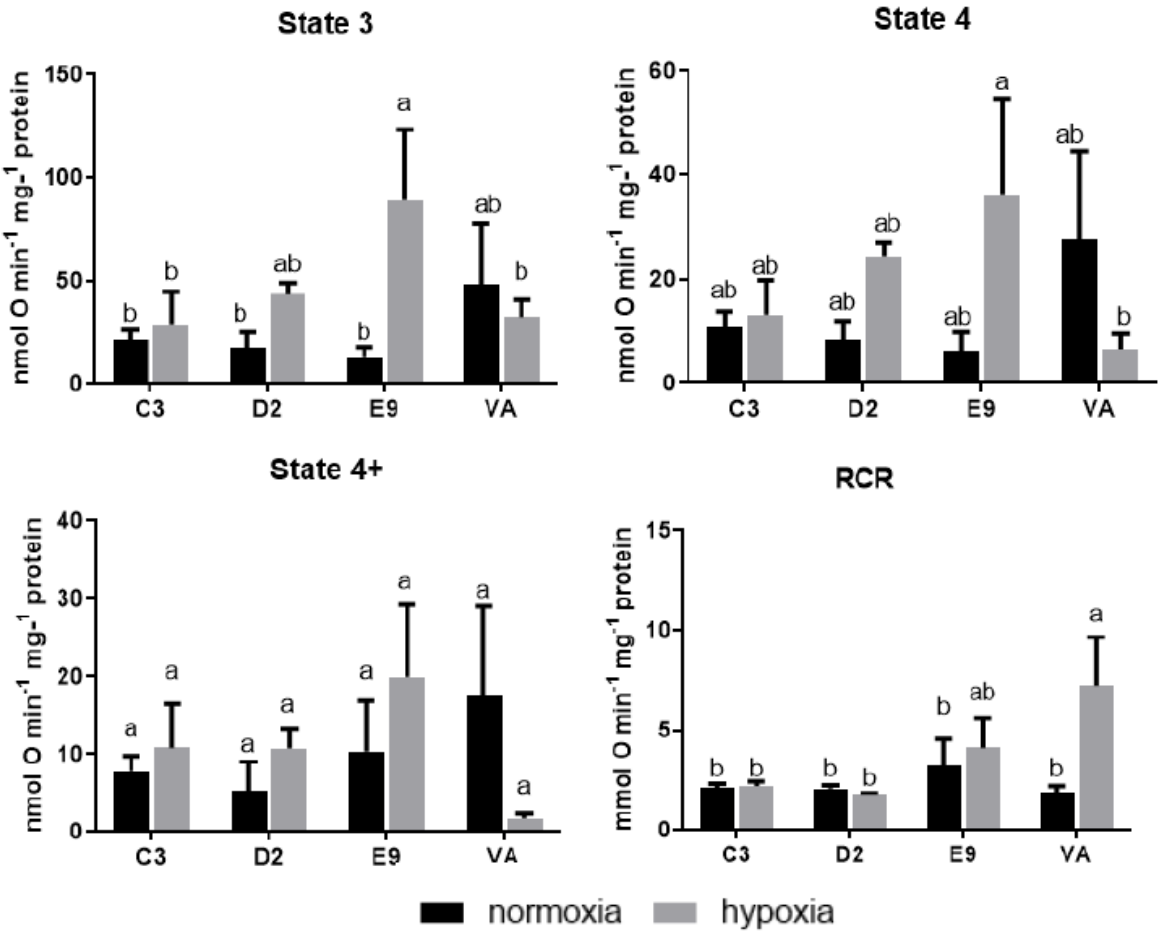

Supplemental 5.5**.** Effect of hypoxia conditions on mitochondrial respirations of oysters from different locations. Different letters indicate the values that are significantly different among *C. virginica* from different locations ($P<0.05$). Vertical bars represent the standard error of means.

SUPPLEMENTAL 5.6

Basal Expression of Stress-sensing and Stress-response Molecules

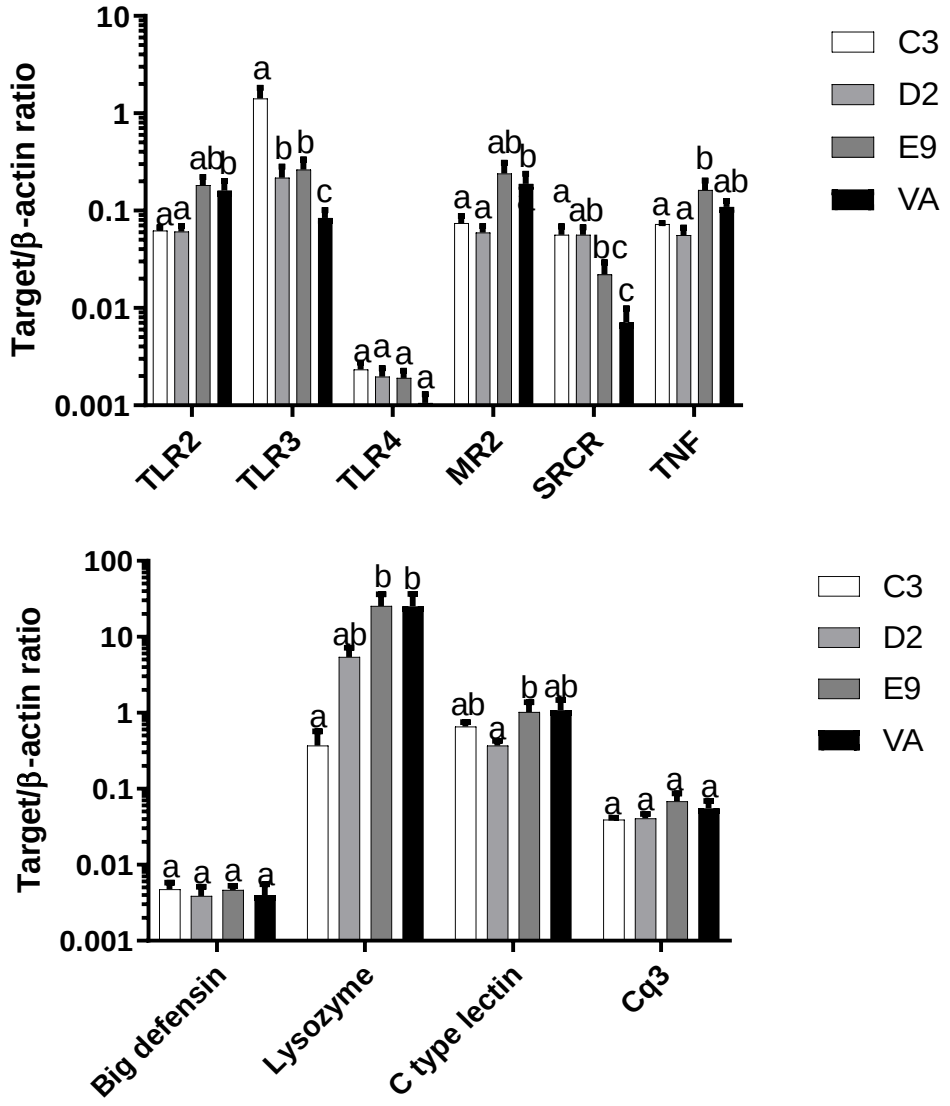

Supplemental 5.6. Basal expression of stress-sensing and stress-response molecules in HCs of *C. virginica* from four different locations. (A) mRNA expression of stress-sensing receptors, relative to β-actin. (B) mRNA expression of humoral stress-response molecules, relative to β-actin. Different letters indicate the values that are significantly different among *C. virginica* from different zones ($P<0.05$); if columns share a letter, the respective values are not significantly different ($P>0.05$). Vertical bars represent the standard error of means, N=5.

SUPPLEMENTAL 6.1

Specimens Sequenced in Chapter 6

Clade	Accession #	Col. Location	Col. Date	16S	H3	ITS-2
1	ASV20209111	Carter Co., TN	Sep-20	X		
1	CU30011	Blount Co., TN	Jul-21	X		X
1	CU30021	Baker Co., GA	Nov-21	X		X
1	NCSM1004701	New Hanover Co., NC	Aug-14	X		
1	NCSM114017	Tyrell Co., NC	Apr-16	X		
1	NCSM41887	Angelina Co, TX	Aug-05	X		
1	NCSM43839	Jefferson Co, AL	Apr-09	X		
1	NCSM64315	San Jacinto Co, TX	Mar-07	X		
1	NCSM64463	Halifax Co., NC	Jul-09	X		
1	SMNC295031	Stanly Co., NC	May-11		X	
1	SMNC295061	Stanly Co., NC	Apr-11		X	
1	SMNC589061	Rutherford Co., NC	Apr-14	X	X	
1	SMNC589131	Mecklenburg Co., NC	Sep-15	X	X	
1	SMNC589151	Cleveland Co., NC	Apr-16	X	X	
1	SMNC632101	Gaston Co., NC	Mar-09		X	
1	SMNC632171	Orange Co., NC	May-13		X	
1	SMNC632231	Rutherford Co., NC	Sep-14		X	
1	SMNC632261	Lexington Co., SC	Apr-15	X		
1	SMNC632281	Mecklenburg Co., NC	Oct-15		X	
1	SMNC632291	Stanly Co., NC	Mar-16	X	X	
1	SMNC9861	Bladen Co., NC	Oct-16		X	
1	SMNC10051	Cleveland Co., NC	Sep-16		X	
1	SMNC10621	Bladen Co., NC	Oct-16	X		
1	SMNC11501	Spartanburg Co., SC	Feb-17		X	
1	SMNC14561	Lincoln Co., NC	Nov-17	X	X	X
1	SMNC17631	Orange Co., NC	Jul-21	X	X	
1	SMNC19261	Cleveland Co, NC	Jul-21		X	
1	SMNC19262	Cleveland Co, NC	Jul-21		X	

1	SMNC19981	Cleveland Co, NC	Aug-21		X	
1	SMNC20421	Gaston Co., NC	Sep-21		X	
1	SMNC20441	Gaston Co., NC	Sep-21		X	X
1	SMNC20481	Gaston Co., NC	Jun-09	X		
1	SMNC20501	Spartanburg Co., SC	Aug-21	X	X	
1	SMNC20521	Henderson Co., NC	Jun-13	X	X	
1	SMNC2076	Cape May Co., NJ	Nov-21	X		
1	SMNC2082	Pickens Co., SC	Oct-21	X		
1	SMNC20931	Cherokee Co., GA	Apr-22	X		
1	UF449229	Clarke Co., AL	Jan-12	X		
1	UF504440	Washington Co., FL	Mar-16	X		
1	UT1094	Little River, Nash, NC	Jul-15	X		
1	SMNC20491	Spartanburg Co., SC	Aug-21		X	X
2	NCSM42075	Greenville Co., SC	Sep-06	X		
2	NCSM64303	Gaston Co., NC	Apr-07	X		
2	NCSM644672	Harnett Co., NC	Jul-09	X		
2	NCSM64950	Wake Co., NC	Dec-14	X		
2	SMNC588341	Stanly Co., NC	May-11		X	
2	SMNC588371	York Co., SC	Oct-14	X		
2	SMNC632141	Gaston Co., NC	May-10			X
2	SMNC632191	Gaston Co., NC	Apr-14	X	X	
2	SMNC632241	Cleveland Co., NC	Sep-14	X	X	
2	SMNC19611	Spartanburg Co., SC	Oct-16	X		
2	SMNC19631	Lexington Co., SC	Feb-17	X		
2	SMNC20491	Spartanburg Co., SC	Aug-21	X		X
2	SMNC20781	Cumberland Co., NJ	Nov-21	X		
2	UF448919	Prince George's Co., MD	Oct-11	X		
2	UF450283	Wake Co., NC	Feb-03	X		
2	UF504549	Stanly Co., NC	Apr-16	X		
2	UT1093	Richmond Co., NC	Jul-15			X
2	UT2731	Montgomery Co., NC	Jul-15	X		

2	UT2733	Richmond Co., NC	Jul-15	X		
2	NCSM114004	Charleston Co., SC	Sep-11	X		
3	ASV2022422	Richland Co., SC	Aug-22	X		
3	SMNC588311	Gaston Co., NC	Apr-14		X	
3	SMNC588361	Gaston Co., NC	Jul-14	X	X	
3	SMNC589141	Stanly Co., NC	Mar-16	X	X	
3	SMNC632111	Gaston Co., NC	Mar-09		X	
3	SMNC632211	Gaston Co., NC	Jun-13		X	
3	SMNC13571	Lexington Co., SC	Feb-17		X	X
3	SMNC20901	Horry Co, SC	Apr-22	X		X
3	UF578837	Hampton Co., SC	Feb-22	X		X
4	NCSM113973	Washington Co., NC	Apr-16	X		
4	NCSM113975	Hyde Co., NC	Apr-16	X		
4	NCSM416233	Dare Co., NC	Nov-99	X		
6	NCSM64699	Berkeley Co., SC	Oct-12	X		
7	ASV2022421	Richland Co., SC	Aug-22	X		
7	CU3003	Anderson Co., SC	Apr-20	X		
7	CU3004	Abbeville Co., SC	Mar-22	X		X
7	NCSM64530	Butler Co., AL	Mar-16	X		X
7	SMNC2051	Spartanburg Co., SC	Aug-21	X		
7	SMNC20961	Cherokee Co., GA	Apr-22	X		X
10	NCSM201643	Watauga Co., NC	Mar-16	X		
10	SMNC19281	Avery Co., NC	Jun-21	X		
10	SMNC21321	Jefferson Co., TN	Jun-22	X		
10	SMNC21331	Jackson Co., AL	Aug-21	X		
11	NCSM2018291	Alleghany Co., VA	Apr-18	X		X
11	NCSM2018292	Alleghany Co., VA	Apr-18	X		
11	UF4470761	Madison Co., VA	May-11	X		
12	NCSM2018481	Iredell Co., NC	Sep-18	X		X
12	NCSM64985	Wilkes Co,, NC	Dec-08	X		X
12	SMNC589051	Iredell Co., NC	May-10		X	

12	SMNC589161	Allegheny Co., NC	May-15	X	X	X
12	SMNC16771	Stokes Co., NC	Jun-19	X	X	X
13	SMNC615011	Mecklenburg Co., NC	Feb-09		X	
13	SMNC615041	Orange Co., NC	May-09	X		
13	SMNC615042	Orange Co., NC	May-09		X	
13	SMNC615091	Mecklenburg Co., NC	Jun-14	X		
13	SMNC615101	Guilford Co. , NC	Sep-15	X	X	
13	SMNC615111	Guilford Co. , NC	Sep-15		X	
13	SMNC655061	Burke Co., NC	Apr-16	X		
13	UF464417	Mecklenburg Co., NC	Mar-13	X		
14	NCSM201427	Burke Co., NC	Jul-19	X		
14	NCSM642531	Burke Co., NC	Jun-08	X		X
14	SMNC655031	Catawba Co., NC	Apr-10		X	
14	SMNC655032	Catawba Co., NC	Apr-10		X	
14	SMNC655033	Catawba Co., NC	Apr-10			X
14	SMNC655041	Catawba Co., NC	May-10	X		
15	UF547091	Harlan Co., KY	Nov-19	X		
15	UF437736	Dickinson Co., VA	May-10	X		
15	UF447154	Dickinson Co., VA	May-11	X		
16	SMNC2153	Carter Co., TN	Jun-22	X		
16	SMNC2160	Carter Co., TN	Jun-22			X
17	NCSM421332	Avery Co., NC	Dec-06	X		
17	NCSM63969	Watauga Co., NC	Jul-08	X		
17	SMNC619161	Floyd Co., VA	Sep-15	X		
17	SMNC13871	Stanly Co., NC	Jun-16	X	X	X
17	SMNC13881	Rutherford Co., NC	Jul-17		X	
17	SMNC13891	Rutherford Co., NC	Apr-17	X	X	
17	SMNC13892	Rutherford Co., NC	Apr-17	X		X
17	SMNC14531	Ashe Co., NC	Aug-17	X	X	
17	SMNC19251	Carter Co., TN	Sep-20	X	X	X
17	SMNC20411	Rutherford Co., NC	Aug-21		X	

17	SMNC20951	Cherokee Co., GA	Apr-22	X		
17	SMNC20991	Oconee Co., SC	Apr-22	X		
17	UF344618	Bledsoe Co., TN	Jun-03	X		
17	UF4470762	Madison Co., VA	May-11	X		
17	UF477870	Greenbrier Co., WV	Jun-14	X		
17	UF479311	Preston Co., WV	Jun-14	X		
17	UF504824	Smythe Co., VA	Jun-16	X		
17	UF505776	Dekalb Co., GA	Oct-16	X		
17	UF505783	Bartow Co., GA	Oct-16	X		
17	UF520694	Sevier Co., TN	Aug-18	X		X
17	UF546814	Grundy Co., TN	Jul-19	X		
17	UF547134	Putnam Co., TN	Nov-19	X		
18	SMNC619211	Polk Co., NC	Jul-16	X		
18	SMNC13551	Polk Co., NC	Jul-16	X	X	X
19	NCSM64911	Northampton Co, NC	Dec-06	X		
19	NCSM64993	Nash Co., NC	Jan-17	X		
19	SMNC589111	Stanly Co., NC	Jun-14	X		
19	SMNC590091	Stanly Co., NC	Jun-14		X	
19	SMNC590101	Gaston Co., NC	Jul-14	X		X
19	SMNC590121	Guilford Co., NC	Sep-15	X		
19	SMNC590141	Stanly Co., NC	Apr-16	X	X	
19	SMNC619192	Stanly Co., NC	Apr-16	X		X
19	SMNC619201	Gaston Co., NC	May-16	X	X	
19	SMNC619202	Gaston Co., NC	May-16		X	
19	SMNC10611	Stanly Co., NC	Apr-16		X	
19	SMNC13511	Durham Co., NC	May-16	X		
19	SMNC17291	Gaston Co., NC	May-19	X	X	X
19	SMNC17641	Orange jCo., NC	Jul-21	X	X	
19	SMNC19271	Granville Co., NC	Jun-21	X	X	
19	UF511981	Marion Co., SC	Jul-18	X		
21	NCSM64895	Pulaski Co., KY	Mar-09	X		X

22	NCSM418592	Dekalb Co., AL	Dec-04	X		
22	SMNC21301	Jefferson Co., TN	Jun-22	X		X
22	SMNC21311	Knox Co., TN	Jun-22	X		X
22	SMNC2156	Greene Co., TN	Jul-22	X		
Meso	ASV202127	Avery Co., NC	Aug-21			X
Meso	CU3009	Sevier Co., TN	Jun-21			X
Meso	CU3010	Sevier Co., TN	Jun-21			X
Meso	CU3012	Carter Co., TN	Jun-22	X		X
Meso	SMNC51921	Gaston Co., NC	Jul-14			X
Meso	SMNC57303	Dade Co., GA	Aug-14			X
Meso	SMNC60002	Burke Co., NC	Oct-09	X	X	
Meso	SMNC655062	Burke Co., NC	Apr-16			X
Meso	SMNC65905	Gaston Co., NC	Jul-14			X
Meso	SMNC66402	Avery Co., NC	Jun-14			X
Meso	SMNC1680	Stokes Co., NC	Jun-19			X
Meso	SMNC2104	Pickens Co., SC	Apr-22	X		X
Meso	SMNC2155	Cherokee Co., GA	Apr-22			X
Meso	SMNC2222	Cherokee Co., GA	Apr-22			X
Trio	ASV201841	Harlan Co., KY	Aug-18	X		
Trio	ASV201843	Bell Co., KY	Aug-18			X
Trio	ASV201937	Harlan Co., KY	Aug-19			X
Trio	ASV2019391	Madison Co., AL	Mar-19			X
Trio	ASV201946	Garland Co., AR	Jul-19			X
Trio	ASV201978	Pushmataha Co, OK	Jul-19			X
Trio	ASV201986	Washington Co., AR	Jul-19			X
Trio	SMNC89402	Beaufort Co, NC	Sep-14			X
Trio	SMNC97502	Stanly Co., NC	Apr-16			X
Trio	SMNC1659	Hancock Co., TN	Jun-16			X
Trio	SMNC1805	New Hanover Co., NC	Sep-17			X
Trio	SMNC19351	Gaston Co., NC	May-19	X		

Supplemental 6.1. All specimens used were *Triodopsis* (with clade numbers) except those designated Meso (Mesodontini), Trio (Triodopsini other than *Triodopsis*). All were sequenced from tissue obtained from these sources: ASV – Amy Van Devender personal collection; NCSM – North Carolina State Museum; CU – Clemson University Mollusk Collection or Anthony Deczynski personal collection;; SMNC – Schiele Museum of Natural History; UF – University of Florida Museum; UT or UTRGV – University of Texas of the Rio Grande Valley.

SUPPLEMENTAL 6.2

GenBank Specimens used as Outgroups in Phylogeny Trees

	Accession number	Identification in Genbank	16S	H3
GenBank	DQ08596.1	Praticolella mexicana	X	
GenBank	DQ085999.1	Millerelix mooreana	X	
GenBank	KJ609125.1	Melampus olivaceus		X
GenBank	KX432016.1	Praticolella salina	X	
GenBank	KY092832.1	Lymnaea stagnalis		X
GenBank	KY512727.1	Vertigo antivertigo		X
GenBank	MF415320.1	Lissachatina fulica		X
GenBank	MK72877.1	Otala lactea		X
GenBank	MK883390.1	Cornu aspersum		X
GenBank	MN022765.1	Haplotrema vancouverense		X
GenBank	MN022774.1	Monadenia fidelis		X
GenBank	MN608010.1	Succinea sp.		X
GenBank	MT181461.1	Limax maximus		X
GenBank	MT266955.1	Patera perigrapta		X
GenBank	MT266961.1	Neohelix albolabris		X
GenBank	MT266964.1	Neohelix dentifera		X
GenBank	MT266964.1	Neohelix solemi		X
GenBank	MT266966.1	Neohelix albolabris		X
GenBank	MT266968.1	Neohelix solemi		X
GenBank	MT266971.1	Mesodon normalis		X
GenBank	MT266972.1	Neohelix dentifera		X
GenBank	MT266974.1	Mesodon normalis		X
GenBank	MT266975.1	Xolotrema fosteri		X
GenBank	MT266979.1	Neohelix alleni		X
GenBank	MT266981.1	Neohelix lioderma		X
GenBank	MT596773.1	Zonites aligirus		X
GenBank	MW443382	Helix pomatia	X	

SUPPLEMENTAL 6.3

Morphological Measurements for *Triodopsis fallax* Group

clade	Access#	width	height	umb	spire	whorls	wdht	wdum	wdsp	notes
1	295.03	9.4	6.2?	1.4	1.5?	5.0?	1.5?	6.7	6.2?	spire broken
1	295.06	9.4	5.4	1.5	1.6	5.0	1.7	6.3	5.9	
1	589.06	10.5	6.5?	2.0	1.6?	5.2	1.6?	6.2	6.7?	spire broken
1	632.17	10.6	6.8	1.8	6.1	4.7	1.6	4.8	6.8	
1	632.26	11.9	7.4	1.5	1.3	5.3	1.6	7.4	9.2	
1	986.1	9.3	?	1.5	?	4.9	?	6.2	?	spire broken
1	987.1	10.3	6.0	1.9	2.2	5.3	1.7	5.4	4.6	
1	1005.1	10.0	6.1?	1.5	?	5.0	1.6?	7.1	?	spire broken
1	1062.1	12.8	8.0	1.9	1.5	5.3	1.7	5.4	4.6	
1	1094.1	9.8	5.3	1.6	1.8	4.9	1.8	6.1	5.5	
1	1150.1	12.0	7.8	1.5	2.5	5.4	1.5	8.0	4.8	
1	1456.1	9.9	5.2?	1.7	1.9?	4.9	1.9?	5.8	5.2?	spire broken
1	1763.1	9.5	4.9	1.5	1.7	4.9	1.9	6.4	5.7	
1	1926.1	9.0	5.0	1.6	1.0	4.8	1.8	5.6	9.0	
1	1926.2	11.2	6.2	2.0	1.5	5.0	1.8	5.6	7.5	
1	1998.1	9.8	5.3	1.5	1.9	5.0	1.8	6.1	5.3	
1	2042.1	9.3	5.4	1.2	1.8	5.0	1.7	7.7	5.3	
1	2043.1	9.4	5.7	1.5	2.0	5.4	1.7	6.3	4.8	
1	2044	10.2	5.0	1.7	0.8	4.5	2.0	6.4	12.8	
1	2048	9.4	6.1	1.8	1.5	5.4	1.5	5.2	6.3	
1	2050.1	12.6	7.3	2.2	2.7	5.4	1.7	5.7	4.7	
1	2052.1	11.2	5.8	2.0	1.8	5.0	1.9	5.6	6.2	
1	2076.1	9.6	5.6	1.5	1.9	4.9	1.7	6.4	5.2	
1	2082.1	10.8	6.7	1.8	1.5	5.2	1.6	6.0	7.3	
1	2093	10.3	5.6	1.8	1.1	5.5	1.8	5.7	9.4	
1	3001.1	11.6	6.4	1.3	1.8	5.3	1.8	8.9	6.5	
1	3002.1	10.9	5.9	1.7	1.5	5.4	1.9	6.4	7.2	
1	449229.1	10.8	5.6	2.0	1.2	4.5	1.9	5.4	9.0	
1	504440	9.8	5.3	1.7	0.9	5.0	1.8	5.8	10.9	
1	295.13.1	9.5	5.3	1.5	1.8	5.2	1.8	6.3	5.2	
1	589.13.1	11.5	6.0	1.4	2.6	5.5	1.9	8.2	4.4	
1	589.15.1	11.2	6.5	1.5	2.3	5.3	1.7	7.5	4.8	
1	632.10.1	10.8	5.8	1.7	2.1	5.4	1.4	6.4	5.1	
1	632.23.1	10.3	5.9	1.6	2.1	5.0	1.8	6.4	5.0	
1	632.28.1	10.2	5.7	1.6	2.0	4.9	1.8	6.4	5.2	
1	632.29.1	10.2	6.1	1.5	2.0	4.9	1.7	7.0	5.0	
2	1093.1	13.1	7.4	2.0	2.9	5.4	1.8	6.6	4.6	
2	1961	9.2	5.4	1.7	0.9	5.1	1.7	5.4	10.2	
2	1963	10.3	5.7	1.5	0.8	4.8	1.8	6.9	12.9	

2	2078.1	11.5	7.4	1.5	3.0	5.8	1.6	7.7	3.9	
2	2079.1	10.6	6.6	1.6	2.3	5.2	1.6	6.6	4.6	
2	2080.1	10.2	5.6	1.5	2.1	5.3	1.8	6.8	4.8	
2	2730.1	11.4	6.7	1.6	2.1	4.9	1.7	7.1	5.5	
2	2731.1	11.4	6.6	1.5	2.4	5.3	1.8	7.6	4.8	
2	2733.1	15.0	10.2	2.2	4.0	5.5	1.5	6.8	3.8	
2	448919	12.6	8.1	1.5	4.7	5.5	1.6	8.4	2.7	
2	450283	10.7	6.8	1.5	5.0	5.0	1.6	7.1	2.1	
2	504549	10.8	6.0	1.4	1.0	5.0	1.8	7.7	10.2	
2	504575.1	10.6	6.5	1.9	2.2	5.5	1.6	5.6	4.8	
2	588.34.1	12.0	8.0	1.8	2.9	5.5	1.5	6.7	4.1	
2	588.35.1	11.8	6.9	2.1	2.5	5.1	1.7	5.6	4.8	
2	588.37.1	11.9	7.6	1.5	2.5	5.6	1.6	7.9	4.7	
2	632.14.1	10.4	6.5	1.2	2.2	5.3	1.6	8.7	4.7	
2	632.19.1	10.8	6.9	1.2	2.4	5.4	1.6	9.0	4.5	
2	632.24.1	11.5	6.6	1.7	2.1	5.3	1.7	6.6	5.4	
3	632.11	11?	?	1.5	?	4.5	?	7.2	?	spire missing
3	1357.1	9.7	6.0	1.7	1.9	5.0	1.6	6.1	5.1	
3	2090	10.3	6.0	1.5	1.5	5.3	1.7	6.9	6.9	
3	578837	13.2	6.8	2.6	1.2	5.5	1.9	5.1	11.0	
3	588.31.1	12.1	7.7	1.8	2.5	5.5	1.6	6.7	4.8	
3	588.36.1	11.2	6.4	1.5	2.2	5.8	1.8	7.5	5.0	
3	589.14.1	10.1	6.7	1.3	2.1	5.5	1.5	7.8	4.8	
3	632.21.1	10.4	6.0	1.1	2.2	5.3	1.7	9.8	4.8	
7	2051	12.4	8.6	2.0	3.6	6.0	1.4	6.2	8.6	
7	2096	10.1	6.5	1.5	1.0	5.5	1.6	6.7	10.1	
7	3003	9.5	5.3	1.5	1.5	5.4	1.8	6.3	6.3	
7	3004	9.4	6.1	1.5	1.5	5.5	1.5	6.3	6.3	

Supplemental 6.3. Measurements of part of the specimens of *Triodopsis fallax* Group, 16S phylogeny. Shaded specimens are not in the final tree but were sequenced and excluded as duplicate sequences. Specimens from NCSM (North Carolina State Museum were not available for measurements.) Those with spires missing or broken were only used for measurements that are not questioned.

SUPPLEMENTAL 6.4

16S Polymorphism of Major *Triodopsis* Clades

Group or Clade	n	Fu's Fs	Tajima's D	h	Hd	Ks	Pi	% var
1	27	0.811	0.562	13	0.895	10.45	0.054	4.03475
2	18	-2.417	-0.726	16	0.987	19.94	0.104	7.69923
3	5	1.138	-0.855	5	1.000	34.50	0.186	13.3205
4	3	n/a	n/a	2	0.667	11.33	0.068	4.3758
7	6	0.452	-0.744	6	1.000	28.67	0.141	11.068
10	4	1.376	-0.868	4	1.000	25.50	0.124	9.84556
11	3	n/a	n/a	3	1.000	6.00	0.036	2.3166
12	4	1.397	-0.868	4	1.000	26.00	0.130	10.0386
13	4	-1.741	-0.650	4	1.000	2.17	0.106	0.83668
14	4	2.944	-0.809	2	0.500	3.00	0.014	1.1583
15,16,17	23	-9.811	-1.066	23	1.000	19.27	0.100	7.43822
19	13	-3.274	-0.389	13	0.987	19.73	0.098	7.61806
21,22	5	-0.299	-0.183	5	1.000	10.30	0.050	3.97683
T. fallax group	60	-8.893	-1.352	41	0.971	19.12	0.114	7.38263
T. fraudulenta group	11	-1.195	-0.601	11	1.000	34.35	0.175	13.2606
T. tridentata group	47	-17.766	-0.714	43	0.995	23.61	0.124	9.11544
All *Triodopsis*	122	-54.494	-0.445	95	0.992	24.13	0.152	9.31506

Supplemental 6.3 16S polymorphism of individual major Triodopsis clades. N – number of sequences in subgroup; Fu' F statistic – analysis of neutrality; Tajima's D – test of nonrandom, directional selection; h – number of haplotypes in subgroup (n); Hd – Haplotype Diversity; Ks - # nucleotide differences; Pi – nucleotide diversity. (DnaSP) % variation is calculated as Ks/259 X 100. A key to clade numbers is in Table 6.1.